

UNIVERSITY OF SOUTHAMPTON

**Linear and Non-linear Dynamics in an
Endo-observer's Frame of Reference**

by

Thomas Erik Schilhabel

A thesis submitted for the degree of

Doctor of Philosophy

in the

Faculty of Engineering and Applied Science

Department of Electronics and Computer Science

June 27, 2001

UNIVERSITY OF SOUTHAMPTON

ABSTRACT

Faculty of Engineering and Applied Science

Department of Electronics and Computer Science

Doctor of Philosophy

Linear and Non-linear Dynamics in an Endo-observer's Frame of
Reference

by Thomas Erik Schilhabel

Industrial applications demand ever-increasing precision in nonlinear system modelling, analysis and control. A prerequisite of high precision in these fields is the thorough analysis of given data from a specific physical system. When no information about the underlying physics is provided but just a time series, one is faced with black box modelling. When additionally the mean dynamics of a physical system are provided one deals with grey box modelling where the states of the mean dynamics are subtracted from the given data. Physical modelling differs from all these approaches since it is not data-driven but based on abstract physical concepts which are left to the experimenter to verify or falsify within physical experiments. Explicit errors and uncertainties are usually included within physical models by employing *stochastic models* which assume certain statistical properties of these errors and uncertainties. Classical physical models do not incorporate general errors and uncertainties which are unspecified prior to physical experiments.

However, the currently proposed techniques known as neural networks, neuro-fuzzy systems, wavelets etc. can be either utilized as statistical tools for *regression analysis* and *pattern analysis* or as purely *heuristic* approaches towards *data analysis* which are, outside a specific statistical setup, neither well understood nor generally explicable. Purely statistical approaches may be able to classify whether a time series stems from a linear, or non-linear system with or without noise. Some more advanced statistical methods known as *chaos theory* have also been developed to quantify the dynamic behaviour, for example the characteristic time-scale, semi-periodic dynamics, generalized Lyapunov-exponents, generalized information measures, fractal dimension etc. None of the tools listed above allows the incorporation of any physical knowledge, and this limits their capabilities in terms of data requirement and predictability.

As an attempt to overcome this unfortunate division between data and physical modelling, this thesis is devoted to the development of a framework which allows the derivation of a physical model that at the same time includes errors and uncertainties

about this system which are as unspecified with respect to their statistical properties as possible. The work can be summarized as: 1. *Grey box modelling*: An appropriate semi-physical model of a ballistic missile with very limited knowledge about the aerodynamical properties of the airframe is being developed. It is shown which kind of dynamics the missile may exhibit and with which methods these dynamics can be analyzed. It is demonstrated that the missile may also show chaotic behaviour, the methods to measure this type of dynamics are presented. The lack of data points may, however, prevent the applicability of these methods which therefore suggests the theoretical framework of an: 2. *Endo-observer for linear systems*: It is proved that real-life observers require a framework such as a stochastic one for incorporating their uncertainties into a physical model. It is shown how minimally specified uncertainties can enter the dynamics of a free particle. The dynamics turn out to be similar to those given by the Schrödinger equation. 3. *Endo-observer for the nonlinear state space*: The concepts of physical dynamics with uncertainties which have been developed for the free particle are exhaustively re-developed for the case when the variance of the uncertainties remains within an arbitrary but fixed bound defined prior to the experiment. The dynamics of a nonlinear vector field with uncertainties are expressed in a form which is very much similar to the Schrödinger equation with a ‘momentum’ consisting of the ‘mechanical momentum’ from which a ‘electromagnetical momentum’ is subtracted which in this case here is the vector field of the state space. 4. *Endo-observer with bias*: It is argued that an observer which has to select permanently among all available variable and parameter values has to favour the more probable ones rather than the less probable ones. The dynamics then lead to the well known nonlinear Schrödinger equation.

The novel approach which is introduced in this work has several advantages over other statistical and stochastical models. 1. The motivation of the formalism is drawn from real-life applications which have strong limitations such as the amount of data and the restriction of unprejudiced model selection, *i.e.*, the model does not utilize any information which is not explicitly available to a real-life observer. 2. The relationship between physical system and observer is clearly defined. 3. The influence of physical parameters on the model is very transparent and clearly separable from the classical physical model itself.

The approach presented here opens up an entire new area of open research problems some of which are discussed at the end of this thesis.

Contents

1	Introduction	1
1.1	The Modelling Task	1
1.2	Motivation	3
1.2.1	State space modelling of ballistic missiles	4
1.2.2	Black box modelling issues	6
1.2.3	Grey box modelling issues	9
1.2.4	White-box modelling	11
1.2.5	Incorporation of physical knowledge into a common framework	12
1.3	The contributions of this thesis	14
1.4	Outline of the thesis	15
2	Physical Models and Black Box Models	18
2.1	Introduction	18
2.2	Physical state space models	20
2.2.1	Assumptions and Requirements	23
2.3	Black-Box modelling techniques	24
2.3.1	Regression techniques	25
2.3.2	Applicability of Black-box models	34
2.4	Conclusion	35
3	Ballistic Missiles	37
3.1	Principles of ballistic missile modelling	38
3.2	The ballistic missile as a point mass	39
3.3	The many particle body of a ballistic missile	44
3.3.1	Desired Flight path during boost phase	58
3.4	The aerodynamic flow around a slender body	59
3.5	Non-linear statistical modelling of time series	74
3.5.1	Time Series pre-processing for Grey-box modelling	75
3.5.2	State space reconstruction and Non-linear statistical analysis . .	77

3.5.3	Possible Routes to chaos in ballistic missiles	82
3.6	Conclusion	85
4	The Endo-Observer of a Linear System	87
4.1	Introduction	88
4.2	Endo- Exo- observers and their relation to each other	89
4.2.1	Observability of a free particle	93
4.3	An endo-observer's dynamics of a free particle	93
4.3.1	Bounds for the variance of the probability distribution of spatial coordinates	105
4.3.2	Conclusion	105
4.4	Analytical Examples	106
4.5	From time series to endo-observer models	110
4.5.1	Probability densities from time series	110
4.6	Conclusion	118
5	Uncertainty in non-linear dynamics	121
5.1	Motivation	121
5.2	Introduction	123
5.3	Propagation of a difference vector field in the state space	125
5.3.1	Dynamics of a difference vector field	126
5.4	Uncertainty of an error-vector field's probability density function in the state space	128
5.5	Computation of dynamics when the probability density function inside the state space is only partially known	133
5.5.1	Introduction	133
5.5.2	Dynamics of an endo-observer's with estimated initial probability density functions	135
5.5.3	Dynamics of an endo-observer's state with bounds	136
5.5.4	Model identification <i>via</i> the incorporation of partially known measurements into non-linear dynamics	137
5.6	Model tracking by representation of new measurements	138
5.6.1	Dynamics of tracking model	140
5.6.2	Computation of likeliness of parameters and non-observable endo-observer state components	143
5.6.3	Examples of prediction models	144
5.7	Conclusion	146

6 The endo-observer's frame of reference for a ballistic missile	148
6.1 Introduction	148
6.2 The Schrödinger equation for a Ballistic Missile	149
6.2.1 Lift- and Drag-coefficients are negligible	152
6.2.2 Drag-coefficient is constant and without Lift-coefficient	154
6.2.3 Drag- and Lift-coefficients are time dependent, a short perturbation through a side wind	157
6.3 Tracking of a Ballistic Missile's Dynamics performed by endo-observers	158
6.4 Conclusions	159
7 Conclusions & Future Research	160
7.1 Utilization of general Non-linear Statistical Modelling techniques . .	161
7.2 Modelling issues of Ballistic Missiles	163
7.3 Endo-observer Models for Linear Dynamical Systems	164
7.3.1 Advantages over black-box and stochastic approaches	166
7.3.2 Open problems and Issues for Future Research	166
7.4 Endo-observer Models for Non-Linear Dynamical Systems	167
7.4.1 Advantages over black-box and stochastic approaches	168
7.4.2 Open problems and Issues for Future Research	169
References	171

List of Figures

3.1	Relationship between two frames of references for a rigid displacement	40
3.2	The diagram of the model ballistic missile	47
3.3	Forces on the airframe, ballistic missile model	55
3.4	Stereographic projection of the ballistic missile	62
3.5	Aerodynamics of a ballistic missile with side-wind	63
3.6	Example: Drag/Lift-forces on a ballistic body	72
4.1	The Relation between endo- and exo-systems	91
4.2	The arrangement of the experiment	92
4.3	The line integral of a probability density function	94
4.4	Endo-observer dynamics - Exo-observer dynamics	119
5.1	A 2-sphere in the state space containing a sub-set of vector field	127
6.1	Ballistic missile trajectory in vacuum and Trajectory's Variance	154
6.2	Superposition of drag-force and perturbation through lift	157

Acknowledgements

I would like to express my sincere gratitude to my supervisor Professor C.J. Harris, who guided and helped me through my PhD studies. Besides giving me valuable advice he always provided his best possible support which allowed me to freely conduct my research. Although there are mutually different opinions about various research issues, his criticism helped me to progress with my work. Thanks are also due to Dr. C.H. Shadle who helped me at some critical stages to arrange my stay within the university.

Special thanks to the DERA Malvern for the financial support of my research during the first three years.

I would like to thank Dr. J.J. Wood who had the patience to listen to my problems during this work, to read my very early drafts, and who helped with his advice whenever he could. Special thanks to Simon Poliakoff who read the latest version of the draft.

Many thanks to all the members in the ISIS group which contributed towards a pleasant working environment.

Lastly I would like to thank my close friends, Anna, and my family for their continued support during the entire period of my PhD research.

List of Symbols

$\overline{(\bullet)}$	Time mean of a variable.
$\langle \bullet \rangle$	Ensemble mean of a variable.
\mathbb{C}	Complex Numbers.
\mathbb{R}	Real Numbers.
a	Geometric measures of the ballistic body.
A_S	Reference area of a body (scaled).
b	Geometric measures of the ballistic body.
b_d	Parameter with $b_d^2/(4m^2)$ as the damping parameter.
B_d	Parameter with $B_d^2/(4j^2)$ as the damping parameter.
β	Damping parameter in Example 3.4.3.
c	Geometric measures of the ballistic body.
c_1, \dots, c_6	Abbreviations of functions given in Section 2.4.
c_9, \dots, c_{14}	Abbreviations of functions given in Chapter 6.
\mathbf{C}_1	Relative aerodynamic force.
$\mathbf{C}_{2,3}$	Relative aerodynamic torques.
$C(\epsilon)$	Correlation integral.
CM	Centre of Mass.
CP	Centre of Pressure.
$C_S(\mathbf{x}_{\text{en}})$	Boundary of orientable smooth surface at \mathbf{x}_{en} .
\overline{D}	Mean drag coefficient.
D_F	Drag coefficient.
$D_{\text{drag, lift}}$	Explicit drag and lift coefficients.
$D(2)$	Box counting dimension.
$d_{\text{attractor}}$	Attractor dimension.
$d_{\text{embedding}}$	Attractor dimension.
$\delta i, j$	Kronecker delta function which is equal to one iff $i = j$ and zero otherwise.
$\delta \mathbf{F}_{(\bullet)}, \delta \mathbf{f}_{(\bullet)}$	Perturbative forces on a body.

δ_s	Thickness of hollow cylinder.
$\delta(x - x')$	Delta function which is ∞ for $x = x'$ and zero otherwise.
\mathcal{E}	Error potential of endo-observer.
$\mathbf{e}_1, \mathbf{e}_2, \mathbf{e}_3$	Unity vectors which span the fixed frame of reference.
$\mathbf{e}'_1, \mathbf{e}'_2, \mathbf{e}'_3$	Unity vectors which span the rigid body fixed frame of reference.
$\mathbf{e}'_{i\text{CM}}$	Unity vectors which span the fixed frame of reference of the rigid body, with the origin at the centre of mass.
$\varepsilon \in \mathbf{R}$	Small parameter for box counting dimension.
$\varepsilon(\bullet)$	Overall error of an endo-observer.
F	Fixed frame of reference
F'	Mobile frame of reference
\mathbf{F}_{ae}	Unperturbed aerodynamic forces on a body.
\mathbf{F}_{th}	Unperturbed thrust forces on a body.
$\mathbf{F}(\mathbf{x})$	Vector field of the state space \mathbf{R}^n
$\mathbf{F}(\mathbf{x}_1)$	Vector field of the sub-state space \mathbf{R}^{k-1} .
$\mathbf{F}_{\text{ex}}(\mathbf{x})$	Vector field of an exo-observer state space model in \mathbf{R}^n
\mathbf{f}	Force on a body.
\mathbf{f}_{ae}	Aerodynamic forces on a body.
\mathbf{f}_{th}	Thrust forces on a body.
\mathbf{g}	Gravitational constant.
$\mathbf{g}_i(\bullet)$	Basis function i
$G(\mathbf{x}_1)$	Hamilton principal function, action function for the endo-observer.
$\Gamma_{1,2,3}$	Torques applied to a body.
γ	Tracking parameter
h	Height of a body
\hbar	Planck's constant
$I_{\Delta x_{\text{en}}}(\mathbf{x}_{\text{en}})$	Finite interval in endo-observer state space.
\mathcal{I}	Inertia tensor
\mathbf{j}_i	Tensor related to the inertia tensor by $\mathcal{I}_i = \rho_i \mathbf{j}_i$
$\mathcal{I}_{1,2,3}$	The three principle moments of the inertia tensor
$\mathbf{J}(i)$	Jacobian matrix at time step i .
$\mathbf{k} \in \mathbf{R}^{k-1}$	Wave-vector
k_d	Parameter with $\sqrt{k/m}$ as angular frequency.
K_d	Parameter with $\sqrt{k/\mathcal{I}}$ as angular frequency.

κ	Constant action function parameter.
λ	Lyapunov exponent.
l	Geometric measures of the ballistic body.
\mathbf{L}	Angular momentum.
L_R	Linear operator.
L	Geometric measure of the ballistic body.
l_d	Reference length of a body.
m	Mass of a body.
μ_{max}	Nyquist frequency.
N	Number of data points.
ω	Rotational velocity of a body.
ω_{R_i}	Characteristic frequency of resonator i .
$\mathbf{p} \in \mathbb{R}^3$	Momentum vector.
\mathbf{q}	Difference vector field between exo-observer and endo-observer vector field.
$\psi(\mathbf{x}, t) \in \mathbb{C}$	‘State space’ function of endo-observer.
$\tilde{\psi}(\mathbf{k}, t) \in \mathbb{C}$	Fourier-transform of $\psi(\mathbf{x}, t)$.
ϕ, ψ	Euler angles.
ψ_{rel}	Roll angle of a body.
φ	Angle in Fig. 4.3.
$\mathcal{R}, \mathcal{R}_t$	Attitude of a rigid body, fixed/at time t .
$\mathbf{r}_0 \in \mathbb{R}^3$	Spatial coordinate vector in the physical space at time $t = t_0$.
$\bar{\mathbf{r}}$	Mean spatial coordinate.
$\mathbf{r} \in \mathbb{R}^3$	Spatial coordinate vector in the physical space
$\mathbf{r}_m \in \mathbb{R}^3$	The mean spatial coordinate vector.
$r_l \in \mathbb{R}$	Distance between CM and applied thrust vector.
$r_{cp} \in \mathbb{R}$	Distance between CM and CP.
r_1, r_2, R	Radii of ballistic body components.
ρ_∞	Free stream air density.
$\rho(\cdot)$	Probability density function.
$\rho(\mathbf{x}_2 \mathbf{x}_1)$	Conditional probability density function, <i>i.e.</i> , probability density of \mathbf{x}_2 when $\rho(\mathbf{x}'_1) = \delta(\mathbf{x}'_1 - \mathbf{x}_1)$.
σ_i	Variance of a function.
σ_r	Variance of spatial coordinates.
σ_v	Variance of velocity distribution.

$s \in \mathbb{R}$	Alternative time parameter
\mathbf{s}_i	Time delay vectors
$S(\mathbf{x}_1)$	Hamilton principal function, action function.
$S_S(\mathbf{x}_{\text{en}})$	Orientable smooth surface at \mathbf{x}_{en}
$t \in \mathbb{R}$	Time
τ	Time delay for time delay vector
τ_f, τ_m	Characteristic time scale of the force/momentum dynamics
θ	Euler angle.
$\theta_{\text{rel}}, \psi_{\text{rel}}$	Angle of attack and roll angle of a body.
$\Theta(\mathbf{r})$	Heaviside function.
$\Theta(t)$	Endo-observer state space function.
\mathbf{v}	Velocity vector for a coordinate system utilised in the literature on flight control.
$V_S(\mathbf{x}_{\text{en}})$	Volume of endo-observer at \mathbf{x}_{en} .
$\mathbf{v} \in \mathbb{R}^3$	Velocity vector.
$\mathbf{v}_0 \in \mathbb{R}^3$	Velocity vector at initial time $t = t_0$.
$\mathbf{v}_{\text{wind}} \in \mathbb{R}^3$	Wind velocity vector.
$\mathbf{v}_{\text{rel}} \in \mathbb{R}^3$	Relative wind velocity vector.
$\bar{\mathbf{v}}$	Mean velocity.
\mathbf{x}	State space vector \mathbb{R}^n .
$\mathbf{x}_1 \in \mathbb{R}^{k-1}$	Sub-state space vector, accessible by endo-observer and exo-observer.
\mathbf{x}_2	Sub-state space vector \mathbb{R}^{n-k+1} accessible by exo-observer.
\mathbf{x}_{en}	State vector of endo-observer state space.
\mathbf{x}_{tr}	State vector of tracking endo-observer state space.
ξ	Stochastic variable in endo-observer state space.

Chapter 1

Introduction

Forward

The purpose of this thesis is outlined and summarized within this chapter. After a short motivation of modelling within the defined problem domain, the state-of-the-art techniques and research issues of data driven black box modelling and purely physical knowledge based dynamical system design are introduced. Each approach is found to offer its own specific advantages and disadvantages. The dynamical systems considered here are implicitly defined by given measurements and physical constraints. It is concluded that neither black-box nor physical modelling is a fully adequate means of dynamical system identification and prediction. The issues considered in the subsequent chapters are summarized in Section 1.3

1.1 The Modelling Task

The objective of this thesis can be summarized as: “*Identification and Prediction of Non-Linear Dynamical Systems with Sparse Time Series and bounds in the State Space.*”

It is assumed that the dynamics of all physical system variables are explicitly defined. A time series is provided which is a set of measured physical variables ordered with respect to the parameter time. Bounds on the non-measurable physical variables are implicitly given by the physical context of the system under consideration. This very general objective is far too ambitious to be dealt within the scope of a single PhD-thesis. Chapter 3 outlines and summarizes the physical knowledge that is in principle

available about a ballistic missile. A toy model for demonstration purposes is introduced. The developed theory in the subsequent chapters applies to all physical state space models which are observed by a real-life experimenter. However, the observer model has just been applied to the toy state space model derived in Chapter 3 in order to keep it analytically trackable. More complicated state space models are in principle possible to model but require the numerical simulation of partial differential equations. The development of the numerical partial differential equation tools as needed here could easily lead to a consecutive PhD-thesis.

Identification and prediction of physical systems is in many cases considered to be a measurement and physical state space modelling problem, *i.e.*, when an experimenter measures a sufficient number of experimental results the physical system can be identified and subsequently utilized for predicting the system's physical variables for all time. This oversimplification of system-observer relations has lead to different kind of statistical and stochastic approaches. This thesis is concerned with the effect physical system interpretation by the observer can have on the modelling of physical systems and thus the prediction of the physical system's future. Some critics may remark that the algorithms developed here are not real identification/prediction algorithms as the emphasis is too strongly put on the available physical knowledge. Indeed, the main part of this work is concerned with clarifying the relationship between observers and physical systems, *i.e.*, the identification/prediction of non-linear dynamical systems is considered to be a purely observational problem. The mathematical reconstruction issues of physical state spaces from observations, as considered by Takens (1981), are not treated here. These reconstruction issues may be effected by the results presented here and may lead to challenging questions for future research.

This thesis' scope has thus been focused on demonstrating the following:

- (i) Real life observers cannot identify state space vectors of physical systems.
- (ii) A relation between real-life observers and abstract physical systems is established (endo-observer, exo-observer concepts).
- (iii) The linear dynamics of a physical systems with respect to observed/estimated probability density functions of real-life observations is derived.
- (iv) The non-linear dynamics of a physical systems with respect to observed/estimated probability density functions of real-life observations is derived for the case when the nominal vector flow in the state space is explicitly given.

1.2 Motivation

All electrical and mechanical appliances in a household, cars, aeroplanes, manufacturers and factories rely on the validity of few physical principles. Because most of the things around us are not static but dynamical systems, physics concentrates on the description of the dynamics of physical variables and their interrelation. The reason for this kind of physical modelling is the simplification of apparently complex phenomena in nature. Physical models are the backbone of engineering because they allow a systematic approach towards the design of all modern technologies around us. Throughout this thesis it is not possible to consider *all* physical dynamical systems. As an example a ballistic missile model is chosen for demonstrating the applicability of the algorithms which are derived in this thesis. It is important to clarify that the algorithms developed below do apply to any kind of (non-linear) dynamical physical system and that the adaptation to other dynamical systems than the ballistic missile is straightforward. The emphasis here is the development of the methodologies devised in Chapter 4, 5 and not the optimization of ballistic missile tracking algorithms. The requirements for such a task are highlighted in Chapter 3.

Assume there is a physical system such as a ballistic missile, which is measured through a specifically chosen arrangement of radars. Information about the physics in form of the precise dynamics of the relevant physical variables and parameters may not be available for two reasons. The dynamics of the physical system (ballistic missile and measurement apparatus) under consideration may not have been explicitly given, or, not all the physical variables required can be identified through the physical arrangement. Deterministic physical dynamical system modelling also requires error-free identification of real numbers which represent the physical variables. The reason why real-life physical systems cannot provide this kind of information is *noise*. The alternative of stochastic dynamical system modelling still requires the dynamics of all relevant physical variables. It is demonstrated in Chapter 3 that this requirement is not fulfilled, *i.e.*, physical modelling as for example employed in classical mechanics is not valid for real-life observers. An alternative approach may be one which does not explicitly require the physical variables' dynamics. When there is no knowledge available about an underlying physical system, data driven modelling techniques have to be utilized which seek to discover the relationship between given data points. These techniques are known as *black-box* modelling. The drawback of black-box, or even grey-box, modelling is that there are always explicit or hidden implicit assumptions about the underlying dynamics which have to be accepted and which cannot be falsified or verified (see Chapter 2 for further details). Additionally, these methods are based on

statistical models which need a considerable amount of data to ensure that the results are statistically significant. It is argued in the following that the amount of data is not sufficient and thus neither black-box nor grey-box modelling can be utilized. The main part of this work is therefore the development of an algorithm which seeks to solve the dilemma of not being able to employ black-box or physical modelling. The requirements and limitations of physical and black-box modelling are briefly discussed in the following two sections.

1.2.1 State space modelling of ballistic missiles

The initial step in dynamical system identification is the analysis of a physical systems with respect to the relevant physical variables and parameters, as this gives indications about the dimension of a state space model, provides possible mathematical relationships between variables and measurements in real-life experiments outside the laboratory, and allows qualitative and quantitative long-term predictions of a physical system with respect to its (non)-linearity and complexity. As the initial focus of this work is in the understanding of ballistic missile trajectories, the algorithm towards ballistic missile state space modelling is devised in Chapter 3. The main purpose of this example is to emphasize the advantages, difficulties and problems of state space modelling.

The investigations in Chapter 3 show that a ballistic missile is precisely and exhaustively described by 16 physical variables which define the state vector \mathbf{x} of an arbitrary ballistic missile. The state vector consists of the spatial coordinate \mathbf{r} , the velocity \mathbf{v} of the body, the wind velocity \mathbf{v}_{wind} and depends explicitly on the time s . Together these describe the dynamics the missile's center-of-mass. Because during the sustain phase the missile can be considered to be a rigid body, the attitude \mathcal{R} and rotational velocity $\omega = \dot{\mathcal{R}}$ complete the list of all necessary physical variables (Arnold, 1978; Hestenes, 1986; Scheck, 1990) and thus the components of the state vector. Cauchy's celebrated theorem (Scheck, 1990) then shows that the dynamics of the ballistic missile can be computed for any time (prediction) by employing the so-called state space vector field which implicitly defines how the combination of the 16 physical variables change as time progresses. The infinitesimal change of the state vector $d\mathbf{x}$ within a infinitesimal time interval dt is defined by a vector field \mathbf{F} . The mathematical notation for that is

$$\mathbf{x} := (\mathbf{r}, \mathbf{v}, \mathbf{v}_{\text{wind}}, \mathcal{R}, \omega, s)^T \quad (1.1)$$

$$d\mathbf{x}/dt := \mathbf{F}(\mathbf{x}) \quad (1.2)$$

In the literature (for example in Blakelock (1965), Garnell (1980), Anonymous (1982), Eichblatt, E.J., Jr (1989), Collinson (1996)) coordinate systems with time dependent rotations have been incorrectly transformed as the authors related non-inertial (time dependent rotations) frame of references to acceleration measurement techniques which belong to inertial (rotationally fixed) frame of references. It has been found that most accelerometers utilized in today's aeroplanes, missiles, etc. (Garnell, 1980) are insensitive to rotational velocities and thus require a modified formula for the solution of centre-of-mass dynamics then the one provided in the references above.

For mechanical systems the forces that are the most relevant physical influences are in many cases very difficult to identify (Hestenes, 1986; Scheck, 1990). For a ballistic missile during the sustain phase, only two forces apply, the aerodynamic and the gravitational force. The gravitational force is—due to the earth's property of almost homogeneous forces on bodies of a size such as a ballistic missile—most easily to model whereas the aerodynamics and the corresponding aerodynamic forces on bodies are little understood, as intensive on-going research *viz* wind-tunnel experiments indicates (Anderson, 1991). The theory is either very imprecise in predicting the aerodynamic properties or far too specialised to specific air frames as to be of little generic value—see for example seen in Anderson (1991). The information required for reasonably realistic ballistic missile modelling is not available. For example Anonymous (1982), Cronvich (1991), or Jenn (1991) provide only details which are incomplete and require too much expert knowledge which is inaccessible for an outsider. Thus, only an (over-)simplified ballistic missile model can be derived which therefore cannot serve as a typical state space model for simulation and prediction, but which may still suffice as a toy model for demonstration purposes. However, if a complete look-up table of all required aerodynamic drag and lift coefficients with respect to all relative wind velocities and relative attitudes of an air-frame towards the relative wind vector were accessible and the inertia tensor were explicitly given, the physical model as outlined in Chapter 3 could provide an adequate model which would correspond to a real-life ballistic body within the precision of the identified physical parameters. Physical reasoning as employed in Chapter 3 certainly provides limited understanding of the system under consideration. However, it remains pure guess-work as long it is not being tested against measurements taken by a sufficient repetition of experiments. The simplicity or complexity of mathematical models which correspond to experiments do generally not reflect the accuracy of the model. The identification and prediction algorithms which have been derived in Chapters 4 & 5 could be realistically tested against the simulated dynamics of a ballistic missile model. The toy model in Chapter 3 thus re-

mains an example which cannot be utilized for validation purposes and may only serve the illustration of the algorithms devised. Deterministic physical dynamical models may be defined through a vector field. However, this does not imply that the dynamics can realistically predicted for all time. The reason for this kind of modelling problem emerges when neighbouring states diverge exponentially as time progresses. Because any real-life measurement incorporates small differences between the state a system is in and the reading on a physical measurement device, a small difference vector enters any kind of modelled phase flow. For dynamical systems where the difference vector decreases or remains constant the modelled error does not significantly influence the prediction. In case that the trajectories of a dynamical system exponentially diverge, the initial small magnitude of an error may after a fixed time interval grow beyond the magnitude of a state vector. This characteristic behaviour is called deterministic chaos. So-called ‘Routes’ to chaos (Schuster, 1989) are indicated within Chapter 3.

Another purpose for considering a precise ballistic missile and its modelling issues is its analysis for identifiability *via* black-box (and grey-box) techniques which are introduced in the following section and outlined in more detail in Chapter 2 and Section 3.5.

1.2.2 Black box modelling issues

Black-box modelling issues are concerned with analysing a given time series (data which is ordered according to time) with respect to the identification of an underlying process which generates this data (Juditsky et al. 1995; Sjöberg et al. 1995). When no information is provided about the source of a time series certain algorithms have to be applied which give an indication (but no proof) about the possible underlying system which may generate the kind of data under consideration. The data is being tested for the following properties in the given order.

1. Does the time series represent pure noise or is it just corrupted with noise?
2. Is the underlying model linear, or non-linear?
3. Is the model predictable, or unpredictable?
4. When the model is predictable how does it evolve with time?

The most elementary tools for time series visualization is either done in graphs, maps or histograms, to show possible trends in the dynamics. When these simple methods fail to show some essential dynamical features several data pre-processing techniques

may be employed before the elementary visualization tools are re-applied to the now pre-processed data. The advantage is, that the pre-processing techniques allow the separation of different time scales in this dynamics (*e.g.* return map, binning, next maxima map), or they may provide for noise reduction and for the elimination of undesired trends in the time series by filtering (*e.g.* linear high-, or low-pass filter). All these methods can for example be found in Kantz et al. (1993), Weigend and Gershenfeld (1993), Kantz and Schreiber (1997), and Schwarz (1994).

Classical time series analysis (Ebeling, Engel and Herzl, 1990; Schwarz, 1994) is based on linear and weakly stationary signals (the first two moments of the distribution are time invariant) for linear processes, or it requires and linear and strongly stationary signals (distribution is time invariant) for nonlinear dynamic system analysis. These requirements have to be proved by generating spectra of various sub-samples in the data set. Tests for linearity can be found in (Keenan, 1985; Tsay, 1986) and white noise test are for example the Kolmogorov-Smirnov-Test (Press, Flannery, Saul and Vetterling, 1993) and the so-called BDS(Brock, Dechert, Scheinkman)-Test (Wolff, 1994). The classical analysis tools may be completed by utilizing the spectral analysis (which includes for example the auto-correlation function, the power spectrum) for the detection of periodicities in the underlying dataset, and the identification of linearly correlated time series, coloured noise Jetschke (1989), by means of n^{th} -order auto-regressive (AR) models (Shumway, 1988; Kurths and Herzl, 1987).

All methods mentioned above are very well suited for providing information about the global behaviour of the time series generating system. Many applications, however, seek some quantitative descriptions about the temporal behaviour of those dynamical systems and the ‘grade’ and complexity of the non-linearity. These quantitative statistical measures have just recently been developed (Beck and Schlögel, 1995; Kantz and Schreiber, 1997) for non-linear dynamical system characterization. Some of the most characteristic qualities emerging through non-linearity are self-similar temporal structures, singularities, intermittence, a *local* spectrum on various scales which changes with time (Beck and Schlögel, 1995; Kantz and Schreiber, 1997). The wavelet analysis has been proven, Daubechies (1992) and Holschneider (1995), to provide such quantitative measures for all the listed qualities of non-linearity. Furthermore, the non-linearity of dynamics can be quantified for small $d_{\text{attractor}}$ -dimensional attractors in a n -dimensional state space by the correlation-integral (Grassberger and Procaccia, 1983a; Grassberger and Procaccia, 1983b; Takens, 1993) which allows an estimate of

the so called (fractal) dimension of the attractor and enables a test of the non-linearity of the underlying system (Takens, 1993). The attractor dimension quantifies some of the geometric properties of attractors. Apart from generalized dimension measures, generalized Lyapunov exponents, generalized information measures there still exists the $f(\alpha)$ -spectrum for characterizing the multi-fractal character (Beck and Schlogel, 1995) to quantify those attractors. All these measures, however, are only suitable for low-dimensional attractors $d_{\text{attractor}} < 11$. Note, that in the sections above it has been noted that n is 16 and there do not seem to be any indications that there is a ‘nice’ attractor inside which has a dimension less than 16. It should be stressed that although it is known that the time series stems from a non-linear dynamical system with some unspecified included noise, the test introduced above ought to be run on some real-life data *prior* to further analysis. The reason for this approach is the validation of the presumed model and at the same time an unbiased view towards the fact, that some crude methods may reveal some general trends inside the time series. However, after all this methodologies for data quantification have been made available, the crucial question has to be raised: what all that has to do with the underlying dynamical system. Remember, all the techniques listed above are qualitative measures to decide from what kind of system the data may originate. For example when the time series only represents the spatial coordinate and velocity components, which are 6 out of the whole $n = 16$ -dimensional state vector, it is not obvious how these components may relate to the entire dynamics. Takens (1981) proved that the entire dynamics of physical system may be reconstructed *via* employing so-called time delay vectors with an embedding dimension $m > 2d_{\text{attractor}}$. The crux is, that the dynamics given by the time delay vectors are diffeomorphic to the original state space and the characteristic measures of complexity, non-linearity mentioned above may be applied to the series of reconstructed state vectors instead of employing the original, non-available state vectors. The quantitative measures deliver the identical values of the original systems, as if they were applied to the series of original state vectors. The problem is that this property only holds when the time series is error free, which means that the application of Taken’s theorem is severely limited, since real-life systems cannot be assumed noise free. A further development of Taken’s theorem to noisy time series data has been provided by Stark (1999), but prior information about the noise is required. The disadvantages of the employment of reconstructed state vectors are obvious: The time series data is never noiseless, nor is the noise defined, and the sufficient amount of data for the application of such an algorithm is $d_{\text{attractor}} < 2 \log_{10} N$ (Ruelle, 1990; Essex and Nerenberger, 1991; Eckmann and Ruelle, 1992) which means that in case of

$d_{\text{attractor}} = n$, the number of 6 component vectors of a time series must be of order $10^8/6$. As a first approach towards circumventing these problems other algorithms may be applied: the recurrence plots by Eckmann et al. (1987), Babloantz (1991), Koebbe and Mayer-Kress (1992) which enable the application of measures developed for symbolic dynamics, the information measures (Shannon-information, Trans-information), and the algorithmic complexity measures (Beck and Schlögel, 1995; Kantz and Schreiber, 1997). Because all quantitative measures above are based on the probability measure, an additional problem is encountered when the algorithms are sought to be applied to a time series. Note, that a time series provides a number of points within the (reconstructed) state space. The only relation between data points and a probability density is given by the frequency a dynamical system visits a small volume element inside the state space. However, the trajectory of a typical ballistic missile is stretched through the 3 spatial coordinates of the state space, which means that there cannot exist a frequency of neighbouring states which may provide an estimate for the probability distribution inside the state space. All methodologies introduced so far prove unsuitable for the dynamics of a ballistic missile whose trajectory is close to a parabola. A related approach to black-box modelling is *grey-box* modelling which may circumvent the just mentioned difficulties.

1.2.3 Grey box modelling issues

Grey-box modelling is strongly related to black box modelling (Juditsky, Hjalmarsson, Benveniste, Deylon, Ljung, Sjöberg and Zhang, 1995; Sjöberg, Zhang, Deylon, Hjalmarsson, Juditsky and Ljung, 1995) but has the advantage that it allows the incorporation of some knowledge by pre-filtering the time series with respect to some mean dynamics, such that only the net dynamics may be analysed. This section shortly introduces the grey-box modelling issues concerning ballistic missile time series.

The dynamical behaviour is strongly dependent on the structure and of how the non-linearity enters these dynamics. The wind is highly unpredictable and changes the trajectory of any flying object in an unpredictable way. Even for a stationary wind a complex relationship exists between all variables due to the geometry of the airframe of a missile. The pure rotational motion of a spinning body with three different principle moments of inertia may exhibit complex (chaotic) behaviour itself, as has been motivated in Section 3.5.3, without any interaction with its environment. There are several ‘routes’ to understanding complex behaviour of a missile and some of them have been summarized in (Schilhabel, 1996). However, the lack of knowledge about the dynamics demands another approach in order to be able to make

any sort of quantitative statements about the missile's dynamics. A semi-physical model that provides a filter for net missile dynamics and therefore may allow the predictability of ballistic missiles has been introduced in Schilhabel (1996) and here in Section 3.5. It has to be emphasized that this algorithm only works for real-life applications when the statistical conditions and physical requirements of a the model are fulfilled. Because necessary information about real-life systems is not provided, the requirements have to be hypothesized in the form of assumptions. The following paragraph summarizes essential issues of the physical modelling which is developed in Chapter 3. The modelling issues described below serve on the one-hand to outline the kind of *modelling* which, in the subsequent chapters and sections, is referred to in the context of physical modelling and on the other-hand to provide a flavour about the kind of physical knowledge which Section 1.2.5 is based on.

A simplified ballistic missile body is one, which is rotationally symmetric and for which the dynamics are completely described by a 6-dimensional state space. The reduction is from 16 to 6 state space components. Ballistic missiles need to be self-stabilizing in the sense that the attitude of the body seeks to be such that the air frame is not prone to lift forces and thus only a single mean drag force applies to the body. This does not mean that there are never any lift forces applied to the air frame of a ballistic body, but in the mean, they average out. Because a missiles dynamics are sensitively dependent on the relative wind, it is also assumed that this information is available. Also, because the model only incorporates part of the physical knowledge it is called a semi-physical ballistic missile model. In short, the semi-physical model is defined by the 6-dimensional 'state space' model of a ballistic body with pure mean drag force with mean drag coefficient $\bar{D}\rho_\infty(\bar{r}_3)$, which consists of a constant and the air density of free stream at the mean altitude \bar{r}_3 . The center-of-mass dynamics of a semi-physical ballistic missile are then completely defined by the mean spatial coordinate $\bar{\mathbf{r}}$ and the mean velocity $\bar{\mathbf{v}}$, with the corresponding state space model

$$d_t \mathbf{v} = (0, 0, -g)^T - \bar{D}\rho_\infty(\bar{r}_3)|\bar{\mathbf{v}}|\bar{\mathbf{v}} \quad (1.3)$$

$$d_t \mathbf{r} = \mathbf{v}. \quad (1.4)$$

The initial condition $\bar{\mathbf{v}}(0), \mathbf{r}(0)$ allows a trajectory $\bar{\mathbf{v}}(t), \bar{\mathbf{x}}(t)$ to be computed in the state space. We now define a set of other 3-dimensional coordinate systems defined by their corresponding bases $\{\bar{\mathbf{e}}'_1, \bar{\mathbf{e}}'_2, \bar{\mathbf{e}}'_3\}(t)$ for any time t with their origin at the corresponding point $\bar{\mathbf{r}}(t)$. Each of these coordinate system is rotated against the original one, such

that

$$\{\bar{\mathbf{e}}'_1, \bar{\mathbf{e}}'_2, \bar{\mathbf{e}}'_3\}(t) = \left\{ \frac{\bar{\mathbf{v}}}{\|\bar{\mathbf{v}}\|}(t), \frac{\bar{\mathbf{v}} \times \mathbf{e}_3}{\|\bar{\mathbf{v}} \times \mathbf{e}_3\|}(t), \frac{\bar{\mathbf{v}} \times \mathbf{e}_3}{\|\bar{\mathbf{v}} \times \mathbf{e}_3\|}(t) \times \frac{\bar{\mathbf{v}}}{\|\bar{\mathbf{v}}\|}(t) \right\}. \quad (1.5)$$

This is, the first vector \mathbf{e}'_1 points in flight direction of the missile, the second axis \mathbf{e}'_2 is orthogonal to the plane where the parabola of the trajectory is embedded in, and the third axis completes the two basis vectors orthogonally. It can be shown that the map described by the equations (1.3), (1.4) is a diffeomorphism, *i.e.*, transformations under a diffeomorphism leave characteristic measures as for example the Lyapunov exponents invariant (a fact that is being utilized in Taken's theorem, otherwise the reconstruction algorithm would not make sense). Each measured $\mathbf{r}(t)$ will generally be different from the ideal one $\bar{\mathbf{r}}(t)$ and the vector $\mathbf{r}(t)$ can be expressed by its corresponding coordinate system at time t leading to the vector $\mathbf{r}'(t)$. The back-transformation of all coordinate systems into one common coordinate system through the diffeomorphism then leads to a very dense distribution of data points, a transformed time series, which then allows the desired computation of all measures required, given that enough time series data points are explicitly available.

1.2.4 White-box modelling

White box modelling refers to a modelling technique assuming that everything about a dynamical system is explicitly known and well defined. This includes the vector field \mathbf{F} of the state space model, the state \mathbf{x} at any time t , the noise and its properties of observed object and observer (Juditsky et al. 1995; Sjöberg et al. 1995). It is apparent that this kind of assumption about real-life dynamical systems is un-realistic and does not reflect the experience of physical observations. It would be desirable to access this kind of information since it allows the only kind of physical modelling which does not require any assumptions, *i.e.*, everything about a dynamical system is explicitly given. Because real-life modelling does not allow any verification or falsification of white-box models its concept itself is an assumption leading to the causal principle introduced before. *Physical modelling throughout this thesis is defined as the systematic approach towards white-box modelling.* The implication is, only models with clearly defined minimal assumptions about non-accessible physical variables and parameters in the state space may be accepted. Black-box or grey-box models which employ parameters with unknown implications regarding the state and the trajectories inside the state space have to be utilized with great care.

1.2.5 Incorporation of physical knowledge into a common framework

The sections above introduced physical modelling which has been shown to be inadequate for the identification and prediction of real-life systems as it requires the measurement of states which cannot be practically performed. Black box modelling has been found very suitable for time series for which the origin is not known or where enough data is available to extract the desired information. It has been indicated that missile tracking algorithms may be difficult to develop when neither the state, nor the state space model, nor enough data is available. Grey-box modelling is black-box modelling with pre-filtered data (Juditsky, Hjalmarsson, Benveniste, Deylon, Ljung, Sjöberg and Zhang, 1995; Sjöberg, Zhang, Deylon, Hjalmarsson, Juditsky and Ljung, 1995), which may help to employ statistical techniques but it does not circumvent the requirement that enough data needs to be made accessible. The problem is that the modelling techniques defined above have nice mathematical properties but the majority are inapplicable due to the strong conditions imposed in the example of a real-life ballistic missile of which the observations are incomplete. Chapters 4–6 are dedicated to the development of a framework which allows the identification and prediction of linear and non-linear dynamical systems under the requirement that

1. Only available physical knowledge is employed: In the linear case the mean velocities at a spatial coordinate and the corresponding probability density function of finding a body's center-of-mass at the coordinate as well as the variance of the total velocity distribution are known. In the non-linear case a mean state space vector field is explicitly given, the probability density distribution inside the state space consists of partially measurable and partially guessed distributions and the stochasticity of the unknown noise is bound through an imposed variance.
2. Only few measurements are available.
3. Uncertainties about the systems dynamics can be modelled through probability distributions.

Before any modelling of uncertainties in linear and non-linear systems can be performed, the nature of the uncertainties needs to be clarified. Following the hypothesis of the causal principle and classical physics, it is assumed throughout this thesis, that there exists an adequate physical model which can in principle be observed and measured. The noise and errors enter the model through the real-life observer. Note the difference. It is not assumed that physical modelling in itself is faulty, only the

real-life observer is incapable of recognizing the underlying physical model. According to Rössler (1992) and Primas (1994) the ideal world of a physical model which exists without erroneous description is defined as the exo-physical state space model with a corresponding exo-physical observer. In contrast real-life observers are called endo-physical observers with their corresponding real-life (endo-physical) state space models. It is the relationship between endo-physics and exo-physics which thus has to be modelled in the following chapters. Chapter 4 first analyses the quality of physical variable measurements a real-life observer is capable of and it is proved that there are some profound qualitative properties of endo-observers which prevent them establishing state spaces as they are modelled in exo-physical (ideal) models. This quality which prevents a real-life observer from relating its measurements to an exo-physical model is then referred to as its uncertainty. The consequences of this type of uncertainty lead to a reformulation of linear dynamics in Chapter 4 and to a corresponding reformulation of non-linear dynamics in Chapter 5. The details of this procedure are extensive and will not be outlined in this section. It is worth mentioning in this context that the properties of endo-observers become the uncertainty's sole model criterion. The form of the uncertainty leads to a novel formulation of state space models. A diffusive term inside the endo-observer's state space model is required which drives the system in the linear and non-linear case away from the nominal vector field and thus shows some similarity to the dynamics defined through the Fokker-Planck equation (Risken, 1996; Gardiner, 1998). However, the meaning of endo-observer models and the Fokker-Planck equation dynamics are fundamentally different because the Fokker-Planck equation models the propagation of probability density functions in the exo-observer state space models when the uncertainty is given by a specific stochasticity. Endo-observer models do not include the knowledge of any kind of stochasticity.

In the linear case the endo-observer dynamics are described in form of the standard Schrödinger equation for a free particle and in the non-linear case the dynamics take the form of generalized Schrödinger equation, a multi-component equation with a ‘momentum’ term which looks the same as the one in the Schrödinger equation for Quantum Mechanics which is subject to a negative vector potential (Ballentine, 1998). A tracking model for endo-observers has been devised in Section 5.6 which is based on the fact that observers who seek a decision about the most likely future state in general tend to put more confidence in the states with higher probability.

The disadvantage of the endo-observer models is that in the linear as well as the non-linear case an initial probability distribution is required as in exo-physical state space models. Although, in either cases algorithms are being devised which allow the

extraction of the required probability density function from the data, it would be more desirable to do system identification and prediction without probability density distribution extraction as an intermediate step, because the probability density distribution already requires the assumption that either enough data is available in order to justify a probability density approximation of an initial state or to estimate the probability density function through bounds on physical variables, the limit theorem and the maximum likelihood principle. Unfortunately the author has not been able to devise such an algorithm. Further, the dynamics of an endo-observer come at a high computational cost. Partial differential equations are analytically almost intractable and numerically very difficult to solve. The examples provided in Chapter 6 do not prove or disprove the framework provided here, they merely stand as analytically solvable illustrations of a ballistic toy model which is being derived in Chapter 3. In order to prove the theory developed here beyond the arguments provided in the following chapters, all solutions of the partial differential equations introduced below and their properties would be required to be analytically checked. This is to date an open research issue and the author has not been able to contribute to the theory of partial differential equations. Required sophisticated numerical modelling for an exhaustive comparison between the dynamics of endo- and exo-observers is a research area in itself and lies outside the possible scope of this thesis. There are still a lot of open questions concerning the endo-observer models presented here, such as the uniqueness, form, and problem specific modelling of the diffusive term introduced for modelling the uncertainty in endo-observer models. A more detailed outline of possible future research issues can be found in Chapter 7.

1.3 The contributions of this thesis

This thesis is not intended to be a complete nor exhaustive exposition of endo-physical modelling techniques. The short reviews on black-box modelling techniques and ballistic missile modelling present genuine examples to illuminate the problems concerning real-life data driven and physical state space motivated modelling. It is not the aim of the thesis to develop a technique for ballistic missile model identification which is competing against well established tracking models for real-life missile defence systems. The theory developed below is a starting point for future developments in endo- and exo-observer physics relations. The ballistic model is far too immature for real applications since it lacks far too much insight into ballistic models which can only be gained through experience with modelling of real ballistic missiles and the

analysis of their trajectories. However, the physical modelling of a proper ballistic missile follows the same physical principles, *i.e.*, the model devised in Chapter 3 is good enough as a toy model to understand the principles of the theory developed here. The thesis' aim is thus to elaborate on certain specific concepts such as exo- and endo-physical state space models, and to outline the possibilities of their extension to fully applicable real-life models. This thesis includes the following new results:

1. The formalism of a ballistic missiles dynamics are reviewed, certain terminology in the literature as well as a flaw in a rigid body dynamics (Anonymous, 1982; Blakelock, 1965; Collinson, 1996; Eichblatt, E.J., Jr, 1989; Garnell, 1980) are corrected. A complete dynamical ballistic missile model for simulation purposes is introduced (see also Schilhabel (1996)).
2. The exo- and endo-physics concepts are shortly reviewed in Section 4.2 and adapted to the real-life measurement problem of physical system states. The real-life measurement issue is analysed and certain properties of real-life observers imply a concept of physical modelling which does not match with the standard physical models of observed systems. As a consequence the novel endo-physical dynamics of linear physical systems (free particle) are derived. Some of the implications of the endo-exo-observer concept have also been utilised in Schilhabel and Harris (1998d), Schilhabel and Harris (1998b), Schilhabel and Harris (1998c).
3. Based on the endo-observer concepts from Chapter 4 a novel endo-physical state space model is derived in Chapter 5. Uncertainties of real-life observers are modeled and taken into account by the model. The issue here is, that little information is available about the kind of stochasticity which enters the dynamics. (See also Schilhabel and Harris (1998d), Schilhabel and Harris (1998a), Schilhabel (1999))
4. Analytically soluble endo-observer models of the simplified ballistic model from Chapter 3 are derived for illustrations purposes in Chapter 6. (See also Schilhabel and Harris (1998a), Schilhabel (2000))

1.4 Outline of the thesis

There are seven chapters in this thesis, whereby the contents from Chapter 4 to Chapter 6 are all original and novel contributions. The concept of grey-box modelling

in Section 3.5.2 has been devised here as well since no further information concerning ballistic missile is in the public domain. Beside this introductory chapter, the remaining chapters are concerned with:

Chapter 2 Physical models and Black-Box Models

After reviewing the basic motivation of physical modelling the nomenclature of state space modelling is introduced and the reason for errors and noises sources in physical systems are listed. The basic ideas of black box modelling techniques are proposed and few typical regression techniques such as neural networks, the Kalman filter, Neuro-fuzzy systems, and wavelets are briefly introduced. The reasons why these regression techniques are unsuitable for the modelling constraints encountered here are highlighted.

Chapter 3 The ballistic missile

A thorough introduction to ballistic state space modelling is presented and the pitfalls and difficulties of aerodynamic models outlined. A toy model is derived as example for future reference. The possible approaches towards black-box and grey box modelling are established and their applicability to ballistic missiles discussed.

Chapter 4 The Endo-Observer of a Linear System

This chapter is a diversion from the main subject of ballistic missile identification and prediction. However, the concepts developed in this chapter are a pre-requisite for the subsequent chapters. The relation between exo-observers (abstract physical concepts) and endo-observers (real life observers) are discussed. Certain qualities of endo-observers are developed to a theory of endo-observer state space models of a free particle, *i.e.*, dynamics of ballistic missile which center-of-mass is moving uniformly. The endo-observer model is applied to an harmonic oscillator, an initial radial Gaussian probability density distribution and an N -point observation of a linear dynamical system.

Chapter 5 Uncertainty in Non-Linear Dynamics

The endo-observer concept from Chapter 3 is utilized for non-linear dynamics.

The generation of vector-field errors in an endo-observer model is demonstrated. A dynamical model of a difference vector-field between endo-observer (real life) vector field and nominal exo-observer (abstract, physical) vector field is developed. Similar mathematical arguments as in the case of the linear endo-observer model are employed to derive the endo-observer model of non-linear dynamical systems. A tracking endo-observer model is also devised.

Chapter 6 The endo-observer's frame of reference for a ballistic model

The toy model from Chapter 3 is revisited for the endo-observer's frame of reference to demonstrate the applicability of the endo-observer model to a real physical system.

Chapter 7 Conclusions

This chapter presents the conclusions of the thesis, together with some suggestions for future research issues. An Endo-observer model for linear and non-linear dynamical systems has been successfully developed. In the linear case the model was tested against the outcome of some typical examples. In the non-linear case the model could not be validated for the general case of observations as the simulation of the model for even the simplest non-linear functions requires the development of techniques which are outside the scope of this thesis. Future research should therefore focus on validating the non-linear endo-observer model for arbitrary non-linear vector flows inside the state space. Besides these major research issues the advantages and disadvantages of statistical state space modelling are listed against those concerning black/grey-box modelling. Issues concerning the ballistic missile model are summarized.

Chapter 2

Physical Models and Black Box Models

Forward

The fundamentals of physical modelling which lead to the concepts of states and vector flow inside the state spaces are summarized. The following motivation presents reasons for noise entering any real-life physical systems which then leads to the requirement of statistical or stochastic state space modelling. It is then argued that neither deterministic nor stochastic state space models can be employed because there is no information provided about the stochasticity, the precise vector flow, and an initial state of the non-linear dynamical systems under consideration. As alternative techniques black-box or grey-box modelling is being considered. Because the number of statistical methods is overwhelming only artificial neural networks, the Kalman filter, Neuro-fuzzy systems, and Wavelets have been depicted as representative examples of regression techniques. Because black-(grey-)box modelling requires large data sets and well known statistical properties which are not defined, it is argued that black-box modelling is unsuitable for our purposes. Because neither stochastic state space modelling nor black-box modelling seem to be an appropriate means of understanding the time series provided, it is argued that new algorithms have to be devised.

2.1 Introduction

The last chapter gave an overview about the work presented. Here, the underlying material is summarized and the corresponding conclusions drawn which motivate the

material presented in following chapters. This chapter is structured as follows. Initially a short overview about the reason of physical system modelling is given. Physical state space models are reviewed in Section 2.2, and Section 2.3 is dedicated for black-box models. In the latter section the advantages and dis-advantages of black-box modelling techniques are reviewed with respect to the task of non-linear system identification and prediction by employing a time series. It is found that neither black-box nor state space modelling are suitable for the just specified task of non-linear system identification with small number of data points. The aim of this chapter is threefold: (i) To motivate grey-box modelling as it has been devised in Chapter 3, under the assumption that enough data points are available. (ii) To highlight the difficulties concerning black-box modelling when insufficient data (*e.g.* a short time series) is given. (iii) To summarize the properties and principles of deterministic, *i.e.* physical, state space modelling.

It is argued below that neither deterministic state space modelling nor black(grey)-box modelling can be applied to non-linear system identification by utilizing time series with a small number of potentially erroneous sample points. The reason for the failure of both modelling techniques is given by the prerequisites of statistical and deterministic modelling. An alternative stochastic model within the concept of endo- and exo-observer's is thus introduced in Chapters 4 and 5. The *physical causality principle* in its form as a mathematical state space model serves as a starting point for stochastic systems modelling. The next paragraph gives a short overview of the causality principle and its applicability to physical systems.

The purpose of scientific investigation is the understanding of natural phenomena in order to predict their future behaviour. The underlying principle which underpins scientific discoveries is the *law of causality* which describes relation between *causes* and their *effects*. Since this principle is so important in science, Ebeling, Engel and Herzl (1990) distinguish between *simple causality*, *strong causality*, and *weak causality*. *Simple causality* means that the same cause leads to the same effect and is thus applicable to phenomena as encountered in classical mechanics. *Strong causality* implies that ‘similar’ causes lead to ‘similar’ effects and therefore applies to statistical and stochastic physical systems. *Weak causality* is defined for the case that ‘similar’ causes lead to very different effects, as typically happens in chaotic scenarios. The success of physical system modelling depends on the underlying system’s complexity. The disadvantage of classical physical models is, that they are generically independent

of the observation due to the level of abstraction. The observer as an analysing and interpreting element in real-life experiments is usually sought to be either eliminated through methodologies such as *gedanken experiments* or to be incorporated through noise and errors in the physical model to allow a more realistic relation between the models and factual measurements. This noise has to be included *via* the introduction of random terms into the state space model which then require analytical and numerical modelling techniques of potentially complex (partial) differential equations with problem-specific boundary conditions. Further information about physical (stochastic) modelling may be found in Scheck (1990), Hestenes (1986), Jetschke (1989), Gardiner (1998) and, Risken (1996).

Alternatively, there have been many empirical or data driven algorithms for establishing relationships between observed or measured data points. These algorithms are usually referred to as *black box modelling* since there is no prior knowledge about the underlying laws between presumed inputs and outputs of the process. The advantage of this approach is, that there exists a systematic approach towards data analysis with the aim of achieving predictions with a certain accuracy. The disadvantage of this approach is that *causality* can *never* be inferred from data alone, there are always at least *assumptions* or *arguments* about the nature of data from outside statistical analysis (Cherkassky and Mulier, 1998) which is usually based on domain knowledge. In many cases statistical modelling techniques, such as ARMA, ARIMA, RBF (Tong, 1995), even require *assumptions* about the architecture of the underlying model. (Statistical measures such as the correlation analysis do not allow the identification of deterministic causalities either as statistics may provide indications but no proof of relationships between physical parameters.) All the prerequisites mentioned above are necessary to allow any explanation or interpretation of the underlying data.

2.2 Physical state space models

[Physical state space models are exhaustively described in (Arnold 1978; Hestenes 1986; Scheck 1990).] *Physical objects* are closed systems of principally measurable variables, *i.e.*, measurable up to a certain error bound. These variables are postulated to be representable by mathematical objects which are *scalars*, *i.e.*, elements of the real numbers. The *state* of a physical object is given by the complete set of all properties of the object which relate the input-time function at any time to a unique output for all time from the instant the input-time function is given. Because all input-variables of a physical system with a finite number of physical elements can be represented in form of

a n -dimensional vector, the *state* is equivalently given by a *state vector* $\mathbf{x}(t)$ (*state variable*). Throughout this text these three definitions of a state will not be distinguished from each other. The state vector is an element of the *state space* $\mathbf{x}(t) \in \Sigma \subset \mathbb{R}^n$ which is the complete set of all possible states. The dynamics of these states is either given in the form of a discrete *map* $\mathbf{F}^\Delta(\mathbf{x}(t))$ which is a function describing the mapping from one state to the following one, or a *vector field* $\mathbf{F}(\mathbf{x}(t))$ which defines a *continuous path*, (*phase*) *flow* or, *orbit* the state follows when the continuous parameter time is altered. The *dynamical system (model)* $(\Sigma, \mathbf{F}(\bullet))$ is defined by the vector field and the state space. Physical models are assumed to be continuous dynamical systems which may in some cases be represented as discretized maps, *e.g.* *stroboscopic* data samples of the state. In fact all real-life measurements are in the ideal case states with equidistant time-lag between each successive data sample. For engineering purposes it may be desirable to distinguish within the dynamical system between the *plant*, the *observer*, and the *controller*. When an observer influences the controller such that the controller output will depend only on the output of the plant and plant's input to the observer, the dynamical system can still be represented by a *common state vector* consisting of state variables describing the plant, the controller, and the observer. In some cases the controller is just defined as a set of certain time constant *control parameters* of a dynamical system. Generally, the relation between plant, controller, and observer are non-trivial: The relation between plant and observer will be carefully analysed in Chapter 4.

In principle physical dynamical systems can be subdivided into the following properties of processes.

- *Reversible*: The state of a physical system for a future time can, in principle, be reached again.
- *Irreversible*: The state of a physical system at an arbitrary instant can never be reached again.
- *Periodic*: The state follows a periodic flow.
- *Non-periodic*: The flow is non-periodic.
- *Deterministic*: The physical system is defined by a dynamical system.
- *Non-deterministic (stochastic)*: The physical system cannot be identified by a unique state of a dynamical system.

- *(Deterministic) Chaotic:* The future state of a dynamical system is sensitively dependent on the initial state.
- *Non-chaotic:* The future state of a dynamical system is not sensitively dependent on the initial state.

When a dynamical system (*i.e.*, the state transition function $\mathbf{F}^\Delta(\bullet)$) with an initial state has been given, a following prediction is trivial. The main concern of modelling is the *identification (estimation)* of state vectors and the underlying dynamical process itself. Let us assume for the moment that a set of stroboscopically spaced state vectors exists. All that has to be done is to find a bijective function $\mathbf{F}^\Delta(\bullet)$ which maps each state to a successive state. The map has to be bijective otherwise some trajectories within the state space would exhibit branches, intersections, or it overlaps with itself which contradicts the causality principle. This also implies that the dynamics inside the state space are reversible. The dynamics in the discrete case are written as

$$\mathbf{x}_{t+1} = \mathbf{F}^{\Delta t}(\mathbf{x}_t). \quad (2.1)$$

When a set of state space vectors is such that Δt is small enough, a continuous model can be generated by ‘smoothing’ over the discrete state vectors. When the time-discrete model (2.1) can be expanded in a Taylor series $\mathbf{x}(t + \Delta t) = \mathbf{x}(t) + \mathbf{F}(\mathbf{x}(t))\Delta t + O((\Delta t)^2)$ and $O((\Delta t)^2) \rightarrow 0$ as Δt approaches zero, then a time-discrete model can be represented as a continuous flow in the state space implicitly given by a vector field $\mathbf{F}(\bullet)$ such that

$$d_t \mathbf{x} = \mathbf{F}(\mathbf{x}(t)). \quad (2.2)$$

Although Eq. (2.1) is a far more general mathematical model than the one given by the flow in Eq. (2.1), the *ordinary differential equation of autonomous systems* $d_t \mathbf{x} = \mathbf{F}(\mathbf{x})$ is considered to be the *standard form* of deterministic models, which is motivated by the fact that a great number of systems can be modelled by this equation, that higher-order differential equations and non-autonomous differential equations can be restated as a system of first-order autonomous ordinary differential equations, and because partial differential equations can be transformed into difference equations for finite approximations by the *Garlekin method*.

When the assumption of error-free state vector estimation does not hold, which is the case for any real-life physical experiment a subsequent problem of system identification has to be addressed which deals with this limitation of real-life experiments. Only a few components of a state vector may be accessible and even these may be corrupted with *random noise*. Essentially, there are three different types of noise (Eberl, 1995):

- **Measurement Noise:** The apparatus for the measurements has some intrinsic statistical errors which can in principle be minimised, but can never be eliminated.
- **System Noise:** The simplification of complex physical system by modelling generically neglects small effects of dynamical influences. These quantities can evolve their own dynamical behaviour which appears like random noise.
- **External Noise or Disturbance:** Physical Systems are in reality never closed. External effects are sought be eliminated such that a quasi closed experiment is obtained which has to cope with the remaining part of small influences.

The measurement noise as well as disturbance are generic and cannot be avoided. System noise might be reduced by taking more system parameters into account, but the model becomes more and more complex and may even become non-tractable. The only way to cope with these undesired effects is to separate the *deterministic* part of model from the *stochastic* one and utilise completely new analytical techniques for mathematical computations (Jentschke, 1989; Risken, 1996). This approach thus leads to stochastic differential equations, or probability distributions of state vectors within the state space.

2.2.1 Assumptions and Requirements

It has just been shown that classical physical modelling is concerned with identifying the state space of an underlying dynamical system. The first hypothesis therefore is that any classical physical system can be represented as a state space model. It is then assumed that the state is, up to a negligible error, accessible. If the error of a state cannot be neglected stochastic state space modelling becomes necessary. If either the state of a physical system is not *completely* measurable, or the flow inside the state space is not explicitly known, physical state space modelling can no longer be applied.

Since the task within this thesis is the identification of non-linear dynamical systems with observed sparse time series, which generally implies that neither all state components nor the vector field of a state space are accessible, this kind of modelling technique is not applicable, *i.e.*, purely data driven modelling techniques might provide sufficient means for dynamical system identification and prediction and are therefore introduced in the following section.

2.3 Black-Box modelling techniques

[Black box modelling techniques are for example introduced in (Papoulis, 1991; Tong, 1995; Cherkassky and Mulier, 1998; Beck and Schlögel, 1995; Kantz and Schreiber, 1997)]

It is worth remembering that the objective of this work is: The identification and prediction of non-linear dynamical systems with sparse time series. This means that the identification of a physical model depends mainly on a time series which is given in form of a set of measurements which, for example, have been taken from a ballistic missile. The arrangement of measurement equipment (radars) do not allow one to measure *all* components of the state vector nor are these measurements error free. An algorithm has to be developed which allows the prediction of the entire trajectory of a ballistic missile based on only few measurements. Thus there are two major application for statistical estimation, *i.e.* predictive learning (Cherkassky and Mulier, 1998). (i) *Regression*, *i.e.* estimation of an unknown continuous function from noisy data, or (ii) *classification*, *i.e.* the recognition or estimation of class decision boundaries between sets of control parameters of the ballistic missile model. Because regression assumes that there is no information available about the vector flow inside the state space, it seems to be unlikely that this methodology can provide a promising modelling tool for state space models. However, the following sections list the advantages and disadvantages of black-box modelling techniques which will be reviewed with respect to either capability.

Scientific rigour requires that the procedure leading from the measured time series of physical variables to the model interpretation is defined prior to further probabilistic analysis, as physical system modelling is generally deterministic state space modelling and the relation between statistics and classical physics is not uniquely defined within the literature (*e.g.* Papoulis (1991), Jetschke (1989)). The following scheme has been inspired by (Dowdy and Wearden, 1991; Cherkassky and Mulier, 1998).

1. *Problem statement:* The clear problem statement is, that control parameters and most state vector components of the dynamical system are not given or known. The dynamical system of for example a ballistic trajectory has to be reconstructed from a time series available.
2. *Hypothesis formulation:* Classification: The relationship between successive data points and control parameters has to be formulated. Regression: Criteria for the general shape of a trajectory in the sub-space of the state space has to be found.

3. *Experimental set-up/Data gathering*: This is a clear *observational* setting of the experiment, the probability distribution of a single estimated data point has to be determined.
4. *Data pre-processing*: This task deals with the selection and transformation of data before it is processed further.
5. *Model estimation*: For generating models with predictive accuracy (so called *generalization* capability).
6. *Model interpretation/Conclusion*: Interpretation of models in terms of trajectories.

The following modelling approaches consider only Item 5–6 of the above list, whilst Item 4 will be dealt with in Chapter 3 where a very carefully assessed pre-processing procedure will be introduced.

The most general approach of black-box modelling allows the extraction of statistical information from any set of data points. That is why the methodologies developed within the framework of black-box modelling have been so successful when applied to a wide range of real-life systems. There are many different approaches (Cherkassky and Mulier, 1998) which are all based on a few similar principles. Black-box modelling has been exhaustively treated in the literature (see *e.g.* (Papoulis, 1991; Cherkassky and Mulier, 1998)), and the next section provides short but sufficient overview about the methodology of black box modelling techniques available today. However, as all models are based on few common features it will suffice to introduce four prototypical models to evaluate their advantages and disadvantages.

2.3.1 Regression techniques

This section summarizes the principles of some of the most common techniques for the estimation of continuous-valued functions from samples—the regression technique. The regression technique approximates a given a time series by a set of functions, whereby this approximation is parameterised in form of a weighted superposition of these basis functions. Let us assume there is a phase flow $\mathbf{f}(\mathbf{x}_0) = \int_{t_0}^t dt' \mathbf{F}(\mathbf{x}(t'))$ approximated by

$$\mathbf{f}_m(\mathbf{x}_0, \mathbf{w}, \mathbf{v}) = \sum_{i=1}^m w_i \mathbf{g}_i(\mathbf{x}_0, \mathbf{v}) + w_0 \quad (2.3)$$

with \mathbf{w} adjustable coefficients (weights) and \mathbf{v} adjustable function parameters depending on the given time series, and $\mathbf{g}_i(\mathbf{x}_0, \mathbf{v})$ as a basis functions. When the statistical model allows the value of \mathbf{v} to be changed depending on the data it is called adaptive, otherwise predetermined or fixed. The number of terms m can be determined following the method suggested by (Moody, 1991; Murata, Yoshizawa and Amari, 1991). A slightly different approach is used by so-called *kernel methods*, where a set of kernel functions $K_i(\mathbf{x}_0, \mathbf{x}_{0_i})$ is applied to represent the trajectory of a model as the weighted combination of the models response values y_i , such that

$$\mathbf{f}(\mathbf{x}_0) = \sum_{i=1}^{m'} K_i(\mathbf{x}_0, \mathbf{x}_{0_i}) y_i. \quad (2.4)$$

\mathbf{x}_{0_i} is the position of the centre of the kernel function inside the state space. As with basis functions (2.3), there are adaptive and fixed kernel functions. A very good review on black box modelling techniques for reconstructed state space models can also be found in ?).

In the following sections various methods will be classified with respect to the above two regression methods.

I.) Neural Networks

[For an overview of Neural networks see (Arbib, 1995)] In recent years there has been an enormous increase of Neural network applications. The general claim states, that they possess adaptability properties similar to those found in a mammalian brain. Despite all efforts the capabilities of neural networks in technical applications fall well short of expectations. The following section summarizes why neural networks still cannot provide the answers required for the identification and prediction of non-linear dynamical systems in the state space.

Principles. Neural networks have been inspired by the biological metaphor of the interconnecting neurons inside the brain. The necessary simplifications lead to mathematical models which very much have the same appearance as Eq. (2.3). There is a huge variety of different neural networks (NN). However, in this context where the data is of statistical nature, only statistical learning in artificial neural networks can be employed. For example radial function networks (Lowe, 1995), linear networks with arbitrary basis functions such as splines as basis functions (Brown and Harris, 1994), Boltzmann machines (Aarts and Korst, 1995), wavelet networks (synonymous

for wavelet representation see further below). All these methods map an input vector \mathbf{x} to an output vector $\mathbf{f}(\mathbf{x})$. In many cases the input and output of a NN are defined by weighted interconnections between input knots (vector) and output knots (vector) (Brown and Harris, 1994; Bishop, 1995). In contrast the Multi-Perceptron weighs the input space first and then creates the output, as does the radial basis function network. More complicated NN are also possible where multi-layers of NN knots are interconnected. In analogy with biological NN the interconnections represent the axons and the knots the neurons found in the brain. The crucial fact though is, that despite all the efforts of modelling increasingly advanced artificial NN the training relies on statistical methods, *e.g.* (Brown and Harris, 1994; Bishop, 1995), or even statistics borrowed from macro-canonical thermodynamics (Bishop, 1995). Since real NN are still not very well understood (Haykin, 1999), mathematical methods of classical statistics have to be employed to put artificial NN for statistical data on a scientific footing. But because statistical mathematics for analysing and training of NN has to be utilized the question arises what contribution NN could provide to enlighten the relationship between data points inside a time series. As an example consider Bayesian neural networks and Singular Value (SV) neural networks. Bayesian neural networks (Pearl, 1995) are a graphical representation of causal relationships in which Baye's rule of inference is employed. Singular Value Neural networks (Bourlard and Kamp, 1988) are for example multiperceptrons which have been shown to evolve weights that in the optimal case are identical to the singular value decomposition. Other NN are trained utilizing Baye's rule and statistics which originates from the maximum entropy principle (Jaynes, 1957) as it has been applied within the framework of statistical physics and can be easily seen in any student textbook such as Schrödgel (1989). As it is evident from the argumentation in (Thodberg, 1996; Haykin, 1999) the theoretical formalism is outside any neural network concepts, *i.e.*, any regression technique which utilises the partition function incorporates the properties of a Bayesian algorithm. There exists a huge variety of regression techniques, among them the pure probabilistic framework and the not so well understood neural networks concept which is so far only justifiable and theoretically tractable through Bayesian statistics and information theory concepts. The question arises which of either concepts should be chosen for explaining and solving dynamical system identification. Since the Bayesian statistics framework in conjunction with the information theoretical concept is chosen to explain neural network capabilities and neural networks seem to offer little more than these statistics, it appears advisable to utilize these statistics given above for the modelling purposes

in the first place.

Advantages. The advantages of artificial neural networks are that they are motivated by real-life complex systems (brains) which exhibit enormous capabilities of pattern recognition, data classification etc.

Disadvantages. The clear disadvantages of artificial neural networks are that they are far from the original aim of incorporating real-life NN's (brain's) capabilities. The relatively simple models being analysed and understood so far, do not differ significantly from any standard statistical models as found for example in (Jaynes, 1957) because the information measure of Shannon, the modified information measure by Akaike, or the trans-information have to be utilized in a statistical framework. The factual overlap is unfortunately not easy to detect due to the difference of language within the NN and statistician communities (Cherkassky and Mulier, 1998).

Conclusion. The employment of classical statistical methods which may also be found in thermodynamics (Schlögel, 1989; Beck and Schrödinger, 1995) and which were developed in the late 50s has little changed over the last decades. Cherkassky and Mulier (1998) argue that the framework of neural networks has only little to offer to a modeller which seeks modelling advantages over classical statistical methods.

II.) The Kalman Filter

The Kalman filter (Kalman, 1960; Kalman and Bucy, 1960; Kalman, 1963; Chui and Chen, 1999) considers deterministic state space models with some additive noise as a dynamical system. The Kalman filter was originally developed for linear state space dynamics with additive Gaussian white noise. The *extended Kalman filter* allows the application of the filter to non-linear systems by utilizing the linear Taylor approximation to non-linear vector flows. This filter, however, is sub-optimal in its performance. The *augmented Kalman filter* includes additive coloured noise in its dynamics by superposing white noise, such that any kind of coloured noise can be generated. The most general filter within this filter class is the *augmented extended Kalman filter*.

Principles. The time continuous or discrete state space formulation of the augmented extended Kalman filter can be written as a set of differential or difference equations

including an equation which determines the observation at an instant and the difference equation which generates the coloured noise for the state and the observer. A filter algorithm as for example given in the (Chui and Chen, 1999) then allows the extraction of a best estimate for a future state (prediction) or the estimation of the system's parameters (system identification). It has been demonstrated that the Kalman filter is nothing but a maximal information, *i.e.*, minimal entropy, preserving filter and derives from the first statistical principles mentioned above in the context of Neural networks.

Advantages. The Kalman filter is a very successful algorithm for real-time applications where the state space models and noises are explicitly given. The underlying theory is sound and the model is well established when prior knowledge about the state dynamics and noise characteristics is provided.

Disadvantages. The algorithm considers only the dynamics of a ‘best’ estimate whether the vector field inside the state space is linear, non-linear, or the noise is Gaussian white, coloured. The drawback therefore is, that the Kalman filter—apart from few linear cases—can generally not provide information about the probability density function inside the state space which quantifies the propensity of finding a system in a particular state. This kind of information can be crucial because even Gaussian distributions do not necessarily stay Gaussian as general non-linear dynamics evolve. Indeed, the probability density function can easily evolve into a distribution with many local minima and a time-dependent variance. This kind of information may become very significant and important, especially when the expectation value of a probability density function is not identical or close to the global maximum of the probability density function. The other disadvantage of Kalman filters is that the algorithm does not allow an estimation of a non-linear dynamical system itself, *i.e.*, the Kalman filter does not support the reconstruction of an entire state space model due to the observation of a subset of state variables.

III.) Neuro-fuzzy systems

Initially this thesis was dealing with the “Intelligent Estimation of the State Space by Neurofuzzy Systems” when modelling problems emerged (Schilhabel and Wu, 1997). In order to develop a scientific argument towards the applicability of such a method the concept of neurofuzzy systems has to be reviewed first.

Principles. Neurofuzzy systems seek to combine the benefits of two concepts, the data driven good generalization of artificial neural-networks and the interpretability of fuzzy rules in terms of human thinking (Brown and Harris, 1994). In short, it is hoped, that on the one-hand a system modeller uses his prior “knowledge” about the underlying dynamical system to initialise a set of fuzzy-rules and that on the other-hand a neural network takes over the job afterwards and optimises these fuzzy-rules with respect to a cost function borrowed from statistics. It turns out that neurofuzzy systems often use piecewise linear functions as fuzzy sets, B-splines of order two, although splines of higher order or completely different functions (*e.g.* Berzin-Bernstein or Gaussian polynomials) can also be used. The idea of the algorithm is as follows. Either an expert decides about the fuzzy rules, *i.e.*, selects the number fuzzy rules, the number and position of fuzzy sets for each rule, or, if this approach is too complex, a so-called construction rule method is applied which chooses the fuzzy set by employing a measure of information content such as the one derived by Shannon or Akaike. In either case statistical learning methods known from information theory (Jaynes, 1957) are applied to the fuzzy sets to find or optimise the fuzzy rules from some training data. These fuzzy rules then define the weight or confidence a modeller has in a particular system represented by these fuzzy rules. Adaptive basis function networks may even change the basis functions in order to learn the fuzzy-rules (Brown and Harris, 1994). As these authors remark there is a direct correspondence between neurofuzzy system and for example radial-basis-function networks.

Closer investigation reveals immediately that in fact neurofuzzy systems are identical to the superposition given in Eq. (2.3) with the only difference that \mathbf{g}_i are considered to have a interpretative meaning for an expert.

This argumentation has several flaws (*e.g.* (Cherkassky and Mulier, 1998)). It is not clear where these fuzzy-sets really come from. Why should a modeller decide to choose for example piecewise linear membership functions as they have been applied by Doyle (1997), Bossley (1997), Brown and Harris (1994)? What does the support of a membership function represent? How does the shape of a membership function effect the model? How does a modeller decide how many membership functions to employ and what shape? How can physical knowledge, as presented in Chapter 3, be translated into membership functions? It is not clear at all when the expert knowledge is so valuable, why it should be optimised? Indeed closer investigation revealed that the definition of fuzzy sets is everything but trivial as the performance of the modelled systems depends sensitively on their choice. Consider the following two examples. The fuzzy representation of a submarine model as utilised in Bossley (1997) is good

enough for a simple short one-time-step-ahead prediction. A controller which has been attempted for the same submarine model could never be stabilized (Mills, 1995; Mills and Harris, 1995). When the fuzzy construction rule/method as for example devised by Brown and Harris (1994), and Wu and Harris (1997) was applied to the Lorenz attractor, the single- and multi- time-step-ahead prediction performed much worse than the Lyapunov exponent allowed (Wu and Schilhabel, 1997; Schilhabel and Wu, 1997). Similar stability problems occurred when neurofuzzy systems were utilised in conjunction with the Institute for Sound & Vibration Research group to brake squeal modelling (Feraday, 1998).

The examples mentioned above are only few of the modelling attempts which have been difficult. The principal concept of neurofuzzy systems is an interesting one: Modelling of physical systems by inclusion of modellers experiences. However, objective knowledge as for example defined by Sir Popper (1972) requires a certain rigour in the argumentation and a particular algorithm which ensures that theories can be put on an objective footing. Neurofuzzy system have been successfully applied in a few cases when the framework of statistics and information theory were employed (Doyle, 1997; Bossley, 1997). For a great majority of non-linear system modelling there does not seem to exist a rigorous framework which formulates a construction rule outside pure statistical modelling that can objectively be tested as experiments revealed (*e.g.* (Feraday, 1998; Wu and Harris, 1997; Schilhabel and Wu, 1997; Wu and Schilhabel, 1997)). Cherkassky and Mulier (1998) conclude that neurofuzzy system are nothing but heuristics. There is a list of questions concerning the rigour of continuous membership functions, the construction of fuzzy sets, etc. As long these questions are not answered prior to any applications it is unclear what neurofuzzy systems have to offer apart from standard statistical modelling techniques and an intriguing intention to perform system modelling beyond classical statistics (Cherkassky and Mulier, 1998). In consideration of the fact that there are too many difficulties arising in combination with neurofuzzy systems (Feraday, 1998; Wu and Harris, 1997; Schilhabel and Wu, 1997; Wu and Schilhabel, 1997) and the clear indication in the statistical literature about the non-applicability of neuro-fuzzy systems Cherkassky and Mulier (1998) to complex system it was decided to discard this framework. The following three paragraphs succinctly summarize the above findings and add few more indications about the usability of neurofuzzy systems.

Advantages. A modeller may be more confident to make some guesses about a particular form of a non-linear function. For simplistic models there may be a

one-to-one correspondence between fuzzy sets and statistical flow in the state space.

Disadvantages. The major disadvantage is that an expert may be lead to believe that the algorithm is working fine because the verification on one particular data set lead to ‘good’ results. However, there is, due to the lack rigour, no criterion beyond statistic models such as validation theory which may help to decide whether the model may work or fail in general*. When neurofuzzy systems are being employed as purely statistical models, generating the B-spline functions can be extremely costly†, such that a real-time application may become non-viable. Although few cases may exist where B-splines are comparatively superior to other methodologies it should be clear that an approximating analytic function which is identical with the underlying system is the most efficient model representation available. It should be mentioned additionally that B-splines of order two are linked to so-called Haar-wavelets. When a vector field is represented by a superposition of Haar-functions then their integral is identical to B-splines of order two. As is well known in combination with wavelets (see also further below) Haar-wavelets are not often used due to their bad convergence properties (Daubechies, 1992).

Conclusion. From a scientific point of view neurofuzzy networks only offer the same qualitative analysis tools as classical statistical methods (Cherkassky and Mulier, 1998). Because the framework does not seem to be able to offer any answers for non-linear system modelling but it poses urgent questions to which the author could not find any answers this method was rejected for the following analysis of non-linear state space models.

IV.) Wavelets

Wavelets are scaled single functions in the form of a short wave. The wavelet transform can be viewed as a projection of functions, data or operators onto a wavelet. Because each wavelet has a specific time-frequency resolution, the component of a wavelet transform quantifies the contribution of functions, data or operators to certain

*It is important to realize that statistical modelling is independent of the appearance of neurofuzzy systems. It is the statistics of input data which decides about neurofuzzy system and not the distribution of fuzzy sets.

†The mathematical properties of B-spline functions are easy to understand, as they provide means of linear superposition of (generally) non-linear functions. However, the problem lies with the understanding of specific shapes of B-spline functions with respect to the rule base interpretation.

frequency contents at a certain time (Chui, 1992; Daubechies, 1992; Mallat, 1998). There are many different kind of (continuous/discrete) wavelets available. The state space considered here is a subset of \mathbb{R}^n which requires a continuous wavelet transform.

Principles. First, a basis wavelet is selected, which is a function with certain mathematical properties. This basis wavelet can be dilated and translated. As with the Fourier transform, the continuous wavelet transform is an integral transform with dilation and translation parameter as new variables. The inverse wavelet transform, which is a weighted superposition of all wavelets, leads then to the original function, data or operator. In contrast to neurofuzzy systems it is not claimed that the wavelet or its weight has a specific meaning or interpretation. As with other basis function techniques the centre, dilation and translation parameters are well defined and the properties of certain basis wavelets are with respect to their approximation capabilities well analysed (Daubechies, 1992; Chui, 1992; Holschneider, 1995).

Advantages. The wavelet is an oscillatory function of which many physical systems consist of. There are many statistical motivations for use of wavelets in signal processing (Mallat, 1998). Because there is no computationally expensive algorithm for finding the wavelet function itself algorithms such as in Donoho et al. (2001), Majid (2001) are capable of computing the wavelet representation of several thousand data points within few seconds. In comparison, the implementation of an algorithm as provided by (Brown and Harris, 1994) may take hours if not days to complete as the shape of the basis functions needs to be computed. Wavelets have been successfully applied to many practical tasks and real life experiments as for example in signal processing/compression (Holschneider, 1995; Chui, 1992), or in physical wavelet models (Kaiser, 1999), etc.

Disadvantages. Wavelets are, however, generally not applicable to state space models and the reconstruction of vector fields. General physical knowledge cannot be incorporated directly and the transform can be computationally costly for high-dimensional state spaces.

Conclusion. Wavelets provide very powerful statistical models for extracting frequency and space coordinate information as well as oscillatory properties out of a time series. However, it is not at all clear how these wavelets may provide physical insight beyond this property,

V.) Non-linear statistics

For completeness reason another analytical tool for statistical data analysis has to be mentioned here. The field of non-linear statistics which emerged in combination with chaos theory (Beck and Schlögel, 1995). The ideas and principles of non-linear statistics are not going to be introduced here since these models will be more closely examined with respect to a ballistic missile trajectory in Section 3.5. For reference the advantages and disadvantages of non-linear statistics are given below.

Advantages. Non-linear statistical methods can provide qualitative information about a non-linear dynamical systems behaviour even when the state is not explicitly given. A state space reconstruction algorithm exists which relies on the implementation of these non-linear statistics.

Disadvantages. Non-linear statistics are of only limited use for noisy time series. Large data sets are required to gain statistically significant information.

Conclusion. Methodologies are very well founded for data-rich time series with no or only very little noise. The theory does not provide sufficient measures in order to allow a clear decision if the time series is sufficient for the algorithms which allow the computations of the characteristic dynamical system quantities.

2.3.2 Applicability of Black-box models

The last section introduced artificial neural-networks, the Kalman filter, Neurofuzzy systems, and wavelets as black-box models and mentioned non-linear statistics as an alternative black-box technique which will be closely examined in Section 3.5.2. It is essential to decide whether these modelling techniques are applicable to the main task (stated on page 1) or not. All four black-box models given above have one feature in common, they must make assumptions about the non-linear systems' noise in order to apply the regression technique introduced before. Additionally, there are always statistical hyper-parameters involved which determine the smoothness of the approximating function $f_m(\mathbf{x}_0)$. The non-linear statistics mentioned last, provides some means of characterising the underlying dynamics which may correspond to the

given time series. Neither of the methods defined above allows an estimate about the evolution of probability densities inside the state space. Note, it is not sufficient to gain a best estimate to an arbitrarily imposed statistical criterion for a statistical algorithm for physical model selection. Scientific rigour requires that additional information is provided about implications on physical system selection when a purely statistical selection criterion is imposed. For example a model which provided a good estimate/prediction in one problem domain (Wu and Harris, 1997) does not necessarily provide a good estimation/prediction in another problem domain (Wu and Schilhabel, 1997). This implies that prior to statistical modelling techniques, which employ the mean and the variance between estimate and system output, information needs to be gained about the system which provides measures for the validity of a certain statistical model/algorithm. Besides these rather genuine modelling issues of statistical models, the main drawback is, that besides these very restricting assumptions about the qualitative stochastic behaviour of dynamical systems, the number of data points must grow exponentially with every added dimension to the state space in order to enable statistically significant answers.

The most suitable approach among the ones listed above towards identification and prediction of a physical system seems still to be the Kalman filter, since it allows incorporation of physical knowledge about the underlying deterministic state space models. Due to the statistical drawbacks, a stochastic differential equation which models entire probability density functions inside the state space is still significantly more powerful than a Kalman filter. Even when stochastic models such as the Fokker-Planck equation cannot analytically be solved, numerical algorithms with proven accuracy still provide predictions of probability densities in the state space with proven error bounds (Langtangen, 1999).

2.4 Conclusion

Deterministic and stochastic physical modelling has been introduced and its properties summarized with respect to its applicability to non-linear dynamical systems identification and prediction. These models were found to be unsuitable for sparse time series modelling, because there is no unique algorithm to identify this time series data with a physical state and the state space models may not explicitly be available. Black-box models are data driven techniques which have to rely on assumptions which are impossible to relate to the physical implications on an underlying state space model and the required number of data points may outstrip the ones given through the sparse

time series. The two models which may be closest to the desired properties are on the one-hand the Kalman filter and on the other-hand stochastic differential equations. If the objectives within the task are not relaxed, no method mentioned so far is applicable. The dilemma seems to be approachable only through thorough reinvestigation of what kind of physical knowledge is really available. The next Chapter explores the problems concerning ballistic missile modelling and the feasibilities of incorporating physical knowledge into statistical techniques.

Chapter 3

Ballistic Missiles

Forward

The general aim of this thesis is to develop the basis of algorithms which enable the prediction of a ballistic missile's trajectory in a three-dimensional spatial co-ordinate system when only a sparse time series is available. As it has been argued in chapter 2 non-linear system approximation can be accomplished either by black-box regression techniques or via the analysis of the state space model of the underlying physical system. Black-box and grey-box modelling (Juditsky et al. 1995; Sjöberg et al. 1995) techniques require a sufficiently large amount of rich data. One regression technique estimates an approximating function which connects data points in a reconstructed state space, whereas an alternative regression technique parameterises a class of state space trajectories which are estimated by employing the given time series. Whichever black-box regression analysis is selected, it is evident that a basic physical understanding of a ballistic body is necessary. Grey-box and white-box modelling require an even deeper insight into the physics of the ballistic missile. Later chapters in this thesis employ models which are based on the precise form of the vector flow inside the state space. It now becomes clear why this chapter first introduces the basic concepts of a ballistic missile before the rigid body dynamics with the most general forces on an arbitrary airframe can be presented. Due to the limitation of access to real-life data of ballistic missiles, this chapter can only present a toy model for demonstration purposes. However, the framework given here could easily be extended to realistic ballistic state space models. Typical properties of the discussed flow inside the state space then would also apply to a real-life framework as is it will be established for grey-box modelling.

3.1 Principles of ballistic missile modelling

Before a ballistic missile can be analysed in any detail a few principles should be explained. The flight of a ballistic missile can be subdivided into three different phases. A missile which covers a distance of about 600km is accelerated, during the *boost phase*, to its maximal velocity of about Mach 6. Additionally a body spin about the symmetry axis is applied to compensate for a-symmetric propulsion forces. The boost phase for this type of missile lasts about 60-90 seconds, during which the missile covers a distance of just 40-60km. After the boost phase is completed the missile enters the *sustain phase*. Missiles with more sophisticated control algorithms enter the *terminal phase* after the sustain phase during which a missile re-ignites its engines and adjusts its final course for the pre-programmed target. The boost phase is the most critical phase for the overall behaviour of a ballistic missile because once the initial physical variables for the sustain phase are defined, the body is left to pure aerodynamic and gravitational influences for the entire sustain phase. During the boost phase the ideal missile maintains a stationary flow of fuel that leaves the boundaries of the air frame with constant velocity and has a constant burning rate. Disturbances as well as aerodynamic forces are compensated for by thrust vector control. The purpose of the boost phase is the acceleration of the missile to a certain velocity, spin and spatial coordinate. The boost takes only few seconds and is accomplished when the velocity reaches its nominal boost velocity and the spin gains its designated magnitude. However, because the boost phase is very short, it is of no significance for flight path interferences. The algorithms for thrust vector control are therefore of limited interest here and will be omitted in the following sections. The precise physical variables of the missile during the boost phase have little significance for its future behaviour and will not be considered here. The initial velocity and spatial coordinate of the missile at the beginning of the sustain phase are the most significant physical variables since they precisely determine the entire missile trajectory for most of the remaining time of flight when the aerodynamic forces are defined. The body of the ballistic missile changes very little under aerodynamic forces and is assumed to be invariant throughout this thesis. The dynamical system consisting of a ballistic missile model is an *open* system due to the loss of mass, the (non-invariant) gravitational forces, and the aerodynamic influences. The precise forms of physical influences on a real-life ballistic missile cannot be modelled due to lack of insight. Sensible approximations have to separate negligible effects from significant effects. The aim of this chapter is to be able to separate specific dynamics with long-term influences on a ballistic body from those which may have only short term effects on the missile's behaviour. This approach may

provide restrictions and simplifications for following prediction techniques in form of the dimensionality of the state space and some bounds on the values of the set of physical parameters. The extraction of the most significant dynamics from the total dynamics is referred to as filtering and is a pre-requisite for grey-box modelling. Grey-box modelling is black-box modelling of pre-processed data. The reason for filtering the dynamics in a state space is because frequently grey-box modelling of dynamical systems turns out to be more successful than black-box modelling. When the measurements of the dynamics of a ballistic missile are filtered the net dynamics may prove to show certain trends or a stochasticity which can be mathematically described far more easily than by modelling the data as it is measured.

The following sections motivate and outline the modelling of real-life ballistic missiles. Section 3.2 introduces the ideal ballistic missile as a point mass, and in Section 3.3 the physics of a three-dimensional extended ballistic body are discussed. The physical modelling is completed in Section 3.4 with the aerodynamic influences on an air frame. Section 3.5 introduces an approach to grey-box modelling. The applicability of grey-box modelling to the sparse time series is discussed.

3.2 The ballistic missile as a point mass

The ideal model of a ballistic body is a point mass with an initial velocity and which is accelerated by a constant gravitational force. Aerodynamic interactions between an air-frame and the atmosphere are ignored in the ideal case. The trajectory of such a point mass is a parabola with a well known parameterisation and precise impact coordinates (Hestenes, 1986).

These ideal properties do not apply in practice; the gravitation changes under coordinate transformations of a point mass with respect to the earth, real live missiles are self-propelling bodies which burn fuel and therefore change their mass, non-rotation invariance of missile bodies lead to the change of their aerodynamic properties with respect to rotations of the air-frame about the relative wind vector. The air-frame's aerodynamics generally change with respect to the magnitude of the relative wind velocity. The earth is not an inertial system, and the air density changes with height. In summary, the modelling of rockets with realistic flight properties is very complex due to the vast amount of physical influences. The following section summarizes necessary definitions of arbitrary particle dynamics, because some literature on aircraft dynamics (Anonymous 1982; Eichblatt, E.J., Jr 1989) seem to mix up certain physical concepts which may lead to misleading interpretations of

the corresponding variables etc. A more detailed treatment may be found in Landau and Lifshitz (1960), Arnold (1978), Hestenes (1986), Scheck (1990), Thornton and Marion (1995)

A *rigid displacement* is an *a priori* hypothesized physical transformation between pair-wise different *reference bodies*, which enables any observer to compare arbitrary length measures with each other and must not be mistaken for a displacement of a *rigid body*. Relations between physical particles at a time t are described by a *position vector* \mathbf{r} with respect to a pre-specified *reference body* or *frame of reference*. The set of all \mathbf{r} , $\{\mathbf{r}\}$, represents an Euclidean space, *i.e.*, the distance between every pair of points in the space is invariant. It has been proved (Arnold, 1978; Hestenes, 1986) that all isometric ($\|\bullet\|_2^2$) displacements are so called *rigid displacements*, which are generated by the *continuous Euclidean group* consisting of just a *translation* and a *rotation*. A *rigid body* is defined to be a set of point masses, whereby any norm of vector differences between these coordinates are constant for all time. The rigid displacement for a coordinate \mathbf{r} at time t in the un-primed frame of reference leads to a change of the coordinate vector which is related the primed frame of reference such that

$$\mathbf{r} = \mathcal{R}'_t \mathbf{r}' + \mathbf{r}_0 \quad (3.1)$$

The velocity and acceleration of any point in either coordinate systems is thus trans-

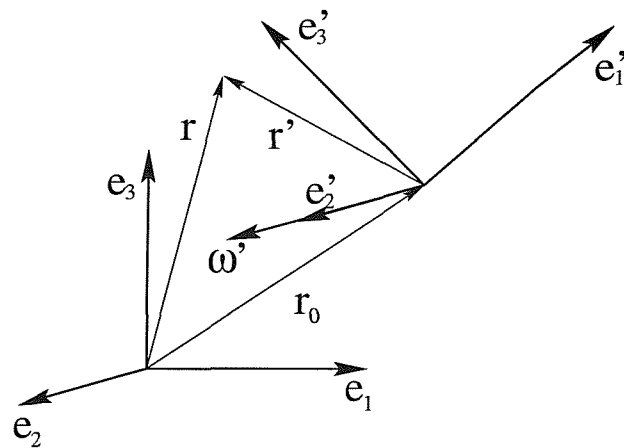


Figure 3.1: The primed frame of reference is supposed to be fixed with respect to a rigid body. The figure shows the case where the primed coordinate system is rotated about the e_2 -axis of the un-primed frame of reference.

formed according to

$$\dot{\mathbf{r}} = \dot{\mathcal{R}}'_t \mathbf{r}' + \mathcal{R}'_t \dot{\mathbf{r}}' + \dot{\mathbf{r}}_0 \quad (3.2)$$

$$= \mathcal{R}'_t (\omega' \times \mathbf{r}' + \dot{\mathbf{r}}') + \dot{\mathbf{r}}_0$$

$$\ddot{\mathbf{r}} = \ddot{\mathcal{R}}'_t \mathbf{r}' + 2\dot{\mathcal{R}}'_t \dot{\mathbf{r}}' + \mathcal{R}'_t \ddot{\mathbf{r}}' + \ddot{\mathbf{r}}_0 \quad (3.3)$$

$$= \mathcal{R}'_t (\dot{\mathbf{r}}' + 2\omega' \times \dot{\mathbf{r}}' + \omega' \times (\omega' \times \mathbf{r}') + \dot{\omega}' \times \mathbf{r}') + \ddot{\mathbf{r}}_0,$$

whereby $\dot{\mathcal{R}}'_t \mathbf{r}' := \omega' \times \mathbf{r}'$ is the velocity of a particle at position \mathbf{r}' due to the rotation about the origin of the primed frame, and ω' is the *rotational velocity* and not the angular velocity. The distinction between either definitions is very significant since the term angular velocity may suggest an angular momentum conservation which would imply that the vector ω' were always constant over time. This is not true as it is known that ω' itself may precess about the angular momentum. An *inertial frame* preserves the form of Newton's law:

$$m\ddot{\mathbf{r}} = \mathbf{f}, \quad (3.4)$$

or equivalently, the acceleration of a free particle is $\ddot{\mathbf{r}} = \mathbf{0}$. Note, that each any mechanical formalism requires an inertial frame of reference which fulfils the above conditions. To prove this substitute the RHS of Equ. 3.4 into Equ. 3.4 and rearrange the result such that

$$m\ddot{\mathbf{r}}' = \mathcal{R}'_t^{-1} \mathbf{f} - [\bullet] = \mathbf{f}'_{net}.$$

Which concludes the proof. All forces in $[\bullet]$ are called *fictitious forces* to distinguish them from the real (field) force $\mathbf{f}' = \mathcal{R}'_t^{-1} \mathbf{f}$. However, due to their physical significance most terms in Eq. (3.4) have specific names. The *inertial force of centre of mass* is given by $m\ddot{\mathbf{r}}_0$, the *inertial force of rotation* is defined as $m\dot{\omega}' \times \mathbf{r}'$, the *coriolis force* is given by $-2m\omega' \times \dot{\mathbf{r}}'$, and depending on whether the sign is positive or negative, the expression $\pm m\omega' \times (\omega' \times \mathbf{r}')$ is called the *centripetal* or *centrifugal force* respectively. The principle of centre-of-mass motion proves that arbitrary external forces applied to an (in)finite number of particles act as if the sum of all external forces applies to the sum of all masses concentrated at the centre of mass (CM) of all those particles. This principle applies in all cases, which means that there does not hold any constraints such as constant distances between particles. The reference frames are therefore selected such that the origin is found in the *centre of mass* rather the *centre of gravity*. The difference vector may be in most cases negligible, but it becomes crucial in the case of celestial mechanics or the mechanics of satellites, where a difference vector between the *centre of gravity* and the *centre of mass* leads to a non-negligible torque about the

centre of mass inside the body which effects the rotational motion. The descriptive variables of a centre of mass bodies, are for translational motions the mass $\sum_i m_i$ of the whole body, the position vector of the centre of mass $\mathbf{r}_{CM} = \sum_j m_j \mathbf{r}_j / (\sum_i m_i)$, its velocity $\dot{\mathbf{r}}_{CM}$, the momentum $\mathbf{p} = m \dot{\mathbf{r}}_{CM}$, the kinetic translational energy $E_{kin} = \mathbf{p}^2 / (2m)$ and the relation between change of momentum and all applied forces $\sum_i f_i$ for constant mass is given by Newton's law $\dot{\mathbf{p}} = m \ddot{\mathbf{r}}_{CM} = \sum_i f_i$. For all coordinate systems that have their origin for all time in the centre of mass (which is only equal to the centre of gravity for homogeneous gravitational field) it follows immediately that

$$\mathbf{f} = m \mathcal{R}_t^{-1} \ddot{\mathbf{r}}_0. \quad (3.5)$$

This equation leads to two essential implications: (i) The transformation of forces between inertial frame of reference and rotating frame of reference is described by rotation operators. (ii) Eq. (3.5) is incompatible with the dynamics given in the literature as for example in Blakelock (1965), Garnell (1980), Anonymous (1982), Eichblatt, E.J., Jr (1989), Collinson (1996). Each force applied to the centre of mass in the rotated coordinate system is equal to the back transformed force in coordinates of the inertial system, *i.e.* the centre of mass of our rigid body can be treated like a inertial system as long as the relation between both vector coordinates \mathcal{R}_t^{-1} is given. Because the centre of mass is a singular vector, the measurement instrument at point \mathbf{r}'_i outside a body's centre of mass mounted on a rigid frame will measure a force, which depends on a shift about \mathbf{r}'_{CM} of the CM due to burning of fuel, that equals to

$$\mathbf{f}' := m_i \left(\ddot{\mathbf{r}}'_{CM} + 2\omega' \times \dot{\mathbf{r}}'_{CM} + \omega' \times (\omega' \times \mathbf{r}'_i) + \dot{\omega}' \times \mathbf{r}'_i + \mathcal{R}'_t^{-1} \ddot{\mathbf{r}}_0 \right). \quad (3.6)$$

This equation is the most general description of a force measurement device mounted on a ballistic body. In most cases all terms but $\mathcal{R}'_t^{-1} \ddot{\mathbf{r}}_0$ are neglected. Equation (3.5) is essential here because other literature include centrifugal like forces which don't occur in this force equation as it has been shown above. Standard literature on flight control *e.g.* (Blakelock, 1965; Garnell, 1980; Anonymous, 1982; Eichblatt, E.J., Jr, 1989; Collinson, 1996) employs the identity

$$d_t \mathbf{V} = \dot{\mathbf{V}} + \omega' \times \mathbf{V} \quad (3.7)$$

which is mathematically correct if there is a distinction between the changing length of the velocity vector and the rotation of its unit vector fixed with missile's coordinate system. Accelerometers mounted on an air-frame of a rocket are today either spring masses, piezo-electrics, or force-balance accelerometers which measure \mathbf{f}' of Equ. (3.6). Note that the centrifugal force there has nothing to do with $\omega' \times \mathbf{V}$ in

Equ. (3.7). For centre of mass dynamics no centrifugal forces exist. Equation (3.7) presumably stems from the case when accelerations were measured by estimation of rotation and change of air velocity displayed by a mercury column of a Pitot tube. Modern accelerometers are not equipped to indicate differences between fictitious and field forces.

It has just been demonstrated that the velocity equation (3.7) for a ballistic missile is wrong in the context of modern acceleration measurements. The inconsistency stems from the simple fact that velocities are concepts which are preserved under transformations between inertial frames of references. Velocity measurements on an air-frame are carried out through the Pitot tube which measures the air-flow in a non-inertial frame of reference. As it is evident from the discussion above acceleration measurements through change of velocity are not equal to acceleration measurements by force estimations. This important distinction has not been appreciated in the literature (Blakelock, 1965; Garnell, 1980; Anonymous, 1982; Eichblatt, E.J., Jr, 1989; Collinson, 1996).

The important result here is, that if all forces on a centre-of-mass body are known, the goal of modelling the trajectory of a ballistic missile has been accomplished. The problem, however, is that these forces consist of a non-homogeneous gravitational force which may apply a torque to the body, and, mainly, aerodynamical forces which depend on the position of an air-frame towards the relative wind direction. This means, that it is crucial to study the complete dynamics of a ballistic body before all the forces can be computed. There are generally four different kind of forces which may influence the trajectory of a missile. (i) The gravitational force, (ii) the propulsion force by expelling exhaust along its path, (iii) aerodynamical forces, (iv) and forces due to an impact on an object. After the proper formulation of centre-of-mass dynamics has been established, some reasonable assumptions about the forces on the ballistic body have to be implied, in order to keep the class of possible models as simple as possible and at the same time as realistic as possible.

The airframe of the rocket without the actual fuel load can be treated as a *rigid body*, *i.e.* forces that may bend, twist, etc. the body are neglected. The centre of gravity is assumed to coincide with the centre of mass which is not the case for the non-uniform gravitational fields like that of the earth. The dimensions of a rocket are so small in comparison to the inhomogeneity of the field that the gravitational force at the centre of gravity, which would normally lead to a torque about the centre of mass, can be neglected. The force then at the centre of mass leads to a force $\mathbf{f}(\mathbf{r}_{CM}) = -Gm\mathbf{r}_{CM}/|\mathbf{r}_{CM}|^3$. This means for all $\mathbf{r}_{CM} \in \mathbb{R}^3$ there exists an $\mathbf{a} \in \mathbb{R}^3$ such that for each $\mathbf{r} \in [\mathbf{r}_{CM} - \mathbf{a}, \mathbf{r}_{CM} + \mathbf{a}]$ the force $\mathbf{f}(\mathbf{r}) = \mathbf{f}(\mathbf{r}_{CM}) + \partial_{\mathbf{r}_{CM}}\mathbf{f}(\mathbf{r}_{CM})(\mathbf{r} - \mathbf{r}_{CM}) + \dots$ has

negligible terms higher than order zero, which is certainly true for $\mathbf{a} \ll \mathbf{r}_{CM}$. All $\mathbf{r} \in [\mathbf{r}_{CM} - \mathbf{a}, \mathbf{r}_{CM} + \mathbf{a}]$ then fulfil $\dot{\mathbf{r}} \approx \mathbf{const.}$ and the torque becomes

$$\Gamma = \sum_i (\mathbf{r}_i - \mathbf{x}) \times (m_i \mathbf{const.}) = \left(\sum_i m_i (\mathbf{r}_i - \mathbf{x}) \right) \times \mathbf{const.} = \mathbf{0} \quad (3.8)$$

whereby $\sum_i m_i (\mathbf{r}_i - \mathbf{x}) = \mathbf{0}$ due to the centre of mass condition. Few additional assumptions have been applied in this equation. The gravitational acceleration \mathbf{g} is independent of the height which thus leads to the simplification, that the gravitational acceleration is assumed to be a *homogeneous* one, *i.e.*, the acceleration vectors \mathbf{g} are parallel with the same length everywhere. The frame of reference, or the observer, is assumed to be in an *inertial frame*, *i.e.*, any rotations of the earth about itself or the sun are omitted.

After the dynamics of point masses have been considered in detail, it becomes clear why it is essential to distinguish between centre-of-mass and centre-of-gravity dynamics. The physical concept of velocity does not trivially transform inside a ballistic missile's frame of reference. It is also clear following the last section that the centre-of-mass dynamics are not sufficient for understanding a missiles trajectory due to the complicated aerodynamic influences. In addition rotational motions have not been considered yet. The dynamics of many-particle-body dynamics have to be derived in the following section. The significance of the fact that a ballistic missile is made up of many particles becomes clear during the forthcoming sections.

3.3 The many particle body of a ballistic missile

The descriptive variables of a many particle bodies for rotational motions about their centre of mass are, the *inertia tensor* \mathbf{J} , the *attitude* \mathcal{R}_t , the *rotational velocity* $\boldsymbol{\omega}$, the *angular momentum* $\mathbf{L} = \mathcal{J}\boldsymbol{\omega}$, the *kinetic rotational energy* $E_{\text{rot}} = (1/2)\boldsymbol{\omega} \cdot \mathbf{L}$, and the *torque* $\Gamma = d_t \mathbf{L}$. The inertia tensor of the whole body is defined by

$$\mathcal{J}_{ij} = \int d^3r \rho_m(\mathbf{r}) \{ \mathbf{r}^2 \delta_{ij} - r_i r_j \} \quad (3.9)$$

with $i, j = 1, 2, 3$ and $\rho_m(\mathbf{r}) d^3r$ mass of particle at position \mathbf{r} relatively to the centre of mass \mathbf{r}_{CM} and has the following properties to be *linear* with respect to $\rho_m(\bullet)$, *i.e.* the inertia tensor of arbitrary rigid bodies may be component-wise built up by taking the sum of the components' inertia tensors with respect to one common coordinate system, and a system of *principle axes* exist for all tensors. This follows immediately from the symmetry of these matrices. The orthogonal transformation is of the type $\mathcal{R} \in SO(3)$

(special orthogonal group). The eigenvalues of the tensor are the *principle moments of inertia*. The relation between changes of the angular momentum and all applied torques Γ is described by Euler's law as

$$\dot{\mathbf{L}} = \mathcal{J}\dot{\boldsymbol{\omega}} + \boldsymbol{\omega} \times \mathcal{J}\boldsymbol{\omega} = \sum_i \mathbf{r}_i \times \mathbf{f}_i \quad (3.10)$$

The *centre-of-mass motion principle* in combination with the properties of an *inertial frame of reference* as well as the *rotational motions about the centre of mass* leads to the conclusions, that any centre of mass trajectory of any body can completely be described by any suitable inertial frame of reference $m\ddot{\mathbf{r}}_{CM} = \mathbf{f}$, whereby \mathbf{r}_{CM} are coordinates of the *centre of mass* related to an inertial reference body. Any forces applied to any points of the body lead to dynamics of its centre of mass as if the resultant force would have been applied directly to the centre of mass. This is in fact particularly important for the calculations of gravitation, propulsion, and aerodynamic forces which generally do not act at the centre of mass. The interrelations between particles of a well defined set of particles may lead to rotations about the centre of mass which is defined through Euler's equation. Newton's law $m\ddot{\mathbf{x}} = \mathbf{f}$ and Euler's equation $\dot{\mathbf{L}} = \Gamma$ together are the most general dynamics of any system of point masses and do not incorporate any simplifications. Since Newton's law can be applied directly to a ballistic missile as long as the accelerations are given, Euler's equation has to be established to provide a complete mathematical formulation of a ballistic missile. In order to keep the problem as simple as possible, the rotational dynamics of the missile's body part which remains unchanged over the whole period of flight (rigid body) is treated first and the influence of burning fuel is incorporated afterwards. For this purpose consider the following schematic Figure 3.2.

The principal aim is to compute the entire inertia tensor of the entire body. The symmetry of the rigid body already indicates that the inertia tensor has three eigenvalues, the principle moments of inertia, of which two are identical in the ideal case but in reality of very similar magnitude. The inertia tensor could be calculated by taking the volume integral over the whole body as in Eq. (3.9) which is generally complicated. However, as it is evident from Figure 3.2 the ballistic missile given here is highly symmetric and can be broken up into simple geometric objects, consisting of a cone, a cropped cone, a hollow cylinder, triangles and squares for the fins. Unfortunately this simplistic model of a ballistic missile is incomplete, since the engine, fuel tanks, and pay load are missing. Because no reliable information about these components is publically available, it is hoped that the simple model leads to a inertia tensor which is not too far from the tensor components of a real missile. The inertia tensor components

1. **Top cone:** Volume = $(1/3)\pi r^2 h = 0.0272 \text{ meter}^3$, CM = $(1/4)h = 0.1175 \text{ meter}$, $\mathcal{J}_{e_1} = \mathcal{J}_{e_2} = (1/20)\rho_M \pi r^4 h + (1/30)\rho_M \pi r^2 h^3 = 0.7042$, $\mathcal{J}_{e_3} = (1/10)\rho_M \pi r^4 h = 0.3841 \text{ kg meter}^2$
2. **Cropped cone:** Volume = $(1/3)\pi h(r_2 - r_1)^2 - \pi h(r_2 - r_1)r_2 + \pi h r_2^2 = 0.9475 \text{ meter}^3$, CM = $h(2r_1/3 + r_2/3)/(r_1 + r_2)$, $\mathcal{J}_{e_1} = \mathcal{J}_{e_2} = (1/30)\rho_M \pi h^3(6r_1^2 + 3r_1 r_2 + r_2^2) + (1/20)\rho_M \pi h(r_1^4 + r_1^3 r_2 + r_1^2 r_2^2 + r_1 r_2^3 + r_2^4) = 662.6097 \text{ kg meter}^2$, $\mathcal{J}_{e_3} = (1/10)\rho_M \pi h(r_1^4 + r_1^3 r_2 + r_1^2 r_2^2 + r_1 r_2^3 + r_2^4) = 75.8523 \text{ kg meter}^2$
3. **Hollow tube:** Volume = $\pi h(r_2^2 - (r_2 - \delta_S)^2) = 0.3079 \text{ meter}^3$, CM = $(1/2)h =$, $\mathcal{J}_{e_1} = \mathcal{J}_{e_2} = (1/4)\rho_M \pi h(r_2^4 - (r_2 - \delta_S)^4) + (1/12)\rho_M \pi h^3(r_2^2 - (r_2 - \delta_S)^2) = 1.8741 \cdot 10^3 \text{ kg meter}^2$, $\mathcal{J}_{e_3} = (1/2)\rho_M \pi h(r_2^4 - (r_2 - \delta_S)^4) = 75.1837 \text{ kg meter}^2$
4. **Fins:** Volume = $2h_t l_t \delta_S + 4h_p l_p \delta_S = 0.0289$, $\mathcal{J}_{e_1} = \mathcal{J}_{e_2} = (1/3)\rho_f l_p \delta_f h_p^3 + (1/6)\rho_f l_p \delta_f^3 h_p + 1/6\rho_f l_p^3 \delta_f h_p + 2\rho_f l_p \delta_f h_p((l_p/2 + r_2)^2 + (h_p/2)^2) + 1/12\rho_f l_t \delta_f^3 h_t + 1/6\rho_f^3 l_t \delta_f h_t + 1/3\rho_f l_t \delta_f h_t^3 + \rho_f l_t \delta_f h_t r_2^2) = 3.8703 \cdot 10^3 \text{ kg meter}^2$, $\mathcal{J}_{e_3} = (1/3)\rho_f l_p^3 \delta_f h_p + 1/3\rho_f l_p \delta_f^3 h_p + 4\rho_f l_p \delta_f h_p(l_p/2 + r_2)^2 + 1/3\rho_f l_p^3 \delta_f h_f + 1/6\rho_f l_p \delta_f^3 h_t + 2\rho_f l_p \delta_f h_t r_2^2) = 15.9111 \text{ kg meter}^2$
5. **Engine:** Volume = $\pi(r_2 - \delta_S)^2 h = 0.5352 \text{ meter}^3$, CM = $(1/2)h = 0.44 \text{ meter}$, $\mathcal{J}_{e_1} = \mathcal{J}_{e_2} = 1/4\rho_M \pi h(r_2 - \delta_S)^4 + 1/12\rho_M \pi h^3(r_2 - \delta_S)^2 = 89.2666 \text{ kg meter}^2$, $\mathcal{J}_{e_3} = (1/2)\rho_M \pi h(r_2 - \delta_S)^4 = 93.0369 \text{ kg meter}^2$

Table 3.1: All physical quantities employ the SI unit system. h is the height of a body, $r = r_1$ and r_2 are radii of the cone and the smaller and larger radii of the cropped cone, respectively. The centre of mass of the empty missile is at 5.4704 meter from the base of the body of Fig. 3.2.

given in Table 3.1 have been computed by hand, but most can be found elsewhere (e.g. (Hestenes, 1986)). The calculus for the inertia tensors is rather straightforward by choosing an affine coordinate system. Steiner's theorem (Scheck, 1990) then leads to the inertia tensor for any body with shifted origin. The only non-symmetric bodies with respect to the missile's symmetry axis are the four fins. However, the following Theorem 3.3.1 (Hestenes, 1986; Scheck, 1990) demonstrates by employing Steiner's theorem how the non-trivial inertia tensor contributions enter the common inertia tensor of all four fins together.

THEOREM 3.3.1 *A body may be composed out of four identical bodies which have the inertia tensor \mathcal{J} with respect to the origin of one arbitrary coordinate system with*

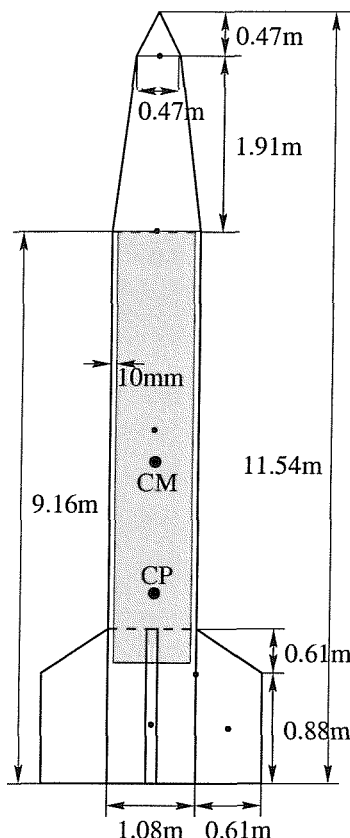


Figure 3.2: The diagram shows a homogeneous mass distribution with $\rho_M = 853 \text{ kg/meter}^3$. The mass of the body (unfueled) is $m = 1.781 \cdot 10^3 \text{ kg}$, the mass of the fuel is $m = 5.699 \cdot 10^3 \text{ kg}$, i.e., the mass of the ballistic missile at time of launch is given by $m = 7.480 \cdot 10^3 \text{ kg}$. The hollow part which is reserved for fuel is highlighted. The measures shown are utilized for calculating the entire mass, centre of mass, and centre of pressure of the ballistic missile. The small solid circles show the origin in which the moments of inertia of the missile's sub-bodies are calculated. The shown centre of mass is only valid for the empty missile, whereas the centre of pressure shown here is the mean centre of pressure which is proved in Example 3.4.3 to vary only by about 0.32 meters. The dimensions of the missile have been inspired by (Systems, 1985; Forden, 1997).

a fixed axis through the origin, and which are shifted by a radius vector \mathbf{r} orthogonal to the axis, and afterwards rotated about of the angles $0, \frac{\pi}{2}, \pi, \frac{3\pi}{2}$, respectively. The compound body then is characterized by the eigenvalues of the inertia tensor

$$\mathcal{J}_1 = \mathcal{J}_2 = 2(I_{xx} + I_{yy}); \quad \mathcal{J}_3 = 4I_{zz} \quad (3.11)$$

Proof: The procedure described above is equal to shift all four bodies about the common vector in the xz-plane

$$\mathbf{a}_s = \begin{pmatrix} r_s \\ 0 \\ z_s \end{pmatrix}. \quad (3.12)$$

and together with Steiner's theorem the inertia tensor becomes

$$I_{xx} = I'_{xx} + Mz_s^2 \quad (3.13)$$

$$I_{yy} = I'_{yy} + M(r_s^2 + z_s^2) \quad (3.14)$$

$$I_{zz} = I'_{zz} + Mr_s^2 \quad (3.15)$$

$$I_{xy} = I'_{xy} \quad (3.16)$$

$$I_{xz} = I'_{xz} - Mr_s z_s \quad (3.17)$$

$$I_{yz} = I'_{yz} \quad (3.18)$$

whereby \mathcal{J}' indicates the inertia tensor of the body components calculated above, and \mathcal{J} is the new tensor with respect to the transformed coordinates.

When a axial-symmetric rigid body is given with rigid sub-bodies for $\psi = 0, \frac{\pi}{2}, \pi, \frac{3\pi}{2}$ the Inertia tensors become

$$\psi = 0 : \begin{pmatrix} I_{xx} & I_{xy} & I_{xz} \\ I_{xy} & I_{yy} & I_{yz} \\ I_{xz} & I_{yz} & I_{zz} \end{pmatrix} \quad (3.19)$$

$$\psi = \frac{\pi}{2} : \begin{pmatrix} I_{yy} & -I_{xy} & I_{yz} \\ -I_{xy} & I_{xx} & -I_{xz} \\ I_{yz} & -I_{xz} & I_{zz} \end{pmatrix} \quad (3.20)$$

$$\psi = \pi : \begin{pmatrix} I_{xx} & I_{xy} & -I_{xz} \\ I_{xy} & I_{yy} & -I_{yz} \\ -I_{xz} & -I_{yz} & I_{zz} \end{pmatrix} \quad (3.21)$$

$$\psi = \frac{3\pi}{2} : \begin{pmatrix} I_{yy} & -I_{xy} & -I_{yz} \\ -I_{xy} & I_{xx} & I_{xz} \\ -I_{yz} & I_{xz} & I_{zz} \end{pmatrix}. \quad (3.22)$$

The inertia tensor for the whole body can simply be obtained by the sum of the inertia tensors of its sub-bodies, when the inertia tensors are all given in one common coordinate system. This follows due to the fact of linearity of inertia tensors with respect to mass distributions. Hence

$$\mathcal{I}_{0, \frac{\pi}{2}, \pi, \frac{3\pi}{2}}^I = \begin{pmatrix} 2(I_{xx} + I_{yy}) & & \\ & 2(I_{xx} + I_{yy}) & \\ & & 4I_{zz} \end{pmatrix} \quad (3.23)$$

$$= \begin{pmatrix} I_{xx;0, \frac{\pi}{2}, \pi, \frac{3\pi}{2}} & & \\ & I_{xx;0, \frac{\pi}{2}, \pi, \frac{3\pi}{2}} & \\ & & I_{zz;0, \frac{\pi}{2}, \pi, \frac{3\pi}{2}} \end{pmatrix} \quad (3.24)$$

with

$$I_{xx;0, \frac{\pi}{2}, \pi, \frac{3\pi}{2}} = 2I'_{xx} + 2I'_{yy} + 2M(r_s^2 + 2z_s^2)$$

and

$$I_{zz;0, \frac{\pi}{2}, \pi, \frac{3\pi}{2}} = 4I'_{zz} + 4Mr_s^2$$

This theorem demonstrates that the ballistic missile's inertia tensor reflects the geometric symmetry about the \mathbf{e}'_3 -axis, when the fins are identical and symmetrically mounted on the air frame such that the conditions of the theorem are fulfilled. This symmetry property is in particular significant for the spin stabilized control of the missile. Breaking the symmetry due to some faulty missile construction will lead to unpredictable behaviour. (This problem is treated in more detail later in this chapter.) However, since there is no information available about the asymmetry of a real missile, perfect symmetry is assumed in the later sections when the dynamics of a missile are employed for prediction purposes. The total inertia tensor of a missile, as it is shown in Figure 3.2 and as the components are given in Table 3.1, is now defined as the sum of the inertia tensors of all components. The inertia tensor of the missile thus becomes in the primed (body fixed) coordinate system

$$\mathcal{I}_{\mathbf{e}'_1} = 3.5830 \cdot 10^4 \text{kgmeter}^2, \quad (3.25)$$

$$\mathcal{I}_{\mathbf{e}'_2} = 3.5830 \cdot 10^4 \text{kgmeter}^2, \quad (3.26)$$

$$\mathcal{I}_{\mathbf{e}'_3} = 260.3681 \text{kgmeter}^2. \quad (3.27)$$

These principle moments of inertia are employed throughout the thesis. The main limitation is that the ballistic missile also carries fuel which strongly effects the inertia tensor of the missile. As has been mentioned before, most of the fuel is burnt during

the initial boost phase. The minor residue of the fuel is neglected here. As it has been argued before the boost phase is of no particular significance for the prediction of the ballistic missile's trajectory since the duration of the boost phase is only about $1/6 - 1/4$ th of the entire time of flight.

During the boost phase the missile is accelerated to a certain initial velocity. The boost takes only few seconds and is accomplished when velocity and spin, reach their initial and stationary magnitude. The ideal rocket has during this time period a stationary flow of fuel that leaves the boundaries of the air frame with constant velocity and has a constant burning rate.

Disturbances as well as aerodynamic forces have to be compensated for. The measured acceleration relative to the rocket has a certain pre-programmed value, *i.e.*, the drag can be compensated for by applying an additional thrust such that the overall acceleration reaches the nominal value. The translation of a body within the time of ignition and maximum acceleration can be neglected. The force on a self-propelling body is given by the following theorem

THEOREM 3.3.2 (Scheck (1990)) *The temporal overall change of a rigid body's momentum (m with its own velocity \mathbf{v}) that has an impact with an infinitesimal small body of velocity \mathbf{u} is equal to the external force \mathbf{f} plus the force $\dot{m}\mathbf{u}$.*

$$\frac{d}{dt}(m\mathbf{v}) = \mathbf{f} + \dot{m}\mathbf{u} \quad (3.28)$$

The proof is rather straightforward (see *e.g.* (Hestenes, 1986)). The conservation of momentum, which follows immediately from Newtons law for closed systems $\frac{d}{dt}(m\mathbf{v}) = \mathbf{0}$, guarantees that

COROLLARY 3.3.3 *A rigid body with velocity $\dot{\mathbf{r}}_{CM}$ and rotational velocity $\boldsymbol{\omega}$ that decays into rigid sub-bodies, that do not interact during the decay, with the difference vector \mathbf{a}_i between the centre of gravity of the new body i and of the former common one, releases these sub-bodies with the rotational velocity $\boldsymbol{\omega}$ each and the translational velocity $\dot{\mathbf{r}}_{CMi} = \dot{\mathbf{r}}_{CM} + \boldsymbol{\omega} \times \mathbf{a}_i$.*

Proof: The general tangential velocity of each point P in rigid body has a translational $\dot{\mathbf{r}}_{CM}$ as well as a rotational component $\boldsymbol{\omega} \times \mathbf{r}_{CMi}$ and the velocity of point P at a particular time t is $\dot{\mathbf{r}} = \dot{\mathbf{r}}_{CM} + \boldsymbol{\omega} \times \mathbf{r}_{CMi}$ which is equivalent with any other choice of frame of reference, *i.e.*, $\dot{\mathbf{r}} = \dot{\mathbf{r}}_{CM} + \boldsymbol{\omega}' \times \mathbf{r}'$. Both coordinate systems are interrelated by

$\mathbf{r} = \mathbf{r}' + \mathbf{a}$, hence

$$\dot{\mathbf{r}}_i = \dot{\mathbf{r}}_{CM} + \omega \times (\mathbf{a} + \mathbf{r}')$$
 (3.29)

$$= \dot{\mathbf{r}}_{CM} + \omega \times \mathbf{a} + \omega \times \mathbf{r}'$$
 (3.30)

$$= \dot{\mathbf{r}}_{CM} + \dot{\mathbf{r}}_{CM_i} + \omega \times \mathbf{a}_i$$
 (3.31)

The definition of a rigid body $\|\mathbf{a}\| = \text{const.}$ means that $\dot{\mathbf{r}}_{CM_i} = \omega \times \mathbf{a}_i$ and Equations (3.30) & (3.31) lead therefore to the identity $\omega' = \omega$. Each body fixed frame of reference fulfils the set of relations:

$$\dot{\mathbf{r}}_{CM} = \dot{\mathbf{r}}_{CM_i} + \omega \times \mathbf{a}$$
 (3.32)

$$\omega = \omega'$$
 (3.33)

In the moment of disconnecting n sub-elements of rigid bodies contained in the former common rigid body the length of the vector \mathbf{a}_i can be altered freely due to the lack of the former constraint of constant distance. When $\mathbf{a}(i)$ are the centres of gravity of these particular rigid bodies then their angular velocities must be zero. The former tangential velocities of the new centres of gravity remain preserved as linear velocities of a magnitude equal to $\|\omega \times \mathbf{a}_i\|$. ■

Note that the last proof does not claim that $\omega'_i = \text{const.}$ will be the same for all sub-bodies at $t >$ time of decay. The initial state of decay defines new angular momenta \mathbf{L}_i which then stay constant. The general case for an open system with internal as well as external forces without torques leads to the theorem

THEOREM 3.3.4 Any closed set of n rigid sub-bodies with mass m_i ($i = 1, \dots, n$) whose centre of mass has momentum \mathbf{p} , and rotates about the CM with rotational velocity ω and decays into its parts at time t_0 whereby arbitrary homogeneous forces \mathbf{f}_i may apply as well leave then the rigid sub-bodies with the velocity $\mathbf{v}_i = \int dt \mathbf{f}_i(t)/m + \dot{\mathbf{r}}_S + \omega \times \mathbf{a}_i$ and angular momentum $\mathbf{L}_i = \mathcal{J}_i \omega$

Proof: The homogeneous force was proved to lead to no torque and the rest follows from the conservation of the angular momentum theorem and corollary 3.3.3. ■

The purpose of the last Theorem was to show that Theorem 3.3.2 is strictly only applicable to centre of mass motions. When the missile incorporates rotational motions as well, Corollary 3.3.3 shows that, depending on the rotation of the missile, an extra acceleration may be gained when mass separates from the missile which is not considered to be part of the air-frames centre of mass. It is obvious from Figure 3.2 and Figure 3.3 that the exit of the exhaust is far outside the air-frames centre of mass which means that Eq. (3.28) does not apply to the ballistic missile considered here. However, there does

not seem to be any attempt in the literature (Eichblatt, E.J., Jr, 1989) to adapt Eq. (3.28) to the real-life problem given above. The general unmotivated assumption probably is that the contribution of rotational motion given by the term $\omega \times \mathbf{a}_i$ is comparatively small in comparison to the main thrust $\mathbf{u}d_t m$. The next corollary shows that a self-propelling rotating ballistic missile which is suddenly decomposed into arbitrary sub-bodies does not change its rotational velocity .

COROLLARY 3.3.5 *A rotating axis-symmetric body with $\omega \parallel \mathbf{e}_3$, whereby \mathbf{e}'_3 is the symmetry axis, which decays at time t_0 into arbitrary rigid sub-bodies, maintains the rotational velocity for all its sub-bodies at all $t > t_0$. Arbitrary homogeneous forces may be applied as well.*

Proof: This follows from the conservation of angular momentum theorem and corollary 3.3.3. ■

Corollary 3.3.5 proves that in the case that fuel is taken evenly from the container of a slender axis symmetric body (as here) and the thrust vector is parallel to the line between nozzle and centre of mass, then the rotational velocity does not change. However, mass is not just removed from the fuel tank. After some fuel has been taken from the tank the vibrational energy of the body and pressure inside the fuel is generally driving the fuel back into an equilibrium of density distribution where the fuel inside the tank seeks an energetic minimum. It is assumed here that there is a constant density of fuel in the containers of the rocket, and Euler's Equ. 3.10 describes the relation between changes of the angular momentum \mathbf{L} with time under the influence of external torques and the loss of mass as it is the case for all self-propelling machines. The linearity of the inertia tensor with respect to ρ_{fuel} proves that the principal axes of the inertia tensor in body coordinates are invariant, *i.e.*, the principle axes of the inertia tensor do not rotate inside the body and the inertia tensor of the fuel is proportional to the total propellant density. Hence

$$d_t \mathbf{L} = d_t \left(\sum_i \rho_i \mathbf{j}_i \omega_i \right) = \Gamma \quad (3.34)$$

whereby i runs over all inertia tensors of the components of a compound (semi)-rigid body. It is important to note that the coordinate vectors must be the same for all inertia tensors employed here. In some cases the inertia tensor may not be fixed with the air-frames coordinate system and it may then become necessary to transform the computed inertia tensor back into the body's system by employing a required rotation about certain angles and perform a shift by employing Steiner's theorem. Because of the symmetry assumption of the fuel distribution inside the tanks with respect to the

entire body's symmetry axis these difficulties do not arise in the model employed here. Euler's law becomes

$$\begin{aligned}\dot{\mathbf{L}} &= \sum_i (\dot{\rho}_i \mathbf{j}_i \omega + \rho_i \mathbf{j}_i \dot{\omega} + \rho_i d_t \mathbf{j}_i \omega) \\ &= \sum_i (\dot{\rho}_i \mathbf{j}_i \omega + \mathcal{J}_i \dot{\omega} + \omega \times \mathcal{J}_i \omega) \\ &= \Gamma\end{aligned}\quad (3.35)$$

The identity $\rho d_t \mathbf{j} \omega = \omega \times \mathcal{J} \omega$ has been derived elsewhere, *e.g.* in (Hestenes, 1986; Scheck, 1990).

The wording above may seem to be rather verbose, but was necessary for the following modelling of rotating semi-rigid bodies. Disturbances in the axis-symmetry of a body may easily lead to changes in the velocity and rotational velocity of a 'rest body' when a certain amount of fuel has been burnt. Although the precise form of \mathbf{L} is not explicitly required for the calculations of the sustain phase considered later but serves as a completion of the insufficient theory provided in the standard literature on ballistic missiles (Blakelock 1965; Garnell 1980; Anonymous 1982; Eichblatt, E.J., Jr 1989; Collinson 1996).

It has been shown that rotational and translational motions can only be treated as a rigid body in case of an open system (semi-rigid body) when certain constraints are fulfilled. It is assumed that Corollary 3.3.5 represents the rotations of the body sufficiently such that Euler's law becomes, in its principle axis components,

$$\dot{\omega}_1 = \frac{\mathcal{J}_2 - \mathcal{J}_3}{\mathcal{J}_1} \omega_2 \omega_3 + \frac{f_{th}^1}{\mathcal{J}_1} r_l(t) + \frac{f_{ae}^1}{\mathcal{J}_1} r_{cp}(t) + \frac{\dot{\rho} j_1}{\mathcal{J}_1} \omega_1 \quad (3.36)$$

$$\dot{\omega}_2 = \frac{\mathcal{J}_3 - \mathcal{J}_1}{\mathcal{J}_2} \omega_3 \omega_1 + \frac{f_{th}^2}{\mathcal{J}_2} r_l(t) + \frac{f_{ae}^2}{\mathcal{J}_2} r_{cp}(t) + \frac{\dot{\rho} j_2}{\mathcal{J}_2} \omega_2 \quad (3.37)$$

$$\dot{\omega}_3 = \frac{\mathcal{J}_1 - \mathcal{J}_2}{\mathcal{J}_3} \omega_2 \omega_1 + \frac{\dot{\rho} j_3}{\mathcal{J}_3} \omega_3 + \frac{\Gamma_{ae}}{\mathcal{J}_3} \quad (3.38)$$

where $\mathcal{J} = \sum_i \rho_i \mathbf{j}_i$ and \mathbf{j}_1 is the inertia tensor of the fuel content divided by the fuel density ρ . The force \mathbf{f}_{th} is the net thrust of the rocket—including the control force—and the corresponding scalar $r_l(t)$ is the distance between the centre of mass $CM(t)$ of the remaining body at time t and the nozzle where the thrust is generated. \mathbf{f}_{ae} is the sum of all aerodynamical forces applied at the centre-of-pressure (CP) which has distance $r_{cp}(t)$ from the centre of mass. The term $\frac{\mathcal{J}_1 - \mathcal{J}_2}{\mathcal{J}_3} \omega_1 \omega_2$ vanishes in Equ. 3.38 due to the axis-symmetry of the body ($\mathcal{J}_1 = \mathcal{J}_2$). It has been shown above that a axis-symmetric body with four identical fins are mounted on the body, such that their centre of mass is on the vertex of a square, remains axis symmetric.

The translational dynamics of the air-frame plus remaining fuel, not the centre of mass, are defined by

$$\dot{\mathbf{v}} = -\dot{m}(t)\mathbf{e}/m(t) + \mathbf{f}_{\text{gr}}/m(t) + \mathbf{f}_{\text{ae}}/m(t) \quad (3.39)$$

which is just the consequence of Theorem 3.3.2. The control force is hidden in $\dot{m}(t)\mathbf{e}/m(t)$ where the mass rate \dot{m} as well as the direction of \mathbf{e} (but not $\|\mathbf{e}\|$) may be varied.

After the general dynamics of a self-propelling ballistic missile have been derived, the *control during boost phase* by simplified inertial control is introduced. The ballistic missile is generally equipped with accelerometers which measure the longitudinal and rotational accelerations of its airframe in its body coordinate system in order to calculate the actual (angular) velocities and (angular) coordinates by twofold temporal integration. Feedback control is always based on the following general algorithm.

1. Define a desired output of a plant.
2. Measure the actual output of the plant and compute the difference between actual and the desired output, *i.e.* the residual (error).
3. Employ adjustable physical parameters to drive the plant towards the desired output by minimizing the error.

The missile considered here can only be steered by thrust vector control, *i.e.*, the direction and magnitude of the thrust.

When the accelerometer measurements are error free, small deviations from the desired trajectory can easily be compensated for. Obviously, real-life systems are never error-free, but it is generally assumed that the deviations are small enough (Eichblatt, E.J., Jr, 1989) such that the control forces can be linearized about their operation point. When the inertial guidance system has a malfunction the body cannot be controlled. *General forces and torques in an equilibrium* consist of the thrust, gravitation, and aerodynamics. The relative wind velocity to the rocket consists of a velocity component parallel to the symmetry axis of the rocket which leads to a drag on the air frame and an orthogonal velocity component leading to a side drift, or lift, as well as a torque about the $\mathbf{e}'_1, \mathbf{e}'_2$ -axes, as long as the centre of pressure does not coincide with the centre of mass, which is assumed here. The thrust is applied with a certain distance vector from the centre of mass, *i.e.*, each deflection of thrust applies a continuous torque on the missile. This problem could be named as the side wind control force dilemma

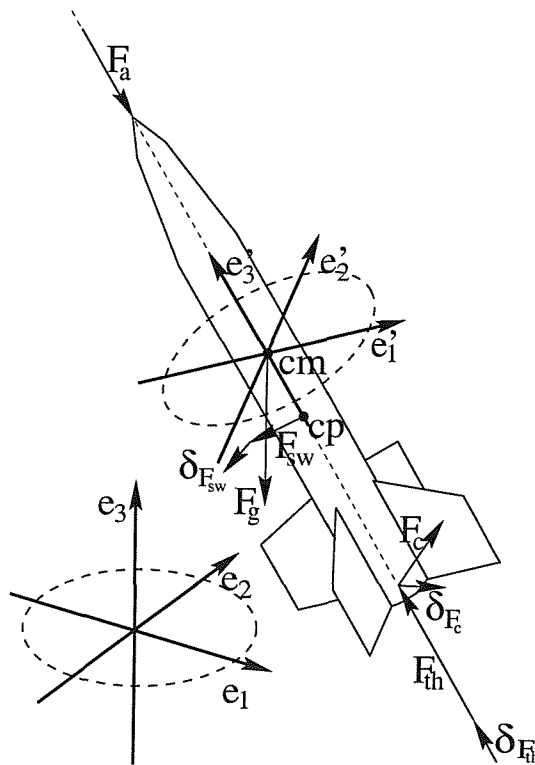


Figure 3.3: Inertial and primed, body fixed, frame of reference as well as the forces on a ballistic missile are being shown. Small disturbances of the nominal forces are indicated by a δ . The centre of mass (CM) and the centre of pressure (CP) are shown as well. Due to the physical arguments above, aerodynamic, gravitational, and thrust forces always apply to the centre of mass. The distances between CM and CP, between CM and centre of gravity, and between CM and nozzle are only relevant for the torques which also apply to the body frame.

since it may be wished to separate torques from translational forces. The solution to this problem may be accomplished by steering the rocket at a certain angle into the wind whilst keeping the angular momentum zero by producing a composite control torque that compensates for the torque of the side wind.

The force equation in combination with the desired flight path and torque compensation is

$$m\ddot{\mathbf{r}}'^0 + m\ddot{\delta}_{\mathbf{r}}' = \mathbf{F}_{th}'^0 + \mathbf{F}_A'^0 + \mathbf{F}_{sw}'^0 (1 - r_l/r_{cp}) + \mathbf{F}_{gravity}'^0 + \delta'_{\mathbf{F}_A} + \delta'_{\mathbf{F}_{sw}} + \delta'_{\mathbf{F}_{th}} + \delta'_{\mathbf{F}_c}, \quad (3.40)$$

whereby the dynamics along the desired trajectory are defined by

$$m\ddot{\mathbf{r}}'^0 = \mathbf{F}_{th}'^0 + \mathbf{F}_A'^0 + \mathbf{F}_{sw}'^0 (1 - r_l/r_{cp}) + \mathbf{F}_{gr}'^0 \quad (3.41)$$

and the linearized net-forces outside the equilibrium are given by

$$m\ddot{\delta}_{\mathbf{r}}' = \delta'_{\mathbf{F}_A} + \delta'_{\mathbf{F}_{sw}} + \delta'_{\mathbf{F}_{th}} + \delta'_{\mathbf{F}_c}$$

with r_{cp} the distance between the centre of mass and the centre of pressure and r_l the distance between the centre of mass and the applied thrust vector. In order to ensure equilibrium, there is only one freely available parameter \mathbf{F}_{th}^{00} which can be chosen to get the pre-determined acceleration $\ddot{\mathbf{r}}^{00}$. The first order approximation of errors in Eq. (3.42) is only justified when the dynamical system stays close enough to an equilibrium, as in this case $\ddot{\mathbf{r}}^{00}$ is the desired first order perturbative acceleration, *i.e.*, $m\ddot{\delta}_{\mathbf{r}}' = \sum_{\mathbf{f}_i} \delta'_{\mathbf{f}_i} = \mathbf{0}$ for all time, and all higher order terms of the Taylor series (3.40) are negligible. The linearized net force and torque equations may therefore be controlled by the following:

$$\delta_{\mathbf{F}^A} + \delta_{\mathbf{F}^{th}} = \mathbf{0} = m(t)\ddot{\delta}_{\mathbf{r}\parallel} + b_d\dot{\delta}_{\mathbf{r}\parallel} + k_d \left(\delta'_{\mathbf{r}\parallel} - \delta'^{00}_{\mathbf{r}\parallel} \right) \quad (3.42)$$

$$\delta_{\mathbf{F}_{sw}} + \delta_{\mathbf{F}^c} = \mathbf{0} = m(t)\ddot{\delta}_{\mathbf{r}\perp} + b_d\dot{\delta}_{\mathbf{r}\perp} + k_d \left(\delta'_{\mathbf{r}\perp} - \delta'^{00}_{\mathbf{r}\perp} \right) - \frac{B_d}{r_l}\dot{\delta}_{\theta_1} - \frac{K_d}{r_l}\delta'_{\theta_1} \quad (3.43)$$

$$\begin{aligned} \delta_{\mathbf{F}_{sw}r_{cp}} + \delta_{\mathbf{F}^c r_{cp}} &= J\ddot{\delta}_{\theta_1} + B_d\dot{\delta}_{\theta_1} + K_d \left(\delta'_{\theta_1} - \delta'^{00}_{\theta_1} \right) - b_d r_l \dot{\delta}_{\mathbf{r}_{sw}} \\ &\quad - k_d r_l \left(\delta'_{\mathbf{r}_{sw}} - \delta'^{00}_{\mathbf{r}_{sw}} \right) \end{aligned} \quad (3.44)$$

with $b_d, B_d, k_d, K_d > 0$ suitable parameter values for the control law. The axial components are due to the (assumed) rotational symmetry of the thrust along the symmetry axis decoupled from the normal force and their related torques. The solution of this equation is well known and leads to the associated design criterion of the *damping parameter* ($b_d^2/4m^2$) and the characteristic angular frequency $\sqrt{k_d/m}$ for *under-damping* ($b_d^2/4m^2 < k_d/m$), *critical damping* ($b_d^2/4m^2 = k_d/m$), and *over-damping* ($b_d^2/4m^2 > k_d/m$) in Eq. (3.42). The combinations of opposite signs in the second force $-\frac{B_d}{r_l}\dot{\delta}_{\theta_1} - \frac{K_d}{r_l}\delta'_{\theta_1}$ in Eq. (3.43) and the momentum equation (3.44) imply that there will be forces that act against each other. The forces which are proportional to the velocities in Eq. (3.43) are meant to damp the system which is sought to be driven back into a nominal equilibrium by the other forces which is proportional to the difference coordinate vector of actual and nominal coordinates. A problem occurs when one set of forces in Eq. (3.42) seeks to stabilize one equilibrium and the other set of forces in Eq. (3.43) seeks to stabilize the other. To ensure that these dynamics work together, the following has to be presumed:

1. Corrections of the spatial coordinates are the prime concern and have to be given preference over the error angle correction.

2. The set of forces for error angle correction as well as for error coordinate correction have a resonance frequency, here $\omega_{R_1} := \sqrt{k_d/m - b_d^2/(4m)}$ and $\omega_{R_2} := \sqrt{K_d/\mathcal{I} - B_d^2/(4\mathcal{I})}$, where a particular system can take up the utmost energy from an outside force. The aim is to decouple both dynamics, such that both may fulfil their task of stabilizing their equilibrium without transmitting energy from one system to another like a resonator, *i.e.*, $\omega_{R_1} \neq \omega_{R_2}$.
3. The characteristic time scale of the force τ_f and momentum dynamics τ_m are related to each other by $\tau_f \ll \tau_m$, *i.e.*, $\delta'_{\theta_1}(\Delta t) \gg \delta'_{\mathbf{r}^\perp}(\Delta t)$.
4. By choosing $-k_d\delta'_{\mathbf{r}^\perp}^0 = \int_{\tau_f} dt B_d \dot{\delta}'_{\theta_1}/r_{cp} + K_d \delta'_{\theta_1} r_{cp} \approx 0$ such that $-br_{cp} \dot{\delta}'_{\mathbf{r}^{sw}} - kr_{cp} (\delta'_{\mathbf{r}^{sw}} - \delta'_{\mathbf{r}^{sw}}^0) = \delta'_{\theta_1}^0 \approx \text{const.}$ for $\Delta t \ll \tau_f$, then both dynamics are virtually decoupled and may be stabilized separately.

However, the assumptions and approximations given above may be true for simple ballistic missile models, the verification or falsification of these models can only be established by obtaining real data. As there is no publically available information, the validity of the model above remains questionable. The most important issue for the following work is, that any kind of general model during the boost phase does not effect the dynamical model during the sustain and terminal phase of the body, because the control of the flight path is restricted to the boost phase and the main trajectory is the one of an uncontrolled, rigid, ballistic body. All equations discussed above simplify in this case to pure rigid motions of the remaining body (air-frame).

$$\dot{\omega}_1 = \frac{\mathcal{I}_2 - \mathcal{I}_3}{\mathcal{I}_1} \omega_2 \omega_3 + \frac{f_{ae}^1}{\mathcal{I}_1} r_{cp} \quad (3.45)$$

$$\dot{\omega}_2 = \frac{\mathcal{I}_3 - \mathcal{I}_1}{\mathcal{I}_2} \omega_3 \omega_1 + \frac{f_{ae}^2}{\mathcal{I}_2} r_{cp} \quad (3.46)$$

$$\dot{\omega}_3 = \frac{\mathcal{I}_1 - \mathcal{I}_2}{\mathcal{I}_3} \omega_2 \omega_1 + \frac{\Gamma_{ae}}{\mathcal{I}_3} \quad (3.47)$$

$$\dot{\mathbf{v}} = \mathbf{f}_{gr}/m + \mathbf{f}_{ae}/m \quad (3.48)$$

The *terminal phase* is defined as the final seconds of flight before the impact, where a dedicated algorithm may correct the rocket's position by fusing camera data with the calculated position. The body here is purely an inertial guidance controlled system, which is running out of fuel during the boost phase, *i.e.*, there is no difference between sustain and terminal phase of the considered ballistic missiles.

3.3.1 Desired Flight path during boost phase

The *desired flight path during the boost phase* is, when the aerodynamical drag is neglected and the gravitational force is approximately homogeneous, *i.e.*,

$$\dot{\mathbf{v}} = -\dot{m}(t)\mathbf{e}/m(t) + \mathbf{g} \quad (3.49)$$

The exhaust velocity \mathbf{e} is assumed to be constant, the velocity of the missile's body, after burn time t and initial velocity $\mathbf{v}(t = 0) = \mathbf{0}$ is then

$$\mathbf{v}(t) = -\mathbf{e} \log(m(t)/m(0)) + \mathbf{g}t. \quad (3.50)$$

The spatial coordinate vector of the missile after burn time t is

$$\mathbf{r}(t) - \mathbf{r}(0) = -(\mathbf{u}/\dot{m}) (m(t) \log m(t)/m(0) - m(t) + m(0)) + (1/2)\mathbf{g}t^2. \quad (3.51)$$

whereby the identity of $\int dx \log x = x \log x - x$ with $x = mt/m(0)$ and therefore $dx/dt = \dot{m}/m(0) = \text{const.}$ has been utilized to compute $\int_0^t \log(\dot{m}/m(0)) dt = m(0)/\dot{m} \int_1^{m(t)/m(0)} dx \log x$. Correcting forces on the boost trajectory of a missile require extra fuel which obviously leads to a loss of mass in addition to the amount which would be needed when no correcting steering movements are applied. The schedule for this problem may be as follows: determine the time of boost t_{boost} with a constant nominal burning rate with the initial angle of $\pi/4$ and determine the accelerations, velocities along its trajectory. Compare then the actual acceleration with the nominal one and change the thrust accordingly. The nominal acceleration itself is dependent on the space coordinate, as the nominal trajectory of the missile during the sustain phase changes with time. The control algorithm requires changing control laws as time progresses in order to successfully drive the missile into its target.

If we choose UDMH as fuel and Nitrogen tetroxide as oxidiser for which the typical exhaust velocity, is $u = 2686 \text{ meters/second}$, for the boost duration Of 60 sec and for a required final speed of $v(t_{\text{boost}}) = 6.5 \text{ Mach} = 6.5 \cdot 340.9 \text{ meters/second} = 2215.9 \text{ meters/second}$, and taking the gravitational acceleration $g = 9.81 \text{ meters/second}^2$, then Eq. 3.50 justifies that the final ratio of the masses has to be $m(t_{\text{boost}})/m(0) \approx 0.6$ when the boost angle is $\pi/4$. To get an estimate of the initial velocity $v_0/\sqrt{2}$, the maximal altitude and the time of flight, the ideal case of an boost angle of $\pi/4$ with uniform gravitational force and no aerodynamic force, *i.e.*

equation $\ddot{\mathbf{x}} = \mathbf{g}$ and its integrals, lead to the ballistic parameters

$$\text{Range}(\pi/4, 6.5M) = \frac{v_0^2}{g} \approx 500.5 \text{ km}, \quad (3.52)$$

$$\text{Height}(\pi/4, 6.5M) = \frac{v_0^2}{4g} \approx 125.13 \text{ km}, \quad (3.53)$$

$$t_{\text{flight}}(\pi/4, 6.5M) = \sqrt{2} \frac{v_0}{g} \approx 5 \text{ min, 19.45 second.} \quad (3.54)$$

The atmosphere has an altitude of $\approx 122 \text{ km}$, *i.e.*, the body can never really leave the atmosphere due to the longest range of this body which is about 500 km . When the body would leave the atmosphere for a certain time interval, certain physical parameters, J_i, m could be adjusted, because apart from the assumed homogeneous gravity there does not exist any other disturbance and the ballistic missile behaves as a *free spinning top* moving along a parabola segment.

In this section some typical physical parameters have been roughly estimated to support some examples which will be used during following chapters. The derivation of the ballistic missile's centre-of-mass dynamics and rotational dynamics (Euler's law) have been presented. The following section completes the derivation of a ballistic missiles dynamics by specifying the aerodynamic forces on an air-frame.

3.4 The aerodynamic flow around a slender body

The aerodynamic airflow around a slender body is generally far too complicated for an explicit description. The net aerodynamic forces and moments on any body are due to *shear stress distributions* and *pressure distributions* over the whole body, whereby for dynamical applications of a rigid body purely net forces and net moments applied to the centre of mass are of interest. A complete parameterization of any airflow around a rigid body then leads to the set of all possible net forces and net moments at this particular body. The fundamental relation between static pressure, dynamic pressure, and the pressure due to the air molecule's weight in an *ideal fluid*, *i.e.*, steady non-turbulent flow of a fluid which is incompressible and non-viscous, is given by Bernoulli's equation

$$p_i + (1/2)\rho_{\text{air}}v_i^2 + \rho_{\text{air}}gr_{3i} = \text{const.} \quad (3.55)$$

for the flow along the streamline, whereby ρ_{air} is the air density which is defined by

$$\rho_{\text{air}}(r_3) = \rho_{\text{air}}(0)e^{-gr_3}. \quad (3.56)$$

The requirements of an incompressible fluid for air are generally not fulfilled. However, the incompressibility approximation of air flow over many air frames, in particular streamlined bodies, is often sufficient. For a constant altitude r_3 , Bernoulli's equation becomes

$$p + (1/2)\rho_{\text{air}}(r_3)v^2 = \text{const.} \quad (3.57)$$

Far ahead and behind the body there is no dynamic pressure and the relation above states therefore that $p(0) = p_{\infty}(v) + (1/2)\rho_{\infty}(r_3)v_{\infty}^2$ whereby the subscript ∞ indicates the free-stream of air-flow far ahead of the moving body. The crucial parameters are thus

1. The magnitude of the free stream velocity, or Mach number
2. The attitude of the body towards the free stream
3. The rotational velocity of the body, because each coordinate \mathbf{r} of a three dimensional body has a velocity $\omega \times \mathbf{r}$ which changes its relative velocity towards the free stream, *i.e.* the Magnus force.
4. The air-density of the free stream.

Furthermore it will be assumed that the air-flow is not *explicitly* dependent on other parameters like thermodynamic variables (*e.g.* temperature) and not dependent on its accelerations relatively to any point on the body surface, since there is no aerodynamic force or torque described in the literature which is explicitly dependent on homogeneous fluid accelerations. When inhomogeneities in an air flow propagate along the body, forces and moments may change as well. This difficulty is avoided when the change of a body's relative velocity Δv_{rel} with a characteristic length l_d during the time interval $\Delta t = l_d/v_{\text{rel}}$ is very small in comparison to unity, *i.e.*, $1 \gg l_d v_{\text{rel}}/\Delta t$. The force and momentum equations of the aerodynamics incorporate 'static coefficients', which are in reality complex functions with respect to the angle of attack, control-surface deflection (not included in the considered ballistic missile), aerodynamic roll angle, and magnitude of velocity (Mach number), as well as 'dynamic coefficients' which are functions depending on the angle of attack rate, control-surface deflection rate (not modelled), aerodynamic roll angle, body rate, and Mach number. The aerodynamic momentum and force equations of a fixed shaped body can be completely described by the undisturbed airflow of magnitude v_{∞} , the actual bodies attitude \mathcal{R} , and its derivative $\dot{\mathcal{R}}$ towards the air flow, the air density ρ , and the bodies invariant surface (Anderson,

1991; Eichblatt, E.J., Jr, 1989).

$$\mathbf{f}_{ae} = \mathbf{C}_1(\psi_{rel}, \dot{\theta}_{rel}, \psi_{rel}, \theta_{rel}, \mathbf{v}_{rel}) A_S \rho_{\infty} \quad (3.58)$$

This equation describes the most general aerodynamic force on a ballistic rigid body with reference area A_S and a non-rotation-invariant surface of a body, *i.e.*, when the vector field $\mathbf{C}_1(\psi_{rel}, \dot{\theta}_{rel}, \psi_{rel}, \theta_{rel}, \mathbf{v}_{rel})$ is completely determined, the desired translational dynamical variables $\mathbf{x}, \dot{\mathbf{x}}$ may immediately be computed. The validity of \mathbf{C}_1 may in many cases even be simplified to $\mathbf{C}_1 = \mathbf{C}_1(\psi_{rel}, \theta_{rel}, \mathbf{v}_{rel})$. The torques on a missiles body are defined (Anderson, 1991; Eichblatt, E.J., Jr, 1989) by

$$\Gamma_{ae} = \mathbf{C}_2(\psi_{rel}, \theta_{rel}, \mathbf{v}_{rel}) \rho_{\infty} l_d A_S + \mathbf{C}_3(\psi_{rel}, \theta_{rel}, \psi_{rel}, \dot{\theta}_{rel}, \mathbf{v}_{rel}) \rho_{\infty} l_d^2 A_S. \quad (3.59)$$

with l_d the reference length of the body. Because the aerodynamics are still in a state where hardly any closed solutions for an air frame exist, the missile modeller has to rely on a sufficient set of data points which have to be interpolated. The assumption in most cases is that the data points are dense enough inside the parameter space in order to justify a first order approximation, such that all higher order terms of the Taylor series are negligible.

Again, the method introduced above can only be utilized if enough data is available. Throughout this project no data has been accessible which leads to the only alternative, the modelling of aerodynamic forces on a body with a fixed surface and its dependence on the aerodynamic parameters $C_d, C_l, \rho_{\infty}, \mathbf{r}, \dot{\mathbf{r}}, \phi, \dot{\phi}, \psi, \theta, \dot{\psi}, \dot{\theta}$. The flow around a body does not explicitly depend on the position of the body in the atmosphere. The implicit dependency comes into play by the changing air densities and variable wind velocities with respect to the earths surface which then leads to different relative wind velocities of the air flow around the body. The crucial drag and lift coefficient C_d, C_l depend on the Mach number of the relative air flow and even the attitude of the body towards the flow. Assuming that the body is approximately ideally controlled during the boost phase, the complex influences when the system runs through four different aerodynamic phases—the subsonic flow $v_{\infty} < 1\text{Mach}$, the transsonic flow $v_{\infty} \approx 1\text{Mach}$, the supersonic flow $v_{\infty} > 1\text{Mach}$, and the hypersonic flow $v_{\infty} \geq 5\text{Mach}$ —can then be omitted, and the only relevant flow during the sustain phase is the high supersonic and hypersonic flow. Supersonic and hypersonic flow are reasonably well described in terms of Newtonian impact theory (Anderson, 1991) as

$$\mathbf{F}_{ae,N} = A \sin^2 \theta \rho_{\infty} v_{\infty}^2, \quad (3.60)$$

with $\mathbf{F}_{ae,N}$ the normal force applying on the surface of impact, A being the total area and θ being the angle between the relative wind velocity and the tangent of the surface. This theory is not exact but produces results very close to actual measurements.

Air flow around a body may be represented by arbitrary Eulerian coordinate systems. Aerodynamic theory usually uses a coordinate system moving with the flow fields, where the crucial forces on a body are defined above to be the *drag* and *lift*. The airframe cones and the long cylinder appear to be circles of different size for a flow field orthogonal to the symmetry axis. The fins may be considered as a combination of flat triangles and rectangles with sharp edges mounted on a circular body. The ballistic missile considered here is due to the four identical fins axis-symmetric whereby the fin-deflection is neglected as an influence for the side wind forces. The following figure shows the stereographic projection which follows from the idealized Newtonian impact theory. The aerodynamic influences on the body are further simplified

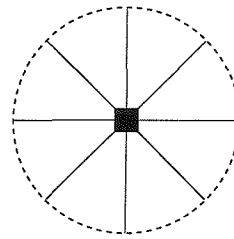


Figure 3.4: The body's symmetries are shown as a stereographic projection. The rectangle denotes the C_4 -symmetry due to rotations of $\pi/2$ about the e_3 -axis. The body has no symmetry to any plane vertically oriented to e_3 , i.e., the dashed circle. The solid lines are planes of reflection parallel to e'_3 under which the body is invariant if and only if the fin deflection may be neglected. The body is in this case D_4 -symmetric.

by approximating the three dimensional extensions of the body towards the free air flow by an effective area towards side winds as well as the axial flow. The area of the body's front is time invariant and consists of a circle and four identical rectangles. The effective area from the side is not time invariant and depends on the actual roll angle between a fin and the side wind. The cones and fins do not lie inside a plane which is orthogonal to the side wind. However, it is assumed that the simplification of the air frame as a convex surface with the characteristic drag/lift coefficient of each component approximate the aerodynamic properties of a real missile sufficiently well. The figure serves as an illustration of how the effective area of a ballistic body changes under rotation of the missile about the axis of roll symmetry. The effective area inside Figure 3.5 is the projection of the 3-dimensional body onto a 2-dimensional plane. The next theorem establishes the relationship between the angle ψ and the effective area as well as the centre of pressure.

THEOREM 3.4.1 *Four identical fins are mounted on a cylindrical tube with outer*

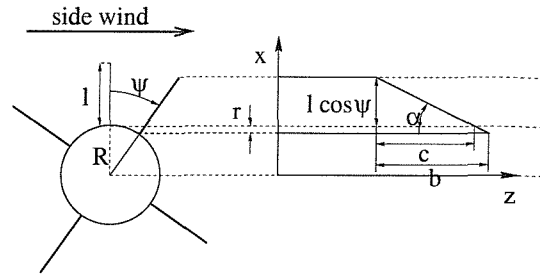


Figure 3.5: This figure shows a cross-section of the ballistic body perpendicular to the axis of symmetry. It may illustrate how the formation of the four fins contributes to the effective area of the whole body. Note that only the fin with the smaller angle $0 \leq \psi \leq \pi/4$ contributes to the effective area, the other fin is just inside the air shadow or in front of it.

radius R . Each fin is made of a triangle of base length b and height l and a rectangle of length L and height l . All fins are radial symmetric with respect to the tubes symmetry axis, and have the angular difference of $\pi/2$ between neighboured fins. The effective area of the combined body towards the side wind is

$$A_{\text{eff}} = A_{\text{sl}} + cd + 2dL \quad (3.61)$$

and the centre of pressure

$$r_{\text{cp}} = A_{\text{eff}}^{-1} [dL^2 + ((1/3)c + L)cd + z_{\text{sl}}A_{\text{sl}} - r_lA_{\text{eff}}], \quad (3.62)$$

with

$$x_{\text{cp}} = y_{\text{cp}} = 0, \quad (3.63)$$

whereby A_{sl} is the area of the slender body and z_{sl} the centre of pressure of the slender body and

$$c = b + bR/l - bR/(l \cos \psi) \quad (3.64)$$

$$d = l \cos \psi - R(1 - \cos \psi) \quad (3.65)$$

with $\psi \in [-\pi/4, \pi/4]$.

Proof: Consider $r = R(1 - \cos \psi)$ the effective area of each triangle is $A_{\text{tri}} = \frac{1}{2}cd$. Note that c follows immediately from calculating $\tan \alpha$ for the bases b and $c-d$ is given by the relation between d , r , and $l \cos \psi$. The common effective area is then $A_{\text{eff}} = 2(A_{\text{tri}} + A_{\text{rec}}) + A_{\text{sl}} = cd + 2Ld + A_{\text{sl}}$. The centre of pressure is therefore $A_{\text{eff}}r_{\text{cp}} = 2z_{\text{rec}}A_{\text{rec}} + 2(z_{\text{tri}} + L)A_{\text{tri}} + z_{\text{sl}}A_{\text{sl}}$ with $z_{\text{rec}} = L/2$ and $z_{\text{tri}} = (1/3)c$. x_{cp} and y_{cp} are automatically

given by the axis' symmetry. ■

After the geometric properties of the rotating body have been found the normal (side wind) force and the axial force for all ballistic missile components can be computed.

THEOREM 3.4.2 1. A circular cone has the axial force $f_a = \rho_\infty(v_{rel}^2)_a \pi r_1^2 \sin^2 \alpha$.

2. A cropped circular cone has the axial force $f_a = \rho_\infty(v_{rel}^2)_a \pi (r_2^2 - r_1^2) \sin^2 \alpha$.

3. Four fins with triangles of angle α lead to the axial force $f_a = 4\rho_\infty(v_{rel}^2)_a a \delta_f \sin^3 \alpha$.

4. The normal force on a cone is $f_n = (2/3)\rho_\infty(v_{rel}^2)_n \pi R$.

5. The normal force on a cropped cone is $f_n = (2/3)\rho_\infty(v_{rel}^2)_n \pi (r_2 - r_1)h$.

6. The normal force on a cylinder is $f_n = (4/3)\rho_\infty(v_{rel}^2)_n \pi R h$.

with α being the angle between axis and generator of the cone, r_1, r_2 the radii of cone and cropped cone, h the height of the cones and cylinder, a the length of the fins triangle hypotenuse, and δ_f the thickness of the fins.

Proof: For axial forces the C_4 -symmetry ensures that forces orthogonal to the symmetry axis cancel each other out. The pressure in the axial direction is therefore $\rho = \rho_\infty(v_{rel}^2)_a \sin^3 \alpha$. The surface integrals over the cone, cropped cone, and triangle lead immediately to $\int_0^R dr 2\pi r \rho / \sin \alpha = \pi R^2 \rho_\infty(v_{rel}^2)_a \sin^2 \alpha$. The total side force on a rotational symmetric body consists of the pressure on the half-shell, i.e., the normal forces on the cone are therefore $f_n = 2R\rho_\infty(v_{rel}^2)_n \int_0^{\pi/2} d\phi \cos^3 \phi \int_0^h dz (h - z/h) = \rho_\infty(v_{rel}^2)_n Rh |\sin \phi - 1/3 \sin^3 \phi|_0^{\pi/2} = 2/3 \rho_\infty(v_{rel}^2)_n Rh$. The surface integral over cylinder and cropped cone follow immediately by changing the limits of integration over r and z accordingly. ■

After the general axial and normal forces on the air frame have been derived the development of the computation is at the stage to return to the particular example of the ballistic missile with the measures as indicated in Figure 3.3. The aerodynamic forces may be calculated by inserting the measures into the formulae of Theorem 3.4.1 and 3.4.2 which then leads to the example below.

EXAMPLE 3.4.3 The fins have a thickness of 0.1m and the rest may be determined by utilizing Fig. 3.3. The common axial force is therefore

$$f_a = 0.1654 \rho_\infty(v_{rel}^2)_a. \quad (3.66)$$

The fins which are mounted on the cylinder are far more complicated with respect to normal forces, because they are not convex and the flow leads to vortices. The simplification is employed that the Newtonian impact theory may produce a normal force on the fin+cylinder section which is identical to a normal force on an effective area identical to the calculated above, i.e., $f = \rho_\infty(v_{rel}^2)_n A_{eff}$. The rest of the tube, including the fins which are in front or behind the tube's air shadow, is assumed to obey the normal force from above.

$$\begin{aligned} f_n &= (20.9622 + 3.3419c + cd + 2dL)\rho_\infty(v_{rel}^2)_n \\ &= 23.855 + 3.3465 \cos \psi + 1.51303 / \cos \psi \end{aligned} \quad (3.67)$$

the normal (side wind) force on the body can thus vary between

$$|f_n| \in [24.4465\rho_\infty(v_{rel}^2)_n, 22.8396\rho_\infty(v_{rel}^2)_n] \quad (3.68)$$

which is about 6.80% variation of the mean force. Since, this small change is of no significance for the model, the normal force will be chosen to be

$$f_n = 23.6431\rho_\infty(v_{rel}^2)_n \quad (3.69)$$

For a cropped cone the centre of pressure (for side wind) is at the coordinate $h((2/3)r_1 + (1/3)r_2)/(r_1 + r_2)$ when the base of the cone is given by the radius r_2 with $r_2 \geq r_1$ which coincides with the origin of the coordinate system and the height of the cone is h . (Note that the special case of a cone with $r_1 = 0$ and a cylinder with $r_1 = r_2$ is also included in the formula.) The centre of pressure for the slender body consists of the cylinder's centre of pressure at coordinate $(0, 0, 4.58 - z'_{CM})^T$, the centre of pressure of the cropped cone $(0, 0, 9.16 + 0.8297 - z'_{CM})^T$ and the cone's centre of pressure at $(0, 0, 9.16 + 1.91 + 0.1567 - z'_{CM})^T$ meters. The centre of pressure of the slender body thus becomes,

$$\begin{aligned} z_{cp_{sl}} &= (\pi/A_{sl})((2/3)r_1 0.47(9.16 + 1.91 + 0.1567 - z'_{CM}) \\ &\quad + (2/3)(r_2 - r_1)1.91(9.16 + 0.8297 - z'_{CM}) \\ &\quad + (4/3)r_2 9.16(4.58 - z'_{CM})) \text{ meters} \\ &= (1/A_{sl})(1.3386 + 5.5506 - 17.8270) = -1.6732 \text{ meters} \end{aligned} \quad (3.70)$$

with $z'_{CM} = 5.4404 \text{ meters}$ and $A_{sl} = 6.5371 \text{ meters}^2$. The centre of pressure follows immediately from Eq. (3.62)

$$\begin{aligned} z_{cp} &= \frac{2.56132 \cos^2 \psi + 0.052488(18.3555 \cos \psi - 1)(25.374 + \cos^{-1} \psi)}{5.5867 \cos \psi + 3.3465 \cos^2 \psi - 0.2916} \text{ meters} \\ &\quad - 5.4404 \text{ meters} \end{aligned} \quad (3.71)$$

The substitution of the value for $\psi = 0, \pi/4$ gives the centre of pressure $r_{cp} = -2.36378$ meters, -2.04127 meters, respectively, which means that the centre of pressure only varies by about 32.251 cm which is just about 15% of the total moment arm. Since a model is sought which is as simple as possible, it may be more convenient to include the variation of the centre of pressure into the noise of the model rather than employing the cumbersome formula (3.70). In order to allow a reasonable missile model it is further assumed that the persistent torque Γ_3 about the symmetry axis is applied due to fin deflection which seeks to accelerate the rotational velocity component ω_3 . Simultaneously the rotational motion of the missile is decelerated by the resistance of the body whilst rotating about the symmetry axis. It is assumed that the net effect is approximately zero, i.e., the axial symmetric rotation is in an equilibrium, i.e., Euler's equations are generally given for $\omega = (0, 0, \omega_3)$. An objection may be that the normal aerodynamic forces will still lead to torques that imply rotational motions with ω_1 and ω_2 non-zero. However, the perturbation of the equilibrium can be considered small in comparison with the torques which therefore dominate the change of the rotational velocity. Although the principle moments of inertia in $\mathbf{e}'_1, \mathbf{e}'_2$ -direction are comparatively large, $\mathcal{J}_{1,2} \approx 3500 \text{ kg} \cdot \text{meters}^2$ (see also Eqs. (3.25)–(3.27)), the normal forces are even larger due to the square of the velocities. The velocities are inside the range of $[2216/\sqrt{2} \text{ meter/sec}, 2216 \text{ meter/sec}$, i.e., the fraction $f_n r_{cp} / \mathcal{J}_1$ for $\theta_{rel} = 10^\circ$ is equal to $[6578, 13156] \rho_\infty$. θ_{rel} is the angle between the negative relative wind velocity and the \mathbf{e}'_3 -axis of the ballistic missile. The un-damped un-coupled equation for the oscillation of the ballistic missile about the equilibrium $\theta_{rel} = 0$ is well known to be $\mathcal{J}_1 \ddot{\theta}_{rel} = f_n r_{cp} \theta_{rel}$ with its characteristic frequency $\sqrt{f_n r_{cp} / \mathcal{J}_1}$. This means that for a driven damped oscillator of this form the resonance frequency is identical with $\sqrt{f_n r_{cp} / \mathcal{J}_1}$ (Scheck, 1990; Hestenes, 1986). Because the resonance frequency is that high the lift-forces cancel each other out over a short period of time. The disadvantage is that the damping is a quadratic term with respect to $\dot{\theta}_{rel}$ because the torque representing the drag through rotational velocity of the body depends on the square of the velocity. For low frequency oscillations the linear approximation of the drag-torque is sufficient and the perturbative dynamics of the ballistic missile could be numerically determined, because of the quadratic dependency only numerical solutions exist. The simplified dynamics of rigid bodies which are employed for the following computations

thus hold

$$\begin{aligned}\ddot{\mathbf{r}} &= \mathbf{g} + 23.6431m^{-1}\rho_\infty|\mathbf{v}_{rel}|(\mathbf{v}_{rel} \cdot \mathbf{e}'_1)\mathbf{e}'_1 + 23.6431\rho_\infty|\mathbf{v}_{rel}|(\mathbf{v}_{rel} \cdot \mathbf{e}'_2)\mathbf{e}'_2 \\ &\quad + 0.1654m^{-1}\rho_\infty|\mathbf{v}_{rel}|(\mathbf{v}_{rel} \cdot \mathbf{e}'_3)\mathbf{e}'_3\end{aligned}\quad (3.72)$$

$$\dot{\omega}'_{rel1} = -2\beta'\omega'^2_{rel1} + 23.6431\mathcal{J}_1^{-1}r_{cp}\rho_\infty|\mathbf{v}_{rel}|(\mathbf{v}_{rel} \cdot \mathbf{e}'_1)\Theta'_{rel1} \quad (3.73)$$

$$\dot{\omega}'_{rel2} = -2\beta'\omega'^2_{rel2} + 23.6431r_{cp}\mathcal{J}_2^{-1}\rho_\infty|\mathbf{v}_{rel}|(\mathbf{v}_{rel} \cdot \mathbf{e}'_2)\Theta'_{rel1} \quad (3.74)$$

$$\dot{\mathbf{r}} = \mathbf{v} \quad (3.75)$$

$$\dot{\Theta}'_{rel} = \omega' \quad (3.76)$$

whereby ρ_∞ depends on the altitude of the missile and β' should be measured from some data, and Θ' is the angle between negative relative wind velocity and symmetry axis \mathbf{e}'_3 . When no data for β' is available an estimate for β' may be employed. Since the centre of pressure is $r_{cp} = -2.20352$ meter and the side wind force is f_n and the air frame rotates with frequency $\dot{\Theta}'_{rel}$ the corresponding wind velocity due to the rotation is approximately $v_{rot} = r_{cp}\dot{\Theta}'_{rel}$, thus the torque on the air frame becomes approximately

$$\beta' = 114.70\rho_\infty \frac{\Theta'^2_{rel,max}}{\omega'^2_{rel}2\mathcal{J}_2} \quad (3.77)$$

Note, that $114.70/(2\mathcal{J}_1) = 0.0165$ is a very small number which implies that the system is only weakly damped. The solutions of the dynamical system is still not explicitly computable but a upper bound for $\dot{\Theta}_{rel}$, \mathbf{f} may be found by introducing the maximum velocity into the damping coefficient. Instead of utilizing ω'^2_{rel} , or $|\mathbf{v}_{rel}|\mathbf{v}_{rel}$, the quadratic function is substituted with $\omega'^2_{max}\omega'_{rel}$, or $|\mathbf{v}_{rel}|_{max}\mathbf{v}_{rel}$. The approximate dynamics can then be solved analytically (Scheck, 1990) when the wind velocity inside the inertial frame of reference is given. The purpose of this chapter is devising an algorithm for dynamical system identification, i.e., the explicit computation of the linearized simplified dynamics of the ballistic missile are not presented here. It is thus sufficient to shortly summarize the required computations. By realizing that the factor $23.6431r_{cp}\rho_\infty|\mathbf{v}_{rel}|(\mathbf{v}_{rel} \cdot \mathbf{e}'_2)$ is independent of Θ' it becomes evident that Eqs. (3.73), (3.74) hold the form of a standard damped oscillator (Hestenes, 1986; Scheck, 1990). When the relative wind velocity is decomposed in the components perpendicular and anti-parallel to the missiles' velocity vector, the rotational motion may be rewritten in terms of a first order approximation for ω^2 which gives

$$\dot{\omega}_{rel1} = -2\beta\omega_{rel1} + 23.6431r_{cp}\rho_\infty|\mathbf{v}_{rel}|(\mathbf{v}_{rel} \cdot \mathbf{v})/\mathcal{J}_1\Theta_{rel1} + \Gamma_1(t)/\mathcal{J}_1 \quad (3.78)$$

$$\dot{\omega}_{rel2} = -2\beta\omega_{rel2} + 23.6431r_{cp}\rho_\infty|\mathbf{v}_{rel}|(\mathbf{v}_{rel} \cdot \mathbf{v})/\mathcal{J}_2\Theta_{rel2} + \Gamma_2(t)/\mathcal{J}_2 \quad (3.79)$$

$$\Gamma_1(t) = 23.6431r_{cp}\rho_\infty|\mathbf{v}_{rel}|(\mathbf{v}_{rel} \cdot \mathbf{e}_i) \quad (3.80)$$

where Γ_i represents the torque in direction of a vector i perpendicular to \mathbf{v} and \mathbf{e}_1 , \mathbf{e}_2 are pair-wise orthogonal to each other as well. This model can immediately be integrated (Marion and Thornton, 1995) to

$$\theta_{rel_i} = \int_{-\infty}^t dt' \Gamma_i(t') Gr_i(t, t') dt' \quad (3.81)$$

$$Gr_i(t, t') = \begin{cases} \frac{1}{J\omega_{n_i}} e^{-\beta(t-t')} \sin \omega_{n_i}(t-t'), & t \geq t' \\ 0, & t < t' \end{cases}, \quad (3.82)$$

where $Gr(\bullet)$ indicates the Greens function with

$$\omega_{n_i} = \sqrt{23.6431 r_{cp} \rho_{\infty} |(\mathbf{v}_{rel} \cdot \mathbf{v}) / J - \beta^2|}. \quad (3.83)$$

Eq. (3.81) defines the angle between relative wind velocities and body axis and thus implies the dynamics of \mathbf{e}'_1 , and \mathbf{e}'_2 . Due to the linearisation a closed form of the ballistic missile model has been found which now reads as

$$\begin{aligned} m\dot{\mathbf{v}} &= m\mathbf{g} - 23.6431 \rho_{\infty} |\mathbf{v}_{rel}|^2 \sum_{i=1}^2 \theta_{rel_i} \mathbf{e}'_i \\ &\quad - 0.1654 \rho_{\infty} |\mathbf{v}_{rel}|^2 \left(1 - \sum_{i=1}^2 \theta_{rel_i}^2 \right) \mathbf{e}'_3 \end{aligned} \quad (3.84)$$

$$\theta_{rel_1} = \int_{-\infty}^t dt' \Gamma_1(t') Gr_1(t, t') dt' \quad (3.85)$$

$$\theta_{rel_2} = \int_{-\infty}^t dt' \Gamma_2(t') Gr_2(t, t') dt' \quad (3.86)$$

$$\mathbf{v}_{rel} = \mathbf{v} - \mathbf{v}_{wind}(\mathbf{x}, t) \quad (3.87)$$

whereby \mathbf{v}_{wind} is an arbitrary environment specific function with respect to the spatial coordinate \mathbf{x} and time t . It is apparent that in real life experiments the wind velocities are the system's variables without an experimenter's influence. For demonstration purposes an arbitrary wind velocity function will be assumed which is a sequence of finite impulse functions with finite width Δt , i.e., a superposition of a finite set of step functions with arbitrary finite magnitude, such that the time mean of the relative angles

θ_{rel_i} is zero and time mean of the wind velocity holds $\bar{\mathbf{v}}_{wind} \perp \mathbf{v}$.

$$\begin{aligned} m\dot{\mathbf{v}} &= m\mathbf{g} - 23.6431\rho_{\infty}|\mathbf{v}|^2 \sum_{i=1}^2 \theta_{rel_i} \mathbf{e}'_i \\ &\quad - 0.1654\rho_{\infty}|\mathbf{v}|^2 \left(1 - \sum_{i=1}^2 \theta_{rel_i}^2 \right) \mathbf{e}'_3 \end{aligned} \quad (3.88)$$

$$\begin{aligned} \theta_{rel_1} &= 23.6431 \frac{\rho_{\infty} r_{cp} \Delta t}{\mathcal{J}_1 \omega_n} \sum_{j=-\infty}^N |\mathbf{v}_{wind_j}|^2 (\mathbf{v}_{wind_j} \mathbf{e}'_1)^2 \\ &\quad \times \exp(-\beta(t - t_j)) \sin \omega_n(t - t_j) \end{aligned} \quad (3.89)$$

$$\begin{aligned} \theta_{rel_2} &= 23.6431 \frac{\rho_{\infty} r_{cp} \Delta t}{\mathcal{J}_2 \omega_n} \sum_{j=-\infty}^N |\mathbf{v}_{wind_j}|^2 (\mathbf{v}_{wind_j} \mathbf{e}'_2)^2 \\ &\quad \times \exp(-\beta(t - t_j)) \sin \omega_n(t - t_j) \end{aligned} \quad (3.90)$$

In Chapter 6 it will become necessary to estimate the mean lift- and drag coefficients which requires the squared angle $\theta_{rel_i}^2$ in order to compute the total drag/lift force over a certain time interval $\propto \Delta t$. It is easy to realize that the integral over the RHS of Eqs. (3.89) & (3.90) is proportional to the integral

$$\begin{aligned} \int_0^{l\Delta t} dt' \sin \omega_n t' \exp(-\beta t') &= \\ \frac{\omega_n}{\beta^2 + \omega_n^2} - \frac{\exp(-\beta l\Delta t)}{\beta^2 + \omega_n^2} (\omega_n \cos(\omega_n l\Delta t) + \beta \sin(\omega_n l\Delta t)) & \end{aligned} \quad (3.91)$$

and the squared angles in Eqs. (3.89) & (3.90) lead to expressions like

$$\begin{aligned} \sum_{j,j'=1}^N \int_0^{l\Delta t} dt \sin \omega_n(t - t_j) \sin \omega_n(t - t_{j'}) \exp(-\beta(2t - (t_j + t_{j'}))) &= \\ = \frac{1}{4} \sum_{j,j'=1}^N \int_0^{2l\Delta t - (t_j + t_{j'})} dt' \exp(-\beta t') [\cos \omega_n(t_{j'} - t_j) - \cos t'] & \\ = \frac{1}{4} \sum_{j,j'=1}^N \frac{\cos \omega_n(t_{j'} - t_j)}{\beta} [1 - \exp(-\beta 2l\Delta t - \beta(t_j + t_{j'}))] & \\ + \frac{\exp(-\beta 2l\Delta t - \beta(t_j + t_{j'}))}{\beta^2 + \omega_n^2} & \\ \times [\beta \cos(\omega_n(2l\Delta t - (t_j + t_{j'}))) - \omega_n \sin(\omega_n(2l\Delta t - (t_j + t_{j'})))] & \\ - \frac{b}{b^2 + \omega_n^2} & \end{aligned} \quad (3.92)$$

with $t' = 2t - (t_j + t_{j'})$. Both, Equations (3.91), (3.92) can significantly be simplified if $\Delta t = 2\pi/\omega_n$, because the sinus- and co-sinus functions become either 0 or ± 1 and the

expressions become

$$\int_0^{l\Delta t} dt' \sin \omega_n t' \exp(-\beta t') = \omega_n \frac{1 - \exp(-\beta l 2\pi/\omega_n)}{\beta^2 + \omega_n^2} \xrightarrow{l \rightarrow \infty} \frac{\omega_n}{\beta^2 + \omega_n^2} \quad (3.93)$$

$$\begin{aligned} \frac{1}{4} \sum_{j,j'=1}^N \int_0^{2l\Delta t - (t_j + t_{j'})} dt' \exp(-\beta t') [\cos \omega_n (t_{j'} - t_j) - \cos t'] \\ = \frac{1}{\beta} [1 - \exp(-\beta 2l\Delta t - \beta(t_j + t_{j'}))] \\ + \frac{\beta}{\beta^2 + \omega_n^2} \{\exp(-\beta 2l\Delta t - \beta(t_j + t_{j'})) - 1\} \\ \xrightarrow{l \rightarrow \infty} \frac{\omega_n^2}{\beta(\beta^2 + \omega_n^2)} \end{aligned} \quad (3.94)$$

It has just become evident that for the choice of $\Delta t = 2\pi/\omega_n$ the angles θ_i as well as the squared angles θ_i^2 are mainly functions of ω_n^2 and b^2 which exponentially increase their effect on the dynamics as time passes by. The maximum is a finite value which can only be reached as the time converges to infinity. For demonstration purposes it is sufficient to consider the mean lift- and drag-coefficients as approximations given by the limits in Eq. (3.93) and Eq. (3.94) which then lead to the mean translational dynamics of a ballistic body

$$\dot{\bar{\mathbf{v}}} = \mathbf{g} - 23.6431 m^{-1} \rho_\infty |\bar{\mathbf{v}}|^2 \sum_{i=1}^2 \theta_{rel_i} \mathbf{e}'_i \quad (3.95)$$

$$- 0.1654 m^{-1} \rho_\infty |\bar{\mathbf{v}}|^2 \left(1 - \sum_{i=1}^2 \theta_{rel_i}^2 \right) \mathbf{e}'_3$$

$$\bar{\theta}_{rel_i} = 23.6431 \frac{\rho_\infty r_{cp}}{l \mathcal{J}(\beta^2 + \omega_n^2)} \sum_{j=-\infty}^N |\mathbf{v}_{wind_j}|^2 (\mathbf{v}_{wind_j} \mathbf{e}'_i)^2 \quad (3.96)$$

$$\bar{\theta}_{rel_i}^2 = 559.00 \frac{\rho_\infty^2 r_{cp}^2 \Delta t}{l \mathcal{J}^2 \beta (\beta^2 + \omega_n^2)} \sum_{j,j'=-\infty}^N |\mathbf{v}_{wind_j}|^2 (\mathbf{v}_{wind_j} \mathbf{e}'_i)^2 |\mathbf{v}_{wind_{j'}}|^2 (\mathbf{v}_{wind_{j'}} \mathbf{e}'_i)^2 \quad (3.97)$$

with l the multiplicity of the time interval Δt over which the mean angles and mean squared angles are taken. As can easily be seen from the formulae given in Eqs. (3.96) & (3.97), for large l Eq. (3.95) converges to the trivial drag-force equation

$$m \dot{\bar{\mathbf{v}}} = m \mathbf{g} - 0.1654 \rho_\infty |\bar{\mathbf{v}}| \bar{\mathbf{v}}. \quad (3.98)$$

It also follows from Eq. (3.95)–(3.97) that the time dependence of θ_{rel_i} with respect to t approximately leads to a perturbative lift- and drag-force which respectively is proportional to $\exp(-\beta(t - t_j)) \sin \omega_n(t - t_j)$, $\exp(-2\beta t) \sin \omega_n(t - t_j) \sin \omega_n(t - t_{j'})$ and thus leading to a perturbative spatial translation which is of similar form,

$$\delta r'_{1,2} = 559.00 \frac{\rho_\infty^2 r_{cp} \Delta t}{m \mathcal{J}_{1,2} \omega_n} |\bar{\mathbf{v}}_j|^2 \sum_{j=-\infty}^N |\mathbf{v}_{wind_j}|^2 (\mathbf{v}_{wind_j} \mathbf{e}'_{1,2})^2 \quad (3.99)$$

$$\begin{aligned} & \times \left[\exp(-\beta t') \frac{\beta^2 - \omega_n^2}{(\beta^2 + \omega_n^2)^2} \sin \omega_n t' + \frac{\beta \omega_n \exp(-\beta t')}{(\beta^2 + \omega_n^2)^2} \cos \omega_n t' \right] \Big|_{t'=t_0}^{t'=t} \\ \delta r'_3 &= 92.457 \frac{\rho_\infty^3 r_{cp}^2 \Delta t^2}{m \mathcal{J}_{1,2} \omega_n^2} |\bar{\mathbf{v}}_j|^2 \sum_{j,j'=-\infty}^N |\mathbf{v}_{wind_j}|^2 (\mathbf{v}_{wind_j} \mathbf{e}'_i)^2 |\mathbf{v}_{wind_{j'}}|^2 (\mathbf{v}_{wind_{j'}} \mathbf{e}'_i)^2 \\ & \times \left[\beta^{-2} \exp(-\beta t') \cos \omega_n(t_{j'} - t_j) - \frac{\beta^2 - \omega_n^2}{(\beta^2 + \omega_n^2)^2} \exp(-\beta t') \cos \omega_n t' \right. \\ & \left. + 2 \frac{\beta \omega_n \exp(-\beta t')}{(\beta^2 + \omega_n^2)^2} \sin \omega_n t' \right] \Big|_{t'=t_0}^{t'=t} \end{aligned} \quad (3.100)$$

Although Eqs. (3.99), (3.100) are only approximations of the real non-linear dynamics of a ballistic missile they nicely illustrate the qualitative behaviour of such a missile. The drag and lift forces applied to a ballistic missile vary as the angles periodically vary with time. Eqs. (3.99), (3.100) serve also as an example in Chapter 6 to illustrate the effect of uncertainties in non-linear dynamics for prediction purposes. As an illustrative example the following parameter values have been chosen in their according SI units

$$\beta = 1 \text{Hz} \quad (3.101)$$

$$\omega_n = 6.804 \text{Hz} \quad (3.102)$$

$$\mathcal{J}_{1,2} = 3.583 \cdot 10^4 \text{kg} \cdot \text{meters}^2 \quad (3.103)$$

$$m = 1781.2 \text{kg} \quad (3.104)$$

$$\Delta t = 1 \text{sec} \quad (3.105)$$

$$\rho_\infty = 0.3506 \text{kg} \cdot \text{meters}^{-3} \quad (3.106)$$

$$r_{cp} = 2.203 \text{meters} \quad (3.107)$$

$$|\bar{\mathbf{v}}_j| = 7 \cdot 340.9 \text{meters/sec} \quad (3.108)$$

$$|\mathbf{v}_{wind_j}| = 0.05 \cdot 340.9 \text{meters/sec} \quad (3.109)$$

$$N = 1 \quad (3.110)$$

such that

$$\delta r'_1 = 84.7347 \text{ meters} \quad (3.111)$$

$$\times \left[-4.6583 \cdot 10^{-4} \exp(-t') \sin \omega_n t' + 1.007 \cdot 10^{-5} \exp(-t') \cos \omega_n t' \right] \Big|_{t'=t_0}^{t'=t}$$

$$\begin{aligned} \delta r'_3 &= 1.8955 \cdot 10^{-3} \text{ meters} \\ &\times \left[\exp(-t') + 4.6388 \cdot 10^{-4} 4^{-1} \exp(-2t') \cos \omega_n t' \right. \\ &\quad \left. + 4.0151 \cdot 10^{-5} \exp(-2t') \sin \omega_n t' \right] \Big|_{t'=t_0}^{t'=t} \end{aligned} \quad (3.112)$$

which can be easily visualised in the following graphs

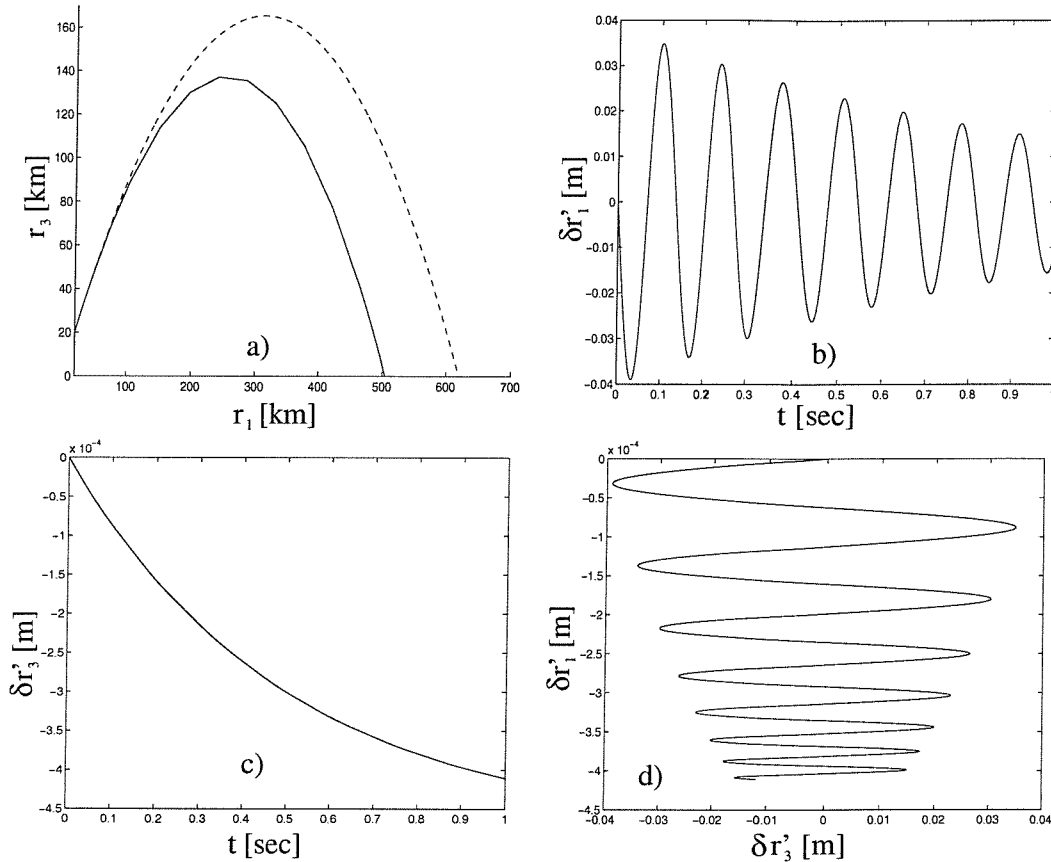


Figure 3.6: This figure shows the effect of lift and drag forces on a ballistic body given by Eq. (3.98) and Eqs. (3.111)–(3.112). Sub-figure a) shows the result (solid line) of Eq. (3.98) as well as the parabola (dashed line) $\mathbf{r} = 2^{-1} \mathbf{g} t^2 + \mathbf{v}_0 t + \mathbf{r}_0$ for comparison. In both cases the initial conditions are $\mathbf{g} = (0, -9.81)^T \text{ meters/sec}^2$, $\mathbf{v}_0 = 1687.37(1, 1)^T \text{ meters/sec}$, $\mathbf{r}_0 = (0, 20000)^T \text{ meters}$. Sub-figure b) shows $\delta r'_1$ as a function of t . Sub-figure c) shows $\delta r'_3$ as a function of t and sub-figure d) shows a $\delta r'_1 - \delta r'_3$ -plot.

After a simplified state space model has been devised the question arises, how well do the dynamics given by Eq. (3.72)–(3.76) approximate a real-life model including all errors in the measurement etc. Strictly speaking this question cannot be answered, even when some real measurements were available. The reason for that is, that radars can only estimate the velocity and position of a ballistic missile. As the simplified model demonstrates the rotational velocity and attitude of the missile's frame of reference with respect to the inertial frame of reference have to be given as well. It is not clear how the errors due to the necessary approximations in the dynamics and the measurement errors enter the dynamics. As mentioned in Chapter 2 the available statistical models can for example perform regression analysis, *i.e.*, the answer provided by the statistical models is to the question which function fits best when assumptions about the underlying noise are being made. Regression analysis cannot be applied in this case since the non-linear function inside the state's (\mathbf{r}, \mathbf{v}) sub-space is dependent on remaining state variables $\omega'_{\text{rel}}, \dot{\omega}'_{\text{rel}}$ which are not measurable, *i.e.*, there is no explicit known function which may be fitted to the data points. Stochastic models such as the Kalman filter are only applicable when the state space dynamics and the stochasticity are explicitly known. The expected answer from employing the Kalman filter to the state space model Eq. (3.72)–(3.76) under the assumption of Gaussian noise with the conjecture of some variance is the estimate of a best parameter set (*e.g.* the mass, ρ_∞ , the principle moments of inertia, etc.) given some past measurements. The problem with this approach is, that the probability density inside the (\mathbf{r}, \mathbf{v}) space does not necessarily have to be initially Gaussian, nor even stay Gaussian as time progresses. The 'best' estimate does not even have to be the best physical estimate. Because there is neither an algorithm available which allows us to establish the state space model itself when only a time series of a few corrupted state vector components are given nor do there exist any statistical models which allow the incorporation of partial physical knowledge to limit the number of possible (\mathbf{r}, \mathbf{v}) sub-state space trajectories. The only technique which remains after the modelling constraints, that neither the stochasticity of the physical model is known nor that the class of functions inside the (\mathbf{r}, \mathbf{v}) sub-state space is given, are imposed is non-linear statistical black-box modelling which seeks to extract qualitative information about the probabilistic distribution inside the (\mathbf{r}, \mathbf{v}) space. This very general approach towards data modelling is presented in the following section.

3.5 Non-linear statistical modelling of time series

Non-linear systems have been shown to exhibit some new qualitative behaviour which is summarized under the name *deterministic chaotic* systems. In order to classify and quantify these dynamics a novel set of statistical tools have been developed over the last two decades (Takens, 1981; Ruelle and Takens, 1971; Ruelle, 1990; Ott, 1993; Abarbanel, Carroll, Pecora, Sidorowich and Tsimring, 1994; Beck and Schlögel, 1995; Tong, 1995; Kantz and Schreiber, 1997). As these methods are statistical a sufficient number of data points are required and the data points have to lie sufficiently densely packed inside the state space. As physical experiments do not allow an arbitrary set of data points this requirement can never be met. However, when the statistical model is confined to a certain subset of the state space, then it has to be proved that for physically viable state vectors the trajectory never leaves the part of the state space under consideration and that this subset of the state space is evenly densely packed with data points. Before these statistical methods are introduced, let us reconsider the general form of a ballistic missile's state space. As it has been argued in this chapter previously, the dynamics of a rigid body (*e.g.* a missile after the boost phase) are described completely by Newton's and Euler's equations.

$$\dot{\mathbf{v}} = -(1/m)(\mathbf{f}_{\text{gr}} + \mathbf{f}_{\text{ae}}) \quad (3.113)$$

$$\dot{\mathbf{r}} = \mathbf{v} \quad (3.114)$$

$$\mathcal{J}\dot{\omega} = -\omega \times \mathcal{J}\omega + \Gamma_{\text{ae}} \quad (3.115)$$

$$\dot{\omega} = \dot{\mathcal{R}} \quad (3.116)$$

$$\dot{\mathbf{v}}_w = \mathbf{F}(\mathbf{v}_w, s) \quad (3.117)$$

$$\rho_{\infty} = \rho_{\infty}(\mathbf{r}, s) \quad (3.118)$$

$$\frac{ds}{dt} = 1 \quad (3.119)$$

This physical insight in the aerodynamic influences on the body gained by the above analysis suggests the use of a *phase space*, or *state space*, of the rigid body together with the wind velocity \mathbf{v}_w and the general non-linear C^1 -function \mathbf{F} defined by

$$\mathbf{x}(t) = (\mathcal{R}, \omega, \mathbf{r}, \dot{\mathbf{r}}, \mathbf{v}_w, s)(t) \quad (3.120)$$

$$\dot{\mathbf{x}}(t) = \mathbf{F}(\mathbf{x}(t)). \quad (3.121)$$

The dependence of aerodynamic forces on the air density ρ_{∞} is implicitly given by Equ. 3.56 and is therefore incorporated in the map above. The wind velocity is defined in the inertial frame of reference of the observer but transforms immediately to $\psi_{\text{rel}}, \dot{\psi}_{\text{rel}}, \theta_{\text{rel}}, \dot{\theta}_{\text{rel}}$ by employing the attitude \mathcal{R} of the body. The non-linear

mapping (3.120) contains 16 components where all are elements of the real line but the three attitude components which are defined on a compact continuous set of real numbers. It is due to the celebrated Cauchy theorem (Scheck, 1990; Arnold, 1978) that a system given in form of Eq. (3.120) is a deterministic one, *i.e.*, for each arbitrary state inside the state space there exists one and only one other state which the system is in after a time interval dt . This means that trajectories inside the state space cannot intersect.

As it turns out some non-linear models of the state space, such as the Duffing oscillator, the Lorenz attractor, Mackey-Glass dynamics, etc., can exhibit some behaviour which leads to a *strange attractor* inside the state space. It is often assumed that the underlying non-linear dynamics follow an attractor with considerably lower dimension than the dimension n of the entire state space (Kantz and Schreiber, 1997; Ott, 1993). However, in many cases this assumption is not true and dynamics do not have any attractors which are of lower dimension or more easily understandable than the state space model itself. However, there are some stochastic systems, where the methodology of non-linear statistics can be applied (*e.g.* Kantz and Schreiber (1998, Schreiber and Kantz (1998). The question therefore arises as to whether the methodology is suitable to be employed in the case of ballistic missile dynamics, when only a time series is being presented. As it is clear from the prerequisite of chaotic statistics which require densely spaced data inside the state space, then initially it would appear these methodologies cannot be applied since the state space model leads to a time series which does not represent the entire state vectors of the dynamics, and also the data is not evenly dense inside the state space. The viable option is to use non-linear statistics to (i) pre-process the data to gain a ‘state space’ model which leads to a state distribution with a small variance in the state vectors probability distribution, and to (ii) employ a method that reconstructs the state space.

3.5.1 Time Series pre-processing for Grey-box modelling

Sjöberg et al. (1995) and Juditsky et al. (1995) suggested an algorithm for pre-processing data when physical knowledge is available. Here, an algorithm for non-linear semi-physical modelling of a ballistic missile is suggested which is based on the physics introduced in the previous sections. Essentially, the following prior physical knowledge will be assumed.

1. The aerodynamic force is independent of \mathbf{r} and only depends $\rho(r_3)$, the origin of inertial frame of reference is therefore arbitrary.

2. The unpredictability comes into play only by variations in the aerodynamic forces on the body.
3. The body is self-stabilizing, *i.e.*, the main flight direction of the body is with the tip in the relative wind direction.
4. According to the three above pointers the principle trajectory of an unperturbed ballistic body is given by the differential equation

$$\ddot{\mathbf{r}} = (0, 0, -g)^T - \bar{D}\rho(\bar{r}_3) |\dot{\mathbf{r}}| \dot{\mathbf{r}} \quad (3.122)$$

which immediately can be integrated to give a unique solution when an estimate for the initial velocity $\dot{\mathbf{r}}$ and spatial coordinate \mathbf{r} and the temporal mean of a drag coefficient \bar{D} are given.

The mean drag coefficient may be employed to compute a mean trajectory which then serves as an origin for a coordinate system that moves along this nominal trajectory with time. The orientation of the coordinate system should follow the actual nominal (unperturbed) direction of the ballistic missile's flight path at each point of the mean trajectory. The trajectory obviously points into the direction as $\dot{\mathbf{r}}$, which therefore suggests the use of the vector of unity $\mathbf{e}_{\dot{\mathbf{r}}} = \dot{\mathbf{r}}/|\dot{\mathbf{r}}|$ to build up an appropriate basis of such a coordinate system

$$\left\{ \mathbf{e}_{\dot{\mathbf{r}}}, \frac{\mathbf{e}_{\dot{\mathbf{r}}} \times \mathbf{e}_3}{\|\mathbf{e}_{\dot{\mathbf{r}}} \times \mathbf{e}_3\|}, \frac{\mathbf{e}_{\dot{\mathbf{r}}} \times \mathbf{e}_3}{\|\mathbf{e}_{\dot{\mathbf{r}}} \times \mathbf{e}_3\|} \times \mathbf{e}_{\dot{\mathbf{r}}} \right\} \quad (3.123)$$

(see also Eq. (1.5)). This new coordinate system is utilized to compute a vector \mathbf{r} with respect to this new coordinates. This algorithm leads to a three-dimensional trajectory about the mobile origin which may then be employed to perform the regular non-linear statistical analysis. Note, this transformation applied to the time series removes the general trend in the time series. The obvious advantage is twofold. Firstly, the net-dynamics of \mathbf{r} contain only the perturbation of the ballistic missile during its flight. Secondly, the desired aim was a state space model with more densely packed state vectors. Because the net-dynamics remove the trend the reconstruction algorithm described in the next section is trend-free as well, which implies that the reconstructed state space is more densely packed with state vectors. It is important to realize that if, apart from the spatial coordinates, other state vector components may be given as well, these components have to be changed according to the net-dynamics which have to be computed according to the dynamics given by Eq. (3.122) and the Basis (3.123).

The time series pre-processing algorithm thus works as follows:

1. Approximate the nominal trajectory of a body by utilizing, apart from the gravitational force, a pure mean drag force.
2. Employ the new coordinate system to calculate the difference vectors (like attitude, velocities, etc.) between reference frame and the new one.
3. Due to Cauchy's theorem the dimension of the deterministic dynamics is 16 which does not change by adding a C^1 -function to the vector field and Taken-Whitney's theorem (Whitney, 1936; Takens, 1981) may now be utilized to reconstruct the state space.

3.5.2 State space reconstruction and Non-linear statistical analysis

As shown in the previous section in Eqs. (3.120), (3.121) the dimension of the deterministic ballistic missile model is 16. When no complete state vector from the phase space is available, *e.g.* only the coordinate vector \mathbf{r} may be measurable as it is the case in the section above, the state space has to be reconstructed by either employing time derivatives of \mathbf{r} , or better, by utilizing delay coordinates to generate time-delay vectors

$$\mathbf{s}_i = [\mathbf{r}_i, \mathbf{r}_{i-\tau}, \dots, \mathbf{r}_{i-(n'-1)\tau}] \quad (3.124)$$

which may be utilized for reconstructing the map between two successive time-delay vectors. The number of employed time-delay components n' depends on the chosen embedding dimension which is n' multiplied with the number of components of \mathbf{r}_i , and τ a sufficient time delay. Taken's theorem ((Takens, 1981)) guarantees that there exists a diffeomorphism between the original state space and the reconstructed state space, if and only if the time series is noise free and a sufficient *embedding dimension* is chosen to be

$$d_{\text{embedding}} \geq 2d_{\text{attractor}} + 1 \quad (3.125)$$

The critical issue here is the *generic intersections* of a trajectory with itself inside the reconstructed state space when the chosen dimension is made too small. The condition (3.125) gives an estimate when this intersection cannot occur, which means that information about the dimensionality of the attractor of the underlying non-linear dynamics is required. As stated above in most cases the attractor, which can have non-integer dimensionality, is not smaller than the dimension of the dynamics, which means that in our case $d_{\text{embedding}} \geq 2 \cdot 16 + 1 = 33$ and n' may be chosen to be 11. Still, all

these considerations are only valid for the noise free case. As soon there is a stochastic driving force inside the dynamics, as it has to be assumed there is in our case, Taken's theorem no longer applies. However, an extension of Taken's theorem exists for the case that the fluctuating driving terms are explicitly known (Casdagli, 1992; Stark, Broomhead, Davies and Huke, 1997; Stark, 1999). Despite these difficulties with noise, it is assumed in the following that Taken's theorem can be utilized. The next section concentrates on the issues to optimise the reconstruction technique.

For a finite amount of data the choice of the time delay τ is critical: When τ is chosen to be too small, the reconstructed attractor is squashed along the phase space diagonal, whereas a τ which is too large leads to the effect that the noise dominates the reconstructed dynamics, *i.e.*, information about the dynamics has been lost (Gershenson, 1988). One approach of choosing τ is based on different autocorrelation methods, in which τ has to be a fraction of autocorrelation time which is chosen by either algorithm.

- The first zero (or the minimum) of the autocorrelation function (Holzfuss and Mayer-Kress, 1986).
- The e-folding time of the autocorrelation function (Frank, Lookman and Nerenberg, 1990)).
- The time, at which the autocorrelation function is equal to 0.5 (Schuster, 1989).
- $(1/10)^{th}$ of the time of the first minimum of the autocorrelation function (Abarbanel, Brown and Kadtke, 1990).

However, the problem is that a number of data sets of an identical underlying physical system show increasing autocorrelation times as the data set length increases (Prichard, 1993). In that case there are mutual information based methods available.

- Choosing the time delay based on the mutual information between the components of the vector. τ is then be chosen to be equal to the first minimum of the mutual information (Fraser and Swinney, 1986).
- One method uses the relation between the mutual information and the generalised correlation integral (Liebert and Schuster, 1988; Theiler, 1986).
- Or using higher order correlation coefficients (Albano, Passamante and Farrel, 1992).

- There are also suggestions to measure distances, which are spanned by the vectors with indices of a ‘window width’ $(d' - 1) \cdot \tau$, which is assumed to be more physically related quantity than the pure embedding dimension (Albano, Muench, Schwartz, Mees and Rapp, 1988; Broomhead, Jones and King, 1987; Gibson, Farmer, Casdagli and Eubank, 1992; Grassberger, 1986).
- Also a good estimate is 1 – 2 times the dominant period of the system (Ruelle and Takens, 1971).

The last methods which are supposed to provide tools for estimating the usefulness of a specific choice of time delays are all based on some statistics, *i.e.*, there is a certain density of data points in the reconstructed state space which is necessary to make some sensible statistics possible.

Returning to our Example 3.4.3, where it is shown that the resonance frequency is within the interval $\rho_\infty[6578, 13156]/\text{sec}$. Following the above arguments τ may be chosen according to the autocorrelation function. Because the periodicity of the time series will be approximately identical to the inverse of the resonance frequency, it can be expected that τ will be within the magnitude of $\rho_\infty^{-1}[7.601, 15.202] \cdot 10^{-5}\text{sec}$.

In principle the state space reconstruction technique may be used for the direct measured time series as well but the sparse density of data points may jeopardise any kind of statistics. To get a more qualitative description of the dynamics the dimension of the attractor may be calculated, which is most easily done by utilizing the box counting dimension

$$D(2) = \lim_{\varepsilon \rightarrow 0} \frac{\ln C(\varepsilon)}{\ln \varepsilon}, \quad (3.126)$$

with the correlation integral $C(\varepsilon) = 2/((N - W)(N - W - 1)) \sum_{j=W}^N \sum_{i=1}^{N-j} \Theta(\varepsilon - \|s_i - s_j\|)$ where $\Theta(\bullet)$ is the Heaviside function, ε the box size and $W \geq 0$ the decorrelation parameter to exclude statistical dependent data points s_i and s_j . The dimension is $0, 1, n, \mathbb{R}_+ \setminus \mathbb{N}$ for a fixed point, limit cycle, n -torus, and a strange attractor, respectively, and contains therefore valuable qualitative information about the dynamics. A strange attractor is a indicator for chaotic dynamics and the global Lyapunov exponents may be computed to gain a measure for the predictability of such dynamics.

$$\bar{\lambda}_i = \lim_{N \rightarrow \infty} (1/N) \ln \lambda_i(N) \quad (3.127)$$

with $\lambda_i(N)$ the local Lyapunov exponent of the matrix which is the direct matrix product of Jacobian matrices after N iterations of the n' -dimensional dynamical system. When one of the global Lyapunov exponents is positive, the dynamics are chaotic and initially neighboured points in the state space diverge exponentially. The predictability of the underlying dynamical systems relates immediately to the largest global Lyapunov exponent, which becomes as difficult and unreliable as larger the global Lyapunov exponent becomes. (Note, that the limit of the temporal mean of the local Lyapunov exponents is only defined to be the global Lyapunov exponent, if and only if the dynamical system is ergodic.) When just time series are given, mathematical values like the Jacobi-matrix and its eigenvalues cannot be computed. The only available numerical method utilizes the data samples to calculate these Lyapunov exponents. This leads to the algorithm developed by (Wolf, Swift, Swinney and Vastano, 1985), which makes two major restriction on the correct selection of neighboured points.

1. The difference $d_i(T) := \|\mathbf{s}(t_i + T) - \mathbf{s}(t_j + T)\|$ between two points should be small enough to fulfil the restrictions of the linear stability analysis.
2. The vector of unity $(\mathbf{s}(t_i + T) - \mathbf{s}(t_j + T)) / \| \mathbf{s}(t_i + T) - \mathbf{s}(t_j + T) \|$ should point into the direction of fastest growth.

The algorithm operates as follows

1. Define a hyper spherical shaped shell $K_{\sigma, \varepsilon}(\mathbf{s}(i)) = \{\mathbf{s} \in \mathbb{R}^n | \sigma < |\mathbf{s} - \mathbf{s}(i)| < \varepsilon\}$ in the reconstructed state space. Each state vector, which is covered by this shell, is a potential neighbour for the following computations. σ cancels out samples which just contain underlying noise and ε preserves the neighborhood of the linearization.
2. Choose two neighbours $\mathbf{s}(t_i)$ and $\mathbf{s}(t_j)$ out of this shell and follow the trajectories for a time interval T and compute $d(T)$.
3. Normalization. Choose another neighbour to $\mathbf{s}(t_i + T)$ out of $K_{\sigma, \varepsilon}(\mathbf{s}(t_i + T))$ which points approximately into the direction of $\mathbf{s}(t_j + T)$. (This step ensures, that the most unstable direction will be approximated.)
4. Repeat this procedure stepping into this algorithm at point 2.
5. After M repetitions, the mean

$$\lambda_1 = \sum_{k=1}^M \frac{1}{MT} \ln \frac{d_k(T)}{d_k(0)} = \frac{1}{T} \overline{\ln \frac{d_k(T)}{d_k(0)}} \quad (3.128)$$

leads then to the global Lyapunov exponent (ergodicity required).

(Eckmann and Ruelle, 1985) as well as Sano and (Sano and Sawada, 1985) employed an alternative numerical algorithm for global Lyapunov exponent estimations for hydrodynamic and chemical data which is based on the local estimation of the Jacobi matrix by observing the trajectories of an entire set of neighboured trajectories. Details of this algorithm are given in (Eckmann, Oliffson Kamphorst, Ruelle and Ciliberto, 1986). To determine the local Lyapunov exponents, one may use the locally linearised map of the perturbations $\delta_{\mathbf{f}_s(o_k)} = \mathbf{s}(o_k) - \mathbf{s}(t)$, where $\mathbf{s}(o_k)$ is a closed neighbour of $\mathbf{s}(t)$ and $k = 1, \dots, m$. This perturbations can then be employed to calculate the maps $\delta_s(t+1) = \mathbf{J}(t) \cdot \delta_s(t)$. The global Lyapunov exponents are then given by the eigenvalues of the matrix

$$\left[(\mathbf{J}(1) \cdot \mathbf{J}(2) \cdots \mathbf{J}(N))^\dagger (\mathbf{J}(1) \cdot \mathbf{J}(2) \cdots \mathbf{J}(N)) \right]^{\frac{1}{2N}}. \quad (3.129)$$

The latter matrix is of particular help if the dynamics are explicitly (including all dynamical parameters) given. The global Lyapunov exponent may be estimated by solving the ballistic missile dynamics and its linearized version at the same time. The mean divergence between both solutions leads for long simulations to an estimate of the global Lyapunov exponents. However this option is not available here, because the dynamical system is not explicitly known, only the time series is given.

Another critical issue of statistical descriptive variables, like the dimension (pointwise dimension, information dimension, Hausdorff dimension, etc.) or the Lyapunov exponents from the time series, is the required amount of data. There are quite different suggestions by (Essex and Nerenberger, 1991; Nerenberg and Essex, 1990; Ruelle, 1990; Smith, 1988; Wolf, Swift, Swinney and Vastano, 1985) but unfortunately, they are at odds over the required amount of data. (Ruelle, 1990; Essex and Nerenberger, 1991; Eckmann and Ruelle, 1992) provide estimates for a set of N data points in the time series, with the dimension estimate $d_{\text{attractor}}$ with

$$d_{\text{attractor}} < 2 \log_{10} N. \quad (3.130)$$

When, as in the worst case for a ballistic missile, the dimension of the reconstructed state space has to be 16 as can easily be seen from Eq. (3.120), (3.121), then identity (3.130) implies that the number of data points should be as much as 10^8 which is equivalent with approximately $10^8/3$ spatial coordinate measurements. It is obvious that this huge amount of data is not available. Still, (Eckmann and Ruelle, 1992) argues, that the number of ‘cycles’ (the correlation time) is a more significant quantity rather than the total number of points. That is, why (Price, Prichard and Hugenson,

1992) prefer a modified version of Ruelle's formula incorporating the delay time τ

$$d_{\text{attractor}} < 2\log(N/\tau), \quad (3.131)$$

in which case the number of required data points could reduce to a magnitude of about $\rho_{\infty}^{-1}[7.601, 15.202] \cdot 10^3$ which may be achievable. However, the applicability of this estimate of the number of data points or the more conservative estimate given above, cannot be decided here, since the verification of either estimate depends very much on the given data set. Despite all the arguments above, there does not seem to be any rigorous derivation of any of the measures and estimates above. Indeed, in many cases spurious results are very difficult to detect and the experimenter has to rely on non-verifiable/falsifyable arguments to justify the data analysis. A fairly recent review on Chaotic time series estimation and state space reconstruction may be found in Kugiumtzis et al. (1994) and Lillekjendlie et al. (1994). The summary principally indicates that the approximation of non-linear functions is possible for prediction purposes, although every approach has its advantages and disadvantages in term of statistical capabilities there is no indication how these statistical criteria may be extended to physical criteria.

3.5.3 Possible Routes to chaos in ballistic missiles

The last section introduced state reconstruction related techniques which not only allow a dynamical system description which is in the ideal case diffeomorphic to the original state space model, but which also enables to check to see if a dynamical system permits long term predictability even when the vector flow is explicitly given. As it is argued above, the global Lyapunov exponents have to be all negative to ensure that the error inside the state estimate decreases. If one global Lyapunov exponent is positive the error expands exponentially, *i.e.*, the long term predictability becomes impossible. This section introduces some dynamical behaviour of the ballistic missile which may lead to unpredictable, chaotic dynamics.

In the simplified rotating ballistic missile model (Eq. (3.45)–(3.47)) the principle moments of inertia have been assumed to be such that $\mathcal{J}_1 = \mathcal{J}_2$. This ideal case can in reality never be achieved. Although this idealisation is never true, the approximate behaviour comes very close to the ideal case. When the difference $\mathcal{J}_1 - \mathcal{J}_2$ is no longer negligible the qualitative behaviour may change significantly. Without loss of generality assume that the moments of inertia are such that $\mathcal{J}_1 > \mathcal{J}_2 > \mathcal{J}_3 > 0$. The Euler equations describe an equilibrium $\omega_0 = (0, \omega, 0)$ which leads in a neighbourhood of $\omega = (0, \omega, 0)$ to a linearized set of Euler's equations which have the eigenvalues

$0, \pm \sqrt{(\mathcal{J}_2 - \mathcal{J}_3)(\mathcal{J}_1 - \mathcal{J}_2)/(\mathcal{J}_1 \mathcal{J}_3)}$, of which one is positive. This implies that the fixed point cannot be stable. Fixed points of rotations about the $\mathbf{e}_{1,3}$ axes are stable, but are not Lyapunov stable. The attractor of a freely spinning top which follows about the unstable equilibrium ω_0 is thus a strange one, *i.e.*, the dynamics of the ballistic missile with three different moments of inertia may be chaotic. As the theory above indicates an unstable fixed point exists in any case since no manufacturer is capable of producing precisely symmetric bodies. The significance and magnitude of chaotic attractors can only be measured in real-life experiments. If and only if a sufficient amount of data points are available to enable a reasonably good approximation of the Lyapunov exponents can the chaoticity be measured. Alternatively, measurements of the inertia tensor provided by the manufacturer are more precise and could provide a very reliable state space model for prediction purposes. Since ballistic missiles are built such that the angle of attack converges to zero, the dynamics are expected to be strongly dissipative and the attractor is very likely to be confined in a small subset of the state space (Schuster, 1989; Ebeling, Engel and Herz, 1990). However, there are many cases where chaotic behaviour has been mistaken for noise (Schuster, 1989; Schwarz, 1994). In short, there is strong evidence that the chaotic behaviour will be exhibited by any real-life ballistic missile, but its relative magnitude to other non-linear effects has to be estimated by employing real-life systems.

It has been shown above that the ballistic body is a dissipative damped system in the air. This paragraph is concerned with the stability of the three body axes in space, *i.e.*, the attitude of the body with respect to the reference coordinate system. The crucial parameters for the stability of the body axis are the centre of mass and the centre of pressure. Generally, as long as the centre of pressure lies behind the centre of mass in desired flight path direction, an aerodynamic force applied to the body leads to a torque which seeks to rotate the body back in opposite direction of the perturbation. This is physically equivalent to a compound pendulum with an arbitrary but fixed axis, where the centre of rotation is the centre of mass and the torque is applied to the time-variable centre of pressure. The variability of the centre of pressure may lead to a parametric resonance: The critical variable for that is the resonance frequency of the compound pendulum. Assume that the body is anti-parallel to the air-flow (global minimum of drag force), then a small disturbance about this equilibrium leads to a torque which seeks to rotate the body back into its minimum. Let the flow be constant for the time of analysis $dv_\infty/dt \ll d\delta_0/dt$, *i.e.*, $f_a e \approx k\delta_0$. The only changing parameter is now the periodic varying centre of pressure. Due to the D_4 -symmetry of the body and spin the centre of pressure will then oscillate with four times the bodies frequency along the

symmetry axis of the body. The linearized Euler equation for small angles about a fixed axis leads therefore to

$$\mathcal{J}_1 \ddot{\delta}_\theta = -r_{cp}(t) k_0^2 \delta_\theta \quad (3.132)$$

whereby \mathcal{J}_1 is the specific moment of inertia about the axis of rotation. (It is here assumed again that $\mathcal{J}_1 = \mathcal{J}_2$.) Euler's equation can now easily be rewritten in term of Arnold's equation (Arnold, 1978)

$$\ddot{\delta}_\theta = -\omega_0^2 (1 + \varepsilon a(t)) \delta_\theta \quad (3.133)$$

with $r_{cp}(t) = \bar{r}_{cp} + \varepsilon a(t)$ and $\omega_0^2 = (k\bar{r}_{cp})/\mathcal{J}_1$ to explicitly parameterize the periodic function $r_{cp}(t)$, whereby the amplitude is $\varepsilon \ll 1$. When the frequency of $a(t)$ is given by ω then it is shown that for the case that $\omega_0/\omega \approx i/2$, ($i = 1, 2, \dots$) Eq. (3.133) becomes unstable for any arbitrary ε , *i.e.*, there is the case of *parametric resonance*. The corresponding ε , ω_0/ω -diagram is also known as the Arnold-tongues diagram. It is obvious from Arnold's equation that this kind of instability may become dominant in our case when the ratio between ω_0 and the rotational velocity component in \mathbf{e}'_1 or \mathbf{e}'_2 is half an integer, whereby the destabilisation may be the strongest for the case that $\omega_0/\omega = 1/2$. Also this specific kind of instability is known as chaos. Again this scenario very much depends on the particular combination of spin velocity of a ballistic missile and $\omega_0^2 = (k\bar{r}_{cp})/\mathcal{J}_1$ which is a purely body intrinsic property. The manufacturer can provide the data required or a sufficient number of measurements may allow an estimate of the chaotic behaviour.

The cases of chaotic missile dynamics just presented may appear to idealized without any experimental justification. However, these idealized examples are typical mathematically reasonably analyzed models where a characteristic behaviour can easily be proved to exist. A real-life ballistic missile may inherit any of those dynamical properties or even a superposition of chaotic attractors which makes the characterization of the missiles behaviour even more difficult. The conclusion of this section therefore is, that the dynamics of a real-life ballistic missile are not easily understood by writing down the vector flow, and the qualitative description of such a missile is an open research issue. All which can be accomplished without any data from real-life ballistic missiles is the theoretical analysis of possible dynamical properties. This section provides the experimental tools and theoretical indications which could be applied with little modifications by a modeller who has access to real-life ballistic missile data. This section also showed which kind of surprising dynamical properties may emerge from non-linear dynamics; any attempt to simplify the modelling task by

introducing *ad hoc* assumptions about the ballistic missile dynamics should be strictly avoided. Because the required information about ballistic missiles is not accessible further work has to be referred to future research when the real data and support may be available. This section provides a profound starting point for this case.

3.6 Conclusion

A ballistic missile has been shown to be modelled by utilizing the basic mechanics of rotating many particle bodies, which are explicitly given by Euler's equations and Newton's force equations. The effect of the gravitational force is well understood and can easily be expressed within the state space's vector flow. In contrast, the aerodynamic forces and torques are found to be very difficult to model when no real-life data is available. The physical assumptions and simplifications may even appear reasonable, but their validity cannot be proven without any physical experiments with sufficiently accurate measurements. Thus the toy models derived here cannot be employed as representative examples to illustrate whether the aerodynamic modelling is satisfactory for a specific ballistic body's dynamics prediction or not. Sections 3.1 to 3.5 outlined the pitfalls of ballistic missile modelling and motivate an (over-) simplified ballistic missile model which allows one to filter the time series data in Section 3.5.1 and which provides an easy-to-integrate model for Chapter 6. Any further interpretation of the results presented within this chapter are not eligible due to their lack of validation with real-life ballistic missile models.

In summary of Section 3.5, the methods developed in conjunction with state space reconstruction techniques can only be justified for the ideal cases when the time series is either noise free or the stochastic forcing is explicitly known, and if the density of (reconstructed) state vectors suggests an approximation of the state vector densities as probabilities. The decision about the applicability of these non-linear statistical black box modelling techniques is shown to be very controversial as some naive approaches to black-box modelling demonstrated (Schilhabel and Wu, 1997; Wu and Schilhabel, 1997). The author does not believe that an it-seems-to-work criterion is sufficient to verify an algorithm of procedures based on heuristics. When a black-box modelling approach was developed for an easy-to-model time series of a hair-dryer given as an example in *matlab* the results seemed to be very promising (Wu and Harris, 1997). However when applied to the time series taken from the Lorenz attractor the algorithm failed, the one-time-step-ahead predictions lead to divergence greater than the largest Lyapunov exponent (Schilhabel and Wu, 1997). The modeller could not even provide

any verifiable rigorous approach about the form or kind of information which could be included in the reconstructed state vectors when the dynamics are explicitly given (Wu and Schilhabel, 1997). It is difficult to justify black-box modelling for larger state space models such as the ballistic missile when fundamental questions *prior* to their implementation cannot be answered. When a time series of real-life measurements is available it can only be shown whether the non-linear statistical methods given above are applicable to this time series or not. Because too many open questions remain in particular with respect to pre-processed time series, a conclusive answer about the applicability and reliability of black-box modelling techniques for general physical system cannot be found.

For any given time series the stochastic forcing is usually not known, the number of data points may not suffice, a specific selection amongst the methods introduced above may be problematic. It is thus desirable to develop methodologies which neither introduce insufficiently understood heuristics (Cherkassky and Mulier, 1998), nor rely on algorithms which may not reveal any insight about physical parameters. The quite considerable amount of physical information available seems to suggest a modelling *ansatz** which seeks to incorporate as much physical knowledge as possible and to include as few prior assumptions into the system's dynamics as possible. The advantage of this kind of approach is twofold. The influence of physical parameter variations is truly transparent and may be proved in a physical experiment or verified through well proven simulations. Because assumptions of a model always introduce vagueness which has to be checked for its reasonableness by utilizing analogies, *gedankenexperiments*, etc. and which always limit the generality of a model, modelling should incorporate as few assumptions as possible. The aim is finding mathematical models with the most general applicability to concrete problems. The work presented in the following chapters therefore focuses on developing modelling techniques which seek to minimize the influence of assumptions and at the same time attempting to incorporate as much prior physical knowledge as possible.

**Ansatz* is a scientific term for approach. The *ansatz* usually refers to utilising a specific form of a function in order to get to the solution.

Chapter 4

The Endo-Observer of a Linear System

Forward

It is shown in this chapter that real-life observers are incapable of relating themselves to the abstract state space models introduced in Chapter 2. A state space model as defined in Chapter 2 is referred to here as the exo-observer state space model. The complementary concept introduced in this chapter is termed endo-observer state space model and allows the modelling of dynamics which are purely based on the knowledge available to a real-life observer. All that is required for an endo-observer state space model is the probability distribution of a free particle's spatial coordinate vector, the mean velocity at each spatial coordinate, and the total variance of the velocity distribution. It is then proved that a Hamilton-Jacobi-like equation and the continuity equation of an endo-observer can be derived and combined in a single partial differential equation which looks identical to the well known Schrödinger equation in Quantum mechanics. The consistency of the derived endo-observer (real-life) state space model with the exo-observer state space model is demonstrated via the comparison of the mean velocity in either model. Two analytically soluble endo-observer state space models are derived and shown to coincide with the exo-observer state space model. Since the motivation of this work is the identification of dynamical systems by utilizing time series data, an algorithm is suggested which allows the reconstruction of the initial conditions for the partial differential equation derived below. These initial conditions at the initial time t_0 are: (i) the mean velocities at all spatial coordinates of a particle, (ii) the variance of the velocity distribution, (iii) and the probability distribution of a particles spatial coordinates. A few illustrative examples are given

below.

4.1 Introduction

In the last chapter it was argued that black-box modelling of time series data is very problematic and that the incorporation of physical knowledge *via* grey-box modelling is very difficult and debatable since the assumptions should be tested against the black box model which is under consideration. The incorporation of physical knowledge into statistical models is thus an open research issue. The only alternative approach to the purely data driven black-box modelling technique is an altered physical state space model which is adapted to the general case that only components of a physical state vector, in the sense of Section 2.2, and bounds on system parameters are given. As it has already been argued in Chapter 2 the uncertainties of physical systems are usually introduced in the form of an additional stochastic term with very specific statistical properties. Since there does not seem to exist any approach which allows the incorporation of unspecified uncertainties into state space models, the following two chapters are dedicated towards developing a theoretical framework which enables the formulation of non-linear dynamical systems based on imprecise measurements, uncertain vector flow identification, and error-based but, up to a bound on the variance, explicitly unspecified stochasticity. Because the problem is too complex to be solved in a single complete theory, the derivation is subdivided into two sub-problems. This chapter is concerned initially with the linear case, where the uniform motion (Landau and Lifshitz, 1960; Arnold, 1978; Hestenes, 1986; Scheck, 1990; Marion and Thornton, 1995) of a particle is considered. The following chapter then shows how the derived framework may be adapted to the non-linear state vector dynamics.

This chapter is organized as follows: In Section 4.2 the information content and availability of a state space is critically reviewed and it is shown that the abstract physical (exo-)observer concept relates measurements to state vectors and vector flow which is in real-life experiments principally not available. The prefix ‘exo’ reflects the abstraction from real life measurements where these nice assumptions do not apply. As it will be shown below, real-life measurements have a profound influence on the accessibility of physical variables which change qualitative real-life physical modelling. It is also outlined how to distinguish classical physical modelling from the kind of physical modelling which takes the real-life observer’s properties into account. These properties of a real-life observer are introduced as endo-observer physics. The prefix ‘endo’ indicates the quality that an observer is somehow incorporated in the

experiment and that it lacks the level of abstraction it desires in order to establish a classical physical model. The purpose of Section 4.3 is to demonstrate how the very well known classical (exo-physical) description of a free, uniformly moving particle, *e.g.*, the centre of mass of an arbitrary body, can be re-formulated in a new framework of an endo-physical observer. The evolution of Gaussian probability density distributions of a free particle and the probability distribution of an oscillating system in endo- and exo-observer variables is utilized in Section 4.4 to demonstrate the models capabilities. In Section 4.5 an algorithm is developed which allows a (sparse) time series within the endo-observer concept to be employed.

Classical statistical methods concerned with the measurement of objects do not usually distinguish between the statistics required for systems which exhibit noise by themselves and statistics which are needed because the observer generates noise entering its measurements. In most cases, however, both situations occur. This chapter derives a new model which takes into account that the object and observer introduce noise into the outcome of the measurement and at the same time that information, which is specified below, is not available to the observer. The modelling of dynamics of this kind of observer (endo-observer) require a new technique which is demonstrated on the dynamics of a uniformly moving particle. Apart from ensuring the conservation of the total energy of an ensemble of particles with a certain mean velocity, also the variance of the probability distribution within the state space has to be preserved. Shannon's theorem (Schlögel, 1989) then leads to an estimated kinetic energy distribution by utilizing the variance of the *action* of the state space ensemble which then delivers the Schrödinger equation. Analytical examples are applied to the derived endo-observer model for an ensemble of free particles with a Gaussian distribution, and to an ensemble of harmonic oscillators to illustrate this approach.

4.2 Endo- Exo- observers and their relation to each other

Physical measurements are a complex mix of abstract concepts and a set of algorithms of how to relate certain quantities to each other. Consider for example the arrangement of two radars depicted in Figure 4.2 which are in principle able to measure the velocity and the position of a particle at the same time. It could be argued that the identification of a centre-of-mass' state vector inside the state space which moves with uniform velocity is trivial because the triangulation for position measurement and the velocity

measurement through the Doppler effect will lead immediately to the desired state vector $(\mathbf{r}, \mathbf{v})^T$. In Chapter 2 this approach was discussed and shown to be wrong for two reasons. A state vector consists of real numbers and real-life measurements cannot determine real numbers. Measurements are always erroneous due to the reasons given in Section 2.2 and it does not seem to be reasonable to take the instrument readings as true physical variables of the system's state. In order to clarify the relationship between the physical system itself and the experiment a more systematic approach towards the definition of a experimental arrangement may be employed as it has been suggested *e.g.* by Primas (1994). The general concepts of endo- and exo-physics were originally introduced by Rössler (1992).

The *universe of discourse* splits this world up into an *observing system* –which in our case is the radars together with the experimenter who interprets the outcome– and the to be observed systems *objects*, which is here the moving particle. The system which has no access to an external observer outside the interrelations of object and observer given by experiments is an *endo system*. This means, that all our models are purely based on measurements are all of an *endo*-character. The *exo-system* is given by a sufficient set of rules of how to communicate measured entities of the endo-system with variables of models created by someone living in the exo-system. A *cut* is defined as the meta-theoretical distinction which generates an exo-system and an object from an endo-system. It has been hypothesized (Hestenes, 1986; Scheck, 1990) that in general for a mechanical system consisting of a uniformly mobile particle, that there exist two *dynamical variables*, coordinate and velocity of a point mass, which can be represented by an exo-observer by two *mathematical objects* which are *real values*. In principle, each of these two *observables* can be measured by the radar, when the mathematics of triangulation and the Doppler effect are employed. Unfortunately, each *physical experiment* which consists of the *preparation*, including the *running* of the experiment and the successive *measurement*, incorporates *errors* due to the limitation of precision in measurable variables, the lack of isolation of the experiment from the environment, and intrinsic noise due to oversimplification of the underlying physical model or non-removable sources of noise. A rigorous approach to overcome this problem is to employ *statistical experiments* where the N -times repetition of the same experiment leads to the frequency distribution of each observable and in the case where $N \rightarrow \infty$ becomes a probability distribution. Alternatively, a conceptual set of replicated experiments, an *ensemble*, may be considered to be the *statistical experiment*, and the probability distribution for each of the observables within the experiment as the *state* of the experiment. The fictitious exo-observer knows for each

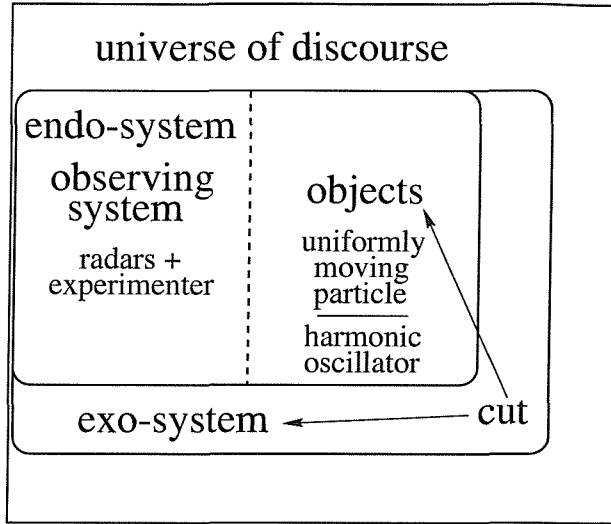


Figure 4.1: The universe of discourse which separates object from the observing systems. An exo-observer is a theoretical construct, because it requires error free knowledge of an arbitrary physical system. The example objects to be observed here in a statistical experiment are a uniform moving particle and a harmonic oscillator.

outcome of the experiment the exact velocity and coordinate of the point mass as well as the measurement of both by the experimenter utilizing the radars. Assume now, that the exo-observer can prepare the experiment such that the point mass at any repetition of the experiment is described by the exact coordinate r_0 and v_0 . The mutually independent probability distributions for the measured coordinate r and velocity v are defined by $\rho(r)$, $\rho(v)$, respectively. Although the combined measurement of r, v suggests a statistical dependence, the fact that the triangulation for the coordinate measurement is independent of the velocity measurement, *i.e.* the noise of r is uncorrelated with the noise of v , leads to the conclusion that the endo-observer is confined to $\rho(r), \rho(v)$. When a similar statistical experiment is performed where the exo-observer prepares the point mass, *i.e.* releases the point mass at an initial state vector and measures repetitively the position and momentum, at every repetition with the probability density $\rho(r_0, v_0)$, then again the measurement is not capable of distinguishing between any specific preparation r_0, v_0 and is confined to the statistics of $\rho(r) = \int \rho(r|r_0, v_0) \rho(r_0, v_0)$ and $\rho(v) = \int \rho(v|r_0, v_0) \rho(r_0, v_0)$ which, however, is generally different from the probability densities in the first preparation. The problem which now arises is, how to perform a prediction of the probability density $\rho(r, v)$ when only the estimates of $\rho(r)$ and $\rho(v)$ are given? The answer seems to be quite straightforward by assuming $\rho(v)$ to be constant with time and shifting $\rho(r)$ about the mean coordinate $\langle r \rangle = \langle v \rangle t$ to

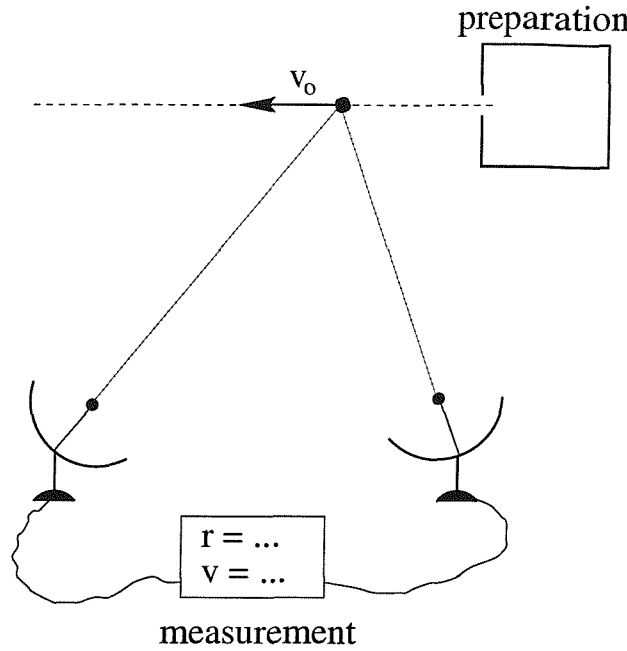


Figure 4.2: After the preparation of the experiment, here the release of an particle with certain but unknown velocity and spatial coordinate, both radars utilize the Doppler effect for velocity measurements and triangulation for position measurements.

compute $\rho(r - \langle v \rangle t)$. This holds only true in case that $\rho(r_0, v_0) = \delta(r'_0 - r_0, v'_0 - v_0)$, but generally it has to be taken into account that the probability distribution $\rho(r)$ is spreading out with time according to $\rho(v)$, whereas $\rho(v)$ is time independent, because the properties of the measurements are time invariant and $\rho(r - v_0 t, v_0) = \rho(r_0, v_0)$. The last section also points towards the problem of different statistics depending on whether the source of the noise comes from the preparation of the experiment, or if the noise stems from the endo-observer measurement itself. When the preparations are all identical, *i.e.* $\rho(r_0, v_0) = \delta(r - r_0)\delta(v - v_0)$, the variance of both, the probability distribution of the coordinates and of the velocity are time invariant. This is in contrast to the opposite case where the endo-observer measures the experiment noise free and all the errors come from the preparations. In this case the variance of the spatial coordinate's probability distribution is time dependent. This means that the statistical characteristics of object and observer should be treated independently in a corresponding model. Obviously, there is the problem that an endo-observer cannot distinguish between either statistics. The following model in the next section treats the statistics which are dependent on the object and observer as if the stochasticity of the measured variables purely originates from the object. As long as care is taken with respect to

the stochastic properties of variables which incorporate both, object and observer, the underlying statistics of an endo-observer state space model will not change. However, the formalism of an endo-observer's state space model can be simplified.

4.2.1 Observability of a free particle

Let us consider an endo-observer which has the capability to observe the probability $\rho(r, t)$. The question which now arises is, if it is in principle possible to reconstruct $\rho(r, v, t)$ from a number of observations. A comparison between this problem and the so-called Radon transform (Helgason, 1980; Herman, 1980; Herman and Natterer, 1981) reveals, that $\rho(r, t) = \int d\nu \rho(r, v, t)$ is similar to the line integral given by the Radon transform $R\rho(r, v, t)$ for which there exists an inverse transform allowing the reconstruction of $\rho(r, v, t)$. The Radon transform requires all line integrals which are parametrized by the variables φ, z which define the coordinates of the ray $Y_{\varphi, z}$ inside the state space by $ze^{i\varphi} + iue^{i\varphi}$ (Kirsch, 1996). The Radon transform thus becomes

$$(R\rho)(\varphi, z) = \int_{-\infty}^{\infty} du \rho(ze^{i\varphi} + iue^{i\varphi}), \quad z \in \mathbb{R}, \varphi \in [0, \pi) \quad (4.1)$$

It becomes obvious from Fig. 4.3, that alternatively $Y_{\varphi, z}$ may be parameterised in terms of the vector flow and the angle φ is implicitly given by $\tan \varphi = t$, which therefore implies that in order to cover the interval $[0, \pi)$, time has to pass from $-\infty$ to ∞ to enable the Radon transform. Hence, the probability density $\rho(r, v, t)$ cannot be reconstructed from observations of a continuous or discrete compact time interval. This proves the non-observability of $\rho(r, v, t)$ for any real-life physical observation process. Therefore, the next section has to deal with estimation techniques when $\rho(r, v, t)$ is not explicitly available.

4.3 An endo-observer's dynamics of a free particle

It has been demonstrated above that the probability density of the exo-observer $\rho(r, v, t)$ is not accessible. On the one hand classical physical models are exo-observer models which assume that any physical variable can precisely be measured, one the other hand endo-observers are only given the information that there is a linear dynamical system, of which the flow in the state space is conservative, and the probability density functions $\rho(r, t), \rho(v)$. Because $\rho(r, v, t)$ cannot be reconstructed within a finite time interval from the information which is provided to an endo-observer, an estimation technique has to be derived based on properties of the linear dynamics of a uniformly

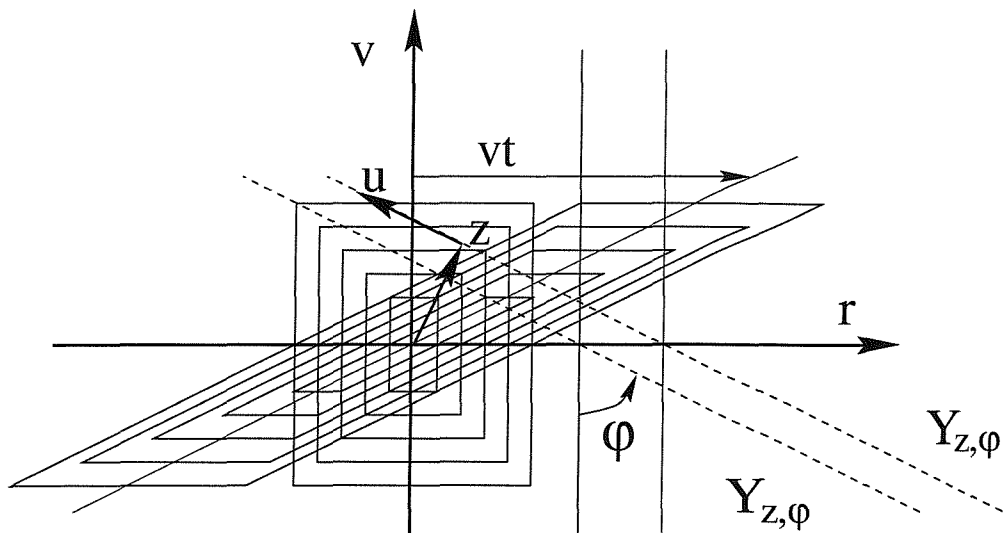


Figure 4.3: This figure demonstrates the Radon transform on a probability density distribution in the state space of a free particle moving along the real line, i.e., there is an initial probability density function at an instant $t_0 = 0$ such that $\rho(r, v, t) = \rho(r - vt, v, 0)$ for all $t \in \mathbb{R}$. This figure shows two instants t_0, t and thus the transformation that the probability density function undergoes as time progresses. The solid lines parallel to the velocity axis illustrate the line integral $\int_{-\infty}^{\infty} dv \rho(r, v, t) = \rho(r, t)$ which is related to the Radon-transform, i.e., the line integral $Y_{z, \varphi} = (R\rho(r, v, t_0))(\varphi, z)$ performed on the initial probability density function $\rho(r, v, t_0)$. The figure demonstrates that the Radon transform for all angles $\varphi \in [0, \varphi]$ can alternatively be performed by employing the line integrals $\int_{-\infty}^{\infty} dv \rho(r, v, t)$ for all $t \in \mathbb{R}$, i.e., $\rho(r, t)$ must be explicitly given for $\{t | t \in \mathbb{R}\}$ in order to reconstruct $\rho(r, v, t_0)$.

moving particles in an exo-observer system. It is well known that the *Liouville* or *continuity equation* holds for any continuous differentiable probability density function $\rho \in C^1$ and any vector flow which is a diffeomorphism (Großmann, 1988) due to Cauchy's theorem (see also page 75). The continuity equation describes the dynamics of preserved quantities, here the probability density which always integrates to unity. The conservative dynamics of $\rho(r, v, t | r_0, v_0)$ in an exo-observer's state space model are thus given by the corresponding *Liouville equation* (Fick, 1988)

$$\partial_t \rho(r, v_0, t | r_0, v_0) = -\partial_r (\rho(r, v_0, t | r_0, v_0) m^{-1} \partial_r S(r, v_0)) \quad (4.2)$$

with $S(r, v_0)$ being *Hamilton's principal function*, given by $\partial_r S(r, v_0) = -H$, $\partial_r S(r, v_0) = mv_0$. The vector field inside the bracket of Eq. (4.2) is implicitly given by the *Hamilton-Jacobi equation* (Fick, 1988) which is only valid for conservative

vector fields in an exo-observer's frame of reference and is defined by

$$\partial_t S(r, v, t) = -(2m)^{-1} (\partial_r S(r, v, t))^2. \quad (4.3)$$

It can easily be demonstrated that $\rho(r - v_0 t, v_0)$ is a solution of Equ. (4.2) by applying the chain rule to $\partial_t \rho(r - v_0 t, v_0)$. It may now become obvious why these dynamics can easily be modelled by an exo-observer, as $\rho(r - v_0 t, v_0)$ is accessible to it throughout the entire experiment. For an endo-observer this model is no longer valid because only $\rho(r, t), \rho(v)$ are given. If the desired model is restricted to the observation and prediction of the probability densities $\rho(r, t)$, the Liouville Equation (4.2) can be modified to

$$\partial_t \rho(r, t) = -\partial_r (\rho(r, t) m^{-1} \partial_r S(r, \langle v \rangle_v(r, t), t)) \quad (4.4)$$

with $\langle v \rangle_v(r, t) = \int dv \rho(v, t | r) v$, which has to be determined prior to the dynamics given in Eq. (4.4). By employing

$$\langle v \rangle_v(r, t) = -\frac{m}{\rho(r, t)} \int_{-\infty}^r dr' \frac{\partial \rho(r', t)}{\partial t} \quad (4.5)$$

the mean vector field (momentum) can be computed and afterwards utilized for the Liouville equation (4.4). Note, that the velocity $\langle v \rangle_v(r, t)$ can only be computed for the 1D-linear case, higher-dimensional endo-observer frames of references cannot even reconstruct $\langle v \rangle_v(r, t)$. This can be demonstrated most easily by employing the Liouville equation for higher spatial coordinate vectors. A relation similar to the one given in Eq. (4.5) can not generally be derived for the multi-dimensional continuity equation. The only velocity which may be available is

$$\langle v_i \rangle_v(r_i, t) = -\frac{m}{\rho(r_i, t)} \prod_{\substack{j=1 \\ j \neq i}}^{k-1} \int_{-\infty}^{\infty} dr'_j \int_{-\infty}^r dr'_i \partial_t \rho(\mathbf{r}', t) \quad i \in \{1, \dots, k-1\}, \quad (4.6)$$

i.e., the vector field (velocity) of a mean taken with respect to all coordinates apart from the dimension i under consideration.

The modelling problem of the particle's dynamics with respect to the confined observation of an endo-observer has now been solved. It has been shown that an endo-observer's dynamics are identical to those of an exo-observer when the mean vector-field $\langle v \rangle_v(r, t)$ can be measured. Further, it has already been demonstrated that in the case of having a number of coordinates greater than one, the mean vector-field with respect to the endo-observer's coordinates cannot be measured. Additionally, the dynamics of the mean vector field which apply to the endo-observer state cannot be

computed, because exo-observer physics do not allow the formulation of any dynamics of the mean vector field. To find a model for the dynamics of $\langle v \rangle_v(r, t)$ a more general approach is required. The following section introduces an estimate for the dynamics of $\langle v \rangle_v(r, t)$ based on the general properties of conservative linear state space models of exo-observers and the accessible probability distributions of endo-observer variables. The *state space* concept in classical mechanics utilizes a well defined set of physical variables which form the state vector which is an element of \mathbb{R}^n . All these physical variables are, at least in principle, measurable quantities. A dynamical system is thus exhaustively represented by a vector field and the state $\mathbf{x} \in \mathbb{R}^n$ in the state space. As introduced in Section 2.2 all these concepts are related to exo-observers. The endo-observers are now assumed to be able to only share a subset of variables $\mathbf{x}_1 := (x_1, \dots, x_{k-1})^T \in \mathbb{R}^{k-1}$ with the exo-observer, *i.e.*, the state space concept as introduced in Section 2.2 no longer applies to endo-observers because there are the variables $\mathbf{x}_2 := (x_k, \dots, x_n)^T \in \mathbb{R}^{n-k+1}$ which are now assumed to be only accessible to the exo-observer.

$$\mathbf{x} = \underbrace{(x_1, \dots, x_{k-1})}_{\text{accessible to an endo-observer}}, \underbrace{x_k, \dots, x_n}_{\text{accessible to an exo-observer}} \quad (4.7)$$

As shown previously, the Liouville or continuity equation still applies to this sub-space of the state space and as such can be formulated with respect to the endo-observer's variables as

$$\partial_\rho(\mathbf{x}_1, t) = -\partial_{\mathbf{x}_1} (\rho(\mathbf{x}_1, t) m^{-1} \partial_{\mathbf{x}_1} S(\mathbf{x}_1, \langle \mathbf{x}_2 \rangle_{\mathbf{x}_2}(\mathbf{x}_1, t), t)) \quad (4.8)$$

with the definition of

$$\langle f(\mathbf{x}) \rangle_{x_i} = \int f(\mathbf{x}) \rho(x_i | x_1, \dots, \check{x}_i, \dots, x_n) dx_i, \quad (4.9)$$

where \check{x}_i denotes the omission of x_i . As already observed, $\partial_{\mathbf{x}_1} S(\mathbf{x}, t)$ is not measurable, however, it might be possible to measure indirectly the mean components of the vector field which is $\langle \partial_{\mathbf{x}_1} S(\mathbf{x}, t) \rangle_{x_1, \dots, \check{x}_i, \dots, x_n}$. For simplicity the endo-observer vector field (momentum) for a particular instant $t = t_0$ when a measurement is taken is defined by

$$\mathbf{F}_{\text{en}}(\mathbf{x}_1, t_0) = \langle \partial_{\mathbf{x}_1} S(\mathbf{x}, t_0) \rangle_{x_1, \dots, \check{x}_i, \dots, x_n}. \quad (4.10)$$

This equation states that the vector field $\mathbf{F}_{\text{en}}(\mathbf{x}_1, t_0)$ is a gradient vector field which may only change according to a gradient as the endo-observer's vector field has to

stay measurable according to Eq. (4.6). This property will become essential for the following arguments.

In order to derive how $\mathbf{F}_{\text{en}}(\mathbf{x}_1, t)$ may change with time once it has been measured, two different frames of reference F, F' have to be introduced. F' is supposed to transform relatively to the fixed frame of reference F following the vector flow defined by $\mathbf{F}_{\text{en}}(\mathbf{x}_1, t)$. Let us consider the instant $t = t_0$ when both frames of references are identical with each other. Within a small time interval Δt the vector field $\mathbf{F}_{\text{en}}(\mathbf{x}_1, t_0)$ will change by

$$\begin{aligned} \partial_t \mathbf{F}_{\text{en}}(\mathbf{x}_1, t)|_{t_0} &= \partial_t \mathbf{F}_{\text{en}, \mathbf{x}_1}(\mathbf{x}_1, t)|_{t_0} \\ &\quad - \lim_{\Delta t \rightarrow 0} [\mathbf{F}_{\text{en}}(\mathbf{x}_1 + \Delta t \mathbf{F}_{\text{en}, \mathbf{x}_1}(\mathbf{x}_1, t_0)/m, t) - \mathbf{F}_{\text{en}}(\mathbf{x}_1, t_0)]/(\Delta t), \end{aligned} \quad (4.11)$$

whereby the change of the vector field $\mathbf{F}_{\text{en}}(\mathbf{x}_1, t)$ depends on two separate contributions. The temporal derivative $\partial_t \mathbf{F}_{\text{en}, \mathbf{x}_1}(\mathbf{x}_1, t)|_{t_0}$ represents the change of the vector field because of the specific probability distribution $\rho(\mathbf{x}_1, \mathbf{x}_2, t)$ about the mean $\int d^n \mathbf{x}_2 \rho(\mathbf{x}_1, \mathbf{x}_2, t) \mathbf{x}_2$. The second expression on the RHS of this equation describes the change of the vector field $\mathbf{F}_{\text{en}}(\mathbf{x}_1, t)$ due to the transform of the probability density function $\rho(\mathbf{x}_1, t)$ under the influence of the vector field. If for example the variance of $\rho(\mathbf{x}_1, \mathbf{x}_2, t)$ were zero with respect to the coordinate \mathbf{x}_2 the first expression on the RHS would vanish and the second expression would describe a deterministic-like flow inside the state space. The change of $\mathbf{F}_{\text{en}, \mathbf{x}_1}(\mathbf{x}_1, t)$ may thus be interpreted as the net dynamics of the vector field $\mathbf{F}_{\text{en}}(\mathbf{x}_1, t)$ of an endo-observer due to the variance of $\rho(\mathbf{x}_2, t | \mathbf{x}_1)$'s at the coordinate \mathbf{x}_1 .

The limit in Eq. (4.11) leads to the definition of the so-called *vector gradient* which thus gives the identity

$$\partial_t \mathbf{F}_{\text{en}}(\mathbf{x}_1, t)|_{t_0} = \partial_t \mathbf{F}_{\text{en}, \mathbf{x}_1}(\mathbf{x}_1, t)|_{t_0} - m^{-1} (\mathbf{F}_{\text{en}}(\mathbf{x}_1, t_0) \partial_{\mathbf{x}_1}) \mathbf{F}_{\text{en}}(\mathbf{x}_1, t_0). \quad (4.12)$$

So far nothing has been proposed for the specific function $\mathbf{F}_{\text{en}, \mathbf{x}_1}(\mathbf{x}_1, t)$. Before dealing with this issue let us consider a corresponding potential of $\mathbf{F}_{\text{en}}(\mathbf{x}_1, t)$ which exists for two reasons. As derived above only the mean vector field at any coordinate x_i with $0 < i \leq k - 1$ can be measured, and the function $\mathbf{F}_{\text{en}, \mathbf{x}_1}(\mathbf{x}_1, t)$ only depends on the variance taken over all \mathbf{x}_2 components for each x_i independently. The potential function G is defined implicitly by the condition that

$$\mathbf{F}_{\text{en}}(\mathbf{x}_1, t) = \partial_{\mathbf{x}_1} G(\mathbf{x}_1, t), \quad (4.13)$$

which allows Eq. (4.12) to be restated in terms of the potential function as,

$$\partial_t \partial_{\mathbf{x}_1} G(\mathbf{x}_1, t)|_{t_0} = \partial_t \partial_{\mathbf{x}_1} G_{\mathbf{x}_1}(\mathbf{x}_1, t)|_{t_0} - (2m)^{-1} \partial_{\mathbf{x}_1} (\partial_{\mathbf{x}_1} G)^2, \quad (4.14)$$

which implies that

$$\partial_t G(\mathbf{x}_1, t)|_{t_0} = \partial_t G_{\mathbf{x}_1}(\mathbf{x}_1, t)|_{t_0} - (2m)^{-1}(\partial_{\mathbf{x}_1} G)^2. \quad (4.15)$$

The original dynamics of $\mathbf{F}_{\text{en}}(\mathbf{x}_1, t)$ have just been reformulated by utilizing a new quantity G but $G_{\mathbf{x}_1}(\mathbf{x}_1, t)$ is as little known as $\mathbf{F}_{\text{en}, \mathbf{x}_1}(\mathbf{x}_1, t)$. In order to identify what the potential means physically, it is returned to the Hamilton-Jacobi equation (4.3) for n dimensions which is integrated with respect to the volume integral over \mathbf{x}_2 , *i.e.*, it is wished to find a function $G(\mathbf{x}_1, t)$ which fulfills Eq. (4.15) and the requirement that

$$\begin{aligned} \partial_t G(\mathbf{x}_1, t)|_{t_0} &= \langle \partial_t S(\mathbf{x}_1, t)|_{t_0} \rangle_{\mathbf{x}_2} = -(2m)^{-1} \left\langle (\partial_{\mathbf{x}_1} S(\mathbf{x}))^2 \right\rangle_{\mathbf{x}_2} \quad (4.16) \\ &= -(2m)^{-1} \sigma_{\mathbf{x}_2}^2(\mathbf{x}_1, t) - (2m)^{-1} (\partial_{\mathbf{x}_1} \langle S(\mathbf{x}) \rangle_{\mathbf{x}_2})^2 \\ &= -(2m)^{-1} \sigma_{\mathbf{x}_2}^2(\mathbf{x}_1, t_0) - (2m)^{-1} (\partial_{\mathbf{x}_1} G_{\mathbf{x}_2}(\mathbf{x}_1, t_0))^2 \end{aligned}$$

with squared variance

$$\sigma_{\mathbf{x}_2}^2(\mathbf{x}_1) = \left\langle \left(\partial_{\mathbf{x}_1} S(\mathbf{x}) - \langle \partial_{\mathbf{x}_1} S(\mathbf{x}) \rangle_{\mathbf{x}_2} \right)^2 \right\rangle_{\mathbf{x}_2} \quad (4.17)$$

and the total squared variance

$$\sigma_{\mathbf{x}_2}^2 = \left\langle \left(\partial_{\mathbf{x}_1} S(\mathbf{x}) - \langle \partial_{\mathbf{x}_1} S(\mathbf{x}) \rangle_{\mathbf{x}_2} \right)^2 \right\rangle_{\mathbf{x}_1, \mathbf{x}_2} \quad (4.18)$$

The last bracket on the right-hand-side of Equ. (4.16) requires some explanation. As stated in Eq. (4.6) only one independent component of the endo-observer vector field can be measured which requires that $\rho(\mathbf{x}_2|\mathbf{x}_1) = \prod_{i=k}^n \rho(x_i|\mathbf{x}_1)$ for all $\mathbf{F}_{\text{en}}(\mathbf{x}_1, t)$ and thus for all S . Bearing this in mind it can be proved that

$$\langle \partial_{\mathbf{x}_1} S(\mathbf{x}) \rangle_{\mathbf{x}_2} = \partial_{\mathbf{x}_1} \langle S(\mathbf{x}) \rangle_{\mathbf{x}_2} \quad (4.19)$$

by observing that

$$\begin{aligned} \int d\mathbf{x}_2 \frac{\partial S(\mathbf{x})}{\partial \mathbf{x}_1} \rho(\mathbf{x}_2|\mathbf{x}_1) &= \frac{\partial}{\partial \mathbf{x}_1} \int d\mathbf{x}_2 S_i(\mathbf{x}) \rho(\mathbf{x}_2|\mathbf{x}_1) \quad (4.20) \\ &- \left[S(\mathbf{x}) \frac{\partial}{\partial \mathbf{x}_1} P(\mathbf{x}_2|\mathbf{x}_1) \right]_{-\infty}^{\infty} + \int d\mathbf{x}_2 \frac{\partial S(\mathbf{x})}{\partial \mathbf{x}_2} \int d\mathbf{x}'_2 \frac{\partial \rho(\mathbf{x}'_2|\mathbf{x}_1)}{\partial \mathbf{x}_1} \end{aligned}$$

with $P(\infty|\mathbf{x}_1) = 1$, $P(-\infty|\mathbf{x}_1) = 0$, and the integral $\int d\mathbf{x}'_2 \partial_{\mathbf{x}_1} \rho(\mathbf{x}'_2|\mathbf{x}_1) = 0$.

Eq. (4.16) is the Hamilton-Jacobi equation of an ensemble of freely moving particles within the exo-observer's state space which has been projected into \mathbb{R}^{k-1} , the exo-observer's state space components are accessible to the endo-observer. Eq. (4.16)

implies the following. Because the action function G derives from the dynamics of the endo-observer's vector field and the Hamilton-Jacobi equation has to hold simultaneously, the squared variance term in Eq. (4.16) has to be equivalent to $G_{\mathbf{x}_1}(\mathbf{x}_1, t)$ in Eq. (4.15). Eq. (4.16) effectively means that if $\sigma_{\mathbf{x}_2}(\mathbf{x}_1)$ were known the Hamilton-Jacobi equation for the endo-observer could be computed exactly. Unfortunately, this requires the knowledge of an exo-observer. Since there is no solution to this problem, estimates of the relative change of $\sigma_{\mathbf{x}_2}(\mathbf{x}_1)$ may still provide a model which produces predictions based on the limited information accessible. The following section derives an estimate for the variation of the squared variance $\sigma_{\mathbf{x}_2}^2(\mathbf{x}_1, t)$ with respect to \mathbf{x}_1 .

It is evident from Eq. (4.16) that the total change of $\sigma_{\mathbf{x}_2}(\mathbf{x}_1)$ is of no relevance here. This can easily be seen if an energy $E(t)$ representing the total mean energy taken over \mathbf{x}_1 is added to the left-hand-side of Eq. (4.16). A new Hamilton principal function given by $G'(\mathbf{x}_1, t) = G(\mathbf{x}_1, t) + \int dt E(t)$ then leads to the same partial differential equation as Eq. (4.16). The crucial contribution to $G(\mathbf{x}_1, t)$ stems from the changes of energy between neighboured \mathbf{x}_1 . The principle idea is as follows. As the variance $\sigma_{\mathbf{x}_2}$ is not available its estimation is needed. This may be accomplished by employing Shannon's principle of unbiased guess of the probability distribution of the residual energy via a constant action $\kappa/2$ defined in Eq. (4.21). After the action distribution has been chosen such that the volume integral with respect to the \mathbf{x}_1 coordinates is identical to $\kappa/2$ (action conservation), the divergence of a vector field corresponding to the distribution of the action may be computed which is a measure of kinetic energy increase at coordinate \mathbf{x}_1 within a infinitesimal volume $d\mathbf{x}_1$ in comparison to its neighboured volume elements. Because the action is a measure of the entire state space, the flux, as will be shown below, can be computed in two different ways, whereby Shannon's approach of unbiased guess then suggests to utilize as the flux the equally weighed sum of both fluxes.

Assume that $\sigma_{\mathbf{x}_1} \sigma_{\mathbf{x}_2}$ is bound by a constant κ ,

$$\sigma_{\mathbf{x}_1} \sigma_{\mathbf{x}_2} \leq \kappa/2 \quad (4.21)$$

The *action* given by Equ. (4.21) is time-invariant because the following integral can be reduced to

$$\begin{aligned} & \int d\mathbf{x} (\mathbf{x}_1 - \langle \mathbf{x}_1 \rangle(\mathbf{x}_2, t))^2 (\mathbf{x}_2 - \langle \mathbf{x}_2 \rangle)^2 \rho(\mathbf{x}, t) \\ &= \int d\mathbf{x}_1 d\mathbf{x}_2 \left(\mathbf{x}_1 - \langle \mathbf{x}_1 \rangle(\mathbf{x}_2, 0) - \frac{\mathbf{x}_2 t}{m} \right)^2 (\mathbf{x}_2 - \langle \mathbf{x}_2 \rangle)^2 \rho \left(\mathbf{x}_1 - \langle \mathbf{x}_1 \rangle(\mathbf{x}_2, 0) - \frac{\mathbf{x}_2 t}{m}, \mathbf{x}_2, 0 \right) \\ &= \int d\mathbf{x} (\mathbf{x}_1 - \langle \mathbf{x}_1 \rangle(\mathbf{x}_2, 0))^2 (\mathbf{x}_2 - \langle \mathbf{x}_2 \rangle)^2 \rho(\mathbf{x}, 0). \end{aligned} \quad (4.22)$$

The only information available about $\kappa/2$ is the value of the integral in Eq. (4.22). The exact distribution of κ with respect to \mathbf{x}_1 is by definition of the experiment inaccessible. Assume that the mean of a variable κ is known, as well as the probability density $\rho(\mathbf{x}_1)$. The question arises what the probability density $\rho(\kappa', \mathbf{x}_1) = \rho(\kappa'|\mathbf{x}_1)\rho(\mathbf{x}_1)$ is. The lack of knowledge about $\rho(\kappa'|\mathbf{x}_1)$, requires an estimate which does not include any biased guess (Schlögel, 1989), *i.e.*, it is assumed that Relation (4.22) holds with respect to any $\rho(\mathbf{x}_1)$. This is only the case if and only if $\rho(\kappa'|\mathbf{x}_1) = \rho(\kappa')$. Thus, the estimated probability density to have the squared action $\kappa^2/4$ at coordinate \mathbf{x}_1 is $\rho(\mathbf{x}_1)$ – which is equivalent to a fictitious ensemble of particles with probability $\rho(\mathbf{x}_1)d\mathbf{x}_1$ within the interval $d\mathbf{x}_1$ at coordinate \mathbf{x}_1 where particles inside the interval share the squared action $\kappa^2/4\rho(\mathbf{x}_1)d\mathbf{x}_1$ – with a corresponding vector field

$$\mathbf{F}(\mathbf{x}_1, t) = -(\kappa^2/4)\partial_{\mathbf{x}_1}\rho(\mathbf{x}_1, t). \quad (4.23)$$

This vector field may be interpreted as the change of squared action, which is proportional to the energy, when its probability density at coordinate \mathbf{x}_1 is being compared with the one at coordinate $\mathbf{x}_1 + d\mathbf{x}_1$. The negative sign takes care of the fact that the squared action increases if the gradient is negative and vice versa. As mentioned above there are two distinct cases for computing the flux of a vector field.

(i) Let us consider the case where each subset of the system's ensemble at any coordinate \mathbf{x}_1 has the same generalized kinetic energy proportional to $|\kappa|^2/4$, in which case the total generalized kinetic energy at \mathbf{x}_1 is $|\kappa|^2/4\rho(\mathbf{x}_1, t)$. The relative change of the total generalized kinetic energy at any state \mathbf{x}_1 is then zero, but the total change of the total generalized kinetic energy at \mathbf{x}_1 is $|\kappa|^2/4\partial_{\mathbf{x}_1}\rho(\mathbf{x}_1, t)$. The negative relative divergence of the vector field (4.23) is thus $-\kappa^2(4\rho(\mathbf{x}_1, t))^{-1}\partial_{\mathbf{x}_1}^2\rho(\mathbf{x}_1, t)$ and therefore defines the generalized energy increase of an event at \mathbf{x}_1 due to the fact that the energy distribution within all ensembles is a δ -function around a specific value and that the probability about a neighbourhood of \mathbf{x}_1 changes. This can be more easily visualized by comparing the system with a distribution of particles as given by $\rho(\mathbf{x}_1, t)$, of which each of these particles has an energy proportional to $\kappa^2/4$. When at an instant t within the interval $d^n\mathbf{x}_1$ $\rho(\mathbf{x}_1, t)d^n\mathbf{x}_1$ particles flow through the interval with a fixed generalized kinetic energy $\propto \kappa^2/4$, the net change of the total generalized kinetic energy inside the interval $d^n\mathbf{x}_1$ at the state \mathbf{x}_1 changes about $-(\kappa^2/4)\partial_{\mathbf{x}_1}^2\rho(\mathbf{x}_1, t)$.

(ii) Let us consider now the case that the relative generalized energy of an event changes with respect to \mathbf{x}_1 . Although the total generalized kinetic energy is still $(|\kappa|^2/4)\rho(\mathbf{x}_1, t)d^n\mathbf{x}_1$, in the mean the vector field for every single event changes according to the relative vector field $(\rho(\mathbf{x}_1, t))^{-1}\mathbf{f}(\mathbf{x}_1, t)$. Because there are $\rho(\mathbf{x}_1, t)d^n\mathbf{x}_1$ events within the interval $d^n\mathbf{x}_1$, the total change of the energy is still equivalent to

Eq. (4.23) and thus the total generalized energy is preserved. The negative divergence of the relative vector field is then identical to $-\partial_{\mathbf{x}_1}[|\kappa|^2(4\rho(\mathbf{x}_1, t))^{-1}\partial_{\mathbf{x}_1}\rho(\mathbf{x}_1, t)]$ and represents the increased energy density at coordinate \mathbf{x}_1 because of the relative generalized energy which is increased with respect to the neighbouring coordinates. This case can be more easily explained by an ensemble of particles within $d^n\mathbf{x}_1$ at \mathbf{x}_1 in which each particle changes its generalized energy from \mathbf{x}_1 to $\mathbf{x}_1 + d\mathbf{x}_1$ about $|\kappa|^2/(4\rho(\mathbf{x}_1, t))\partial_{\mathbf{x}_1}\rho(\mathbf{x}_1, t)$. The net change of the total generalized energy in the interval $d^n\mathbf{x}_1$ at \mathbf{x}_1 due to the change of energy of each particle is then identical to $-\rho(\mathbf{x}_1, t)\partial_{\mathbf{x}_1}[\kappa^2(4\rho(\mathbf{x}_1, t))^{-1}\partial_{\mathbf{x}_1}\rho(\mathbf{x}_1, t)]$. The negative sign of the divergences in both cases takes care of the fact that a source is proportional to the negative divergence of a vector field. In the above argument the magnitude of the constant κ has been employed, now it will be clarified what κ really is in terms of a physical constant. It is well known that the units of \mathbf{x}_1 are meters and the second derivative of G^2 becomes

$$(2m)^{-1}\partial_{\mathbf{x}_1}^2 G_{\text{res}}^2 = m^{-1}p_{\text{res}}^2 + G_{\text{res}}\partial_{\mathbf{x}_1}^2 G_{\text{res}}, \quad (4.24)$$

which demonstrates that it is proportional to the kinetic energy of the ensemble of free particles subject to an endo-observer, the units of κ must be therefore in $\text{kg} \cdot \text{meter}^2 \cdot \text{sec}^{-1}$. Two estimates of $\partial_t G_{\mathbf{x}_1}(\mathbf{x}_1, t)|_{t_0}$ are possible. The question arises which is the optimal one. As there is no additional information with which to make a choice, Jaynes principle of unbiased guess requires that both estimates have to be included with equal weight into a common estimate.

$$\begin{aligned} E_{\text{res}}(\mathbf{x}_1, t_0) = & \kappa^2(8m\rho(\mathbf{x}_1, t_0))^{-1}\partial_{\mathbf{x}_1}^2\rho(\mathbf{x}_1, t_0) \\ & + \kappa^2(8m)^{-1}\partial_{\mathbf{x}_1}[\rho^{-1}(\mathbf{x}_1, t_0)\partial_{\mathbf{x}_1}\rho(\mathbf{x}_1, t_0)], \end{aligned} \quad (4.25)$$

which is valid for all $\rho(\mathbf{x}_1, t_0) > 0$. The form of $E_{\text{res}}(\mathbf{x}_1, t_0)$ is very crucial for the following analysis of $G(\mathbf{x}_1, t)$ in Eq. (4.16), because the origin of G derives from the meaning of $\partial_t G_{\mathbf{x}_1}(\mathbf{x}_1, t)|_{t_0}$ which is generally dependent on the coordinate system, *i.e.*, the mean vector flow is dependent on the Jacobian matrix which defines the transform between the two frames of reference F and F' . It is only because of the specific form of $E_{\text{res}}(\mathbf{x}_1, t_0)$, which is expressed in coordinates of F rather than F' , that the endo-observer dynamics can be formulated for any instant $t \neq t_0$. Since Eq. (4.16) is a partial differential equation which is only dependent on \mathbf{x}_1, t , the action $G(\mathbf{x}_1, t)$ can be integrated for all $t \neq t_0$ and is thus *not* limited to an infinitesimal time interval at a specific t_0 . It also becomes clear why the action function is chosen to be $\kappa/2$ instead of just κ . The addition of the two fluxes in Eq. (4.25) leads to $2E_{\text{kin}}$ where the factors in the numerator and denominator cancel each other out. Equation (4.25) is very

unwieldy and can be simplified by defining $A(\mathbf{x}_1) = \sqrt{\rho(\mathbf{x}_1)}$, so that the left-hand-side of Eq. (4.25) can then be rewritten in terms of $\rho(\mathbf{x}_1, t)$ as

$$\begin{aligned} & \frac{\kappa^2}{8m} \frac{1}{\rho(\mathbf{x}_1)} \frac{\partial^2 \rho}{\partial \mathbf{x}_1^2}(\mathbf{x}_1) + \frac{\kappa^2}{8m} \frac{\partial}{\partial \mathbf{x}_1} \left(\frac{1}{\rho(\mathbf{x}_1)} \frac{\partial \rho}{\partial \mathbf{x}_1}(\mathbf{x}_1) \right) \\ &= \frac{\kappa^2}{2m\sqrt{\rho(\mathbf{x}_1)}} \left(\frac{1}{2} \frac{1}{\sqrt{\rho(\mathbf{x}_1)}} \frac{\partial^2 \rho}{\partial \mathbf{x}_1^2}(\mathbf{x}_1) - \frac{1}{4} \frac{1}{\sqrt{\rho^3(\mathbf{x}_1)}} \left(\frac{\partial \rho}{\partial \mathbf{x}_1} \right)^2 \right) \\ &= \frac{\kappa^2}{2m\sqrt{\rho(\mathbf{x}_1)}} \frac{\partial}{\partial \mathbf{x}_1} \left(\frac{1}{2\sqrt{\rho(\mathbf{x}_1)}} \frac{\partial \rho}{\partial \mathbf{x}_1}(\mathbf{x}_1) \right) \\ &= \frac{\kappa^2}{2m A(\mathbf{x}_1)} \frac{\partial^2 A(\mathbf{x}_1)}{\partial \mathbf{x}_1^2}. \end{aligned} \quad (4.26)$$

After this long digression the purpose of deriving the specific form for the estimate $\sigma_{\mathbf{x}_2}(\mathbf{x}_1)/2$ in Eq. (4.16), it will become evident when it is considered how the Liouville and Hamilton-Jacobi equations (4.2) & (4.3) can easily be rewritten in terms of $A(\mathbf{x}_1)$ as

$$\begin{aligned} (2A\partial_t A)(\mathbf{x}_1, t) &= -\partial_{\mathbf{x}_1} (A^2(\mathbf{x}_1, t)m^{-1}\partial_{\mathbf{x}_1} G(\mathbf{x}_1, t)) \\ &= -2A(\mathbf{x}_1, t)\partial_{\mathbf{x}_1} A(\mathbf{x}_1, t)m^{-1}\partial_{\mathbf{x}_1} G(\mathbf{x}_1, t) - A^2(\mathbf{x}_1, t)m^{-1}\partial_{\mathbf{x}_1}^2 G(\mathbf{x}_1, t) \end{aligned} \quad (4.27)$$

and accordingly,

$$\partial_t G(\mathbf{x}_1, t) = \kappa^2 (2mA(\mathbf{x}_1))^{-1} \partial_{\mathbf{x}_1}^2 A(\mathbf{x}_1) - (2m)^{-1} (\partial_{\mathbf{x}_1} G(\mathbf{x}_1, t))^2 \quad (4.28)$$

Multiplication of Eq. (4.27) by $i\kappa(2A(\mathbf{x}_1, t))^{-1} \exp(iG(\mathbf{x}_1, t)/\kappa)$ and the addition of the result with the product of $-A(\mathbf{x}_1, t) \exp(iG(\mathbf{x}_1, t)/\kappa)$ and Eq. (4.28) leads to

$$\begin{aligned} & i\kappa\partial_t [A(\mathbf{x}_1, t) \exp(iG(\mathbf{x}_1, t)/\kappa)] \\ &= -\frac{\kappa^2}{2m} \left[2i\kappa^{-1} \partial_{\mathbf{x}_1} A(\mathbf{x}_1, t) \partial_{\mathbf{x}_1} G(\mathbf{x}_1, t) + iA(\mathbf{x}_1, t) \kappa^{-1} \partial_{\mathbf{x}_1}^2 G(\mathbf{x}_1, t) \right. \\ & \quad \left. + \partial_{\mathbf{x}_1}^2 A(\mathbf{x}_1) - A(\mathbf{x}_1) \kappa^{-2} (\partial_{\mathbf{x}_1} G(\mathbf{x}_1, t))^2 \right] \exp(iG(\mathbf{x}_1, t)/\kappa) \\ &= -\kappa^2 (2m)^{-1} \partial_{\mathbf{x}_1}^2 A(\mathbf{x}_1, t) \exp(iG(\mathbf{x}_1, t)/\kappa) \end{aligned} \quad (4.29)$$

By introducing the notation $\psi(\mathbf{x}_1, t) = A(\mathbf{x}_1, t) \exp(iG(\mathbf{x}_1, t)/\kappa)$ this equation can be restated as

$$i\kappa\partial_t \psi(\mathbf{x}_1, t) = -\kappa^2 (2m)^{-1} \partial_{\mathbf{x}_1}^2 \psi(\mathbf{x}_1, t). \quad (4.30)$$

which is the well known *Schrödinger equation* (Ballentine, 1998) in Quantum mechanics (QM). It is important to realize that although this partial differential equation

is intriguingly equivalent to that form in QM, the motivation is somewhat different. Firstly κ represents in QM \hbar which is Planck's constant up to a factor 2π . In the case considered here, κ is a parameter which characterizes the preparation procedure within the experiment. Secondly, QM postulates that the velocity and momentum operator are non-commutative. This has not been postulated in the above derivation. Pure statistics of observables of an endo-observer with respect to the variables of an exo-observer are developed here. It is remarkable that this equation even holds when $A(\mathbf{x}_1, t) = 0$, *i.e.* when the probability density function is zero at any \mathbf{x}_1 . During the derivation of Eq. (4.30) a term for $E_{\text{res}}(\mathbf{x}_1, t_0)$ was derived in Eq. (4.25) which does only hold for $\rho(\mathbf{x}_1, t) \neq 0$. The reason for this apparent contradiction is, that Eq. (4.25) refers to a quantity which is relative with respect to $\rho(\mathbf{x}_1, t)$ whereas Eq. (4.30) refers to a function which is absolutely dependent on $\rho(\mathbf{x}_1, t)$.

When the final form of the estimated dynamics of the probability density function for an ensemble of free particles has been found, it has to be demonstrated that these dynamics are consistent with the mean behaviour of this ensemble, more specifically, the invariance of the mean momentum for any exo-observer has to be demonstrated together with the Galilean invariance of the dynamics with respect to an arbitrary mean velocity.

Initially consider the mean value of any variable which is measured by the endo-observer defined by

$$\langle \mathbf{x}_2 \rangle = \int d^n \mathbf{x} \mathbf{x}_2 \rho(\mathbf{x}, t) \quad (4.31)$$

for any $t \in \mathbb{R}$; the exo-observer measures obviously the same mean coordinate. The mean momentum of the endo-observer is given by the integral over the flux of Eq. (4.8), *i.e.*,

$$\begin{aligned} \langle \mathbf{p} \rangle &= \int d^{k-1} \mathbf{x}_1 \rho(\mathbf{x}_1, t) \partial_{\mathbf{x}_1} G(\mathbf{x}_1, t) \\ &= -i\kappa \int d^{k-1} \mathbf{x}_1 (\psi^*(\mathbf{x}_1, t) \partial_{\mathbf{x}_1} \psi(\mathbf{x}_1, t) - \psi(\mathbf{x}_1, t) \partial_{\mathbf{x}_1} \psi^*(\mathbf{x}_1, t)), \end{aligned} \quad (4.32)$$

By definition $\langle \mathbf{p} \rangle$ has to be proportional to the change of the mean coordinate of the probability distribution of $\rho(\mathbf{x}_1, t)$

$$\begin{aligned} d_t \langle \mathbf{x}_1 \rangle(t) &= - \int d^{k-1} \mathbf{x}_1 \rho(\mathbf{x}_1, t) \frac{\partial}{\partial \mathbf{x}_1} G(\mathbf{x}_1, t) \mathbf{x}_1 = \\ &= [\mathbf{x}_1 \rho(\mathbf{x}_1, t) \partial_{\mathbf{x}_1} G(\mathbf{x}_1, t)]_{-\infty}^{\infty} + \int d^{k-1} \mathbf{x}_1 \rho(\mathbf{x}_1, t) \partial_{\mathbf{x}_1} G(\mathbf{x}_1, t) \end{aligned} \quad (4.33)$$

The bracket in Eq. (4.33) is equal to zero due to the decay of $\rho(\mathbf{x}_1, t)$ which is assumed to be faster than the increase of $|\mathbf{x}|$. (This is a reasonable assumption since it indirectly

defines bounds for the variance of $\rho(\mathbf{x}_1, t)$.) To ensure that $d_t \langle \mathbf{x}_1 \rangle(t) = \text{const.}$ for all time, the higher order time derivatives have to vanish. In order to show this, it is easier to consider the inverse transform of the Fourier transform of $\psi(\mathbf{x}_1, t)$ in Eq. (4.30). When $\tilde{\psi}(\mathbf{k}, t)$ denotes the Fourier transform of $\psi(\mathbf{x}_1, t)$,

$$\tilde{\psi}(\mathbf{k}, t) = (2\pi)^{-(k-1)/2} \int_{-\infty}^{\infty} d^{k-1} \mathbf{x}_1 \psi(\mathbf{x}_1, t) \exp(-ikr) \quad (4.34)$$

the Schrödinger equation becomes

$$i\kappa \partial_t \tilde{\psi}(\mathbf{k}, t) = -\kappa k^2 (2m)^{-1} \tilde{\psi}(\mathbf{k}, t) \quad (4.35)$$

with the trivial solution

$$\tilde{\psi}(\mathbf{k}, t) = \exp(-it\kappa k^2 (2m)^{-1}) \tilde{\psi}(\mathbf{k}, 0) \quad (4.36)$$

The mean momentum (4.32) can thus be expressed in terms of $\tilde{\psi}(\mathbf{k}, t)$ which is

$$\begin{aligned} -i\kappa \int d\mathbf{x}_1 \psi^*(\mathbf{x}_1, t) \frac{\partial}{\partial \mathbf{x}_1} \psi(\mathbf{x}_1, t) &\propto \\ \int d\mathbf{x}_1 \int d^k(\kappa \mathbf{k}) \int d^k(\kappa \mathbf{k}') \tilde{\psi}^*(\mathbf{k}, 0) \tilde{\psi}(\mathbf{k}', 0) \mathbf{k}' \times \\ \exp\left(i\mathbf{x}_1(\mathbf{k}' - \mathbf{k}) - \frac{it\kappa}{2m}(\mathbf{k}'^2 - \mathbf{k}^2)\right) &= \int d^k(\kappa \mathbf{k}') \rho(\mathbf{k}', 0) \mathbf{k}' \end{aligned} \quad (4.37)$$

whereby $\rho(\mathbf{k}', 0) = \tilde{\psi}^*(\mathbf{k}, 0) \tilde{\psi}(\mathbf{k}', 0)$ which proves that $d^a t \langle \mathbf{x}_1 \rangle(t) = 0$ for all $a > 1$.

Now that it has been shown that the Schrödinger equation serves as an appropriate model for the ensemble of free particles requiring the initial probability distribution $\rho(\mathbf{x}_1, 0)$, the measured mean velocities $\langle \mathbf{v} \rangle(\mathbf{x}_1, 0)$ and the variance of the velocity distribution for prediction purposes, the question arises how the mean momentum enters the model Eq. (4.30). By definition Eq. (4.30) has to hold for all mean velocities. In the following consider the frames of reference of two endo-observers one \mathbf{x}_1 is attached to a coordinate system which is immobile with respect to an exo-observer and the other one \mathbf{x}'_1 moves uniformly with the mean velocity $\langle \mathbf{p} \rangle/m$ of the ensemble. The preparation of the experiment is obviously the same for both endo-observers, thus the probability distributions have to be the same, *i.e.*,

$A^2(\mathbf{x}_1, t) = \psi^*(\mathbf{x}_1, t) \psi(\mathbf{x}_1, t) = A'^2(\mathbf{x}'_1, t') = \psi'^*(\mathbf{x}'_1, t') \psi'(\mathbf{x}'_1, t')$. Hence the only available difference between ψ' and ψ is a phase shift, *i.e.*, $\psi'^*(\mathbf{x}'_1, t') = \psi^*(\mathbf{x}_1, t) \exp[i\phi(\langle \mathbf{p} \rangle, \mathbf{x}_1, t)]$ (Ballentine, 1990; Ballentine, 1998). The coordinate transformation between the two endo-observers is $\mathbf{x}_1 = \mathbf{x}'_1 + \langle \mathbf{p} \rangle t' / m, t = t'$, where the gradients in both coordinate systems must be identical due to the linear shift, and the partial time differential is $\partial/\partial t' = \partial/\partial t + \langle \mathbf{p} \rangle / m \partial/\partial \mathbf{x}_1$. The second summand

represents the change of a function at a point \mathbf{x}_1 due to the velocity of mobile frame of reference. Applying the derivatives in coordinates of the uniformly moving frame of reference to Eq. (4.30) to an equation which contains terms as in Eq. (4.30) for the fixed endo-observer plus some additional terms which vanish as the endo-observer model is independent of the mean velocity. For these additional terms to become zero the phase shift must be equal to

$$\phi(\langle \mathbf{p} \rangle, \mathbf{x}_1, t) = \langle \mathbf{p} \rangle \mathbf{x}_1 / \kappa - \langle \mathbf{p} \rangle^2 t / (2m\kappa). \quad (4.38)$$

This identity therefore defines how the initial state of an endo-observer changes, when the mean velocity is added to the initial state.

4.3.1 Bounds for the variance of the probability distribution of spatial coordinates

Although the Schrödinger equation for a free particle is reasonably easy to solve, sometimes an approximation to the variance is sufficient. In that case the variance of the action enables the estimation of $\sigma_{\mathbf{x}_1}(t)$ by calculating the strongest growth possible. Without loss of generality assume that the mean velocity of the ensemble is zero. When at a time t' the variance $\sigma_{\mathbf{x}_1}(t')$ and $\kappa/2$ are given, then due to the bound (4.21) the increase of the variance is limited by $\kappa/(2\sigma_{\mathbf{x}_1}(t'))$, *i.e.*,

$$\sigma_{\mathbf{x}_1}(t) = \sigma_{\mathbf{x}_1}(t') + \kappa t / (2\sigma_{\mathbf{x}_1}(t')). \quad (4.39)$$

4.3.2 Conclusion

This Section 4.3 introduced first the Hamilton-Jacobi and continuity equation for an ensemble of free particles for classical conservative physical systems; this concept has been defined (Hestenes, 1986; Scheck, 1990) to be an exo-observer concept. Following the arguments in Section 4.2 it was demonstrated that exo-observer physics are not available to real-life observers, as the formalism of the Hamilton-Jacobi and Liouville equation has been adapted to the endo-observer. The endo-observer is nothing but an ideal real-life observer in the sense that it has only access to a subset of the physical state space. The problem that a real-life observer cannot measure real numbers as physical variables, since any kind of measurement involves floating point numbers, is not considered here. Modelling of endo-observers remains an open research issue. Few examples within the next section will illustrate the endo-observer model capabilities as they can easily be compared with analytical exo-observer models.

4.4 Analytical Examples

EXAMPLE 4.4.1 (Gaussian distribution for spatial coordinate and velocity) *In the motivation above, a uniformly moving particle whose coordinate and velocity are measured by two radars, may be prepared such that the initial probability density is Gaussian,*

$$\rho(r, v, t) = \frac{1}{2\pi\sigma_1\sigma_2} \exp\left(-\frac{(r - r_0 - vt)^2}{2\sigma_1^2} - \frac{(v - v_0)^2}{2\sigma_2^2}\right) \quad (4.40)$$

$$= \frac{1}{2\pi\sigma_1\sigma_2} \exp\left(c_1 + \frac{c_2^2}{4c_3} - c_3 \left(v - \frac{c_2}{2c_3}\right)^2\right). \quad (4.41)$$

As the endo-observer model implies, the experiment does not allow the measurement of $\rho(r, v)$, since only $\rho(r)$ and $\rho(v)$ are explicitly known, i.e., the prediction has to be confined to employing the Hamilton-Jacobi (4.3) and Liouville equations (4.2). The measurable probability $\rho(r, t)$ is then given by

$$\rho(r, t) = \frac{1}{\sqrt{2\pi}} \frac{1}{\sqrt{\sigma_2^2 t^2 + \sigma_1^2}} \exp\left(\frac{((r - r_0) - v_0 t)^2}{2(\sigma_2^2 t^2 + \sigma_1^2)}\right), \quad (4.42)$$

hence,

$$\langle v \rangle_r(r, t) = \frac{c_2}{2c_3} = \frac{\sigma_2^2(r - r_0)t + \sigma_1^2 v_0}{\sigma_2^2 t^2 + \sigma_1^2} \quad (4.43)$$

$$\left(\langle v^2 \rangle_r - \langle v \rangle_r^2\right)(r, t) = \frac{1}{2c_3} = \frac{\sigma_1^2 \sigma_2^2}{\sigma_2^2 t^2 + \sigma_1^2} \quad (4.44)$$

this follows immediately from the fact that $\rho(r, v, t) = \exp(c_1 + c_2 v - c_3 v^2) = \exp(c_1 + c_2^2/2c_3 - c_3(v - c_2/2c_3)^2)$, with

$$c_1 = -\frac{(r - r_0)^2}{2\sigma_1^2} - \frac{v_0^2}{2\sigma_2^2} \quad (4.45)$$

$$c_2 = \frac{\sigma_2^2(r - r_0)t + \sigma_1^2 v_0}{\sigma_1^2 \sigma_2^2} \quad (4.46)$$

$$c_3 = \frac{\sigma_2^2 t^2 + \sigma_1^2}{2\sigma_1^2 \sigma_2^2} \quad (4.47)$$

$$\frac{c_2}{2c_3} = \frac{\sigma_2^2(r - r_0)t + \sigma_1^2 v_0}{\sigma_2^2 t^2 + \sigma_1^2} \quad (4.48)$$

$$\frac{c_2^2}{4c_3} = \frac{(\sigma_2^2(r - r_0)t + \sigma_1^2 v_0)^2}{2\sigma_1^2 \sigma_2^2(\sigma_2^2 t^2 + \sigma_1^2)} \quad (4.49)$$

$$c_1 + \frac{c_2^2}{4c_3} = -\frac{(r - r_0)^2}{2(\sigma_2^2 t^2 + \sigma_1^2)} + \frac{(r - r_0)v_0 t}{(\sigma_2^2 t^2 + \sigma_1^2)} - \frac{t^2 v_0^2}{2(\sigma_2^2 t^2 + \sigma_1^2)} \quad (4.50)$$

$$= -\frac{((r - r_0) - v_0 t)^2}{2(\sigma_2^2 t^2 + \sigma_1^2)} \quad (4.51)$$

Note the derivation of Eq. (4.42) is based purely on the possible observation an endo-observer can perform. Eq. (4.30) for the 1-dimensional case reads

$$\frac{\partial}{\partial t} \Psi(r, t) = \frac{ih}{2m} \frac{\partial^2}{\partial r^2} \Psi(r, t). \quad (4.52)$$

What an exo-observer measures at a time $t = 0$ is the Gaussian distribution in Eq. (4.42), where $\langle v \rangle(r, 0) = 0$ as long as the mean velocity of the ensemble is equal to zero, i.e., the action function $G(r, 0)$ is in that case is zero as well. The square-root of Eq. (4.42) and Eq. (4.38) leads to the initial state function.

$$\Psi(r, 0) = e^{ik_0 r} e^{\frac{(r - r_0)^2}{4\sigma_1^2}}, \quad (4.53)$$

with $\langle v \rangle = \kappa k_0$ the mean momentum and $\sigma_2 = h/2\sigma_1$ the variance of the initial velocity probability distribution. The solution of Equation (4.53) is computed best by utilizing the Fourier transform of Eq. (4.36). Its solution is well known (Fick, 1988; Ballentine, 1998), and is identical to Eq. (4.42). Note, the appearance of the mass inside the above parameters follow from the fact that Eq. (4.53) deals with momenta rather than velocities as in Eq. (4.42).

EXAMPLE 4.4.2 (The Harmonic Oscillator) Consider again the arrangement of the above experiment, where the objects are harmonic oscillators. The radars are now

employed to measure the momentum p (velocity v) probability distribution $\rho(p, t)$ and the spatial coordinate probability distribution $\rho(r, t)$ for the elongation of the oscillator. Now the time parameters play a crucial role. A typical radar can take say N measurements per second, i.e., it has a resolution for frequencies of up to $\mu_{\max} = 1/(2N)$ which means that changes of a probability distribution greater than v_{\max} cannot be detected. The experiment consists of the following steps.

- Prepare the oscillator with frequency ω . The errors of each individual preparation require the utilization of a model of ensembles with the probability density $\rho(r_0, p_0)$.
- The statistical experiment, i.e. many times repetition of the momentum (velocity) and, separately, coordinate measurement lead to $\rho(r, t), \rho(p, t)$

A harmonic oscillator is described best within the phase space, which is the r, mv -diagram where each individual oscillator with initial momentum mv_0 and initial spatial coordinate r_0 is represented by a uniform rotation about the origin, i.e.,

$$r(t) = \sqrt{r_0^2 + p_0^2} \sin(\omega t + \phi) \quad (4.54)$$

$$v(t) = \sqrt{r_0^2 + p_0^2} \cos(\omega t + \phi), \quad (4.55)$$

with $\tan \phi = p_0/r_0$. This means that the dynamics of an ensemble of oscillators are defined as the rotation of the probability density in the phase space. As in Example 4.4.1 assume that the initial probability distribution is Gaussian which leads for the exo-observer to the phase diagram of the ensemble of oscillators,

$$\rho(r, v, t) = \frac{1}{2\pi\sigma_1\sigma_2} \exp\left(-\left(c_4 - \frac{c_5^2}{c_6}\right)r^2 - c_6\left(p - \frac{c_5}{c_6}r\right)^2\right), \quad (4.56)$$

whereby

$$c_4 = \frac{1}{2\sigma_1^2} - \frac{\sigma_2^2 - \sigma_1^2}{2\sigma_1^2\sigma_2^2} \sin^2(\omega t) \quad (4.57)$$

$$c_5 = \frac{\sigma_2^2 - \sigma_1^2}{4\sigma_1^2\sigma_2^2} \sin(2\omega t) \quad (4.58)$$

$$c_6 = \frac{1}{2\sigma_2^2} - \frac{\sigma_2^2 - \sigma_1^2}{2\sigma_1^2\sigma_2^2} \sin^2(\omega t) \quad (4.59)$$

The measurable probability $\rho(r, t)$ is then given by

$$\rho(r, t) = \frac{1}{2\sqrt{\pi c_6}\sigma_1\sigma_2} \exp\left[-r^2\left(c_4 - \frac{c_5^2}{c_6}\right)\right] \quad (4.60)$$

$$\rho(p, t) = \frac{1}{2\sqrt{\pi c_4}\sigma_1\sigma_2} \exp\left[-p^2\left(c_6 - \frac{c_5^2}{c_4}\right)\right], \quad (4.61)$$

with the simplifying assumption that the measurable probability densities of the endo- and exo- observer are identical. If the model of the harmonic oscillator is known and the probability densities are given as the limit of the frequencies gained by the statistical experiment, the total energy can be easily computed. This is exo-observer modelling as it requires unlimited access to all physical variables. However, as an endo-observer this includes too many assumptions which are not based on the available measurements. Therefore, an endo-observer is confined to a model which deals with the differences between all measured $\rho(r, t + i\tau), \rho(r, t + i\tau)$, where, $i \in \mathbf{N}$ and τ defines the time difference between two successive measurements. Because an exo-observer determines the kinetic energy by

$$\langle T \rangle_{r,p} = \frac{1}{2m} \iint dp dr p^2 \rho(r, p, t), \quad (4.62)$$

which means that the maximal kinetic energy difference of a corresponding endo-observer estimate is equal to

$$E_{osc} = \frac{1}{2} \langle T_{\max} - T_{\min} \rangle_{r,p} = \frac{1}{4m} \iint dv dr p^2 (\rho(r, v, 0) - \rho(r, v, \pi/2\omega)), \quad (4.63)$$

when $\sigma_v(\rho(r, 0)) = \max(\sigma_v)$, and E_{osc} denotes the total energy of a fictitious, non-statistical oscillator with frequency ω . As in our example the energy difference becomes

$$\langle T_{\max} - T_{\min} \rangle_{r,p} = \frac{1}{2} \frac{1}{4m} \|(\sigma_1^2 - \sigma_2^2)\|, \quad (4.64)$$

Consider next the probability density

$$\rho(r_0, p_0, 0) = \frac{1}{2\pi\sigma_1^3\sigma_2^3} r_0^2 p_0^2 \exp\left(-\frac{r^2}{2\sigma_1^2} - \frac{v^2}{2\sigma_2^2}\right) \quad (4.65)$$

and the corresponding energy difference which is

$$\langle T_{\max} - T_{\min} \rangle_{r,p} = \frac{3}{2} \frac{1}{4m} \|(\sigma_1^2 - \sigma_2^2)\| \quad (4.66)$$

The problem above is a purely stationary one, i.e., the probability density is up to a rotational coordinate transformation time invariant. Returning to the approach given in Example 4.4.1 now requires the computation of endo-observer-model (4.30). First, the stationarity of the dynamics has to be taken into account. Stationarity here means, that the function $\psi(r, t)$ consists of two parts, one which is purely time dependent $\Theta(t)$ and the other which is a function of space coordinates only. To accomplish this

the product-ansatz* is utilized (Fick, 1988), i.e., $\psi(r,t) = \psi_n(r)\theta(t)$. Schrödinger's equation becomes due to the mean potential energy $\frac{m\omega^2}{2}r^2$ at coordinate r

$$\left[-\frac{\kappa^2}{2m} \frac{d^2}{dr^2} + \frac{m\omega}{2} r^2 - E_n \right] \psi_n(r) = 0, \quad (4.67)$$

with $E_n \propto \kappa\omega$, because the substitution of $\psi_n(r)\theta(t)$ into Eq. (4.30) leads to $-\frac{\kappa\dot{\theta}}{i\theta} = -\frac{\kappa^2}{2m} \frac{d^2}{dr^2} + \frac{m\omega}{2} r^2 = \text{const.}$ with $\text{const.} = \kappa\omega$ due to the physical requirement that the dynamics are ω -periodic. It can be shown (Fick, 1988) that the solutions of Eq. (4.67) require the discrete set of functions which are defined as $\psi_n(r) = \sqrt{\frac{m\omega}{\kappa\pi}} \frac{(-1)^n}{\sqrt{2^n n!}} e^{r^2/2} \frac{d^n}{dr^n} e^{-r^2/2}$, and $E_n = (n + 1/2)\kappa\omega$. The square of the first two functions for $n = 0, 1$ is in both cases identical with the probability densities in Eqs. (4.61), (4.65), if and only if $\kappa\omega \equiv \frac{1}{4m} \|\langle \sigma_2^2 - \sigma_1^2 \rangle\|$. The equivalence is physically evident because it represents the variance of the total energy.

4.5 From time series to endo-observer models

The above examples have illustrated the differences between endo- and exo-observers. It is now necessary to devise an algorithm which defines the framework of an endo-observer state space model for time series in order to compute (predict) the future likelihood of finding a particle (or an arbitrary bodies center-of-mass) at a spatial coordinate when only a time series is given.

4.5.1 Probability densities from time series

After the dynamics of an endo-observer have been established, its probabilistic formalism has to be related to real-life measurements from experiments (see Section 4.2) which utilize a radar for the spatial coordinates and the velocities. Initially it is assumed that nothing is known about the radar or the experiment's statistical properties.

When the experiment is repeated N times and each time, after t seconds have passed, the velocity and the centre of mass coordinate of a body are measured, a frequency distribution of discrete sets of possible velocities v and spatial coordinates r can be extracted. Under the assumption that N is very large, probability distribution functions for v and r can be fitted to the discrete distribution. However, in most cases an experiment is established only once and the experiment's outcome is only defined by a unique times series consisting of two components, r and v . In this case a modified

*Ansatz is a scientific term for approach.

approach to probabilistic system modelling has to be devised. Assume the modeller is given N data pairs $(\mathbf{r}, \mathbf{v})_i$ with $i = 1, \dots, N$. The mean velocity is thus equal to $\bar{\mathbf{v}} = \sum_i \mathbf{v}_i / N$. A probability distribution of coordinate vectors may be approximated by utilizing a set of transformed data points $(\mathbf{r} - \bar{\mathbf{v}}t, \mathbf{v})_i$ which then lead under the assumption that ensemble mean is equivalent with temporal mean to the identical probability distribution as in the first case. Once the probability density distributions $\rho(\mathbf{r}), \rho(\mathbf{v})$ are available, an initial probability distribution $\rho(\mathbf{r}, t_0) = \rho(\mathbf{r} + N\bar{\mathbf{v}}t)$ can be calculated. The mean velocity distribution can either be approximated by $\langle \mathbf{v} \rangle_{\mathbf{v}}(\mathbf{r}, t_0) = \bar{\mathbf{v}}$, or $\langle \mathbf{v} \rangle_{\mathbf{v}}(\mathbf{r}, t_0)$ may be estimated by utilizing the difference of two initially derived probability distribution functions at two separate instances t_0, t_1 . The latter mean velocity estimation at a coordinate is based on Eq. (4.5). The problem here is that the estimated probability density function $\rho(\mathbf{r}, t_0)$ is a very rough approximation of the exo-observer's probability density function $\rho(\mathbf{r}, t_0)$. In many case much more information is available about the radar's stochastic properties.

Assume that a radar is an ideal one in the sense that the noise which enters the time series is purely random and the central limit theorem (Schlögel, 1989) applies. In this case the probability density function takes the form of a Gaussian distribution function. When the variance for each \mathbf{v} component is $\sigma_{\mathbf{v}}$ and for each \mathbf{r} component is $\sigma_{\mathbf{r}}$, the maximum likelihood method (Papoulis, 1991) of this probability density function then requires that the Gaussian distribution is centered about each measured state $(\mathbf{r}, \mathbf{v})_i$. The probability density function for N data points may be extracted by the following basic relationship between statistical events E_A, E_B, E_C : The probability of event E_A and E_B happening under the constraint of event E_C is given by

$$P(E_A \text{ AND } E_B | E_C) = P(E_A | E_C)P(E_B | E_C), \quad (4.68)$$

whereas the probability of event E_A or E_B happening under the constraint of event E_C is given by

$$P(E_A \text{ OR } E_B | E_C) = P(E_A | E_C) + P(E_B | E_C) - P(E_A \text{ AND } E_B | E_C) \quad (4.69)$$

If the probability density function is required for the special case that N data points are given and at the same time $(\mathbf{r}, \mathbf{v})_i$ and $(\mathbf{r}, \mathbf{v})_j$ are valid measurements for all $1 \leq i, j \leq N$ with $i \neq j$ then Eq. (4.68) needs to be employed. However, when one seeks the probability density estimation for N data points for the case that $(\mathbf{r}, \mathbf{v})_i$ or $(\mathbf{r}, \mathbf{v})_j$ are valid measurements for all $1 \leq i, j \leq N$ with $i \neq j$ then Eq. (4.69) describes the statistical relationship between all measurements correctly. Here it is assumed that the measurements of all data pairs $(\mathbf{r}, \mathbf{v})_i$ are statistically independent



$P((\mathbf{r}, \mathbf{v})_i \text{AND} (\mathbf{r}, \mathbf{v})_j) = 0$ for all $i \neq j$, as well as for any arbitrary statistical combination of the form $P((\mathbf{r}, \mathbf{v})_{i'} \text{AND} \dots \text{AND} (\mathbf{r}, \mathbf{v})_{j'}) = 0$. This assumption is justified as each measurement is performed independently from any of the other ones. A statistical model which defines a common event of N data point measurements each of which leads to the appropriate statistical endo-observer state estimate has thus to employ Eq. (4.69) which then becomes

$$\begin{aligned} \rho_{\{(\mathbf{r}, \mathbf{v})_i | i \leq N\}}(\mathbf{r}, \mathbf{v}, t_0) &= N^{-1} \sum_{i=1}^N (2\pi\sqrt{\sigma_r \sigma_v})^{-3} \\ &\times \exp(-(\mathbf{r} - (\mathbf{r}_i - i\bar{v}t))^2(2\sigma_r^2) - (\mathbf{v} - \mathbf{v}_i)^2/(2\sigma_v^2)). \end{aligned} \quad (4.70)$$

It has to be mentioned that another approach may consider the probability of a model which can generate the common event that $(\mathbf{r}, \mathbf{v})_1 \text{AND} \dots \text{AND} (\mathbf{r}, \mathbf{v})_N$ do occur. This approach has not been utilised as this would assume a statistical exo-observer. Endo-observers require statistics due to the performed measurements which in the ideal case are statistically independent of each other. (A more detailed motivation and derivation of this probability distribution function may be seen in Sections 4.4 and 5.5.) The probability density function $\rho(\mathbf{r}, t_0)$ employed for an endo-observer model is thus given by

$$\rho(\mathbf{r}, t_0) = N^{-1} \sum_{i=1}^N (2\pi\sigma_r \sigma_v)^{-3/2} \exp(-(\mathbf{r} - (\mathbf{r}_i - i\langle \mathbf{v} \rangle_v(\mathbf{r}, t_0)t_0))^2/(2\sigma_r^2)). \quad (4.71)$$

and the three mean velocity components at an arbitrary spatial coordinate \mathbf{r} become

$$\langle v_{j'} \rangle_v(\mathbf{r}, t) = \int_{-\infty}^{\infty} d^3 \mathbf{v} d^3 \mathbf{r} \rho_{\{(\mathbf{r}, \mathbf{v})_i | i \leq N\}}(\mathbf{r}, \mathbf{v}, t_0) v_{j'} \quad (4.72)$$

with the total velocity variance of

$$\sigma_{\{\mathbf{v}_i | i \leq N\}}^2 = N^{-1} \sum_{i=1}^N (2\pi\sigma_v)^{-3/2} \int_{-\infty}^{\infty} d^3 \mathbf{v} (\mathbf{v} - \bar{\mathbf{v}})^2 \exp(-(\mathbf{v} - \mathbf{v}_i)^2/(2\sigma_v^2)). \quad (4.73)$$

The formulae (4.70)–(4.73) just derived may in some cases be interpreted as the probability distribution functions utilized for calculating $\rho(r, v, t)$ at any instant t in the future (Papoulis, 1991), thus providing predictions. However, as argued in Section 4.2, the probability density function $\rho(r, v, t)$ of an exo-observer cannot be extracted from the kind of measurement performed by the radar arrangement. The argumentation so far is thus based on the same principle as in the beginning of this section. Instead of utilizing the data points themselves and superimposing them, which could be interpreted as the superposition of N δ -probability distributions, a Gaussian probability distribution

with fixed variance about each data point has been employed for the estimation of the relevant endo-observer's initial variables. However, the prediction model of an endo-observer's time series is very much different from the kind of prediction algorithm utilized in black-box modelling. As in Example 4.4.1 the total variance of an initial probability density function $\rho(r, v, t_0)$ will be employed in the following example for estimating the dynamics of $\rho(r, v, t)$ with $t > t_0$. Since a complete endo-observer model with respect to a time series has been established, an example is presented where a set of two data pairs $(r, v)_j$ are chosen for computing the future distribution (prediction) of $\rho(r, t)$ in endo- and exo-physical variables in order to compare the models with each other. As the endo-observer model for three spatial coordinates does not add anything new to the principles under discussion, the without loss of generality the following examples focus on a particle moving uniformly along a line. The following calculations may be simplified by realizing that the dynamics of a superimposed Gaussian probability distribution is identical to the superposition of the dynamics of each individual Gaussian probability distribution. This is a property of the linearity of all operators in case of the exo-observer's continuity equation as well as the endo-observer's Schrödinger equation. The limitation to only two measured data pairs $(r, v)_i$, with $i = 1, 2$ is due to the analytical difficulties which arise if when the endo-observer model is applied to larger sets of data pairs.

EXAMPLE 4.5.1 An endo-observer's states with erroneous mean velocity measurements *The purpose of this example is to demonstrate how the probability density function $\rho(r, t)$ of an endo-observer compares to the one of an exo-observer. Because numerical simulations are far beyond the scope of this thesis only a simple analytically tractable example may be chosen. It is therefore assumed that the variances σ_r, σ_v are known and that an endo-observer is just given two observations. Additionally, the estimates of an endo-observer's mean velocities $\langle v \rangle_v(r, t)$ are assumed to be faulty in the sense that an endo-observer identifies a linear function of $\langle v \rangle_v(r, t)$ rather than the correct one. This example is structured as follows: (i) The probability density function of the exo-observer is calculated. (ii) The product of variances of the initial spatial coordinate and velocity probability distributions are determined. (iii) An estimate for the mean velocity distribution for each spatial coordinate is introduced. (iv) The initial endo-observer state is composed. (v) The Fourier transform is employed for computing the endo-observer state for all time t . (vi) The probability density function of an endo-observer is compared with the one of an exo-observer.*

The difficulty of finding examples is not because the theory which has been developed in this chapter is only applicable to few cases, instead it is because it becomes

difficult finding examples which can be treated analytically as the complexity increases. Since numerical simulations are not within the scope of this thesis the example given below may be realistic in its computation but it lacks the complexity of real-life time series which are sets of at least several hundred of data points. In order to keep the calculations simple few additional modelling issues are taken into account. Because the multi-dimensional case does not give any new insights about the model, only the one-dimensional case is considered here. It has been proven above that the Schrödinger equation is invariant under inertial transformations, it can always be found a coordinate system such that two spatial coordinate estimates are $r_1 = -r_2$ and two velocity measurements hold $v_1 = -v_2$.

The state space's probability density function of a particle which moves along the line is assumed to be defined by

$$\begin{aligned} \rho(r, v, t) = & \frac{1}{4\pi\sigma_1\sigma_2} \left[\exp\left(-\frac{(\sigma_1^2 + \sigma_2^2)}{4\sigma_1^2\sigma_2^2} ((r - r_1 - vt)^2 + (v - v_1)^2)\right) \right. \\ & + \frac{(\sigma_1^2 - \sigma_2^2)(r - r_1 - vt)(v - v_1)}{4\sigma_1^2\sigma_2^2} \Big) \\ & + \exp\left(-\frac{(\sigma_1^2 + \sigma_2^2)}{4\sigma_1^2\sigma_2^2} ((r + r_1 - vt)^2 + (v + v_1)^2)\right) \\ & \left. + \frac{(\sigma_1^2 - \sigma_2^2)(r + r_1 - vt)(v + v_1)}{4\sigma_1^2\sigma_2^2} \Big) \right], \end{aligned} \quad (4.74)$$

which therefore exhibits the dynamics of $\rho(r, t)$ according to

$$\begin{aligned} \rho(r, t) = & \frac{1}{2\sqrt{\pi}\sqrt{\sigma_2^2(t-1)^2 + \sigma_1^2(t+1)^2}} \left[\exp\left(-\frac{(r - r_1 + tv_1)^2}{\sigma_2^2(t-1)^2 + \sigma_1^2(t+1)^2}\right) \right. \\ & \left. + \exp\left(-\frac{(r + r_1 + tv_1)^2}{\sigma_2^2(t-1)^2 + \sigma_1^2(t+1)^2}\right) \right] \end{aligned} \quad (4.75)$$

with the mean state $(\bar{r}, \bar{v})^T = (0, 0)^T$. These dynamics hold for all time $t \in \mathbb{R}$. In order to compute the endo-observer dynamics, the total variance of $\rho(r, v, t)$ needs to

be determined.

$$\begin{aligned}
 \kappa_1^2/4 &= \int_{-\infty}^{\infty} dr dv \rho(r, v, 0) r^2 v^2 = \sigma_r^2 \sigma_v^2 = \\
 &= \int_{-\infty}^{\infty} dr dv \frac{r^2 v^2}{4\pi\sigma_1\sigma_2} \left[\exp\left(-\frac{(\sigma_1^2 + \sigma_2^2)}{4\sigma_1^2\sigma_2^2} ((r - r_1)^2 + (v - v_1)^2)\right) \right. \\
 &\quad \left. + \frac{(\sigma_1^2 - \sigma_2^2)(r - r_1)(v - v_1)}{4\sigma_1^2\sigma_2^2} \right) \\
 &\quad + \exp\left(-\frac{(\sigma_1^2 + \sigma_2^2)}{4\sigma_1^2\sigma_2^2} ((r + r_1)^2 + (v + v_1)^2)\right) \\
 &\quad \left. + \frac{(\sigma_1^2 - \sigma_2^2)(r + r_1)(v + v_1)}{4\sigma_1^2\sigma_2^2} \right] \\
 &= \frac{3\sigma_1^4 + 3\sigma_2^4 + 4(1 + r_1^2)v_1^2 + 2\sigma_2^2(1 + r_1^2 - 4r_1v_1 + v_1^2)}{8\sqrt{\sigma_1^2 + \sigma_2^2}} \\
 &\quad + \frac{2\sigma_1^2(1 + r_1^2 - \sigma_2^2 + 4r_1v_1 + v_1^2)}{8\sqrt{\sigma_1^2 + \sigma_2^2}},
 \end{aligned} \tag{4.76}$$

which may be compared with a single Gaussian probability density function

$$\rho(r, v, t) = \frac{1}{2\pi\sigma_1\sigma_2} \left[\exp\left(-\frac{(\sigma_1^2 + \sigma_2^2)}{4\sigma_1^2\sigma_2^2} ((r - r_i - vt)^2 + (v - v_i)^2)\right) \right. \\
 \left. + \frac{(\sigma_1^2 - \sigma_2^2)(r - r_i - vt)(v - v_i)}{4\sigma_1^2\sigma_2^2} \right] \tag{4.77}$$

with the variance

$$\begin{aligned}
 \kappa_2^2/4 &= \int_{-\infty}^{\infty} dr dv \rho(r, v, 0) (r - r_i)^2 (v - v_i)^2 = \sigma_r^2 \sigma_v^2 = \\
 &= \frac{3(\sigma_1^4 + \sigma_2^4) - 2\sigma_1^2\sigma_2^2 + 2(\sigma_1^2 + \sigma_2^2)}{16\sqrt{\sigma_1^2 + \sigma_2^2}}
 \end{aligned} \tag{4.78}$$

All that is now needed for the endo-observer model is the mean velocity at an instant $t_0 = 0$ and at the spatial coordinate r which is defined by

$$\begin{aligned}
 \langle v \rangle_v(r, t) &= \int_{-\infty}^{\infty} dv \rho(r, 0|v)v \\
 &= r \frac{\sigma_1^2 - \sigma_2^2}{\sigma_1^2 + \sigma_2^2} - \frac{\exp\left(\frac{4rr_1}{\sigma_1^2 + \sigma_2^2}\right) - 1}{\exp\left(\frac{4rr_1}{\sigma_1^2 + \sigma_2^2}\right) + 1} \left(r_1 \frac{\sigma_1^2 - \sigma_2^2}{\sigma_1^2 + \sigma_2^2} - v_1 \right).
 \end{aligned} \tag{4.79}$$

This equation is superimposed by two functions of which the first term is linear in r and the second term which is nothing but the hyperbolic tangents $\tanh[2rr_1/(\sigma_1^2 + \sigma_2^2)]$

multiplied with a constant $r_1(\sigma_1^2 - \sigma_2^2)/(\sigma_1^2 + \sigma_2^2) - v_1$. It is now assumed that the endo-observer is incapable of estimating the precise mean velocity as given in Eq. (4.79). Because of the imprecision the endo-observer estimates a pure linear relationship in form of $\langle v \rangle_v(r, t) \propto r$. The initial state is defined as before through the identity $\psi(r, t_0) = \sqrt{\rho(r, t_0)} \exp(im \int_0^r dr' \langle v \rangle_v(r', t_0))$ and therefore holds

$$\begin{aligned} \psi(r, 0) = & \frac{1}{\sqrt{2\sqrt{\pi}\sqrt{\sigma_2^2 + \sigma_1^2}}} \left[\exp\left(-\frac{(r-r_1)^2}{\sigma_2^2 + \sigma_1^2}\right) \right. \\ & \left. + \exp\left(-\frac{(r+r_1)^2}{\sigma_2^2 + \sigma_1^2}\right) \right]^{(1/2)} \exp\left(\frac{im}{2} \frac{\sigma_1^2 - \sigma_2^2}{\sigma_1^2 + \sigma_2^2} r^2\right) \end{aligned} \quad (4.80)$$

where it has to be borne in mind that the endo-observer state function $\psi(\bullet)$ incorporates the momentum and not the velocity, which is the reason for the mass m appearing in the exponent of the function.

The Schrödinger equation now can easily be set up by employing Eq. (4.80) and the estimate of κ in Eq. (4.78). In order to compute the dynamics it is not very advisable to perform the corresponding calculation in the spatial coordinate representation of the Schrödinger equation. However, the Fourier transform may be applied to Eq. (4.80) which according to Eq. (4.35) leads for any t to $\tilde{\Psi}(k, t)$ in Eq. (4.36). The inverse Fourier transform then provides $\psi(r, t)$ for all $t \in \mathbb{R}$. In order to simplify the computation even further another approximation is utilized. In case that $r_0 \gg \sigma_1$ the square root of the sum of exponential functions in Eq. (4.80) may be approximated with the sum of the square roots taken from the exponential functions individually.

$$\begin{aligned} \psi(r, 0) \approx & \frac{1}{\sqrt{2\sqrt{\pi}\sqrt{\sigma_2^2 + \sigma_1^2}}} \left[\exp\left(-\frac{(r-r_1)^2}{2\sigma_2^2 + 2\sigma_1^2}\right) \right. \\ & \left. + \exp\left(-\frac{(r+r_1)^2}{2\sigma_2^2 + 2\sigma_1^2}\right) \right] \exp\left(\frac{im}{2} \frac{\sigma_1^2 - \sigma_2^2}{\sigma_1^2 + \sigma_2^2} r^2\right) \end{aligned} \quad (4.81)$$

The Fourier transform is now easily performed via Eq. (4.34) which thus leads with Eq. (4.36) to the Fourier transform

$$\begin{aligned} \tilde{\Psi}(k, t) = & \sum_{j=1}^2 \sqrt{\frac{\sqrt{\sigma_1^2 + \sigma_2^2}}{2\sqrt{\pi}(1 - im(\sigma_1^2 - \sigma_2^2))}} \exp\left(-i \frac{t\kappa k^2}{2m}\right) \\ & \times \exp\left(\frac{-ik^2(\sigma_1^2 + \sigma_2^2)^2 - 2kr_0(\delta_{j1} - \delta_{j2})(\sigma_1^2 + \sigma_2^2) + mr_0^2(-\sigma_1^2 + \sigma_2^2)}{2(\sigma_1^2 + \sigma_2^2)(i + m\sigma_1^2 - m\sigma_2^2)}\right). \end{aligned} \quad (4.82)$$

The endo-observer state space function may now be determined through the inverse Fourier transform applied to $\tilde{\Psi}(k, t)$ which immediately gives

$$\begin{aligned} \Psi(r, t) = & \sum_{j=1}^2 \sqrt{\frac{m\sqrt{\sigma_1^2 + \sigma_2^2}}{2\sqrt{\pi}(i\kappa t + m\sigma_2^2(1 - \kappa t) + m\sigma_1^2(1 + \kappa t))}} \\ & \times \exp\left(\frac{imr^2(\sigma_1^2 + \sigma_2^2)(i + m(\sigma_1^2 - \sigma_2^2)) - 2m(\delta_{j1} - \delta_{j2})rr_0(\sigma_1^2 + \sigma_2^2)}{2(\sigma_1^2 + \sigma_2^2)(i\kappa t + m\sigma_2^2(1 - \kappa t) + m\sigma_1^2(1 + \kappa t))}\right) \\ & \times \exp\left(-\frac{mr_0^2(\sigma_2^2(1 - \kappa t) + \sigma_1^2(1 + \kappa t))}{2(\sigma_1^2 + \sigma_2^2)(i\kappa t + m\sigma_2^2(1 - \kappa t) + m\sigma_1^2(1 + \kappa t))}\right). \end{aligned} \quad (4.83)$$

The corresponding probability density $\rho(r, t) = \Psi(r, t)\Psi^*(r, t)$ is then given by the product between each summand in Eq. (4.83) and its conjugate complex form, because the approximation above considers the Fourier transform of each component, i.e.,

$$\begin{aligned} \rho(r, t) = & \sum_{j=1}^2 \frac{m\sqrt{\sigma_1^2 + \sigma_2^2}}{2\sqrt{\pi}\sqrt{\kappa^2 t^2 + m^2(\sigma_2^2(1 - \kappa t) + \sigma_1^2(1 + \kappa t))^2}} \\ & \times \exp\left(\frac{-m^2[r\sigma_1^2 + r\sigma_2^2 + r_0(\delta_{i1} - \delta_{i2})[\sigma_2^2(1 - \kappa t) + \sigma_1^2(1 + \kappa t)]]^2}{(\sigma_1^2 + \sigma_2^2)(\kappa^2 t^2 + m^2[\sigma_2^2(1 - \kappa t) + \sigma_1^2(1 + \kappa t)]^2)}\right) \end{aligned} \quad (4.84)$$

in order to utilize the inverse transform to calculate the probability density function $\rho(r, t)$ in an endo-observer's spatial coordinates. Function (4.84) describes the estimation of $\rho(r, t)$ when only the initial probability density function $\rho(r, 0)$ and the action κ are given. This result may be compared with Eq. (4.75) and the endo-observer model which utilizes the estimated probability density function of each measurement. The endo-observer model for Example 4.4.1 leads here to

$$\begin{aligned} \rho(r, t) = & \frac{\sqrt{\sigma_1^2 + \sigma_2^2}}{2\sqrt{\pi}\sqrt{\sigma_1^4 + 2\sigma_1^2\sigma_2^2 + \sigma_2^4 + \kappa_2^2 t^2}} \\ & \sum_{i=1}^2 \exp\left(-\frac{(\sigma_1^2 + \sigma_2^2)(r + (\delta_{i,1} - \delta_{i,2})(r_i - v_i t)^2)}{(\sigma_1^2 + \sigma_2^2)^2 + \kappa_2^2 t^2}\right) \end{aligned} \quad (4.85)$$

As can be seen in Figure 4.4 the large value of κ leads to a very rapid dispersion of the probability density function $\rho(r, t)$. The reason the estimated probability density function spreads much more quickly than in the case of Eq. (4.75) is given by the variance of $\rho(r, 0)$. When no further insight about the specific probability density function $\rho(r, v, 0)$ is available, as it has been demonstrated in case of an endo-observer, the given estimate in Eq. (4.84) is the only one which does not include any further assumptions about

the two measurements. In some cases not only a time series $\{(r_1, v_1, t_1), (r_2, v_2, t_2)\}$ but also few properties of an endo-observer are explicitly known. When through repeated experiments the additional properties such as the mean and variance of an estimated probability density function $\rho_i(r, v, t_i)$ for the two instants t_1, t_2 are known, the estimate of $\rho(r, t)$ based on $\rho_i(r, v, t_i)$ can be improved significantly. The constant κ is in this particular case based on the integral

$$\kappa_2 = \int_{-\infty}^{\infty} dr dp r^2 p^2 \rho_i(r, p, t_i) \quad (4.86)$$

which is generally much smaller than the value given in Eq. (4.76). The reason for that is that κ in Eq. (4.76) does not only include the variance of $\rho_i(r, p, t_i)$ at each observation but also the variance of the probability distribution among all $\rho_i(r, p, t_i)$. To give a flavour about the effect different estimates of κ have on the endo-observer model, the following Figure 4.4 shows three different computations of $\rho(r, t)$. (i) As a reference the probability density function of the exo-observer (4.74) is presented in Fig. 4.4.a. (ii) κ_1 is chosen according to Eq. (4.76) and the corresponding probability function $\rho(r, t)$ is plotted in Fig. 4.4.b. (iii) The information about κ_2 which is available to an endo-observer is given by Eq. (4.78) and the probability density function is shown in Fig. 4.4.c.

4.6 Conclusion

The notion of endo- and exo-observer have been introduced and the difficulties arising by applying probability theory to this concept established. The method of unbiased guess by Shannon was applied for estimating the residual variance of kinetic energy which enters the Hamilton-Jacobi equation of an endo-observer. The Liouville and Hamilton-Jacobi equations for endo-observer dynamics were then reformulated in a common partial differential equation, the Schrödinger equation. After important properties characterizing an ensemble of free particles, such as the time invariance of the mean velocity and preservation of the variance of action of the state space, have been proved, analytical examples then demonstrate the applicability of the model.

Although this experimental arrangement of coordinate and velocity measurements of a particle or a body's center-of-mass is very realistic and refers immediately to the measurements as they are provided in case of a ballistic missile trajectory estimation, the dynamics of ballistic missile are certainly neither uniform nor linear as the analysis in Chapter 3 suggests. The problems which have to be solved in the forthcoming chapter are as follows. (i). The endo-observer's state space concept has to be extended

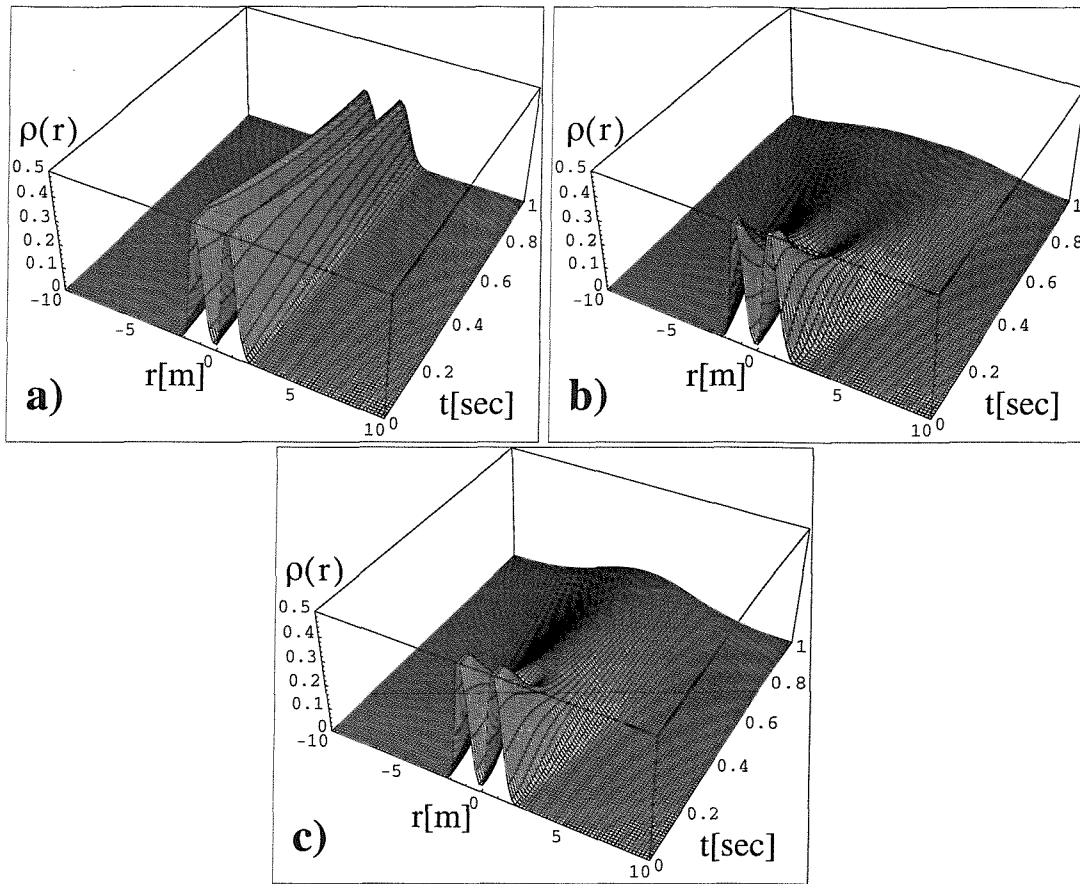


Figure 4.4: This figure illustrates the difference between exo-observer models and endo-observer model by choosing a non-Gaussian distribution function. In order to keep the problem analytically tractable the superposition of two Gaussian functions defined in Eq. (4.74) in the state space are chosen. The first sub-figure a) therefore shows the kind of prediction which could be possible if endo-observer had access to $\rho(r, v, t)$ [see Eq. (4.75)], whereas the second sub-figure b) is based on an estimate of κ_1 given in Eq. (4.76) and the corresponding dynamics defined in Eq. (4.84). The last sub-figure corresponds to Eq. (4.85) which employs additional information of an endo-observer about the statistics of individual observations $\rho_i(r, p, t_i)$ which then leads to a more precise prediction since the dynamics of an endo-observer are applied to individual data points taken from a time series rather than applied to an estimate of $\rho(r, t)$ which has been extracted from the total set of data points taken from a time series. The parameters are as follows: $\sigma_1 = 0.5, \sigma_2 = 0.1, r_1 = 1, v_1 = 0.25$

to the case that the vector field is non-linear and that the state vector's coordinate components depend on more than just one variable. (ii). A real-life physical model also incorporates system parameters which have to be included as well. (iii), the new formalism must provide a means of system identification and tracking with respect to given data points.

Chapter 5

Uncertainty in non-linear dynamics

Forward

An algorithm is proposed which seeks to extend the endo-observer concept from linear to non-linear dynamics. It is argued that the identification of non-linear vector flows leads to uncertainties which differ from the kind of uncertainties introduced for linear systems. Uncertainties of the vector fields inside the classical (exo-observer) state space are shown to be time dependent and to propagate through the state space. The dynamics of the endo-observer's trajectories thus consist of the exo-observer dynamics which are superimposed with dynamics originating from the observer's uncertainty. Additionally, an algorithm towards estimating initial probability density functions of the endo-observer's states under the constraint of a sparse time series data is derived. A tracking model for endo-observers completes the analysis of non-linear endo-observer models.

5.1 Motivation

In the last chapter the endo-observer dynamics of a linear dynamical system, *i.e.*, a uniformly moving center-of-mass, were derived. It was found that no real-life observer (endo-observer) can access the system state vectors which are required for physical models. The framework derived above allows the incorporation of unprejudiced uncertainty of a real-life observer in a physical model which thus bridges two concepts. The abstract purely theoretical (exo-observer) concept is related through a probabilistic model to the real-life endo-observer description based on real experimental processes. This chapter is devoted to arbitrary non-linear dynamical system modelling and gen-

eral non-linear system identification and prediction under strong modelling constraints such as unprejudiced assumptions about the stochasticity of an endo-observer. These constraints are as follows.

(i) The non-linear dynamics are known up to their parameters and state of the system. (ii) Because physical experiments always include noise the resulting errors have to be taken into account by the dynamics. It is shown that endo-observer (real-life observer) measurements lead to dynamics which are different from exo-observer (ideal observer) dynamics. (iii) Because state vector components and parameters are not directly accessible, estimates have to be employed which enter the dynamics derived below. (iv) The uncertainty of a system requires a probabilistic model with initial probability density functions for the initial state and parameter space. (v) The probability density function of an initial state is not accessible all which is known are the bounds on system parameters, bounds on non-observable state vector components and the measurements in form of rational numbers, *i.e.*, the algorithm has to provide a consistent model for giving an estimate of any initial probability density function of the state and parameter space. The algorithm must allow that any measurement at any time enters the dynamics consistently with respect to prior measurements. After a framework for system identification has been developed, future predictions have to be based on this identified system and most recent observations.

There are many algorithms (*e.g.* the Kalman filter (Chui and Chen, 1999), stochastic differential equations (Jetschke, 1989)) which claim to be able to do the kind of estimation and identification of non-linear systems mentioned above, however, in most cases the assumptions utilised prior to these algorithms include specific kind of noises for a stochastic differential equation, particular distributions of the probability density, accessibility of the entire state or parameter space to an observer, certain density of data points within the state space about an attractor, time invariance of stochasticity, etc.

No such prior assumptions or claims have been presumed during the derivation of this model below. The algorithm introduced here thus uses a very general approach with a minimum of assumptions required. This versatility comes at a price. It is expected that algorithms which have been developed for stochastic systems with specific properties will perform better when these specific confines are met by a dynamical system.

It has to be stressed that it is not the subject of this work to analyse under what circumstances a particular stochastic model performs best, this is an open research issue left for future research. This work is solely focused on developing an algorithm

which incorporates the above restrictions and no other hidden constraints.

This chapter is organized as follows. The introduction 5.2 specifies the endo-observer concept which is employed in this chapter to non-linear dynamical systems. Section 5.3 is dedicated to deriving a model for non-linear dynamics when vector fields with uncertainties enter the state space. This section is followed by Section 5.4 which explores the non-linear dynamics of a state space when a stochastic distribution of erroneous vector fields drive the system. The incorporation of bounds for unavailable state vector components and physical parameters into the endo-observer's dynamics is made in Section 5.5. How a sparse time series (set of all past observational data points) can be included into the derived models of the sections above is demonstrated in Section 5.5.4. The prediction of dynamics may also require model tracking which is introduced in Section 5.6. The conclusion in Section 5.7 shortly summarises the properties of non-linear observers in this chapter.

5.2 Introduction

This chapter introduces a new concept of non-linear systems modelling in the coordinates of an endo-observer. The aim is to find a model based on the premise that the state of a system is only accessible by statistical means and that the dynamics are given for a deterministic system. Although there exists a huge variety of models (Papoulis, 1991; Jetschke, 1989; Gardiner, 1998), their motivations and assumptions are insufficient for our purpose. Most models either make assumptions about the stochasticity of the noise and how it enters the state space model, which is not explicitly given here, or they consider the evolution of an initial probability density function which is unknown in this analysis. It has been shown in the last chapter how profound the nature of an endo-observer's observations are in their effect on the model of a linear system. This model was based on a *Hamiltonian* which can be derived analytically in case of an ensemble of free particles. In the general non-linear case there does not exist an exact analytical solution only numerically evaluated integrals may exist. An approach as employed in Chapter 4 may be utilised to derive a similar model for the non-linear case, however, this approach has not been attempted here, as the derivation of a numerical model is computational costly and cumbersome and it is unclear if the approach can be proved for a general non-linear system. Even if the Hamiltonian in form of Eq. (4.16) could be derived, a Schrödinger equation is not suitable for the identification of the flow in the state space. The reasons for this are:

- (i) The non-linear dynamics of a physical system are derived for an exo-observer.

- (ii) The flow within the exo-observer's state space depends on the initial state. An endo-observer model cannot access all components of an exo-observer's state which prevents utilising the model derived in Chapter 4.
- (iii) Because the initial state cannot be measured by an endo-observer the state space flow itself is subject to errors which has to be incorporated in the model.
- (iv) Since the non-linear dynamics of a physical system are derived for an exo-observer, an endo-observer state space model has to be derived which employs the knowledge of the state space of an exo-observer and includes an error of the endo-observer at the same time.

When there is an observation given by an endo-observer which identifies that the system is at a particular state, then there exists an endo-observer specific probability distribution which describes the probability the system can be found at a specific state for a given observation. Because the endo-observer knows the dynamics of the state, a flow is expected which is different from that identified by the exo-observer. The vector field which arises due to the difference between the observation by the endo-observer and the nominal one given by the exo-observer is called the difference vector field. It is shown below how a difference vector field enters the dynamics of an exo-observer and also how the difference vector field evolves with time. As the initial state of a difference vector field is inaccessible to an endo-observer, this lack of knowledge has to be included in the model. A similar approach is that presented in Chapter 4 which then leads to the state space dynamics of an endo-observer. The model presented here cannot be applied to any arbitrary subset of the state space. To circumvent this problem the model will be extended to the case where, apart from lower dimensional observations through the endo-observer, bounds for variables and parameters are given which cannot be accessed by the endo-observer. This will complete the estimation (identification) task of this modelling approach. Prediction may easily be accomplished by evolving the dynamics over time. Obviously, the quality of the predictions depends on the precision with which an endo-observer fits its state space model to the one of the exo-observer. For longer prediction times the dynamics will become increasingly inaccurate. It is therefore shown how to represent the system more accurately when the probability distribution of the parameter space is defined through the previous endo-observer's measurements and when recent measurements are subsequently given. As it will become evident in this chapter, the main drawback of this model is that it only applies to continuous dynamics for which the vector field, apart from few unknown parameters, is explicitly defined. The quality of the identification and prediction very

much depends on the accuracy of bounds for the state vector components which have to be included in the model.

5.3 Propagation of a difference vector field in the state space

The dynamics of a deterministic system are specified by a differentiable vector field $\mathbf{F}_{\text{ex}}(\mathbf{x}_{\text{ex}})$ in the *state space* with a *state vector* $\mathbf{x}_{\text{ex}} \in \mathbb{R}^n$, such that

$$d_t \mathbf{x}_{\text{ex}} = \mathbf{F}_{\text{ex}}(\mathbf{x}_{\text{ex}}). \quad (5.1)$$

The fact that a deterministic system requires error-free measurements of the vector field and state vector is emphasised by the index ‘ex’ which refers to the concept of an exo-observer in Section 4.2. The hypothetical observer of a deterministic, *i.e.* error free, experiment is an *exo-observer*. An observer that is not error free which seeks to relate its observation through an endo-observer model to a deterministic model is an *endo-observer*. The measurement of an endo-observer can therefore be interpreted as the alignment of an endo-observer model to an exo-observer model. Since any measurement is corrupted with noise, physical measurements relate, by definition, to endo-observer models whereas classical mechanics are exo-observer models. We distinguish here two different kind of errors which enter an endo-observer model. The misalignment of the endo-observer model with respect to the deterministic model, *i.e.*, the endo-observer identifies co-ordinate $\mathbf{x}_{\text{ex}} + \Delta \mathbf{x}_{\text{ex}}$ instead of co-ordinate \mathbf{x}_{ex} , and the misidentification of a measured variable, *i.e.*, the endo-observer measures $\mathbf{F}_{\text{ex}}(\mathbf{x}_{\text{ex}}, t) + \Delta \mathbf{F}$ instead of $\mathbf{F}_{\text{ex}}(\mathbf{x}_{\text{ex}}, t)$. An estimate for an endo-observer model can be found by taking the mean over many (N) repetitive measurements, *i.e.*,

$$\langle \mathbf{F}_{\text{ex}} \rangle(\mathbf{x}_{\text{en}}, t) = \frac{1}{N} \sum_{i=1}^N \mathbf{F}_{\text{ex}}(\mathbf{x}_{\text{en}}, t, i). \quad (5.2)$$

The endo-observer model seeks to identify a specific trajectory of an exo-observer’s state space for a given experiment. If within a finite interval $I_{\Delta \mathbf{x}_{\text{en}}}(\mathbf{x}_{\text{en}}) = [\mathbf{x}_{\text{en}} - \Delta \mathbf{x}_{\text{en}}, \mathbf{x}_{\text{en}} + \Delta \mathbf{x}_{\text{en}}]$ there is an overall error

$\varepsilon(I_{\Delta \mathbf{x}_{\text{en}}}(\mathbf{x}_{\text{en}})) = \int_{-\Delta \mathbf{x}_{\text{en}}}^{\Delta \mathbf{x}_{\text{en}}} d^n \mathbf{x}_{\text{en}} (\mathbf{F}_{\text{en}} - \langle \mathbf{F}_{\text{en}} \rangle)^2(\mathbf{x}_{\text{en}}, t) \rho(\mathbf{x}_{\text{en}}, t)$, this information can be employed to estimate the deviation of the vector field from the mean vector field of the endo-observer by introducing $\mathbf{q}(\mathbf{x}_{\text{en}}, t) = \lim_{\Delta \mathbf{x}_{\text{en}} \rightarrow 0} \varepsilon(I_{\Delta \mathbf{x}_{\text{en}}}(\mathbf{x}_{\text{en}})) / \Delta \mathbf{x}_{\text{en}}$. The vector field of an endo-observer’s has to take this estimate into account

$$d_t \mathbf{x}_{\text{en}} = \mathbf{F}_{\text{en}}(\mathbf{x}_{\text{en}}, t), \quad (5.3)$$

with $\mathbf{F}_{\text{en}}(\mathbf{x}_{\text{en}}, t) = \mathbf{q}(\mathbf{x}_{\text{en}}, t) + \langle \mathbf{F}_{\text{ex}} \rangle(\mathbf{x}_{\text{en}}, t)$.

The following Section 5.3.1 shows that the difference vector field is not constant, even when the exo-observer model is time invariant, because the additional shift which is imposed on a trajectory subsequently changes the vector field to which the trajectory is subject of for the future states.

5.3.1 Dynamics of a difference vector field

It has been argued above that the dynamics of an endo-observer *vector field* \mathbf{F}_{en} are defined by a superposition of the nominal exo-observer vector field $\langle \mathbf{F}_{\text{ex}} \rangle(\mathbf{x}_{\text{en}}, t)$ and a difference vector field $\mathbf{q}(\mathbf{x}_{\text{en}}, t)$ which represents the noise in a vector field effecting the dynamics an endo-observer system incorporates. Because there is no information available to the endo-observer of how $\mathbf{q}(\mathbf{x}_{\text{en}}, t)$ may change with time t and state \mathbf{x}_{en} , assumptions about these dependencies have to be included into the endo-observer model. The choice of an initial distribution $\mathbf{q}(\mathbf{x}_{\text{en}}, t_0)$ for a particular time t_0 will be treated in the next section. This section is concerned with the derivation of the estimation of the difference–vector–field’s dynamics.

Let $V_S(\mathbf{x}_{\text{en}}) \subset \mathbb{R}^n$ be a subset of the endo-observer state space with its corresponding piecewise smooth orientable surface $S_S(\mathbf{x}_{\text{en}})$ —i.e., S_S has a parametric representation $\mathbf{x}_{\text{en},S}(t)$ such that $\mathbf{x}_{\text{en},S}(t)$ has a continuous derivative $d_t \mathbf{x}_{\text{en},S}(t)$ which is nowhere a zero vector—with \mathbf{x}_{en} at its center. Then $C_S(\mathbf{x}_{\text{en}})$ is defined to be the boundary of $S_S(\mathbf{x}_{\text{en}})$ which is a piecewise smooth simple closed curve with \mathbf{x}_{en} at its centre. For simplicity let us choose the shape of the volume to be a n -dimensional sphere. As argued above, there is a genuine error of an endo-observer which enters the model because of misalignment between exo- and endo-observers. Assume that the endo-observer vector field is given by $\mathbf{F}_{\text{en}}(\mathbf{x}_{\text{en}}, t) = F_{\text{en}}(x_{\text{en}_i}, t)\mathbf{e}_j$ such that the vector field points towards the j th component of the state space and only varies with respect to its i th component. Now it is further assumed that the diameter of the sphere represents the distance between two states which cannot be resolved by an endo-observer. This implies that the endo-observer may apply at an instant t a vector field $\mathbf{F}_{\text{en}}(\mathbf{x}_{\text{en}}, t)$ to the state $\mathbf{x}_{\text{en}} + \Delta\mathbf{x}_{\text{en}}$, with $|\Delta\mathbf{x}_{\text{en}}| = \varepsilon$ equal to the diameter of the sphere, due to the misalignment between observers. The vector field within the sphere changes according to $(F_{\text{en}}(x_{\text{en}_i} + \varepsilon, t) - F_{\text{en}}(x_{\text{en}_i} - \varepsilon, t))/(2\varepsilon)$ which can be interpreted as an error vector field within the sphere (see also Fig. 5.1). An endo-observer thus incorporates a trajectory within the time interval Δt which is identical to $\Delta F_{\text{en}_i} = [F_{\text{en}}(x_{\text{en}_i} + \varepsilon, t) - F_{\text{en}}(x_{\text{en}_i} - \varepsilon, t)]\Delta t$. This trajectory is subject to the vector flow itself. Because the mean endo-observer vector field is still $\mathbf{F}_{\text{en}}(\mathbf{x}_{\text{en}}, t)$ a differ-

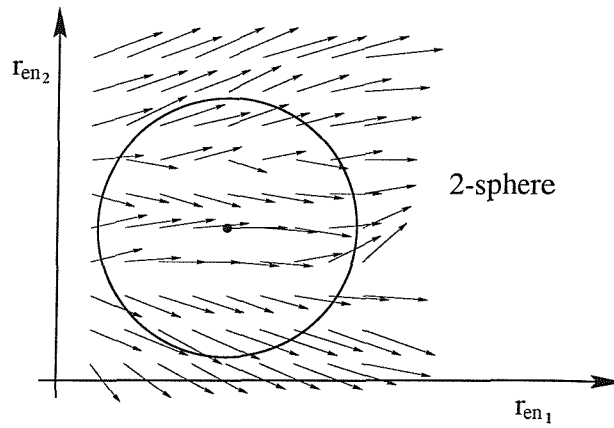


Figure 5.1: A 2-sphere inside an exo-observer's state space is shown. The area inside the sphere covers all these vector fields of an endo-observer which may be mistaken for the vector field at the centre of the sphere due to misalignment between endo- and exo-observer.

ence vector Δs flows in the ensemble mean with the vector flow $\mathbf{F}_{\text{en}}(\mathbf{x}_{\text{en}}, t)$. In the limit as the volume and time interval go to zero the flow of the difference vector Δs approaches $F_{\text{en}_j}(x_{\text{en}_i}, t) \partial_{x_{\text{en}_i}} F_{\text{en}_j}(x_{\text{en}_i}, t)$ which is identical to $(1/2) \partial_{x_{\text{en}_i}} F_{\text{en}_j}^2(x_{\text{en}_i}, t)$. Generally $\mathbf{F}_{\text{en}}(\mathbf{x}_{\text{en}}, t)$ has all components j and changes with respect to all components i which means that the flow of the difference vector is superimposed by $\sum_{i,j} (1/2) \partial_{x_{\text{en}_i}} F_{\text{en}_j}^2(x_{\text{en}_i}, t)$. The net flow of difference vectors out of the sphere is given by the divergence of the flow of the difference vector $\text{div} \sum_{i,j} (1/2) \partial_{x_{\text{en}_i}} F_{\text{en}_j}^2(x_{\text{en}_i}, t)$ when the diameter of the sphere approaches zero. When the net flow of the difference vector is positive the error inside the sphere decreases by the same amount. An error potential is therefore defined as $\mathcal{E}(\mathbf{x}_{\text{en}}, t)$ which represents the net flow of Δs out of the sphere when the time interval Δt approaches zero. The change of $\mathcal{E}(\mathbf{x}_{\text{en}}, t)$ with time t is therefore

$$\partial_t \mathcal{E}(\mathbf{x}_{\text{en}}, t) = - \sum_{i,j} (1/2) \text{div} \left[\partial_{x_{\text{en}_i}} F_{\text{en}_j}^2(x_{\text{en}_i}, t) \right] \quad (5.4)$$

$$= -(1/2) \partial_{\mathbf{x}_{\text{en}}}^2 \mathbf{F}_{\text{en}}^2(\mathbf{x}_{\text{en}}, t). \quad (5.5)$$

$\mathcal{E}(\mathbf{x}_{\text{en}}, t)$ is a new quantity which has to be related to the already defined error vector field above. This is easily done by realising that $\mathcal{E}(\mathbf{x}_{\text{en}}, t)$ is the net flow of an error out of a fixed volume inside the state space. This net flow is also defined by the divergence of $\mathbf{q}(\mathbf{x}_{\text{en}}, t)$, *i.e.*, $\mathcal{E}(\mathbf{x}_{\text{en}}, t) = \text{div} \mathbf{q}(\mathbf{x}_{\text{en}}, t)$. The latter identity allows the substitution of $\mathcal{E}(\mathbf{x}_{\text{en}}, t)$ in Eq. (5.4). Because $\partial_{\mathbf{x}_{\text{en}}}^2 \mathbf{F}_{\text{en}}^2$ is equivalent with $\text{div}(\text{grad} \mathbf{F}_{\text{en}}^2)$, Eq. (5.4)

implies that

$$\partial_t \mathbf{q}(\mathbf{x}_{\text{en}}, t) = -(1/2) \partial_{\mathbf{x}_{\text{en}}} \mathbf{F}_{\text{en}}^2(\mathbf{x}_{\text{en}}, t). \quad (5.6)$$

Because this identity is the gradient of the difference vector field $\mathbf{q}(\mathbf{x}_{\text{en}}, t)$ and the initial difference vector field $\mathbf{q}(\mathbf{x}_{\text{en}}, t_0)$ is derived from a potential, $\mathbf{q}(\mathbf{x}_{\text{en}}, t)$ remains the gradient of a potential for all time, *i.e.*,

$$\partial_t S(\mathbf{x}_{\text{en}}, t) = -(1/2) (\partial_{\mathbf{x}_{\text{en}}} S(\mathbf{x}_{\text{en}}, t) + \langle \mathbf{F}_{\text{ex}} \rangle)^2(\mathbf{x}_{\text{en}}, t), \quad (5.7)$$

as $\partial_t \partial_{\mathbf{x}_{\text{en}}} S(\mathbf{x}_{\text{en}}, t) = \partial_{\mathbf{x}_{\text{en}}} \partial_t S(\mathbf{x}_{\text{en}}, t)$. This means that any potential $S(\mathbf{x}_{\text{en}}, t)$ with the gradient $\mathbf{q}(\mathbf{x}_{\text{en}}, t)$ may be utilised for representing the difference vector field. This potential is required for the dynamics derived in the following section.

5.4 Uncertainty of an error-vector field's probability density function in the state space

The last section treated the case of a state \mathbf{x}_{en} where there exists one single difference vector field $\mathbf{q}(\mathbf{x}_{\text{en}}, t)$ which influences the endo-observer vector field $\mathbf{F}_{\text{en}}(\mathbf{x}_{\text{en}}, t)$. Because the preparation of an experiment (see Section 4.2) will lead to a set of non-repetitive initial variables and measurements the vector field $\mathbf{F}_{\text{en}}(\mathbf{x}_{\text{en}}, t)$ will vary depending on a specific experiment as well, *i.e.*, a probability density function can be assigned to the distribution of the measured vector field $\mathbf{F}_{\text{en}}(\mathbf{x}_{\text{en}}, t)$. This section derives the dynamics of an endo-observer when the variance of the probability density function which describes the distribution of $\mathbf{F}_{\text{en}}(\mathbf{x}_{\text{en}}, t)$ is bounded. This bound is assumed to hold despite the fact that $\mathbf{F}_{\text{en}}(\mathbf{x}_{\text{en}}, t)$ is not necessarily a conservative vector field.

So far, only the case of a single trajectory of an endo-observer has been considered, *i.e.*, the error of the endo-observer consisted of the erroneous identification of a co-ordinate. As mentioned above an endo-observer may also assign a wrong vector field to the system irrespective to the misalignment treated earlier. In order to take care of this influence consider an additional stochastic variable $\xi(\mathbf{x}_{\text{ex}}, t)$ which is assumed to enter the endo-observer dynamics as follows

$$\partial_t \mathbf{q}(\mathbf{x}_{\text{en}}, t) = -(1/2) \nabla_{\mathbf{x}_{\text{en}}} (\xi + \mathbf{F}_{\text{en}})^2(\mathbf{x}_{\text{ex}}, t). \quad (5.8)$$

These dynamics are not explicitly available to an endo-observer because $\xi(\mathbf{x}_{\text{ex}}, t)$ is not accessible, *i.e.*, an endo-observer model may be derived which employs the probability density function $\rho(\mathbf{x}_{\text{en}}, \xi, t)$. However, $\rho(\mathbf{x}_{\text{en}}, \xi, t)$ is not accessible to an endo-observer

as it comprises the variable $\xi(\mathbf{x}_{ex}, t)$ which cannot be measured as \mathbf{x}_{ex} is not measurable. As the required information is not accessible, alternative statistics have to be employed where the information given is utilised. As demonstrated below instead of employing the dynamics of the difference vector field $\xi(\mathbf{x}_{ex}, t)$ the dynamics of a *mean vector field* are utilised which is defined by an “energy” potential $\sigma_{\mathbf{F}_{en}}(\mathbf{x}_{en}, t)$ introduced in the next paragraph.

For the time being it is assumed that the endo-observer identifies the vector field \mathbf{F}_{en} with a probability $\rho(\mathbf{F}_{en}(\mathbf{x}_{en}, t) + \langle \mathbf{F}_{en} \rangle_{\mathbf{F}_{en}}(\mathbf{x}_{en}, t)) d^n \mathbf{F}_{en} = \rho(\xi(\mathbf{x}_{en}, t)) d^n \mathbf{x}_{en}$. This means that the endo-observer considers a state space model in which a probability density function is attached to each individual trajectory in the state space. This probability density function $\rho(\xi, \mathbf{x}_{en}, t)$ then describes the *propensity* that an endo-observer at any instant t measures a vector field $\mathbf{F}_{en}(\mathbf{x}_{en}, t) = \langle \mathbf{F}_{en} \rangle_{\xi}(\mathbf{x}_{en}, t) + \xi$ with the mean vector field identical to $\langle \mathbf{F}_{en} \rangle_{\xi}(\mathbf{x}_{en}, t)$. This implies for an experiment that either the actual vector field $\langle \mathbf{F}_{en} \rangle_{\xi}(\mathbf{x}_{en}, t) + \xi$ is explicitly given to extract the error ξ , or, that the error is known in order to extract the vector field. Neither is possible, according to the arrangement of an endo-observer experiment. Since there is no approach which may avoid this problem the only alternative is the application of an estimate for the endo-observer dynamics by the mean of an ensemble which has a distribution equivalent to $\rho_{est}(\mathbf{x}_{en}, \xi, t)$. It is assumed in the following that the probability density function $\rho(\xi | \mathbf{x}_{en}, t)$ is not explicitly accessible, what may be given instead is a bound on its variance

$$\sigma_{\mathbf{x}, \xi}^2 = \int d^n \mathbf{x} d^n \xi \rho(\mathbf{x}, \xi, t) (\mathbf{F}_{en} - \langle \mathbf{F}_{en} \rangle_{\mathbf{x}, \mathbf{F}_{en}})^2 \leq \kappa^2 / 4. \quad (5.9)$$

Further it is assumed that the mean of ξ is zero at all times, *i.e.*,

$$\langle \xi \rangle(t) = \int d^n \xi \rho(\xi, t | \mathbf{x}) \xi = 0. \quad (5.10)$$

In the statistical case the ensemble mean of all ξ is utilized and the Liouville equation of the probability density function $\rho(\mathbf{x}_{en}, \xi, t)$ thus becomes

$$\partial_t \rho(\mathbf{x}_{en}, t) = -\partial \mathbf{x}_{en} (\rho(\mathbf{q} + \langle \mathbf{F}_{ex} \rangle)) (\mathbf{x}_{en}, t), \quad (5.11)$$

as ξ is just an additive constant to the flow which in the mean cancels out due to the Identity (5.10). Eq. (5.11) therefore does not include any estimation or approximation as long as the net-flow on the right-hand-side of the Liouville equation are error-free. Precise knowledge of $\rho(\xi | \mathbf{x}_{en}, t)$ is required for the Hamilton-Jacobi equation derived below.

The dynamics of $\mathbf{q}(\mathbf{x}_{en}, t)$ have to take the distribution $\rho(\xi | \mathbf{x}_{en}, t)$ into account as it is the case for the identity (5.11). However, the dynamics of $\mathbf{q}(\mathbf{x}_{en}, t)$ do not just cancel out in the mean, because the right-hand-side in Eq. (5.8) is a quadratic function of ξ . The crucial property of ξ is that the mean is considered to be zero and the variance is bounded. For the moment assume that $\rho(\xi | \mathbf{x}_{en}, t)$ is known such that the dynamics of $\mathbf{q}(\mathbf{x}_{en}, t)$ can be computed by taking the mean with respect of ξ over $\mathbf{q}(\xi, \mathbf{x}_{en}, t)$. Some dynamics of a vector field may now be defined which employ the mean potential $\langle [\xi + \mathbf{F}_{en}(\mathbf{x}_{ex}, t)]^2 \rangle_\xi$. The gradient of the mean of $[\xi + \mathbf{F}_{en}(\mathbf{x}_{ex}, t)]^2$ at time t is

$$\partial_t \mathbf{q}_\xi(\xi, \mathbf{x}_{en}, t) = -(1/2) \partial_{\mathbf{x}_{en}} \langle (\xi + \mathbf{F}_{en}(\mathbf{x}_{ex}, t))^2 \rangle_\xi, \quad (5.12)$$

where the subscript in \mathbf{q}_ξ indicates that the mean potential with respect to the stochastic variable ξ has been utilised. The right-hand-side of Eq. (5.12) can be rewritten as

$$\langle (\xi + \mathbf{F}_{en}(\mathbf{x}_{ex}, t))^2 \rangle_\xi = \langle (\xi + \langle \xi \rangle_\xi)^2 \rangle_\xi + \langle (\langle \xi \rangle_\xi + \mathbf{F}_{en}(\mathbf{x}_{ex}, t))^2 \rangle_\xi \quad (5.13)$$

$$= \langle \xi^2 \rangle_\xi(\mathbf{x}_{ex}, t) + \mathbf{F}_{en}^2(\mathbf{x}_{ex}, t), \quad (5.14)$$

because the mean $\langle \xi \rangle_\xi$ vanishes. This fact then implies that $\langle \xi^2 \rangle_\xi$ is nothing but the squared variance of ξ .

As it has been argued above \mathbf{q} can be derived from a potential, which implies that \mathbf{q}_ξ stems from a potential as well, *i.e.*, the Hamilton-Jacobi-like equation for the statistical case becomes

$$\begin{aligned} \partial_t S_\xi(\mathbf{x}_{en}, t) &= -(1/2) \sigma_{\mathbf{F}_{en}}^2(\mathbf{x}_{en}, t) \\ &\quad -(1/2) (\partial_{\mathbf{x}_{en}} S_\xi(\mathbf{x}_{en}, t) + \langle \mathbf{F}_{ex} \rangle(\mathbf{x}_{en}, t))^2, \end{aligned} \quad (5.15)$$

with the squared variance

$$\sigma_{\mathbf{F}_{en}}^2(\mathbf{x}_{en}, t) = \langle \xi^2 \rangle_\xi(\mathbf{x}_{ex}, t) \quad (5.16)$$

The Hamilton-Jacobi-like equation states that the mean vector field can be computed for any time t as long as the squared variance $\sigma_{\mathbf{F}_{en}}^2(\mathbf{x}_{en}, t)$ is given. What is required are either the explicit dynamics of $\rho(\xi | \mathbf{x}_{en}, t)$ or a look-up table for any $\sigma_{\mathbf{F}_{en}}^2(\mathbf{x}_{en}, t)$. As it has been argued above neither is accessible during the experiment of an endo-observer, which therefore demands an estimate for $\sigma_{\mathbf{F}_{en}}^2(\mathbf{x}_{en}, t)$. This estimate should take into account that $\sigma_{\mathbf{x}_{en}, \mathbf{F}_{en}}^2$ is bounded by $\kappa^2/4$ but no further assumptions about the distribution $\sigma_{\mathbf{F}_{en}}^2(\mathbf{x}_{en}, t)$ have to be included. Note that $\sigma_{\mathbf{F}_{en}}^2$ denotes the *generalized kinetic energy density* at the state \mathbf{x}_{en} . Because there is no information available about the dependency of $\sigma_{\mathbf{F}_{en}}^2(\mathbf{x}_{en}, t)$ with respect to the state \mathbf{x}_{en} , a homogeneous *generalized kinetic energy*

density distribution has to be assumed due to *Jayne's law of unbiased guess* (Jaynes, 1957). The *generalized kinetic energy* is therefore defined by $(\kappa^2/4)\rho(\mathbf{x}_{en}, t)d^n\mathbf{x}_{en}$, which may be interpreted as an energy potential with a corresponding vector field

$$\mathbf{f}_{en}(\mathbf{x}_{en}, t) = (|\kappa|^2/4)\partial_{\mathbf{x}_{en}}\rho(\mathbf{x}_{en}, t), \quad (5.17)$$

which represents the change of energy within the estimated infinitesimal interval $d^n\mathbf{x}_{en}$. The divergence of a vector field as given in Eq. (5.17) can be interpreted as an energy source $(\partial_{\mathbf{x}_{en}}^2 G_{\text{res}}^2 = 2\mathbf{f}_{en}^2(\mathbf{x}_{en}) + G_{\text{res}}\partial_{\mathbf{x}_{en}}^2 G_{\text{res}})$ which is proportional to the *residual energy* E_{res} . The residual energy is sought as an estimate for $\sigma_{\mathbf{F}_{en}}(\mathbf{x}_{en}, t)$, up to a constant energy $E(t)$. These arguments explain why the vector field (5.17) estimates the change of the generalized squared action at point \mathbf{x}_{en} rather than estimating the change of action at this coordinate. However, care has to be taken with respect to Jayne's principle (Jaynes, 1957) of unbiased guessing which extends to two distinct cases.

First, let us consider the case where each subset of the system's ensemble at any coordinate \mathbf{x}_{en} has the same generalized kinetic energy proportional to $\kappa^2/4$, in which case the total generalized kinetic energy at \mathbf{x}_{en} is $|\kappa|^2/4\rho(\mathbf{x}_{en}, t)$. The relative change of the total generalized kinetic energy at any state \mathbf{x}_{en} is then zero, but the total change of the total generalized kinetic energy at \mathbf{x}_{en} is $|\kappa|^2/4\partial_{\mathbf{x}_{en}}\rho(\mathbf{x}_{en}, t)$. The negative relative divergence of the vector field (5.17) is thus $-\kappa^2(4\rho(\mathbf{x}_{en}, t))^{-1}\partial_{\mathbf{x}_{en}}^2\rho(\mathbf{x}_{en}, t)$ and therefore defines the generalized energy increase of an event at \mathbf{x}_{en} due to the fact that the energy distribution within all ensembles is a δ -function around a specific value and that the probability about a neighbourhood of \mathbf{x}_{en} changes. This can be more easily visualized by comparing the just mentioned system with a distribution of particles given by $\rho(\mathbf{x}_{en}, t)$, of which each of these particles has an energy proportional to $\kappa^2/4$. When at an instant t within the interval $d^n\mathbf{x}_{en}\rho(\mathbf{x}_{en}, t)d^n\mathbf{x}_{en}$ particles leave the interval with a fixed generalized kinetic energy $\propto \kappa^2/4$, the net change of the total generalized kinetic energy inside the interval $d^n\mathbf{x}_{en}$ at the state \mathbf{x}_{en} changes about $-(\kappa^2/4)\partial_{\mathbf{x}_{en}}^2\rho(\mathbf{x}_{en}, t)$.

Secondly, let us consider now the case that the relative generalized energy of an event changes with respect to \mathbf{x}_{en} . Although the total generalized kinetic energy is still $(|\kappa|^2/4)\rho(\mathbf{x}_{en}, t)d^n\mathbf{x}_{en}$, in the mean the vector field for every single event changes according to the relative vector field $(\rho(\mathbf{x}_{en}, t))^{-1}\mathbf{f}(\mathbf{x}_{en}, t)$. Because there are $\rho(\mathbf{x}_{en}, t)d^n\mathbf{x}_{en}$ events within the interval $d^n\mathbf{x}_{en}$, the total change of the energy is still equivalent to (5.17) and thus the total generalized energy remains preserved. The negative divergence of the relative vector field is then identical to $-\partial_{\mathbf{x}_{en}}[|\kappa|^2(4\rho(\mathbf{x}_{en}, t))^{-1}\partial_{\mathbf{x}_{en}}\rho(\mathbf{x}_{en}, t)]$ and represents the increased energy density at coordinate \mathbf{x}_{en} because of the relative generalized energy which is increased with respect to the neighbouring coordinates. This case can be more easily explained by an

ensemble of particles within $d^n \mathbf{x}_{\text{en}}$ at \mathbf{x}_{en} of which each particle changes its generalized energy from \mathbf{x}_{en} to $\mathbf{x}_{\text{en}} + d\mathbf{x}_{\text{en}}$ about $|\kappa|^2/(4\rho(\mathbf{x}_{\text{en}}, t))\partial_{\mathbf{x}_{\text{en}}}\rho(\mathbf{x}_{\text{en}}, t)$. The net change of the total generalized energy in the interval $d^n \mathbf{x}_{\text{en}}$ at \mathbf{x}_{en} due to the change of energy of each particle is then identical to $-\rho(\mathbf{x}_{\text{en}}, t)\partial_{\mathbf{x}_{\text{en}}}[\kappa^2(4\rho(\mathbf{x}_{\text{en}}, t))^{-1}\partial_{\mathbf{x}_{\text{en}}}\rho(\mathbf{x}_{\text{en}}, t)]$. The negative sign of the divergence in both cases takes care of the fact that a source is proportional to the negative divergence of a vector field.

The *residual energy* E_{res} is the evenly weighted sum of both contributions, the relative divergence of the vector field as well as the divergence of the relative vector field

$$\begin{aligned} E_{\text{res}} &= -\kappa^2(8\rho(\mathbf{x}_{\text{en}}, t))^{-1}\partial_{\mathbf{x}_{\text{en}}}\rho(\mathbf{x}_{\text{en}}, t) \\ &\quad -\kappa^2(8\rho(\mathbf{x}_{\text{en}}, t))^{-1}\partial_{\mathbf{x}_{\text{en}}}[\rho^{-1}(\mathbf{x}_{\text{en}}, t)\partial_{\mathbf{x}_{\text{en}}}\rho(\mathbf{x}_{\text{en}}, t)], \end{aligned} \quad (5.18)$$

according to Jayne's principle. Because $\rho(\mathbf{x}_{\text{en}}, t) \geq 0$ it is now possible to introduce the function $A(\mathbf{x}_{\text{en}}, t) = \sqrt{\rho(\mathbf{x}_{\text{en}}, t)}$ which allows us to rewrite the residual energy in terms of the *generalized quantum potential*

$$E_{\text{res}} = -\kappa^2(2A(\mathbf{x}_{\text{en}}, t))^{-1}\partial_{\mathbf{x}_{\text{en}}}^2 A(\mathbf{x}_{\text{en}}, t) \quad (5.19)$$

and subsequently leads to a set of two coupled partial differential equations, which derive from the Liouville equation

$$\partial_t A(\mathbf{x}_{\text{en}}, t) = -\partial_{\mathbf{x}_{\text{en}}} A(\mathbf{x}_{\text{en}}, t)(\partial_{\mathbf{x}_{\text{en}}} G(\mathbf{x}_{\text{en}}, t) + \langle \mathbf{F}_{\text{ex}} \rangle(\mathbf{x}_{\text{en}}, t)) \quad (5.20)$$

$$-A(\mathbf{x}_{\text{en}}, t)(\partial_{\mathbf{x}_{\text{en}}}^2 G(\mathbf{x}_{\text{en}}, t) + \partial_{\mathbf{x}_{\text{en}}} \langle \mathbf{F}_{\text{ex}} \rangle(\mathbf{x}_{\text{en}}, t))/2 \quad (5.21)$$

and from the Hamilton-Jacobi-like equation

$$\partial_t G(\mathbf{x}_{\text{en}}, t) = \kappa^2(2A(\mathbf{x}_{\text{en}}, t))^{-1}\partial_{\mathbf{x}_{\text{en}}}^2 A(\mathbf{x}_{\text{en}}, t) \quad (5.22)$$

$$-(1/2)(\partial_{\mathbf{x}_{\text{en}}} G(\mathbf{x}_{\text{en}}, t) + \langle \mathbf{F}_{\text{ex}} \rangle(\mathbf{x}_{\text{en}}, t)) \quad (5.23)$$

which can be combined into a common partial differential equation. This may most conveniently be proved by multiplying the negative function of $\psi(\mathbf{x}_{\text{en}}, t) = A(\mathbf{x}_{\text{en}}, t) \exp(iG(\mathbf{x}_{\text{en}}, t)/\kappa)$ with Eq. (5.22) and taking the sum of the result with the product of Eq. (5.20) with $i\kappa \exp(iG(\mathbf{x}_{\text{en}}, t)/\kappa)$ which immediately gives the generalized Schrödinger equation

$$i\kappa \partial_t \psi(\mathbf{x}_{\text{en}}, t) = (1/2)(-i\kappa \partial_{\mathbf{x}_{\text{en}}} + \langle \mathbf{F}_{\text{ex}} \rangle(\mathbf{x}_{\text{en}}, t))^2 \psi(\mathbf{x}_{\text{en}}, t). \quad (5.24)$$

This equation has the same appearance like the Schrödinger equation for a particle moving in an electromagnetic field with a vector potential which is identical to

$-\langle \mathbf{F}_{\text{ex}} \rangle(\mathbf{x}_{\text{en}}, t)$. Although the appearance is the same the motivation of Eq. (5.24) is completely different of that of the Schrödinger equation. In summary, the equation above describes the estimated dynamics of an endo-observer which has to include the dynamics of an error vector field which originates from the mis-alignment and mis-identification of an exo-observer's vector field. The statistical properties of the stochastic variable ξ , which represents the mis-identification of the vector field at a time t , lead to a generalized estimated energy distribution which is equivalent to an expression known from the quantum potential. Hamilton-Jacobi equation and Liouville equation can be combined in a single differential equation which is given by Eq. (5.24).

5.5 Computation of dynamics when the probability density function inside the state space is only partially known

It has been shown above, that an initial probability density function of the state space has to be explicitly given for the computations of the future state. The purpose of this thesis has been to develop an algorithm which allows predictions of non-linear dynamics with included errors despite limitations that the state cannot be measured. All that is available are the measurements of corrupted state vector components and some gross bounds on the possible variables and parameters of a dynamical system. This section aims to introduce an algorithm which combines the dynamics of a system as given in Section 5.4 with the bounds for the variable and parameter space which is not accessible to an endo-observer.

5.5.1 Introduction

In Section 4.2.1 it was argued that the Radon transform may be employed for the computation of the conditional probability density function at a time t when the observations of the entire time-axis is utilized. This is an un-practical procedure because if the observations at all time for re-constructing the joint probability density function are required a prediction becomes redundant. Since there is far less information available than that required for deterministic dynamics with a stochastic initial distribution, an alternative model of a dynamical system has to be developed which tackles several issues simultaneously.

1. **The Schrödinger equation:** Physical observations are of an endo-observer type which means that uncertainties in a system's dynamics due to erroneous measurements have to be taken into account by utilizing the model derived above and defined in Eq. (5.24).
2. **The measurement issue:** The dynamics developed so far require the probability distribution of an initial state and the precise dynamics of a system. For most physical experiments the exact parameters are not explicitly given. Instead of the probability density function of an initial state only few components of a state vector are measurable in form of a noisy rational number.
3. **Estimating probability density function of measurable state vector components:** As the initial state vector is unavailable it can only be estimated. An initial state vector estimate has to take into account the measurement in form of a rational number. It is shown below how the given stochasticity of measurements can be employed for estimating the probability density function of the state vector components which are accessible to an endo-observer.
4. **Estimating probability density function of non-measurable state vector components and guessing the system parameter distribution:** The state vector and the dynamical system parameters which are non-measurable will be shown to require a bound. This bound then motivates a particular probability density function which can be combined in a common probability density function incorporating all components of a state vector and components which represent the parameter space.
5. **System identification:** After generating an estimate for the state vector and parameter space, the dynamics given by Eq. (5.24) produce an estimate of the future states. Usually there is more than one possible estimate, *i.e.*, a single estimate of a future state has to allow the incorporation of measurements taken at different instances into a consistent model. It has to be shown why an estimate of the future state is given by the dynamics (5.24) applied to the product of all probability density functions at a particular instance after they have been estimated and evolved with time to that particular instance. The initial estimate of the parameter probability distribution is shown to be improved by utilizing the integral of the product of the evolved state vectors' probability density functions subject to a specific parameter set as a correlation measure.

6. **Prediction following System identification:** The system identification procedure leads to a dynamical system which allows the prediction of a system's future states. The identification procedure involves probability density functions dependent upon measurements taken at a previous time of a state, the prediction should rely more on the most recent measurements without discarding the older ones. An algorithm is proposed which seeks to do that. The difference to other algorithms such as statistical, learning algorithms is that these algorithms are based on finding a fixed point (limit cycle). It is argued below that this algorithm must not employ dynamics which converge to a fixed point.
7. **System tracking:** When Jayne's approach of unbiased guessing for system identification leads to a too conservative probability estimate for the propensity of finding a system in a particular state, biased statistics—in the information theoretical sense—may be employed which incorporate some kind of decision-making process allowing the selection of states for which the observer feels more confident about finding a dynamical system. It is important to realize that this kind of approach does not involve any kind of further information about the system which is provided additionally to the information. Tracking always involves some algorithm which changes the information measure based on non-Bayesian statistics.
8. **Prediction following System tracking:** The prediction process is identical to that given in Point 6 up to the fact that it is being applied to the state function of the tracking model introduced in Point 7.

The issues addressed above are derived in the sections below. Section 5.5.2 derives a probability density function estimate of an initial state when some state vector components are not attainable. Section 5.5.4 and Section 5.6 expand the concept of endo-observer dynamics to system identification and tracking, respectively.

5.5.2 Dynamics of an endo-observer's with estimated initial probability density functions

In Section 5.4 a model has been derived which requires an initial probability density function for computing the likelihood that the system at some future time will be found in a particular state. A probability density function *per se* cannot be measured. Only in the limit when the number of experimental repetitions approaches infinity does the relative frequencies of particular outcomes represent the probabilities of these events.

Because time series are unique events, the experiment cannot be repeated. When, however, the statistics of an endo-observer are explicitly given, then the *maximum likelihood method* allows an estimation of the probability density function. A measurement of the state leads for an endo-observer to a distribution of measurement events. Utilizing the event's relative frequencies a probability density function can be approximated, which represents the likelihood that an observer estimates a state under the condition that a particular fixed state is presented to the observer. It is now assumed that the statistics of an endo-observer are independent of the non-linear system's state, further it is assumed that the observer's events are pure random such that the central limit theorem guarantees a Gaussian (standard, normal) distribution with a given variance. (This last assumption can, if required, be relaxed; it becomes relevant further below when a concrete probability density function has to be included in the model.) Because there is possibly only one single observation at a time, the question arises what is the best estimate of a probability density function $\rho(\mathbf{x}_1|\mathbf{x}_{10})$, after an observation \mathbf{x}_{10} and the probability density function and therefore the likelihood $l(\mathbf{x}_{11}) = \exp((\mathbf{x}_1 - \mathbf{x}_{11})^2/(2\sigma^2))$ is given. The maximum likelihood method seeks to find the likelihood $l(\mathbf{x}_{10})$ for which the probability density function becomes maximal when \mathbf{x}_{10} has been observed. This is only the case if

$$\rho(\mathbf{x}_1|\mathbf{x}_{10}) = \exp\left(-\frac{(\mathbf{x}_1 - \mathbf{x}_{10})^2}{2\sigma^2}\right). \quad (5.25)$$

After the probability density function has been estimated for observable states, an estimate of the probability density function has to be derived for the case when this variable/parameter cannot be observed.

5.5.3 Dynamics of an endo-observer's state with bounds

In Section 5.4 it has been shown how uncertainty must be included if further knowledge is not available. The central idea is that no prejudice about the probability distribution enters an estimate. The same idea is exploited in this section. Consider in the following an arbitrary variable for which the probability distribution has to be estimated. If there is no additional information available a uniform distribution has to be chosen. For any variable as an element of the real line the uniform distribution does not exist and even if it existed it would not convey a lot of information for a future state. Fortunately any physical system is subject to constraints which leads to bounds in the variable and parameter space. Under the assumption that at a particular time a bound of the unknown state vector components is known, an initial

probability distribution can be computed. Because the probability density function inside an interval which is given by the bound is homogeneous and since outside the interval the probability density function is zero, the probability density function for the unobservable variable and parameter space has a shape of a hypercube. The choice of such a probabilistic function represents $\rho(\mathbf{x})$, *i.e.*, an estimate of the probability density function that a event occurs within a finite interval. However this is not the probability density function which can be employed for the endo-observer model for two reasons. Firstly, a function which represents such a shape contains discontinuities which are for a system's dynamics impossible to incorporate. Secondly, this distribution assumes that the events are real values with a conditional probability $\rho(\mathbf{x}_2|\mathbf{x}_{20}) = \delta(\mathbf{x}_2 - \mathbf{x}_{20})$ which is an unreasonable assumption. Although the probability density function is not motivated by observations, the properties of an endo-observer have to be taken into account because the bounds are motivated by observations of past experiments as well. Therefore, instead of considering the probability density function $\rho(\mathbf{x}_2) = 1/\Delta\mathbf{x}_2$ for $|\mathbf{x}_2 - \mathbf{x}_{20}| \leq \Delta\mathbf{x}_2/2$, an estimate is being sought which represents the probability density function $\rho(\mathbf{x}_2, \{\mathbf{x}_{20} \in I_{\Delta\mathbf{x}_2}(\mathbf{x}_{20})\}|\mathbf{x}_{20})$. For the case that $\rho(\mathbf{x}_2, |\mathbf{x}_{20})$ is the Gaussian distribution, $\rho(\mathbf{x}_2) = \rho(\mathbf{x}_2, \{\mathbf{x}_{20} \in I_{\Delta\mathbf{x}_2}(\mathbf{x}_{20})\}|\mathbf{x}_{20})\rho(\mathbf{x}_{20})$ becomes the error function

$$\rho(\mathbf{x}_2) = \frac{\sigma}{\sqrt{\pi}\Delta\mathbf{x}_2} \int_{\frac{-\Delta\mathbf{x}_2}{2}}^{\frac{\Delta\mathbf{x}_2}{2}} d\langle\mathbf{x}_2\rangle_o \exp\left(-\frac{(\mathbf{x}_2 - \langle\mathbf{x}_2\rangle_o)^2}{2\sigma^2}\right). \quad (5.26)$$

The above probability density function of the state space could be used to evolve the system over time, and thus employ the result for prediction purposes. However, this estimate is very crude since the bounds have to be carefully chosen.

5.5.4 Model identification *via* the incorporation of partially known measurements into non-linear dynamics

Eq. (5.26) allows the estimation of the probability density function for variables and parameters which are not explicitly measurable but which may be bound by a compact subset of the real line in an exo-observer system. Eq. (5.25) allows the estimation of a probability density function for measurable variables. A joint probability density function may be generated by taking the product of both probability density functions

$$\rho(\mathbf{x}, \mathbf{u}, t) = \rho(\mathbf{x}_1, t)\rho(\mathbf{x}_2, t)\rho(\mathbf{u}_2, t) \quad (5.27)$$

with \mathbf{u} the system's parameters at time t . When there is given a set of probability density functions for different instances the information can be combined by multiplying

the evolved probability density functions at a particular time t .

$$\rho(\{\mathbf{x}\}_{i=1}^N, \{\mathbf{u}\}_{i=1}^N, t) = \frac{\prod_{i=1}^N \rho(\mathbf{x}_{1t_i}, t) \rho(\mathbf{x}_{2t_i}, t) \rho(\mathbf{u}_{t_i}, t)}{\int d^n \mathbf{x} d^n \mathbf{u} \prod_{i=1}^N \rho(\mathbf{x}_{1t_i}, t) \rho(\mathbf{x}_{2t_i}, t) \rho(\mathbf{u}_{t_i}, t)} \quad (5.28)$$

The multiplication derives from the fact that the measurements at different instances are assumed to be statistically independent. This assumption is reasonable since experiments are set up in such a manner that the outcome of a measurement does not depend on the past measurements.

This Section has introduced a new concept of initial probability density function estimation which is a prerequisite of the end endo-observer dynamics, Eq. (5.24). All estimates have been derived using Jayne's principle, the maximum likelihood method, presumed bounds on non-measurable variables/parameters, measured parameters and a random endo-observer which is stochastically independent of the system's state. The estimate of the probability density function is already sufficient for the predictions of future states. However, this model does not allow the tracking of dynamical systems which is investigated in Section 5.6.

5.6 Model tracking by representation of new measurements

As demonstrated in Section (5.4) the identification of an endo-observer system is possible within certain bounds of the required variable and parameter space. However, in many cases a probability density function in a high dimensional state space is unhelpful for decision making, *e.g.*, for answering the question at which spatial coordinates the system is most likely to be within the next time step. An argument may be put forward which states that the maximum of a probability density function can easily be found by analysis of the probability density function's spatial partial derivatives becoming zero. This may be convenient when the probability density function has only one maximum, this approach does become more complicated when the probability density function contains many local maxima. This section intends to introduce an approach towards estimating the probability that a particular parameter and a non-measurable endo-observer variable may be measured with respect to past measurements. This approach is different from system identification because it is no longer purely based on the information available to an endo-observer, the system tracking process includes assumptions about the relationship of the dynamical system probability density function and the measurement which are based on assumptions which cannot be justified

by a purely information theoretical approach. It is going to be shown that this approach includes ‘subjectivity’ for this tracking model.

Tracking is a widespread issue within the control community and deals with the question in which state a dynamical system may be. In Bar-Shalom and Fortmann (1988), for example, tracking is defined as the processing of measurements obtained from a target for maintaining its current state estimate. Although there is no mention about the prediction and selection of state space estimations, the emphasis is placed on maintaining a state estimate. In order to be able to maintain a system’s state, several things have to be guaranteed. The underlying dynamical system must either be given or extracted, and a state estimation procedure is available. Part of the tracking algorithm is the *association* of data with a specific trajectory (track) inside the state space to minimize the influences of errors on the trajectory identification procedure. The crux of tracking algorithms is the employment of a *decision-making process* which decides on selecting either a single trajectory in a deterministic model or the *prior probabilities* in a Bayesian framework. It is important to realize that these decisions in either case are not based on the data alone but rather on some statistical assumptions about the distribution of the data about a nominal track (trajectory): Some illustrative examples of recent tracking algorithms can be found in Mahapatra and Mehrotra (2000), Kirubarajan et al. (2000). The Kalman filter is a deterministic model (Kalman, 1960; Kalman and Bucy, 1960), which utilizes as a decision-making process the minimisation of estimation variance (Chui and Chen, 1999). A probabilistic model based on Bayesian inference requires as a decision-making process the initial prior. A stochastic process, as it has been derived in the previous sections, requires a decision-making process about the stochasticity of the dynamical system at each instant. The problem which emerges within the framework of non-linear system identification, as developed in Section 5.5.4, is the probability density function inside the state space which does not necessarily convey more relevant information about the likelihood that a particular state (track) may be chosen by a dynamical system than any other arbitrary guess. As in the case of a Kalman filter, neighbouring states may stem from a common but undefined probability distribution. The postulate of the tracking model derived below will thus be that

POSTULATE 5.6.1 *The confidence of a tracking endo-observer in its observations of a state is proportional to the probability of this state.*

This postulate has profound consequences on the model. As it has been argued above, the unbiased guess approach of Jayne’s which entered the stochastic models before is

now violated. This fact may also be termed as ‘subjectiveness’ towards the observers own measurements.

The following section states more precisely which properties the tracking endo-observer has, and then the dynamics based on these pre-defined tracking model properties are derived.

5.6.1 Dynamics of tracking model

In Section 5.4 the dynamics of an endo-observer are derived which include the dynamics of errors entering the system. In this section, the focus is placed on the tracking of trajectories within the endo-observer’s dynamics.

After a fitness landscape has been defined, an endo-observer model has to be derived which provides a probability density function representing the specific selection of state and parameter variables within the limitations of a fitness landscape. The tracking of a state is defined here as the selection of the state with the most salient probability density function. This most likely kind of probability density function cannot be selected by just utilising the gradient of the state’s probability density function and then replacing the nominal probability density function of the state with a delta function $\delta(\mathbf{x}_{tr} - \mathbf{x}_{tr0})$. Such a choice would neglect all the information provided by the state’s probability density function. What is needed is a tracking algorithm which takes the following issues into account

- (i) The dynamics are of the type given in Eq. (5.24) when no tracking is pursued.
- (ii) Tracking of a state is performed inside the endo-observers state space.
- (iii) New estimates provide the most recent information about a systems state.
- (iv) Former estimates are as relevant as the last estimates. However, system parameters may change with time, a time dependent weighting of the state estimates may be justified.
- (v) The dynamics given by Eq. (5.24) represent the likelihood that a state may be at a state \mathbf{x}_{tr} .
- (vi) All states are equally probable before any initial probability density functions have been presented to the model.
- (vii) The dynamics of the tracking models probability density function have to drive the system towards a locally single state, the locally most probable one.

- (viii) All local maxima of the state space's probability density function have to be considered.
- (ix) Closely neighboured states attract each other more strongly than states which are further apart

The modelling of an endo-observer which is capable of recognizing a non-linear system requires dynamics which according to Point (i) are identical to Eq. (5.24) when no tracking is pursued. The local competition between neighbouring states \mathbf{x}_{tr} depends on the likelihood that a state is selected by the exo-physical system. Because the likelihood is estimated by $\rho(\mathbf{x}_{tr}, t)$, the dynamics of the difference vector field $\mathbf{q}(\mathbf{x}_{tr}, t)$ have to evolve such that $\mathbf{q}(\mathbf{x}_{tr}, t)$ approaches the state with the locally higher probability density function $\rho(\mathbf{x}_{tr}, t)$.

The tracking of trajectories involves the selection of the most suitable models (*e.g.* trajectories, vector flows, non-linear functions, etc.) with respect to a performance criterion of past measurements. Here, in this case the suitability of a model is expressed by the local maxima of a probability density, *i.e.*, the propensity or likelihood, that a state occurs. For the purpose of deriving auto-selective dynamics within a framework of state space models, let us reconsider the dynamics of the error potential $\mathcal{E}(\mathbf{x}_{tr}, t)$ in Eq. (5.4). The increase of $\mathcal{E}(\mathbf{x}_{tr}, t)$ is defined as the negative divergence of a vector field, which is given as the gradient of $\mathbf{F}_{tr}^2(\mathbf{x}_{tr}, t)$. Because it is demanded that the auto-selective dynamics choose the state representing the maximum of the probability density function $\rho(\mathbf{x}_{tr}, t)$, the vector field has to be proportional to the gradient of $\rho(\mathbf{x}_{tr}, t)$. When γ is defined to be the parameter of competitiveness, the increase of the error potential due to the probability density function is given by the negative divergence of the just defined vector field, *i.e.*,

$$\partial_t \mathcal{E}(\mathbf{x}_{tr}, t) = -\gamma \partial_{tr}^2 \rho(\mathbf{x}_{tr}, t), \quad (5.29)$$

which represents just the contribution to the change of the error potential due to $\rho(\mathbf{x}_{tr}, t)$ and a proportionality constant γ . The total change of $\mathcal{E}(\mathbf{x}_{tr}, t)$ with time t is therefore the sum of $\partial_t \mathcal{E}(\mathbf{x}_{tr}, t)$ in Eq. (5.4) and that in Eq. (5.29)

$$\partial_t \mathcal{E}(\mathbf{x}_{tr}, t) = -(1/2) \partial_{tr}^2 \mathbf{F}_{tr}^2(\mathbf{x}_{tr}, t) - \gamma \partial_{tr}^2 \rho(\mathbf{x}_{tr}, t). \quad (5.30)$$

The following argument is the same as in Section 5.3.1 which therefore leads to an identity similar to Eq. (5.12) which thus becomes

$$\partial_t \mathbf{q}_\xi(\xi, \mathbf{x}_{tr}, t) = -(1/2) \partial_{\mathbf{x}_{tr}} \langle (\xi + \mathbf{F}_{tr}(\mathbf{x}_{ex}, t))^2 \rangle_\xi - \gamma \partial_{\mathbf{x}_{tr}} \rho(\mathbf{x}_{tr}, t), \quad (5.31)$$

and defines the change of the error vector field under the constraint of tracking trajectories represented by a gradient $-\gamma\partial_{\mathbf{x}_{\text{tr}}}\rho(\mathbf{x}_{\text{tr}}, t)$. The difference vector field between exo-observer and endo observer thus changes according to the identity given above. The potential defined in Eq. (5.15) differs only by an additional potential $-\gamma\rho(\mathbf{x}_{\text{tr}}, t)$ that has to be employed here. The Liouville equation thus remains the same as defined in Eq. (5.20), *i.e.*,

$$\begin{aligned}\partial_t A(\mathbf{x}_{\text{tr}}, t) &= -\partial_{\mathbf{x}_{\text{tr}}} A(\mathbf{x}_{\text{tr}}, t) (\partial_{\mathbf{x}_{\text{tr}}} G(\mathbf{x}_{\text{tr}}, t) + \langle \mathbf{F}_{\text{ex}} \rangle(\mathbf{x}_{\text{en}}, t)) \\ &\quad - A(\mathbf{x}_{\text{tr}}, t) (\partial_{\mathbf{x}_{\text{tr}}}^2 G(\mathbf{x}_{\text{tr}}, t) + \partial_{\mathbf{x}_{\text{tr}}} \langle \mathbf{F}_{\text{ex}} \rangle(\mathbf{x}_{\text{tr}}, t)) / 2\end{aligned}\quad (5.32)$$

and the Hamilton-Jacobi-like equation incorporates the potential defined above and yields

$$\begin{aligned}\partial_t G(\mathbf{x}_{\text{tr}}, t) &= \kappa^2 (2A(\mathbf{x}_{\text{tr}}, t))^{-1} \partial_{\mathbf{x}_{\text{tr}}}^2 A(\mathbf{x}_{\text{tr}}, t) - \gamma\rho(\mathbf{x}_{\text{tr}}, t) \\ &\quad - (1/2) (\partial_{\mathbf{x}_{\text{tr}}} G(\mathbf{x}_{\text{tr}}, t) + \langle \mathbf{F}_{\text{ex}} \rangle(\mathbf{x}_{\text{tr}}, t))\end{aligned}\quad (5.33)$$

which again can be combined into a single partial differential equation. This may most conveniently be proved by multiplying the negative function of $\psi(\mathbf{x}_{\text{tr}}, t) = A(\mathbf{x}_{\text{tr}}, t) \exp(iG(\mathbf{x}_{\text{tr}}, t)/\kappa)$ with Eq. (5.33) and taking the sum of the gained result with the product of Eq. (5.20) with $i\kappa \exp(iG(\mathbf{x}_{\text{tr}}, t)/\kappa)$ which immediately gives the *generalized nonlinear Schrödinger equation*

$$i\kappa\partial_t \psi(\mathbf{x}_{\text{tr}}, t) = (1/2)(-i\kappa\partial_{\mathbf{x}_{\text{tr}}} + \langle \mathbf{F}_{\text{ex}} \rangle(\mathbf{x}_{\text{tr}}, t))^2 \psi(\mathbf{x}_{\text{tr}}, t) - \gamma|\psi(\mathbf{x}_{\text{tr}}, t)|^2 \psi(\mathbf{x}_{\text{tr}}, t). \quad (5.34)$$

which differs from the formulation of quantum mechanics *via* the *nonlinear Schrödinger equation* by an included vector potential $-\langle \mathbf{F}_{\text{ex}} \rangle(\mathbf{x}_{\text{tr}}, t)$. This equation is therefore up to the non-linear term $\gamma|\psi(\mathbf{x}_{\text{tr}}, t)|^2 \psi(\mathbf{x}_{\text{tr}}, t)$ identical to the Schrödinger equation which describes the dynamics of a particle which interacts with an electromagnetic field. The term $|\psi(\mathbf{x}_{\text{tr}}, t)|^2$ may be interpreted as a time-dependent potential which coincides with the probability density function of finding a particle at the tracking endo-observer state \mathbf{x}_{tr} . Unfortunately, as also in the model (5.24), the solutions of this equation are not well understood and in the general case only exist as a numerical approximation.

The derivation of a tracking endo-observer model has almost been accomplished. After the dynamics have been derived the explicit choice of the function $\psi(\mathbf{x}_{\text{tr}}, t)$ in the state space is motivated in Section 5.6.2.

5.6.2 Computation of likeliness of parameters and non-observable endo-observer state components

As in Section 5.5.4 a probability density function estimation of non-explicit measurable variables and parameters through Eq. (5.26) has to be performed prior to the utilization of the tracking endo-observer model (5.34). As Eq. (5.25) allows the estimation of a probability density function for measurable variables, a joint probability density function may now be approximated by taking the product of the probability density functions of the state space's subsets, *i.e.*,

$$\rho(\mathbf{x}_{\text{tr}}, \mathbf{u}_{\text{tr}}, t) = \rho(\mathbf{x}_{\text{tr}_1}, t)\rho(\mathbf{x}_{\text{tr}_2}, t)\rho(\mathbf{u}_{\text{tr}}, t), \quad (5.35)$$

with, as before, \mathbf{u} the system's parameters at time t . The set of probability density functions given for different instances can then be combined by the normalized product of the evolved probability densities functions at time t . In contrast to Section 5.5.4 in which Eq. (5.24) is being utilized, the probability density of the tracking endo-observer model has to be computed by employing the squared magnitude of model (5.34), *i.e.*,

$$\rho(\mathbf{x}_{\text{tr}}, t) = \frac{\prod_{i=1}^N \rho(\mathbf{x}_{\text{tr}_1 t_i}, t)\rho(\mathbf{x}_{\text{tr}_2 t_i}, t)\rho(\mathbf{u}_{\text{tr} t_i}, t)}{\int d^n \mathbf{x}_{\text{tr}} d^{n_u} \mathbf{u}_{\text{tr}} \prod_{i=1}^N \rho(\mathbf{x}_{\text{tr}_1 t_i}, t)\rho(\mathbf{x}_{\text{tr}_2 t_i}, t)\rho(\mathbf{u}_{\text{tr} t_i}, t)}, \quad (5.36)$$

with the index t_i indicating that there are N state functions $\psi(\mathbf{x}_{\text{tr}}, t_i)$ at the initial time t_i . As before, the multiplication derives from the fact that the measurements at different instances are assumed to be statistically independent. This assumption is reasonable since experiments are set up such that the outcome of a measurement does not depend on the past measurements. Finally, the initial state functions for each t_i are given by $\psi(\mathbf{x}_{\text{tr}}, t_i) = \sqrt{\rho}(\mathbf{x}_{\text{tr}_1 t_i}, t_i)$ because the initial phase of $\psi(\mathbf{x}_{\text{tr}}, t_i)$ is zero as follows from Eq. (5.10) and Identity (5.15). It is important to realize that there is no physical meaning attached to the state functions $\psi(\mathbf{x}_{\text{tr}}, t_i)$ for tracking purposes. The justification of these state functions is only done by the prediction model given in Eq. (5.36).

After the derivation of the tracking model has been completed, the following example illustrates the application to a realistic but analytically simple model. Extension to more complex problems is limited by the need for the numerical approximation of Eq. (5.34).

5.6.3 Examples of prediction models

After the dynamics of a prediction model have been derived an example should demonstrate the use and applicability of the dynamics given by Eq. (5.36).

The example given below is a rather simple dynamical case, not because the model (5.34) only applies to this simple model, but in the general case there does not exist an analytical solution but only numerical approximations.

An analytical example of the tracking endo-observer model

As for an example which can be easily calculated assume that there is a zero vector field applied to the state's probability density function. The endo-observer model (5.34) becomes the general non-linear Schrödinger equation

$$i\kappa\partial_t\psi(\mathbf{x}_{\text{tr}}, t) = (1/2)(-\kappa\partial_{\mathbf{x}_{\text{tr}}}^2)^2\psi(\mathbf{x}_{\text{tr}}, t) - \gamma|\psi(\mathbf{x}_{\text{tr}}, t)|^2\psi(\mathbf{x}_{\text{tr}}, t), \quad (5.37)$$

which can be solved analytically (Zakharov and Mikhailov, 1978; Satsuma and Yajima, 1947) by means of the inverse scattering technique when an arbitrary $\psi(\mathbf{x}_{\text{tr}}, t_0)$ has been given. Here, it has to be shown that this endo-observer model is capable of identifying a zero vector field, *i.e.*, there exists a stationary solution of the partial differential equation (5.34). This has been demonstrated for example in (Mills, 1998). The stationary solution *ansatz* $\psi(\mathbf{x}_{\text{tr}}, t) = \psi_s(\mathbf{x}_{\text{tr}})\exp(i\omega t)$ leads to the probability density function

$$(-1/2)\kappa\partial_{\mathbf{x}_{\text{tr}}}^2\psi_s(\mathbf{x}_{\text{tr}}) + E\psi_s(\mathbf{x}_{\text{tr}}) - \gamma\psi_s^3(\mathbf{x}_{\text{tr}}) = 0$$

whereby it has to be borne in mind, that $\psi_s(\mathbf{x}_{\text{tr}})$ and $\partial_{\mathbf{x}_{\text{tr}}}\psi_s(\mathbf{x}_{\text{tr}})$ have to vanish as $\mathbf{x}_{\text{tr}} \rightarrow \pm\infty$. These conditions now lead immediately to a solution,

$$\psi(\mathbf{x}_{\text{tr}}, t) = \prod_{j=1}^n \frac{\sqrt{2E}}{\cosh^2(\sqrt{2E}x_{\text{tr},j})} \exp(i\omega t) \quad (5.38)$$

The tracking algorithm for N identical observations

In the following let us assume that an endo-observer estimates at initial time t_h the probability density

$$\rho(\mathbf{x}_{\text{tr},t_h}, t_h) = \frac{\prod_{j=1}^n \frac{\sqrt{2E}}{\cosh^2(\sqrt{2E}x_{\text{tr},j})}}{\int_{-\infty}^{\infty} d^n \mathbf{x}_{\text{tr}} \prod_{j=1}^n \frac{\sqrt{2E}}{\cosh^2(\sqrt{2E}x_{\text{tr},j})}}. \quad (5.39)$$

As argued above the initial phase is zero, thus the initial state function becomes

$$\psi(\mathbf{x}_{\text{tr}t_h}, t) = \frac{\prod_{j=1}^n \frac{\sqrt{2E}}{\cosh^2(\sqrt{2E}x_{\text{tr}j})}}{\int_{-\infty}^{\infty} d^n \mathbf{x}_{\text{tr}} \prod_{j=1}^n \frac{\sqrt{2E}}{\cosh^2(\sqrt{2E}x_{\text{tr}j})}} \exp(i\omega(t - t_h)), \quad (5.40)$$

and the tracking model becomes,

$$\rho(\mathbf{x}_{\text{tr}}, t) = \frac{\prod_{h=1}^N \prod_{j=1}^n \frac{\sqrt{2E}}{\cosh^2(\sqrt{2E}x_{\text{tr}j})}}{\int_{-\infty}^{\infty} d^n \mathbf{x}_{\text{tr}} \prod_{h=1}^N \prod_{j=1}^n \frac{\sqrt{2E}}{\cosh^2(\sqrt{2E}x_{\text{tr}j})}}. \quad (5.41)$$

Depending on the total number of sample points the probability density function is more or less peaked about the origin of the state space model.

The tracking algorithm for N non-identical observations

Now, let us assume that an endo-observer estimates at an initial time t_h the probability density

$$\rho(\mathbf{x}_{\text{tr}t_h}, t_h) = \frac{\prod_{j=1}^n \frac{\sqrt{2E}}{\cosh^2(\sqrt{2E}(x_{\text{tr}j}) - x_{0j_h})}}{\int_{-\infty}^{\infty} d^n \mathbf{x}_{\text{tr}} \prod_{j=1}^n \frac{\sqrt{2E}}{\cosh^2(\sqrt{2E}(x_{\text{tr}j} - x_{0j_h}))}}, \quad (5.42)$$

in which case the tracking model derives to

$$\rho(\mathbf{x}_{\text{tr}}, t) = \frac{\prod_{h=1}^N \prod_{j=1}^n \frac{\sqrt{2E}}{\cosh^2(\sqrt{2E}(x_{\text{tr}j}) - x_{0j_h})}}{\int_{-\infty}^{\infty} d^n \mathbf{x}_{\text{tr}} \prod_{h=1}^N \prod_{j=1}^n \frac{\sqrt{2E}}{\cosh^2(\sqrt{2E}(x_{\text{tr}j} - x_{0j_h}))}}. \quad (5.43)$$

Depending on the distribution of the origin \mathbf{x}_{0h} of all data points h , the density function $\rho(\mathbf{x}_{\text{tr}}, t)$ can take any shape which is possible as a superposition of basis functions given by Eq. (5.42).

The reason for Eq. (5.42) being a solution of the dynamical system (5.37) is the invariance of this equation towards shifts in the origin.

Prediction with the tracking model

The prediction of an arbitrary non-linear system becomes straightforward, as long as the dynamics (5.37) and the initial probabilities (5.42) are given explicitly. As demonstrated in this example, any future state can be computed by utilizing Eq. (5.37) and

the future probability density distribution is then defined by

$$\rho(\mathbf{x}_{\text{tr}}, t_{\text{future}}) = \rho(\mathbf{x}_{\text{tr}}, t) = \frac{\prod_{h=1}^N \prod_{j=1}^n \frac{\sqrt{2E}}{\cosh^2(\sqrt{2E}(x_{\text{tr}_j} - x_{0j_h}))}}{\int_{-\infty}^{\infty} d^n \mathbf{x}_{\text{tr}} \prod_{h=1}^N \prod_{j=1}^n \frac{\sqrt{2E}}{\cosh^2(\sqrt{2E}(x_{\text{tr}_j} - x_{0j_h}))}}. \quad (5.44)$$

It has to be admitted that this case is rather trivial because a stationary state has been assumed in the first place, but the principle is also valid for the most general case.

5.7 Conclusion

The goal of this chapter has been the development of an algorithm which incorporates few specified uncertainties about a non-linear dynamical system of a state space model. The concept of endo-observers in Chapter 4 has been extended to the case that the abstract error-free state space model is given and about the stochastic property of noise in the vector field is only known in that the variance is bounded by an arbitrary but fixed value. State space models with this kind of stochastic forcing are here defined as endo-observer concepts. (Note, that the endo-observer concept which is utilized in Chapter 4 is a slightly different one, since the stochasticity is of a different origin.)

After a short introduction about the problem domain, the source or erroneous vector fields in a real-life physical system has been motivated, and the necessary minimal qualitative assumptions about the nature of the noise have been introduced. The implications for the dynamics of a difference vector field between the estimated and nominal vector field then lead to a differential equation which follows the dynamics of a negative potential's gradient. This potential is the squared magnitude of the vector field at any point of the state space. It was then shown how very similar arguments to these utilized in Chapter 4 lead to a set of differential equations similar to the Schrödinger equation with a negative vector potential. Obviously the motivation in our case is very much different from the one in Quantum Mechanics. The meaning of the derived Schrödinger equation lies in the identification of the squared magnitude of the state function ψ as the probability distribution density in the real-life observer's state space (endo-observer) and the gradient of the phase of this complex function as the mean error-vector field at a state. It is then argued that the initial mean difference vector field is zero. Any initial state function of an endo-observer can thus easily be generated by taking the square root of the estimated probability density function in the endo-observer's state space. The identification of a state space is defined here as the composition of a probability density function consisting of

the measured state vector components, estimated state vector components, and the control parameters of the dynamical system. Information and physical insight about the underlying dynamical system, and the explicit availability of the variables' and parameters' bounds are a prerequisite for the applicability for the methods devised in this chapter. System identification for many data points is then defined through the superposition of all pre-defined probability distributions in the state space. In order to include tracking in this model an approach towards decision-making has been established which places more confidence on higher probabilities in the state space. Because this confidence is no-longer based on physical knowledge but rather biased preference, these corresponding dynamics could be interpreted as a 'subjective' choice. The dynamics modelling this tracking behaviour are given by the generalized non-linear Schrödinger equation which is very similar to the differential equation for the non-linear system identification procedure. The crucial term is a cubic term with respect to the magnitude of ψ which drives the tracking system towards focusing the probability density function at a specific state. Section 5.5 first motivated the various algorithms which have to be devised for non-linear system identification, tracking and prediction. The non-linear Schrödinger equation has been put in the context of these three issues. A simple model serves in Section 5.6.3 as an illustrative example.

Having devised an algorithm in Chapter 4 for purely linear dynamical systems and having derived a similar procedure in Chapter 5, the applicability of endo-observer models to general non-linear dynamical systems has to be proven. It is desirable to prove analytically which dynamics the non-linear and the generalized non-linear Schrödinger equations can exhibit. Unfortunately, only a comparatively small number of all known partial differential equations are analytically soluble and for the majority of partial differential equations solubility is an open research issue as mathematical tools for investigating their behaviour are currently immature. Even the numerical integration of partial differential equations is the object of an intensive research effort. Because of the limited time and effort which can be spent on this work the author had to drop the ambitious aim towards developing a closed theory of endo-observers for estimation and tracking non-linear dynamical systems. The following chapter thus presents only a few soluble endo-observer models which are unfortunately stripped of some of the interesting features that the Schrödinger equations may exhibit. It is hoped that the simple models given in the next chapter serve sufficiently as an exemplar of the applied algorithms developed here.

Chapter 6

The endo-observer's frame of reference for a ballistic missile

Forward

This chapter is purely dedicated to demonstrate the capabilities of the endo-observer models as developed in Chapters 4 & 5. The most general cases of endo-observer models require the numerical integration of a multidimensional elliptic partial differential equation. Only examples have been depicted which are analytically tractable. The numerical implementation problems of the endo-observer identification algorithm have been left for future research.

6.1 Introduction

The dynamics of a ballistic missile have been derived in Chapter 4. A ballistic's body dynamics require the functional dependency of lift and drag coefficients with respect to relative wind velocity, attitude, and rotational velocity of a ballistic missile. It has been argued that modelling without this kind of information requires some reasonable assumptions about those coefficients, which are based on physical arguments. Because, the speed of a typical ballistic missile is at its peak velocity about Mach 7, Newton's theory of drag/lift has to be applied. These assumptions are being upheld in this chapter. The most general dynamics as given in Eq. (5.24) are not analytically soluble, *i.e.*, numerical integration has to be applied. The purpose of this chapter is not to present the solution of a nonlinear probability density function, but the application of the derived dynamics to an example which is easy to comprehend and which can

be compared with ones expectations about the result of a model. It is therefore being argued that the perturbation theory of an unperturbed parabolic trajectory of a missile is adequate to demonstrate the feasibility and reasonableness of the model derived in Chapter 3. This chapter motivates and solves the dynamics of the simplified ballistic missile model, utilizes the identification algorithm devised in Chapter 5 for exhibiting the usefulness of that approach and exerts the tracking algorithm of Section 5.6 on the identified system in Section 6.2. The conclusion summarizes the findings.

6.2 The Schrödinger equation for a Ballistic Missile

The vector field of a ballistic missile under certain physical assumptions to estimate the drag and lift coefficients has been given in Example 3.4.3. Since any vector field $\langle \mathbf{F}_{ex} \rangle(\mathbf{x}_{en}, t) \in C^1$ is suitable for the dynamics of the endo-observer model given in Eq. (5.24), also the vector field defined in Example 3.4.3 can be introduced in the endo-observer model. Straightforward numerical computation then leads to the endo-observer dynamics of the ballistic model given. Because there does not seem to exist any analytical solution, this model is not suitable for demonstrating the capabilities of the endo-observer model, since much of the result were down to the simulation itself which is a different modelling issue all-together. For demonstration purposes it is sufficient to utilize a model which is close enough to the real trajectory but which may be analytical tractable. The model being proposed here is based on first order perturbation theory. Instead of considering the physically correct trajectory, the unperturbed (without drag) trajectory is being employed which is corrected by adding a first order perturbation term to the nominal unperturbed trajectory. The vector \mathbf{v}_0 defines the velocity for a ballistic missile without aerodynamic forces, \mathbf{v}_{lift} is the velocity of the body due to first order perturbation which stems from aerodynamics forces on the body which are orthogonal to the unperturbed velocity vector, and \mathbf{v}_{drag} is the velocity of the ballistic missile due to the first order perturbation which originates from the aerodynamic forces on the missile which are parallel to the unperturbed velocity vector \mathbf{v}_0 . The vector field thus becomes

$$\dot{\mathbf{r}} = \mathbf{gt} + \mathbf{v}_0 + \mathbf{v}_{drag} + \mathbf{v}_{lift} \quad (6.1)$$

$$\dot{\mathbf{v}}_{drag} = -D_{drag}(t)|\mathbf{gt} + \mathbf{v}_0 + \mathbf{v}_{w\parallel}|(\mathbf{gt} + \mathbf{v}_0 + \mathbf{v}_{w\parallel}) \quad (6.2)$$

$$\dot{\mathbf{v}}_{lift} = D_{lift}(t)|\mathbf{v}_{w\perp}|(\mathbf{v}_{w\perp}), \quad (6.3)$$

with $\mathbf{v}_{w\parallel}$ being the component of the wind velocity which is parallel to $\mathbf{gt} + \mathbf{v}_0$, and $\mathbf{v}_{w\perp}$ being the component of the wind velocity which is orthogonal to $\mathbf{gt} + \mathbf{v}_0$. It has

to be emphasised that $\mathbf{v}_0/|\mathbf{v}_0|$ does not necessarily coincide with the symmetry axis of the ballistic missile. This model also has the advantage that there are no rotations of the body frame of reference about certain angles involved which requires even more care when choosing the basis functions of ψ since the periodic boundary conditions have to be included within the model. The lift coefficient $D_{\text{lift}}(t)$ is chosen according to Eqs. (3.99) & (3.100)

$$D_{\text{drag}}(t) = 84.7347 \exp(-t) \sin 46.3t \quad (6.4)$$

$$D_{\text{lift}}(t) = 1.8955 \cdot 10^{-3} \exp(-2t) \sin^2 46.3t \quad (6.5)$$

The drawback of this model is that the deviations $\mathbf{v}_{\text{drag}}, \mathbf{v}_{\text{lift}}$ are only well approximated by the terms given above as long as a time interval $t - t_0$ leads to the relations $|\mathbf{g}t + \mathbf{v}_0 + \mathbf{v}_{\text{w}||}| \gg |\mathbf{v}_{\text{drag}}|$ and $|\mathbf{g}t + \mathbf{v}_0 + \mathbf{v}_{\text{w}||}| \gg |\mathbf{v}_{\text{lift}}|$. As the model given in Eq. (3.98)—and repeated here for convenience

$$m\dot{\bar{\mathbf{v}}} = m\mathbf{g} - 0.1654\rho_\infty|\bar{\mathbf{v}}|\bar{\mathbf{v}}, \quad (6.6)$$

cannot be analytically solved, the endo-observer model can only be represented in form of a numerical integration shown in the top-left sub-figure of Figure 3.6. As the perturbation of the mean-drag-coefficient dynamics Eq. (6.6) was derived to be

$$\delta r'_1 = 84.7347 \text{meter} \quad (6.7)$$

$$\times \left[-4.6583 \cdot 10^{-4} \exp(-t') \sin \omega_n t' + 1.007 \cdot 10^{-5} \exp(-bt') \cos \omega_n t' \right] \Big|_{t'=t_0}^{t'=t}$$

$$\delta r'_3 = 1.8955 \cdot 10^{-3} \text{meter} \quad (6.8)$$

$$\times \left[\exp(-t') + 4.6388 \cdot 10^{-4} \exp(-2t') \cos \omega_n t' \right. \Big|_{t'=t_0}^{t'=t}$$

$$\left. + 4.0151 \cdot 10^{-5} \exp(-2t') \sin \omega_n t' \right] \Big|_{t'=t_0}^{t'=t},$$

it follows that the endo-observer dynamics as presented in Section 6.2.3 can be interpreted as a superposition of the dynamics given by Eqs. (6.6)–(6.8) which defines the dynamics of the mean value of the probability density function $|\psi|^2(\mathbf{r}, t)$ and the dynamics governed by the Schrödinger equation.

Eq. (6.1)–(6.3) implies several essential properties of the state function ψ . Because $\dot{\mathbf{v}}_{\text{drag}}$ is independent of $\dot{\mathbf{v}}_{\text{lift}}$ and both accelerations are independent of \mathbf{r} the state function ψ can be decomposed into a product of three components of which each relates to a sub-set of state variables $\mathbf{r}, \mathbf{v}_{\text{drag}}, \mathbf{v}_{\text{lift}}$

$$\psi(\mathbf{x}_{\text{en}}, t) = \psi(\mathbf{r}, t)\psi(\mathbf{v}_{\text{drag}}, t)\psi(\mathbf{v}_{\text{lift}}, t) \quad (6.9)$$

The substitution of the vector field Eq. (6.1)–(6.3) into the nonlinear Schrödinger equation (5.24) leads to

$$\begin{aligned} i\kappa\partial_t\psi(\mathbf{x}_{en}, t) = & -(\kappa^2/2)\left(\partial_{\mathbf{r}}^2 + \partial_{\mathbf{v}_{\text{drag}}}^2 + \partial_{\mathbf{v}_{\text{lift}}}^2\right)\psi(\mathbf{r}, \mathbf{v}_{\text{drag}}, \mathbf{v}_{\text{lift}}, t) \quad (6.10) \\ & -i\kappa(\mathbf{g}t + \mathbf{v}_0 + \mathbf{v}_{\text{drag}} + \mathbf{v}_{\text{lift}})\partial_{\mathbf{r}}\psi(\mathbf{r}, \mathbf{v}_{\text{drag}}, \mathbf{v}_{\text{lift}}, t) \\ & +i\kappa D_{\text{drag}}(t)|\mathbf{g}t + \mathbf{v}_0 + \mathbf{v}_{\text{w}\parallel}|(\mathbf{g}t + \mathbf{v}_0 + \mathbf{v}_{\text{w}\parallel})\partial_{\mathbf{v}_{\text{drag}}}\psi(\mathbf{r}, \mathbf{v}_{\text{drag}}, \mathbf{v}_{\text{lift}}, t) \\ & -i\kappa D_{\text{lift}}(t)|\mathbf{v}_{\text{w}\perp}|(\mathbf{v}_{\text{w}\perp})\partial_{\mathbf{v}_{\text{lift}}}\psi(\mathbf{r}, \mathbf{v}_{\text{drag}}, \mathbf{v}_{\text{lift}}, t) \\ & +(1/2)\left[(\mathbf{g}t + \mathbf{v}_0 + \mathbf{v}_{\text{drag}} + \mathbf{v}_{\text{lift}})^2 + D_{\text{drag}}^2(t)(\mathbf{g}t + \mathbf{v}_0 + \mathbf{v}_{\text{w}\parallel})^4\right. \\ & \left.+ D_{\text{lift}}^2(t)(\mathbf{v}_{\text{w}\perp})^4\right]\psi(\mathbf{r}, \mathbf{v}_{\text{drag}}, \mathbf{v}_{\text{lift}}, t) \end{aligned}$$

because the divergence of $\langle \mathbf{F}_{\text{ex}} \rangle(\mathbf{x}_{en}, t)$ vanishes for all time t . This differential equation cannot be solved in the \mathbf{x}_{en} coordinates. However, by substitution of

$$\psi(\mathbf{r}, \mathbf{v}_{\text{drag}}, \mathbf{v}_{\text{lift}}, t) = \frac{1}{(2\pi)^{9/2}} \int_{-\infty}^{\infty} d^9\mathbf{k} \tilde{\psi}(\mathbf{k}, t) \exp(i\mathbf{k} \cdot (\mathbf{r}, \mathbf{v}_{\text{drag}}, \mathbf{v}_{\text{lift}})) \quad (6.11)$$

into Eq. (6.10) leads immediately to

$$\begin{aligned} i\kappa\partial_t\tilde{\psi}(\mathbf{k}, t) = & (\kappa^2/2)\mathbf{k}^2\tilde{\psi}(\mathbf{k}, t) \quad (6.12) \\ & +\kappa(\mathbf{g}t + \mathbf{v}_0 + \mathbf{v}_{\text{drag}} + \mathbf{v}_{\text{lift}})\mathbf{k}_1\tilde{\psi}(\mathbf{k}, t) \\ & -\kappa D_{\text{drag}}(t)|\mathbf{g}t + \mathbf{v}_0 + \mathbf{v}_{\text{w}\parallel}|(\mathbf{g}t + \mathbf{v}_0 + \mathbf{v}_{\text{w}\parallel})\mathbf{k}_2\tilde{\psi}(\mathbf{k}, t) \\ & +\kappa D_{\text{lift}}(t)|\mathbf{v}_{\text{w}\perp}|(\mathbf{v}_{\text{w}\perp})\mathbf{k}_3\tilde{\psi}(\mathbf{k}, t) \\ & +(1/2)\left[(\mathbf{g}t + \mathbf{v}_0 + \mathbf{v}_{\text{drag}} + \mathbf{v}_{\text{lift}})^2 + D_{\text{drag}}^2(t)(\mathbf{g}t + \mathbf{v}_0 + \mathbf{v}_{\text{w}\parallel})^4\right. \\ & \left.+ D_{\text{lift}}^2(t)(\mathbf{v}_{\text{w}\perp})^4\right]\tilde{\psi}(\mathbf{k}, t) \end{aligned}$$

with $\mathbf{k} = (\mathbf{k}_1, \mathbf{k}_2, \mathbf{k}_3)$. The rather lengthy expression in Eq. (6.12) can be simplified to

$$i\kappa\partial_t\tilde{\psi}(\mathbf{k}, t) = c_9(\mathbf{k}, t)\tilde{\psi}(\mathbf{k}, t) \quad (6.13)$$

with the solution

$$\tilde{\psi}(\mathbf{k}, t) = \tilde{\psi}(\mathbf{k}, t_0) \exp\left(-(i/\kappa) \int_{t_0}^t dt' c_9(\mathbf{k}, t')\right). \quad (6.14)$$

with

$$\begin{aligned} c_9(\mathbf{k}, t) = & (\kappa^2/2)\mathbf{k}^2 + \kappa(\mathbf{g}t + \mathbf{v}_0 + \mathbf{v}_{\text{drag}} + \mathbf{v}_{\text{lift}})\mathbf{k}_1 \quad (6.15) \\ & -\kappa D_{\text{drag}}(t)|\mathbf{g}t + \mathbf{v}_0 + \mathbf{v}_{\text{w}\parallel}|(\mathbf{g}t + \mathbf{v}_0 + \mathbf{v}_{\text{w}\parallel})\mathbf{k}_2 + \kappa D_{\text{lift}}(t)|\mathbf{v}_{\text{w}\perp}|(\mathbf{v}_{\text{w}\perp})\mathbf{k}_3 \\ & +(1/2)\left[(\mathbf{g}t + \mathbf{v}_0 + \mathbf{v}_{\text{drag}} + \mathbf{v}_{\text{lift}})^2 + D_{\text{drag}}^2(t)(\mathbf{g}t + \mathbf{v}_0 + \mathbf{v}_{\text{w}\parallel})^4 + D_{\text{lift}}^2(t)(\mathbf{v}_{\text{w}\perp})^4\right] \end{aligned}$$

The determination of any $\psi(\mathbf{r}, \mathbf{v}_{\text{drag}}, \mathbf{v}_{\text{lift}}, t)$ is therefore reduced to determining the flow of the vector field which is given by the time integral over $c_9(\mathbf{k}, t)$ and a subsequent inverse Fourier transform of $\tilde{\psi}(\mathbf{k}, t)$

$$\begin{aligned}\psi(\mathbf{r}, \mathbf{v}_{\text{drag}}, \mathbf{v}_{\text{lift}}, t) &= \frac{1}{(2\pi)^{9/2}} \int_{-\infty}^{\infty} d^3 \mathbf{r} d^3 \mathbf{v}_{\text{drag}} d^3 \mathbf{v}_{\text{lift}} \tilde{\psi}(\mathbf{k}, t_0) \\ &\times \exp \left(i \mathbf{k} \cdot (\mathbf{r}, \mathbf{v}_{\text{drag}}, \mathbf{v}_{\text{lift}}) - (i/\kappa) \int_{t_0}^t dt' c_9(\mathbf{k}, t') \right).\end{aligned}\quad (6.16)$$

The probability density function $\rho(\mathbf{r}, \mathbf{v}_{\text{drag}}, \mathbf{v}_{\text{lift}}, t)$, which represents the likelihood to find the ballistic missile at coordinate \mathbf{r} and having a drag force and lift force which add the velocities \mathbf{v}_{drag} and \mathbf{v}_{lift} respectively to the nominal one, is, as before, given by

$$\rho(\mathbf{r}, \mathbf{v}_{\text{drag}}, \mathbf{v}_{\text{lift}}, t) = |\psi(\mathbf{r}, \mathbf{v}_{\text{drag}}, \mathbf{v}_{\text{lift}}, t)|^2. \quad (6.17)$$

The dynamics of an endo-observer can be determined by utilizing a predefined initial state $\rho(\mathbf{r}, \mathbf{v}_{\text{drag}}, \mathbf{v}_{\text{lift}}, t_0)$ which determines the future state *via* Eq. (6.14) and therefore the probability density function for any time in the future by Eq. (6.17). The following concrete examples given below may illustrate the dynamics of an endo-observer.

6.2.1 Lift- and Drag-coefficients are negligible

This section shows the simplest endo-observer model, when the Lift- and Drag- coefficients can be set to zero. The exo-observer model in this case is given by

$$\dot{\mathbf{r}} = \mathbf{g}t + \mathbf{v}_0 \quad (6.18)$$

or, equivalently,

$$\mathbf{r} = (1/2)\mathbf{g}t^2 + \mathbf{v}_0 t + \mathbf{r}_0. \quad (6.19)$$

The endo-observer model is being formally given by the following conditions.

1. Drag and Lift coefficients are zero $D_{\text{lift}}(t) = D_{\text{drag}}(t) = 0$.
2. The endo-observer is assumed to be unbiased, *i.e.*, the mean difference vector field vanishes for the initial state $\partial_{\mathbf{x}_{\text{ex}}} (G(\mathbf{x}_{\text{ex}}, t_0)) = \mathbf{0}$.
3. The initial probability density function is assumed to be Gaussian $|\psi(\mathbf{r}, t_0)|^2 = 1/(\sqrt{\pi^3 \sigma^3}) \exp(-\mathbf{r}^2/\sigma^2)$ with a corresponding state function which is a Gaussian as well $\psi(\mathbf{r}, t_0) = 1/\sqrt{\sqrt{\pi^3 \sigma^3}} \exp(-\mathbf{r}^2/(2\sigma^2))$

The choice of the initial state function is not very restrictive in terms of the system's dynamics, it has been selected for convenience sake. The Fourier transform of the state function is

$$\tilde{\psi}(\mathbf{k}_1, t_0) = \sqrt{\sigma^3}/\pi^{3/4} \exp\left(-\frac{\sigma^2 \mathbf{k}_1^2}{2}\right) \quad (6.20)$$

The state function can now straightforwardly be computed by utilizing Eq. (5.24)

$$\begin{aligned} \psi(\mathbf{r}, t) &= \frac{1}{(2\pi)^{3/2}} \int_{-\infty}^{\infty} d^3 \mathbf{k}_1 \tilde{\psi}(\mathbf{k}_1, t_0) \exp(i\mathbf{k}_1 \mathbf{r}) \\ &\quad \times \exp\left(-(i/\kappa) \int_{t_0}^t dt' \left[(\kappa^2/2) \mathbf{k}_1^2 + \kappa(\mathbf{g}t + \mathbf{v}_0) \mathbf{k}_1 + (1/2)(\mathbf{g}t + \mathbf{v}_0)^2\right]\right) \end{aligned} \quad (6.21)$$

$$\begin{aligned} &= \frac{1}{(2\pi)^{3/2}} \int_{-\infty}^{\infty} d^3 \mathbf{k}_1 \tilde{\psi}(\mathbf{k}_1, t_0) \exp(-i\mathbf{k}_1^2 \kappa t/2 - i((1/2)\mathbf{g}t^2 + \mathbf{v}_0 t + \mathbf{r}_0 - \mathbf{r}) \mathbf{k}_1) \\ &\quad \times \exp(-i/(2\kappa) [(1/3)g^2 t^3 + \mathbf{v}_0 \mathbf{g}t^2 + \mathbf{v}_0^2 t + \mathbf{r}_1]) \end{aligned} \quad (6.22)$$

Because the initial state is supposed to be a Gaussian function, The endo-observer state at time t becomes

$$\begin{aligned} \psi(\mathbf{r}, t) &= \frac{\sigma^{3/2}}{(2)^{3/2} \pi^{9/4}} \int_{-\infty}^{\infty} d^3 \mathbf{k}_1 \exp\left(-\frac{\sigma^2 + i\kappa t}{2} \mathbf{k}_1^2 - i((1/2)\mathbf{g}t^2 + \mathbf{v}_0 t + \mathbf{r}_0 - \mathbf{r}) \mathbf{k}_1\right) \\ &\quad \times \exp(-i/(2\kappa) [(1/3)g^2 t^3 + \mathbf{v}_0 \mathbf{g}t^2 + \mathbf{v}_0^2 t + \mathbf{r}_1]) \end{aligned} \quad (6.23)$$

$$\begin{aligned} &= \frac{\sigma^{3/2}}{(2)^{3/2} \pi^{9/4}} \exp(-i/(2\kappa) [(1/3)g^2 t^3 + \mathbf{v}_0 \mathbf{g}t^2 + \mathbf{v}_0^2 t + \mathbf{r}_1]) \\ &\quad \times \exp(-((1/2)\mathbf{g}t^2 + \mathbf{v}_0 t + \mathbf{r}_0 - \mathbf{r})^2 / (2i\kappa t + 2\sigma^2)) \end{aligned} \quad (6.24)$$

$$\times \int_{-\infty}^{\infty} d^3 \mathbf{k}_1 \exp\left(-\frac{\sigma^2 + i\kappa t}{2} \left(\mathbf{k}_1 + \frac{i((1/2)\mathbf{g}t^2 + \mathbf{v}_0 t + \mathbf{r}_0 - \mathbf{r})}{i\kappa t + \sigma^2}\right)^2\right)$$

$$\begin{aligned} &= \sqrt{\frac{\sigma^3}{(\sigma^2 + i\kappa t)^3 \pi^{3/2}}} \exp(-i/(2\kappa) [(1/3)g^2 t^3 + \mathbf{v}_0 \mathbf{g}t^2 + \mathbf{v}_0^2 t + \mathbf{r}_1]) \\ &\quad \times \exp(-((1/2)\mathbf{g}t^2 + \mathbf{v}_0 t + \mathbf{r}_0 - \mathbf{r})^2 / (2i\kappa t + 2\sigma^2)). \end{aligned} \quad (6.25)$$

The probability density follows by the product of the state with the complex conjugate state,

$$\rho(\mathbf{r}, t) = \frac{\sigma^3}{\sqrt{\pi^3 (\sigma^4 + \kappa^2 t^2)^3}} \exp\left(-\frac{\sigma^2 ((1/2)\mathbf{g}t^2 + \mathbf{v}_0 t + \mathbf{r}_0 - \mathbf{r})^2}{\sigma^4 + \kappa^2 t^2}\right),$$

which is the Gaussian distribution centered at the coordinate $(1/2)\mathbf{g}t^2 + \mathbf{v}_0 t + \mathbf{r}_0$ of the deterministic ballistic trajectory, and the squared variance $(\sigma^4 + \kappa^2 t^2)/(2\sigma^2)$ which increases quadratically according to $\kappa^2 t^2/(2\sigma^2)$ as time progresses. As has just been

demonstrated, the endo-observer model developed here allows the computation of a ballistic trajectory including the errors which an endo-observer inevitable may include during measurements.

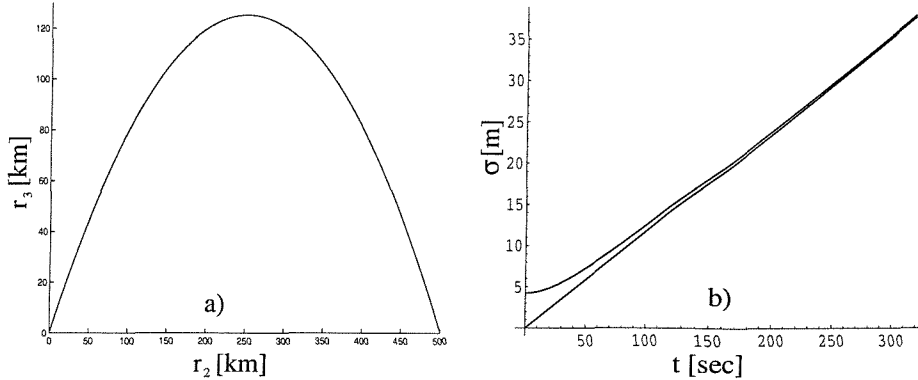


Figure 6.1: a) The trajectory of a ballistic missile with initial velocity $\mathbf{v}_0 = (0, 1566.84, 1566.84)^T$ meters/sec. The abscissa represents the second component of the coordinate vector \mathbf{r} and the ordinate is the height and third component of \mathbf{r} . b) The abscissa is the time axis in seconds. (The time of flight is 319.44 sec.) The ordinate is the length in meters. The non-linear function represents the variance as it evolves with time, when $\kappa = 1, \sigma = 6$. The linear function is given by $\kappa t / (\sqrt{2}\sigma)$ and is defined as a lower bound for σ which converges towards the function $\kappa t / (\sqrt{2}\sigma)$ as $t \rightarrow \infty$.

6.2.2 Drag-coefficient is constant and without Lift-coefficient

This section is concerned with an endo-observer model, when the Lift- coefficient can be set to zero but the drag coefficient applies. The exo-observer model in this case is given by (Hestenes, 1986)

$$\begin{aligned} \dot{\mathbf{r}} &= \mathbf{g} + \mathbf{v}_0 \\ &- D_{\text{drag}}(t) \mathbf{v}_0 \left\{ \mathbf{g} \left| (1/2)t^2 + (1/3)\mathbf{g}\mathbf{v}_0^{-1}t^3 \right| + \mathbf{v}_0 \left| t + (1/2)\mathbf{g}\mathbf{v}_0^{-1}t^2 \right| \right\} \end{aligned} \quad (6.26)$$

or, equivalently,

$$\begin{aligned} \mathbf{r} &= c_{11} = (1/2)\mathbf{g}t^2 + \mathbf{v}_0t + \mathbf{r}_0 \\ &- D_{\text{drag}}(t) \mathbf{v}_0 \left\{ \mathbf{g} \left| (1/6)t^3 + (1/12)\mathbf{g}\mathbf{v}_0^{-1}t^4 \right| + \mathbf{v}_0 \left| (1/2)t^2 + (1/6)\mathbf{g}\mathbf{v}_0^{-1}t^3 \right| \right\}. \end{aligned} \quad (6.27)$$

The endo-observer model is being formally given by the following conditions.

1. The Lift coefficient is zero $D_{\text{lift}}(t) = 0$.

2. The endo-observer is assumed to be unbiased, *i.e.*, the mean difference vector field vanishes for the initial state $\partial_{\mathbf{x}_{\text{ex}}}(G(\mathbf{x}_{\text{ex}}, t_0)) = \mathbf{0}$.
3. The initial probability density function is assumed to be Gaussian $|\psi(\mathbf{r}, \mathbf{v}_{\text{drag}}, t_0)|^2 = 1/(\sqrt{\pi^6 \sigma^6}) \exp(-(r^2 + v_{\text{drag}}^2)/\sigma^2)$ with a corresponding state function which is a Gaussian as well $\psi(\mathbf{r}, \mathbf{v}_{\text{drag}}, t_0) = 1/\sqrt{\sqrt{\pi^6 \sigma^6}} \exp(-(r^2 + v_{\text{drag}}^2)/(2\sigma^2))$

The choice of the initial state function is not very restrictive in terms of the system's dynamics, it has been selected for convenience sake. The Fourier transform of the state function is

$$\tilde{\psi}(\mathbf{k}_1, \mathbf{k}_2, t_0) = \sqrt{\sigma^6}/\pi^{6/4} \exp\left(-\frac{\sigma^2 \mathbf{k}_1^2 + \mathbf{k}_2^2}{2}\right) \quad (6.28)$$

The state function can now straightforwardly be computed by utilizing Eq. (6.14). Since most of the computations to follow had to be repeated during the following sections, all computations are being as much generalized as possible.

$$\psi(\mathbf{r}, \mathbf{v}_{\text{drag}}, \mathbf{v}_{\text{lift}}, t) = \frac{1}{(2\pi)^{9/2}} \int_{-\infty}^{\infty} d^3 \mathbf{k}_1 d^3 \mathbf{k}_2 d^3 \mathbf{k}_3 \tilde{\psi}(\mathbf{k}_1, t_0) \tilde{\psi}(\mathbf{k}_2, t_0) \tilde{\psi}(\mathbf{k}_3, t_0) \quad (6.29)$$

$$\times \exp(i\mathbf{k}_1 \mathbf{r} + i\mathbf{k}_2 \mathbf{v}_{\text{drag}} + i\mathbf{k}_3 \mathbf{v}_{\text{drag}}) \times \exp\left(-(i/\kappa) \int_{t_0}^t dt' \left[(\kappa^2/2) \mathbf{k}_1^2 + \kappa \dot{\mathbf{r}} \mathbf{k}_1 + \kappa \dot{\mathbf{v}}_{\text{drag}} \mathbf{k}_2 + \kappa \dot{\mathbf{r}}_{\text{lift}} \mathbf{k}_3\right]\right)$$

$$\times \exp\left(-(i/\kappa) \int_{t_0}^t dt' \left[(1/2)(\dot{\mathbf{r}}, \dot{\mathbf{v}}_{\text{drag}}, \dot{\mathbf{r}}_{\text{lift}})^2\right]\right)$$

$$= \frac{1}{(2\pi)^{9/2}} \int_{-\infty}^{\infty} d^3 \mathbf{k}_1 d^3 \mathbf{k}_2 d^3 \mathbf{k}_3 \tilde{\psi}(\mathbf{k}_1, t_0) \tilde{\psi}(\mathbf{k}_2, t_0) \tilde{\psi}(\mathbf{k}_3, t_0) \quad (6.30)$$

$$\times \exp(-(i/2)(\mathbf{k}_1^2 + \mathbf{k}_2^2 + \mathbf{k}_3^2)\kappa t - i(c_{11} - \mathbf{r})\mathbf{k}_1)$$

$$\times \exp(-i(c_{12} - \mathbf{v}_{\text{drag}})\mathbf{k}_2 - i(c_{13} - \mathbf{v}_{\text{lift}})\mathbf{k}_1 - i/(2\kappa)c_{14})$$

with

$$c_{11} = \int_{t_0}^t dt' \dot{\mathbf{r}} \quad (6.31)$$

$$c_{12} = \int_{t_0}^t dt' \dot{\mathbf{v}}_{\text{drag}} \quad (6.32)$$

$$c_{13} = \int_{t_0}^t dt' \dot{\mathbf{v}}_{\text{lift}} \quad (6.33)$$

$$c_{14} = \int_{t_0}^t dt' (\dot{\mathbf{r}}, \dot{\mathbf{v}}_{\text{drag}}, \dot{\mathbf{r}}_{\text{lift}})^2 \quad (6.34)$$

Because the initial state is supposed to be a Gaussian function, The endo-observer state at time t becomes

$$\psi(\mathbf{r}, \mathbf{v}_{\text{drag}}, \mathbf{v}_{\text{lift}}, t) = \frac{\sigma^{9/2}}{(2)^{9/2}\pi^{27/4}} \int_{-\infty}^{\infty} d^3\mathbf{k}_1 d^3\mathbf{k}_2 d^3\mathbf{k}_3 \quad (6.35)$$

$$\begin{aligned} & \times \exp(-(i\kappa t + \sigma^2)/2(\mathbf{k}_1^2 + \mathbf{k}_2^2 + \mathbf{k}_3^2) - i(c_{11} - \mathbf{r})\mathbf{k}_1) \\ & \times \exp(-i(c_{12} - \mathbf{v}_{\text{drag}})\mathbf{k}_2 - i(c_{13} - \mathbf{v}_{\text{lift}})\mathbf{k}_1 - i/(2\kappa)c_{14}) \\ & = \frac{\sigma^{9/2}}{(2)^{9/2}\pi^{27/4}} \exp(-i/(2\kappa)c_{14} - (c_{11} - \mathbf{r})^2/(2i\kappa t + 2\sigma^2)) \quad (6.36) \end{aligned}$$

$$\begin{aligned} & \times \exp(-(c_{12} - \mathbf{v}_{\text{drag}})^2/(2i\kappa t + 2\sigma^2) - (c_{13} - \mathbf{v}_{\text{lift}})^2/(2i\kappa t + 2\sigma^2)) \\ & \times \prod_{i=1}^3 \int_{-\infty}^{\infty} d^3\mathbf{k}_i \exp\left(-\frac{\sigma^2 + i\kappa t}{2} \left(\mathbf{k}_i + \frac{i(c_{1i} - c_{2i})}{i\kappa t + \sigma^2}\right)^2\right) \\ & = \sqrt{\frac{\sigma^9}{(\sigma^2 + i\kappa t)^9 \pi^{9/2}}} \exp(-i/(2\kappa)c_{14} - (c_{11} - \mathbf{r})^2/(2i\kappa t + 2\sigma^2)) \quad (6.37) \\ & \times \exp(-(c_{12} - \mathbf{v}_{\text{drag}})^2/(2i\kappa t + 2\sigma^2) - (c_{13} - \mathbf{v}_{\text{lift}})^2/(2i\kappa t + 2\sigma^2)). \end{aligned}$$

with $c_{2,1} = \mathbf{r}$, $c_{2,2} = \mathbf{v}_{\text{drag}}$, and $c_{2,3} = \mathbf{v}_{\text{lift}}$. The probability density follows by the product of the state with the complex conjugate state,

$$\begin{aligned} \rho(\mathbf{r}, \mathbf{v}_{\text{drag}}, \mathbf{v}_{\text{lift}}, t) &= \frac{\sigma^9}{\sqrt{\pi^9(\sigma^4 + \kappa^2 t^2)^9}} \exp(-(c_{11} - \mathbf{r})^2/(2i\kappa t + 2\sigma^2)) \quad (6.38) \\ & \times \exp(-(c_{12} - \mathbf{v}_{\text{drag}})^2/(2i\kappa t + 2\sigma^2) - (c_{13} - \mathbf{v}_{\text{lift}})^2/(2i\kappa t + 2\sigma^2)) \end{aligned}$$

which shows that the solution of the probability density function is a purely based on integration of $\dot{\mathbf{r}}, \dot{\mathbf{v}}_{\text{drag}}$. The distribution is, as before, Gaussian centered at the coordinate (c_{11}, c_{12}, c_{13}) of the deterministic ballistic trajectory in Eq. (6.1)–Eq. (6.3), and the squared variance $(\sigma^4 + \kappa^2 t^2)/(2\sigma^2)$ which increases quadratically according to $\kappa^2 t^2/(2\sigma^2)$ as time progresses. This demonstrates again that the endo-observer model developed here allows the computation of a ballistic trajectory including the errors which an endo-observer inevitable may include during measurements. The drag- and lift-coefficients do not change anything about the predictability of the system. The dominant influence is the variance of the difference vector field given by κ which determines the overall stochasticity of the dynamical system. As an example consider the dynamical system as plotted in Figure 6.1. However the predictability of the missile trajectory is limited by condition on the first order approximations given by the expressions in the curly brackets as defined in Eq. (6.26) and Eq. (6.27). As long as $|D_{\text{drag}} v_0 \{\bullet\}|$ in Eq. (6.26) is very small in comparison to $|gt + \mathbf{v}_0|$, the approximation

is valid. The special case of having a lift-coefficient equal to zero thus leads to

$$\rho(\mathbf{r}, \mathbf{v}_{\text{drag}}, t) = \frac{\sigma^6}{\sqrt{\pi^6(\sigma^4 + \kappa^2 t^2)^6}} \exp\left(-(c_{11} - \mathbf{r})^2/(2i\kappa t + 2\sigma^2)\right) \times \exp\left(-(c_{12} - \mathbf{v}_{\text{drag}})^2/(2i\kappa t + 2\sigma^2)\right) \quad (6.39)$$

with c_{11} and c_{12} given in Eq. (6.26) and Eq. (6.27) respectively.

6.2.3 Drag- and Lift-coefficients are time dependent, a short perturbation through a side wind

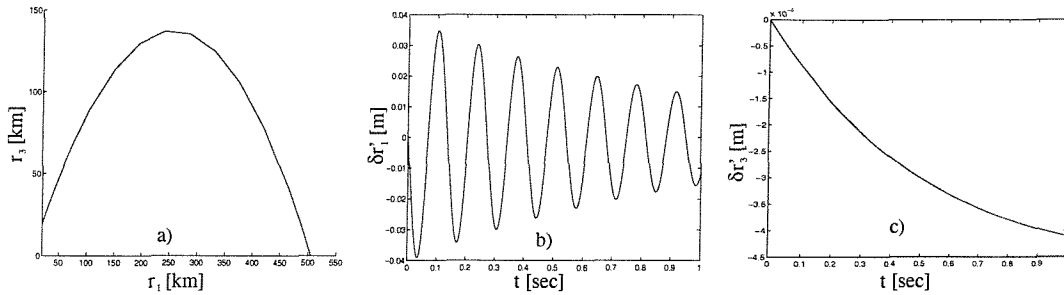


Figure 6.2: This figure shows the effect of lift and drag forces on a ballistic body given by Eq. (6.6) and Eqs. (6.7)–(6.8). Figure a) shows the result of Eq. (6.6). Figures b), c) show the perturbation of drag- and lift-forces due to angular oscillations of the body about its equilibrium in the bodies $\delta r'_1$ and $\delta r'_3$ coordinates, respectively. The superposition defined by Eq. (6.40) gives the desired dynamics of c_{11} . As the variations of $\delta r'_1, \delta r'_3$ are too small in comparison with $\bar{\mathbf{r}}(t)$ a graphical superposition has been omitted. An example of the dynamics of the variance of the probability density function (6.41) may be looked up in the RHS of Figure 6.1

This case does not introduce anything principally new, as the dynamics of the spatial coordinate are explicitly given in Eqs. (6.6)–(6.8). The mean spatial coordinate vector c_{11} is given by the following superposition:

$$c_{11} = \bar{\mathbf{r}}(t) + L_R(\delta r'_1, \delta r'_2, \delta r'_3) \quad (6.40)$$

with L_R a linear operator which translates the body fixed coordinate transformations given by $\delta r'_1, \delta r'_2, \delta r'_3$ into the corresponding transformations of an immobile frame of reference. The probability density function is then explicitly defined as

$$\rho(\mathbf{r}, t) = \frac{\sigma^3}{\sqrt{\pi^3(\sigma^4 + \kappa^2 t^2)^2}} \exp\left(-(c_{11} - \mathbf{r})^2/(2i\kappa t + 2\sigma^2)\right) \quad (6.41)$$

6.3 Tracking of a Ballistic Missile's Dynamics performed by endo-observers

As there has been demonstrated in Section 5.6 the state of an endo-observer $\psi(\mathbf{x}_{\text{tr}}, t)$ is a complex function and is thus defined up to an arbitrary phase $\phi(\mathbf{x}_{\text{tr}}, t)$. A state $\psi'(\mathbf{x}'_{\text{tr}}, t')$ which only differs from a state $\psi(\mathbf{x}_{\text{tr}}, t)$ by a complex phase shift is physically equivalent to a system described by $\psi'(\mathbf{x}'_{\text{tr}}, t')$ in the sense that the probability densities of finding either system at a state vector \mathbf{x}_{tr} are identical. The following derivation below shows the transformation of the generalized nonlinear Schrödinger equation when a system given by $\psi(\mathbf{x}_{\text{tr}}, t)$ is replaced by $\psi'(\mathbf{x}'_{\text{tr}}, t')$. To interpret the physical meaning of that phase shift, let us consider two endo-observer's frames of references F with a state vector \mathbf{x}_{tr} and F' which follows at time $t = t'$ the vector field $\langle \mathbf{F}_{\text{ex}} \rangle(t)$ such that the coordinates between both frames of references transform as $\mathbf{x}_{\text{tr}} = \mathbf{x}'_{\text{tr}} + \int_{t_0}^{t'} dt \langle \mathbf{F}_{\text{ex}} \rangle^2(t)$. The differential operators transform according to

$$\partial_{\mathbf{x}_{\text{tr}}} = \partial_{\mathbf{x}'_{\text{tr}}} \quad (6.42)$$

$$\partial_t = \partial_{t'} - \langle \mathbf{F}_{\text{ex}} \rangle(t) \partial_{\mathbf{x}_{\text{tr}}}. \quad (6.43)$$

Because ψ' and ψ differ only by a phase it can be defined that

$$\psi(\mathbf{x}_{\text{tr}}, t) = \psi'(\mathbf{x}'_{\text{tr}}, t') \exp(i\phi'(\mathbf{x}'_{\text{tr}}, t')) \quad (6.44)$$

In the frame of reference F the generalized nonlinear Schrödinger Equation (5.24) takes the form

$$\begin{aligned} i\kappa \partial_t \psi(\mathbf{x}_{\text{tr}}, t) &= (1/2) \left(-i\kappa \partial_{\mathbf{x}'_{\text{tr}}} + \langle \mathbf{F}_{\text{ex}} \rangle(t) \right)^2 \psi(\mathbf{x}_{\text{tr}}, t) \\ &\quad - \gamma |\psi(\mathbf{x}_{\text{tr}}, t)|^2 \psi(\mathbf{x}_{\text{tr}}, t) \\ &= -(\kappa^2/2) \partial_{\mathbf{x}_{\text{tr}}}^2 \psi(\mathbf{x}_{\text{tr}}, t) - i\kappa \langle \mathbf{F}_{\text{ex}} \rangle(t) \partial_{\mathbf{x}_{\text{tr}}} \psi(\mathbf{x}_{\text{tr}}, t) \\ &\quad + (1/2) \langle \mathbf{F}_{\text{ex}} \rangle^2(t) \psi(\mathbf{x}_{\text{tr}}, t) - \gamma |\psi(\mathbf{x}_{\text{tr}}, t)|^2 \psi(\mathbf{x}_{\text{tr}}, t) \end{aligned} \quad (6.45)$$

By introducing the Identities (6.42), (6.43), (6.44) into Eq. (6.45) the generalized nonlinear Schrödinger equation for the immobile frame of reference leads straightforwardly to the standard nonlinear Schrödinger equation

$$\begin{aligned} i\kappa \partial_{t'} \psi'(\mathbf{x}'_{\text{tr}}, t') - \kappa \psi'(\mathbf{x}'_{\text{tr}}, t') \partial_{t'} \phi'(t') &= -(\kappa^2/2) \partial_{\mathbf{x}'_{\text{tr}}}^2 \psi'(\mathbf{x}'_{\text{tr}}, t') \\ &\quad + (1/2) \langle \mathbf{F}_{\text{ex}} \rangle^2(t') \psi'(\mathbf{x}'_{\text{tr}}, t') - \gamma |\psi'(\mathbf{x}'_{\text{tr}}, t')|^2 \psi'(\mathbf{x}'_{\text{tr}}, t') \end{aligned} \quad (6.46)$$

by choosing the phase to be equal to $\phi'(t') = -1/(2\kappa) \int_t^{t'} \langle \mathbf{F}_{\text{ex}} \rangle^2(t) dt$ which then allows to cast the Schrödinger equation into its original form

$$i\kappa \partial_{t'} \psi'(\mathbf{x}'_{\text{tr}}, t') = -(\kappa^2/2) \partial_{\mathbf{x}'_{\text{tr}}}^2 \psi'(\mathbf{x}'_{\text{tr}}, t') - \gamma |\psi'(\mathbf{x}'_{\text{tr}}, t')|^2 \psi'(\mathbf{x}'_{\text{tr}}, t'). \quad (6.47)$$

This means that the solution of the generalized nonlinear Schrödinger equation, in case that the function $\langle \mathbf{F}_{\text{ex}} \rangle(t)$ is purely time dependent, can be computed by solving the nonlinear Schrödinger equation in the mobile frame of reference of an endo-observer. The derivation above can be summarized as follows. Because the difference between Eq. (6.45) and Eq. (6.47) is just a phase shift of the state, the probability density functions are identical which proves that both solutions are physically identical to each other. The phase shift represents a transformation between two endo-observer systems of which F' is the one that follows the defined by $\langle \mathbf{F}_{\text{ex}} \rangle(t)$ and F is the frame of reference which is supposed to be immobile with respect to the flow induced by this vector field. It has just been demonstrated that the results from Section 5.6 can be utilized. The probability density is thus

$$\rho(\mathbf{x}_{\text{tr}}, t, t_j) \propto \prod_{i=1}^n \prod_{j=1}^N \text{sech}^2 \kappa(x_{\text{tr}i} - r_i(t_j, t)) \quad (6.48)$$

where the indices i and j represent the dimensions of the state space and the observations, respectively.

6.4 Conclusions

This section applied the framework of an endo-observer model successfully to the ballistic missile with pre-selected parameter values as the outcome of the computations reflect the expectations. The requirement of analytic computability unfortunately limits the model to an initial Gaussian probability density function with a quasi-homogeneous vector-field in the state space. The tracking model in form of the non-linear Schrödinger equation was proved to be form invariant with respect to the mean value dynamics which demonstrates that the proposed tracking model generates a soliton with its mean spatial coordinate vector at the mean of the non-linear dynamics at any time t .

Chapter 7

Conclusions & Future Research

This thesis deals with the real-life data and abstract state space model correspondence problem. The problem domain of this work focuses on the identification of non-linear dynamical systems for short and noisy time series, where only components of the state vector are explicitly given and neither further knowledge about the errors exist nor assumptions about the noise may be utilized. It is demonstrated in Chapter 2 that stochastic and statistical systems require very specific properties with respect to the underlying deterministic physical system as well as the data to allow meaningful statistical modelling. The dimensions of the state space imply lower bounds on the required number of data points and the stochastic properties of the noise determine the stochastic model to be utilized. Neither information is usually available prior to the modelling task. Usually it is presupposed (*e.g.* (Brown and Harris, 1994; Bossley, 1997)) that certain model requirements are fulfilled rather than carefully checking whether certain conditions hold (Wu and Schilhabel, 1997). Information measure driven algorithms may easily underestimate the (reconstructed) flow in the state space due to lack of data points. Hence, there is no rigorous criterion which allows a decision about the validity of such a statistical model. In combination with statistical modelling it should be mentioned that revived methodologies such as the Vapnik-Chervonenkis' (VC) learning theory do not solve the difficulties encountered above (Vapnik, 1999; Cherkassky, 1999; Cherkassky and Mulier, 1998), as *all* statistical modelling techniques are inherently ill-posed (Cherkassky, 1999). It has been demonstrated in Section 3.5.2 that the constraints imposed by the experimental arrangement refute meaningful statistical modelling. As mentioned earlier, in some cases a black-box model performs well (Wu and Harris, 1997) in another case it fails (Wu and Schilhabel, 1997). The global Lyapunov exponent measurement algorithm does not provide a rigorous criterion either as it depends on the data, on a pre-selected

time-delay etc. (Weigend and Gershenfeld, 1993; Prichard, 1993). In short, there does not seem to exist a rigorous statistical framework which generally allows the incorporation of physical knowledge such as a parameterised non-linear vector field in a state space when just components of the vector field, which are corrupted with noise, are explicitly given (Cherkassky and Mulier, 1998; Cherkassky, 1999). In Section 3.5 it is argued that physical driven modelling state space modelling cannot be utilized due to the lack of physical insight and the fact that real-life systems always include noise. These difficulties have been found to be insurmountable. Chapter 4 and Chapter 5 are thus dedicated to deriving a framework of stochastic modelling which is based on as few stochastic assumptions as possible. It is shown in Chapter 4 how a real-life observer effects the interpretation of physical measurements when the linear or non-linear state space model is *a priori* known. The advantage of this model is that the assumptions, requirements and information to a real-life observer are transparent. The requirements of these models are found to be twofold. (i) The abstract physical state space model with its dynamical system parameters must be explicitly given. (ii) Bounds on non-measurable state space components and parameters have to be either estimated or guessed. Although several new results and novel theoretical techniques have been derived many interesting and important problems concerning the proposed approach remain very much an open research issue, *e.g.* how can past measurements provide information which allows a mathematically rigorous constraint for possible state space models etc. The chosen modelling issues on ballistic missiles in Chapter 3 exemplify the problems faced when concerned with incorporating physical knowledge in a data and physical system driven hybrid model. This concluding chapter reviews the methodologies presented in this thesis in such an appraisal is presented with respect to black-box modelling, as is for example defined in Eckmann and Ruelle (1985) or Casdagli (1989), and physical driven modelling, as for example summarized in Chui and Chen (1999), Jetschke (1989). Some open research problems and suggestions for future research are also presented.

7.1 Utilization of general Non-linear Statistical Modelling techniques

Non-linear statistical modelling techniques provide the few means of testing some given time series with respect to data generated by some generically underlying dynamics. It is important to note that there does not exist any rigorous proof which provides a test for a finite set of data whether the data was generated by a particular non-

linear dynamical system or not. The difficulty of system identification *via* statistical data is known by statisticians as an ill-posed problem, see also *e.g* (Cherkassky and Mulier, 1998; Cherkassky, 1999), as there does not exist a unique stochastic non-linear dynamical system which may generate the data. Section 2.3 reviewed the methodologies which try and identify whether the time series stems from a deterministic or stochastic system, or if the underlying dynamics are linear or non-linear, chaotic or non-chaotic, and what information content is provided by information measures etc. Despite these being reasonably well developed theories based on probability theory, it has been found in Section 3.5.2 that most practical implementations of algorithms are very problematic since the state space reconstruction problem is ill-posed (Cherkassky, 1999). The lack of information about a physical system cannot be compensated by any statistical framework, *i.e.*, there does not exist any statistical significance measures for state space identification algorithms outside the pure data driven framework for a real-life implementations (Cherkassky, 1999) and most statistical algorithms are based on assumptions, such as Takens theorem which assumes noise-free data, which are not fulfilled by the time series provided. The most significant drawback, however, is the vast amount of data required for non-linear dynamical systems modelling as in the case of a ballistic missile, since there is not much evidence of a simple attractor inside the state space which would enable the identification of a dynamical system with small data sets. The grey-box modelling *ansatz* as derived in Chapter 3 lead back to the same algorithms as employed for black-box modelling, *i.e.*, grey-box modelling encounters the same difficulties as statistical black-box modelling. It thus becomes apparent that purely data driven statistical models lack the property of incorporating physical knowledge in their analysis. In summary the black-box and grey-box modelling techniques as reviewed by Eckmann and Ruelle (1985, Casdagli (1989, Sjöberg et al. (1995, Juditsky et al. (1995) cannot be employed for the following reasons:

- (i) **Insufficient data:** For example the number of data points is of the order $10^8/6$ for a time series consisting of space-coordinate and velocity measurements of a ballistic missile which may have a 16-dimensional attractor.
- (ii) **Non-available statistical error criterion:** The inverse problem of state space reconstruction is ill-posed, *i.e.*, there does not exist among all the (non-linear) statistical methodologies a criterion which measures the performance of the state space reconstruction techniques according to their accuracy and robustness towards variations in the state space models. The extracted probability estimation *via* the frequency of events relates to the output space, probability densities in the state space cannot be extracted.

(iii) **Physical Knowledge does not simplify the analysis:** All that physical insight may provide is a pre-filtering of the time series which enables grey-box modelling. There does not seem to exist an approach that allows the ill-posedness of problems of the data-driven modelling techniques to be overcome or which reduces the dimension of the attractor inside the state space model.

The counter argument by researchers within the black-box modelling community may be that their derived heuristics have been performing well in practice as it is the case in Kantz and Schreiber (1998), or Schreiber and Kantz (1998). However, these kind of arguments are flawed since the precise mechanisms behind these statistical algorithms are not very well understood (Ott, 1993; Weigend and Gershenfeld, 1993; Tong, 1995). Because black-box and grey-box models seem to be inappropriate for the kind hypothetical ballistic missile time series modelling under the constraint of a relatively small set of data points with respect to the dimensions of the dynamical system alternative approaches had to be taken into account. An alternative to pure statistical system modelling of time series is physical system modelling of a ballistic missile which has been reviewed with respect to the applicability to real-life system identification and prediction.

7.2 Modelling issues of Ballistic Missiles

The aim of the move towards non-linear system identification and prediction is the incorporation of as much physical knowledge into the model as possible. Chapter 3 has two purposes. The dynamics of a ballistic missile were reviewed and the problems concerning aerodynamic modelling were highlighted, followed by the determination of a very much a simplified toy model which served for illustration purposes in Chapter 6. The difficulties of physical knowledge inclusion in non-state space models became clear in Section 3.5, after the available physics had been summarized. The encountered problems with relating state space models to real-life data are varied.

- (i) State space models are a physical abstraction and cannot *per se* be identified, as noise corrupts measurements (see *e.g.* (Gardiner, 1998)).
- (ii) A state vector component is a real number. Experiments do not allow the measurements of real numbers, as finite precision only allows the measurement of rational numbers.
- (iii) A state does not account for errors in the measurements.

- (iv) Not all state vector components are accessible or observable (see *e.g.* (Ott, 1993)).

However, state space models are very appealing since they allow the prediction of a dynamical system for all time once a state of the underlying dynamics has been identified. The inclusion of physical knowledge is efficient and very clearly defined. Deterministic models are therefore often related to erroneous measurements through the incorporation of stochastic terms (*e.g.* Kalman (1960), Kalman and Bucy (1960)). However, the stochasticity has to be very well defined *prior* to the identification and prediction as has been shown in Fig. 4.3 where it is demonstrated that the reconstruction of stochasticity is ill-posed. For example, even when the dynamical system is explicitly known the Kalman filter can only estimate stationary noise, *i.e.*, the statistic properties of noise are time invariant. Due to the limitations statistical modelling under consideration imposes on the system being modelled, this approach has been found unacceptable since these assumptions are unjustified and serve purely as an argument for the motivation of black/grey-box modelling.

The dilemma which had to be faced in this work can thus be described as follows: Black-box modelling techniques do not work on a hypothetical time series of a ballistic missile because there is not enough data available, and at the same time the state space model cannot be employed since neither the precise state space dynamics nor the ballistic missile's state are explicitly given. The non-linear dynamical system identification problems have been found in the previous section as to be ill-posed (Cherkassky, 1999) which implies that no approach could be found which is capable of overcoming this dilemma. Because the incorporation of physical knowledge in the to be derived model has priority over black box modelling due to the lack of time series data, the models which have been derived in the Chapters 4 and 5 are motivated by state space models which then have been sought to incorporate the uncertainty of real-life observers.

7.3 Endo-observer Models for Linear Dynamical Systems

Linear system identification may appear to be a very exhaustively researched subject. This may be true for certain stochastic systems such as the linear Kalman filter, however, for only partially observed linear dynamical systems the identification procedure is very much dependent on the underlying assumptions about the system's stochasticity. As the argument about the observability of a free particle showed (see Fig. 4.3),

any real-life observation contains insufficient information in order to reconstruct the probability density inside a free particle's state space. Mathematicians may refer to the state space reconstruction approach as an *inverse problem* which is *ill-posed* as the question of which dynamical model may correspond to the provided time series is not sufficiently defined (Kirsch, 1996). Because there does not seem to exist a conclusive mathematical argument which allows a generic decision of how this kind of uncertainty may be taken into account, the statistical technique of minimal prejudice has been utilized in Chapter 4, after the concepts of exo-(ideal, abstract, physical model) observer and endo-(real-life) observer had been introduced in Section 4.2. The dynamics as defined for an exo-observer have been derived in Section 4.3 in an endo-observer's frame of reference. It was demonstrated in the same section that an endo-observer can only measure the probability density function of the spatial coordinate vector components of the (exo-observer) state space irrespective of the velocity. Apart from the probability density function the mean vector field at a particular spatial coordinate may be estimated and the mean variance of the velocity probability distribution at each spatial coordinate can be determined. It became evident, that if an endo-observer (real-life observer) just relies on the measured vector field, the predictions could lead to spurious results. The novel approach which has been devised in Section 4.3 allows the computation of a net vector field which has to be added to the observed vector field in order to apply a correcting term to the vector flow. The correcting term minimises the divergence of the predicted vector flow from the underlying vector flow of an exo-observer. It has to be emphasised that no assumption about the probability density distribution inside an exo-observer state space model has been made. All that is required, for the additional vector field computation, is the upper bound of the total variance of the velocity's probability distribution and the probability distribution of the free particle's observable spatial coordinates. It is then proved that the *ansatz* employed leads to the corrected dynamics of a real life observer's mean state which has been proved to coincide with the dynamics of the exo-observer's mean state. An algorithm towards extracting the probability distribution of spatial coordinate was also presented in Chapter 4. After the system had been identified (the state function has been computed), the prediction was shown to just consist of calculating the state function for any desired instant. The squared magnitude of the state function is always the probability density, which estimates the probability inside an infinitesimal interval of finding a systems state at a specific spatial coordinate.

7.3.1 Advantages over black-box and stochastic approaches

The theory developed in this thesis is rigorously derived from an information theory conceptual framework, and does not include any assumptions about probability density functions inside the state space. The results found appear to be satisfactory, in particular when only a little information about the exo-physical state space and the endo-observer is given. As argued above the endo-physical approach is an attempt towards combining the information extraction capabilities of black-box models with the means of the physical framework of classical (exo-observer) state space models.

7.3.2 Open problems and Issues for Future Research

The derivation of the endo-observer model is not very elegant. The estimate of the exo-physical influence on an endo-observer is imposed by two energy components entering the energy balance of an endo-observer. Although the fact that both energy contributions have to be included with equal probability due to Jayne's principle is well founded, the validity of this approach is shown through the computation of the solutions of the endo-observer state model and not by employing the framework which motivated the dynamics in the first place. It is desirable to develop a mathematical framework in which all requirements of the model can be incorporated at once and the endo-observer dynamics follow as a necessary consequence of these specific requirements. It has not been shown why higher order variations of the probability density function should not effect the endo-observer's estimate. It is not clear how much the probability density functions of the spatial coordinates in the endo-observer's state model may differ from those of the exo-observer in the best and worst case as time progresses. Does there exist an approach which generalizes the linear endo-observer model to an arbitrary non-linear system with many exo-physical non-accessible components where the vector flow is not explicitly known?

Future research should focus on the theoretical consolidation of this model and some generalization of this approach towards variable stochastic properties of the endo-observer. The applicability of this model ought to be proved by developing some performance bounds to enable an experimenter to judge the reliability of his probability density estimate. The implications of this algorithm for control applications may be of interest.

7.4 Endo-observer Models for Non-Linear Dynamical Systems

Non-linear system identification is despite the vast amount of literature still an immature field (Cherkassky and Mulier, 1998). The problem an experimenter is faced with is the lack of understanding of non-linear dynamical systems, as the theory of non-linear systems has not developed much yet (Jetschke, 1989). The efforts towards a generalization of endo-observer models, as it is proposed in Chapter 4, for non-linear systems has been unsuccessful. The author could not develop an approach which would allow a probabilistic model selection of non-linear systems when no precise information about the exo-physical vector flow is incorporated in the endo-physics dynamics. The only workable model developed here extends the components of the endo-physics observer to all exo-physics components of the state space plus the components which completely incorporate the system parameters. Instead of just considering the probability density distribution of the spatial coordinate, the probability density distribution of all exo-physics state vector components and system parameters are employed. Because, generally, most of the exo-physical (ideal, physically abstract) state vector components and the system parameters are not accessible, the probability distributions inside the endo-physical state space need to be estimated *via* an imposed probability distribution which follows from lower and upper bounds of physical variables and parameters. The inaccessibility of non-linear system components to an endo-observer is thus modelled differently to the linear case. It is first shown in Section 5.3 how a difference vector field between the one measured by an endo-observer and a nominal vector field enters the endo-observer dynamics. It is then demonstrated in Section 5.3 that this difference vector field is subject to changes as time progresses. It emerges that the squared magnitude of the endo-observer vector field (nominal vector field plus the difference vector field) serves as a potential which can be incorporated in a Hamiltonian required for the formalism. The dynamics of the difference vector field follow the negative gradient of this potential landscape, *i.e.*, the error in the vector field persistently increases along the steepest ascent of the total vector field towards the system's local vector field maximum. Under the assumption that the initial variance of the magnitude distribution of the difference vector field is within an arbitrary but fixed bound, the dynamics of the difference vector field can be cast in a form which is very much similar to that found for the total vector field in the linear case. Although the motivation and interpretations of the resultant dynamics of an endo-observer in the non-linear case are very different to that found in the linear case, the mathematical derivation of the

non-linear endo-observer dynamics can be easily adopted. The result is the generalized Schrödinger equation with a term which is similar to the vector potential in quantum mechanics. An exhaustively developed algorithm for system identification has been derived in Section 5.5. It is suggested how an endo-observer with a given time series and certain variable and parameter bounds composes a probability density distribution for the endo-observer state space to firstly identify and secondly predict the non-linear dynamical exo-observer system. Prediction here means, as in the linear case, evolving the probability distribution in the endo-observer state space with time and then utilizing the computed probability of a state as a propensity to expect the exo-observer to be at this state.

For many applications the precise information about a probability distribution is not required. It may be only desirable to focus on the local maximums of the distribution. This kind of aim is then being implemented in form of a specific tracking algorithm. The crux here is that the endo-observer is assumed to have more confidence in the endo-observer states with a higher value of the probability density function. Based on that assumption the generalized non-linear Schrödinger equation is derived, which then leads to the tracking algorithm outlined in Section 5.6.1.

Because general numerical simulations of the endo-observer model for non-linear dynamical systems are far too difficult to implement and go far beyond the scope of this work, some toy models have been assembled separately in Chapter 6 to illustrate and outline the theory in the form of analytical solutions.

7.4.1 Advantages over black-box and stochastic approaches

Because the emphasis is placed on the dynamics of an endo-observer, little attention has been paid towards developing a model for the probability density estimation in the endo-observer state space from the given time-series data. The emerging problem which has not been addressed in this thesis is the suitability of a particular parameterised state space model for predictions. Throughout this thesis it was assumed that the dynamical system is well defined up to a parameterisation. An algorithm for the identification of an *a priori* undefined vector flow could not be devised. Although this weakness may effect the algorithm as a whole, this criticism is unjustified as for a physical system the endo-observer model is in most particular cases well parameterised. Another weakness in Chapter 5 emerged within the framework of probability density estimation through data. Although the estimation procedure is well established as can for example be seen in (Papoulis, 1991), the statistical significance decreases with the number of given data points. Neither an estimate for the statistical significance of the

probability density estimation algorithm nor the effect of an estimate which deviates from the nominal probability density distribution has been derived. This complex problem has been left for future research. The probability estimation as for example provided in Chapter 5 is just a mean of providing an example of how the endo-observer concept could be applied in a framework of non-linear dynamical system identification. However, the endo-observer state space model no longer requires a comparatively large number of data points in order to estimate some of the qualitative measures introduced in Chapter 2 and Section 3.5.2. A regression technique which assumes stochastic properties of the exo-observer model is no longer required. The derived algorithm simplifies the estimation technique of probability density functions as they may be alternatively implemented in form of regression techniques for the phase flow such as artificial neural networks, radial basis functions, neuro-fuzzy system etc. (Bishop, 1995; Lillekjendlie, Kugiumtzis and Christoffersens, 1994; Kugiumtzis, Lillekjendlie and Christoffersen, 1994; Brown and Harris, 1994). The only assumption about the uncertainty of an endo-observer model is an initial probability distribution of an error vector field with mean zero and fixed variance. The rest follows from Jayne's principle of unbiased guessing. This *ansatz* therefore ensures that only the information available is taken into account and no other hidden assumptions enter the model.

7.4.2 Open problems and Issues for Future Research

The major drawback of the endo-observer model presented here is the fact that exo-physical state space models must be explicitly given, or must at least be known up to some parameterisation when the corresponding parameters have a certain *a priori* given probability distribution. Also, the probability distributions of the state space components and parameters which are not measurable have to be guessed up to the second order of their cumulants (Schlögel, 1989). Thus, the model presented here is not as close to a complete approach as desired where, without the knowledge of all exo-physical vector flow components and without a given probability distribution for non-measurable state vector components, the endo-physics dynamics can be modelled by just employing the given or observed time series. This aim has proved to be too difficult to overcome within this thesis. In many cases the statistical community employs the variance of a predicted system output with the given data points of a time series in order to validate and quantify a statistical model. This kind of measure cannot be applied here, since entire probability density distributions are under consideration. A comparison between the endo-physics model and the flow in an exo-physical state space is hard to justify since the exo-physical model does not propagate any errors

in its dynamics whereas the endo-physics model inherits the errors performed by a real-life observer. Objective comparison between the model proposed here and other models on the level of time series data comparison is very difficult as there does not exist a universally valid algorithm which is capable of generating a probability density function in a reconstructed state space which could be compared with the probability density function of an endo-observer model.

Further research could aim at even further relaxing the information required of an endo-observer model. The variance of the system uncertainty cannot be chosen dependent on the endo-physical state space component, which may become a necessity for some dynamical systems. The noise applied to the endo-physical vector field has been assumed as homogeneous. Further developments on this model may seek to provide means of real-life measurement equipment which may exhibit state dependent error sources which cannot yet be incorporated in the endo-physics dynamics. So far there does not exist a truly objective performance measure which allows the comparison of existing statistical methodologies. It could be very challenging to provide such a performance measure.

References

Aarts, E. and J. Korst (1995). Boltzman machines. In M. Arbib (Ed.), *The Handbook of Brain Theory and Neural Networks*, pp. 162–165. Mass: The MIT Press.

Abarbanel, H., R. Brown, and J. Kadtke (1990). Prediction in Chaotic Nonlinear Systems: Methods for Time Series with Broadband Fourier Spectra. *Phys. Rev. A* 41, 1742.

Abarbanel, H. D. I., T. A. Carroll, L. M. Pecora, J. J. Sidorowich, and L. S. Tsimring (1994). Predicting physical variables in time-delay embedding. *Phys. Rev. E* 49, 1840–1853.

Albano, A., J. Muench, C. Schwartz, A. Mees, and P. Rapp (1988). Singular-value decomposition and the Grassberger–Procaccia algorithm. *Phys. Rev. A* 38, 3017.

Albano, A., A. Passamante, and M. Farrel (1992). Using higher-order correlations to define an embedding window. *Physica D* 54, 85.

Anderson, J. J. (1991). *Fundamentals of Aerodynamics* (2nd ed.). Aerospace Science Series. New York: McGraw-Hill International Editions.

Anonymous (1982). *Guided Weapons Handbook* (7th ed.). The Royal Military College of Science.

Arbib, M. (Ed.) (1995). *The Handbook of Brain Theory and Neural Networks*. The MIT Press.

Arnold, V. (1978). *Mathematical Methods of Classical Mechanics*. Graduate Texts in Mathematics. New York: Springer Verlag.

Babloyantz, A. (1991). Evidence for slow brain waves: A dynamical approach. *Electroencephalography and Neurophysiology* 78(5), 402–405.

Ballentine, L. (1990). *Quantum Mechanics*. Prentice Hall, Inc.

Ballentine, L. (1998). *Quantum Mechanics*. Singapore: World Scientific.

Bar-Shalom, Y. and T. Fortmann (1988). *Tracking and Data Association*. Mathematics in Science and Engineering. San Diego, London: Academic Press, Inc.

Beck, C. and F. Schlögel (1995). *Thermodynamics of chaotic systems*, Volume 4 of *Cambridge Nonlinear Science Series*. Cambridge University Press.

Bishop, C. (1995). *Neural networks for Pattern recognition*. Oxford: Clarendon Press.

Blakelock, J. (1965). *Automatic Control of Aircraft and Missile*. New York: John Wiley & Sons, Inc.

Bossley, K. (1997). *Neurofuzzy Modelling Approaches in System Identification*. Ph.D. thesis, University of Southampton.

Bourlard, H. and Y. Kamp (1988). Auto-association by multilayer perceptrons and singular value decomposition. *Biol. Cybern.* 59, 291–294.

Broomhead, D., R. Jones, and G. King (1987). Topological dimension and local coordinates form time series data. *J. Phys. A* 20, L563.

Brown, M. and C. J. Harris (1994). *Neurofuzzy Adaptive Modelling and Control*. International Series in Systems and Control Engineering. New York, London: Prentice Hall.

Casdagli, M. (1989). Nonlinear Prediction of Chaotic Time Series. *Physica D* 35, 335.

Casdagli, M. (1992). A dynamical systems approach to modeling input-output systems. In M. Casdagli and S. Eubank (Eds.), *Nonlinear modeling and forecasting*, pp. 265–281. Redwood City: Addison Wesley.

Cherkassky, V. (1999). Guest editorial vapnik-chervonenkis (vc) learning theory and its applications. *IEEE Transactions on Neural Networks* 10(5), 985–987.

Cherkassky, V. and F. Mulier (1998). *Learning from Data, Concepts, Theory, and Methods*. New York: John Wiley & Sons, Inc.

Chui, C. (1992). *An Introduction to Wavelets*. Academic Press.

Chui, C. and G. Chen (1999). *Kalman Filtering with Real-Time application* (3rd ed.). Springer Series in Information Sciences. Berlin: Springer-Verlag.

Collinson, R. (1996). *Introduction to Avionics* (1st ed.). Number 11 in Microwave Technology Series. London: Chapman & Hall.

Cronvich, L. (1991). Aerodynamic considerations for autopilot design. In M. Hemsch (Ed.), *Tactical Missile Aerodynamics: General Topics*, Volume 141 of *Progress in Astronautics & Aeronautics*, pp. 29–67. American Institute of Aeronautics and Astronautics.

Daubechies, I. (1992). *Ten Lectures on Wavelets*. CBMS 61. SIAM.

Donoho, D., M. Duncan, X. Huo, L. Levi, J. Buckheit, M. Clerc, J. Kalifa, S. Mallat, T. Yu, S. Chen, I. Johnstone, J. Scargle, and R. von Sachs (2001). Wavelab 802 for matlab5.x. <http://www-stat.stanford.edu/~wavelab/>.

Dowdy, S. and S. Wearden (1991). *Statistics for Research*. New York: Wiley.

Doyle, R. (1997). *A Helicopter Obstacle Avoidance System Incorporating Non-linear Neurofuzzy Multi-Sensor Data Fusion*. Ph.D. thesis, University of Southampton.

Ebeling, W., H. Engel, and H. Herzl (1990). *Selbstorganisation in der Zeit*, Volume 309 of *Wissenschaftlich Taschenbücher: Mathematik/Physik*. Berlin: Akademie-Verlag.

Eberl, W. (1995). Grundlagen und Methoden zur nichtlinearen Dynamik. In *Skript zur Vorlesung: "Chaotische Dynamik und Strukturbildung"*. Chaosgruppe e.V. und TU München: Verlag Kunst und Alltag.

Eckmann, J.-P., O. Kamphorst, and D. Ruelle (1987). Recurrent plots of dynamical systems. *Europhys. Lett.* 4(9), 973–977.

Eckmann, J.-P., S. Oliffson Kamphorst, D. Ruelle, and S. Ciliberto (1986). Lyapunov exponents from a time series. *Phys. Rev. A* 34, 4971.

Eckmann, J.-P. and D. Ruelle (1985). Ergodic theory of chaos and strange attractors. *Rev. Mod. Phys.* 57, 617.

Eckmann, J.-P. and D. Ruelle (1992). Fundamental limitations for estimating dimensions and Lyapunov exponents in dynamical systems. *Physica D* 56, 185 – 187.

Eichblatt, E.J., Jr (1989). Simulation. In S. M. (Ed.), *Test and Evaluation of the Tactile Missile*, Volume 119 of *Progress in Astronautics and Aeronautics*, Chapter 5, pp. 129–194. Washington, DC: American Institute of Aeronautics and Astronautics.

Essex, C. and M. Nerenberger (1991). Comments on ‘Deterministic Chaos: the science and the fiction’ by d. ruelle. *Proc. R. Soc. Lond. A* 435, 287.

Feraday, S. (1998). Modelling brake squeal with neuro-fuzzy systems. Personal communications.

Fick, E. (1988). *Einführung in die Grundlagen der Quantentheorie* (6. ed.). Aula-Verlag Wiesbaden.

Forden, G. (1997). The airborne laser. *IEEE Spectrum* 34(9), 40–49.

Frank, G., T. Lookman, and M. Nerenberg (1990). Recovering the attractor: A review of chaotic time-series analysis. *Can. J. Phys.* 68, 711.

Fraser, A. and H. Swinney (1986). Independent coordinates for strange attractors from mutual information. *Phys. Rev. A* 33, 1134.

Gardiner, C. (1998). *Handbook of Stochastic Methods* (2nd. ed.), Volume 13 of *Springer Series in Synergetics*. Berlin: Springer Verlag.

Garnell, P. (1980). *Guided Weapon Control Systems* (2nd. ed.). Pergamon Press.

Gershenfeld, N. (1988). An experimentalist’s introduction to the observation of dynamical systems. In H. Bai-Lin (Ed.), *Directions in Chaos*, pp. 311. World Scientific.

Gibson, J., J. Farmer, M. Casdagli, and S. Eubank (1992). An analytic approach to practical state space reconstruction. *Physica D* 57, 1 – 30.

Grassberger, P. (1986). Do climatic attractors exist? *Nature* 323, 609.

Grassberger, P. and I. Procaccia (1983a). Characterization of strange attractors. *Phys. Rev. Lett.* 50(5), 346–349.

Grassberger, P. and I. Procaccia (1983b). Measuring the strangeness of strange attractors. *Physica D* 9(1–2), 189–208.

Großmann, S. (1988). *Funktionalanalysis, im Hinblick auf Anwendungen in der Physik* (4th ed.). Aula-Verlag Wiesbaden.

Haykin, S. (1999). *Neural Networks, A Comprehensive Foundation* (2nd. ed.). Prentice Hall.

Helgason, S. (1980). *The Radon transform*. Boston: Birkhäuser-Verlag.

Herman, G. (1980). *Image Reconstruction from Projections: The Fundamentals of Computerized Tomography*. New York: Academic Press.

Herman, G. and F. Natterer (1981). *Mathematical Aspects of Computerized Tomography*, Volume 8 of *Lecture Notes in Medical Informatics*. New York: Springer-Verlag.

Hestenes, D. (1986). *New Foundations for Classical Mechanics*. Dordrecht: D. Reidel Publishing Company.

Holschneider, M. (1995). *Wavelets : an analysis tool*. Oxford mathematical monographs. Oxford: Oxford University Press.

Holzfuss, J. and G. Mayer-Kress (1986). An approach to error-estimation in the application of dimension algorithms. In H. Haken (Ed.), *Dimensions and Entropies in Chaotic Systems – Quantification of Complex Behaviour*, Volume 32 of *Springer Series in Synergetics*, pp. 114. Berlin: Springer-Verlag.

Jaynes, E. T. (1957). Information theory and statistical mechanics. *Phys. Rev.* 106(4), 620–630.

Jenn, A. (1991). Drag prediction methods for axisymmetric missile bodies. In M. Mendenhall (Ed.), *Tactical Missile Aerodynamics: Prediction Methodology*, Volume 142 of *Progress in Astronautics & Aeronautics*, pp. 37–62. American Institute of Aeronautics and Astronautics.

Jetschke, G. (1989). *Mathematik der Selbstorganisation*. Verlag Harri Deutsch.

Juditsky, A., H. Hjalmarsson, A. Benveniste, B. Deylon, L. Ljung, J. Sjöberg, and Q. Zhang (1995). Nonlinear black-box models in system identification: Mathematical foundations. *Automatica* 31(12), 1725–1750.

Kaiser, G. (1999). *A Friendly Guide to Wavelets* (6th ed.). Birkhäuser-Boston.

Kalman, R. (1960). A new approach to linear filtering and prediction problems. *Trans. ASME, J. Basic Eng.* 82, 35–45.

Kalman, R. (1963). *A new method in Wiener filtering theory*. Proc. Symp. Eng. Appl. Random Function Theory and Probability. New York: Wiley.

Kalman, R. and R. Bucy (1961). New results in linear filtering and prediction theory. *Trans. ASME, J. Basic Eng.* 83, 95–108.

Kantz, H. and T. Schreiber (1997). *Nonlinear time series analysis*. Cambridge, UK: Cambridge University Press.

Kantz, H. and T. Schreiber (1998). Nonlinear projective filtering i: Background in chaos theory. In *Proceedings of NOLTA 1998*, Lausanne. Presses Polytechniques et Universitaires Romandes.

Kantz, H., T. Schreiber, I. Hoffmann, T. Buzug, G. Pfister, L. G. Flepp, J. Simonett, R. Badii, and E. Brun (1993). Nonlinear noise reduction: A case study on experimental data. *Phys. Rev. E* 48, 1529–1538.

Keenan, D. (1985). A Tuckey Nonadditivity-Type test for times series nonlinearity. *Biometrika* 72(1), 39–44.

Kirsch, A. (1996). *An Introduction to the Mathematical Theory of Inverse Problems*, Volume 120 of *Applied Mathematical Sciences*. New York: Springer Verlag.

Kirubarajan, T., Y. Bar-Shalom, K. Pattipati, and I. Kadar (2000). Ground target tracking with variable structure imm *IEEE Transactions on Aerospace and Electronic Systems* 36(1), 26–44.

Koebbe, M. and G. Mayer-Kress (1992). Use of recurrence plots in the analysis of time-series data. In M. Casdagli and S. Eubank (Eds.), *Nonlinear Modelling and Forcasting*, SFI Studies in the Science of Complexity, Proc. Vol. XXI, pp. 361–378. Santa Fe: Addison-Wesley.

Kugiumtzis, D., B. Lillekjendlie, and N. Christoffersen (1994). Chaotic time series, part I. Estimation of some invariant properties in state space. *Modeling, Identific. & Control* 15, 205–224.

Kurths, J. and H. Herzel (1987). An attractor in solar time series. *Physica D* 25(1–3), 165–172.

Landau, L. and E. Lifshitz (1960). *Mechanics*. Oxford: Pergamon Press Ltd.

Langtangen, H. (1999). *Computational Partial Differential Equations*, Volume 2 of *Numerical methods and Diffpack Programming series*. Springer-Verlag.

Liebert, W. and H. Schuster (1988). Proper choice of the time delay for the analysis of the chaotic time series. *Phys. Lett. A* 142, 107.

Lillekjendlie, B., D. Kugiumtzis, and N. Christopersens (1994). Chaotic time series, part II: System identification and prediction. *Modeling, Identific. & Control* 15, 225–243.

Lowe, D. (1995). Radial basis function networks. In M. Arbib (Ed.), *The Handbook of Brain Theory and Neural Networks*, pp. 779–782. The MIT Press.

Mahapatra, P. and K. Mehrotra (2000). Mixed coordinate tracking of generalized maneuvering targets using acceleration and jerk models. *IEEE Transactions on Aerospace and Electronic Systems* 36(3), 992–1000.

Majid, F. (2001). The wave packet analysis tool xwpl. <http://www.math.yale.edu/pub/wavelets/software/xwpl/>.

Mallat, S. (1998). *A Wavelet Tour of Signal Processing*. Academic Press.

Marion, J. and S. Thornton (1995). *Classical Dynamics of Particles and Systems* (4th ed.). Saunders College Publishing.

Mills, D. (1995). Control of a six degree of freedom auv. Personal communications.

Mills, D. (1998). *Nonlinear Optics* (2.nd ed.). Springer Verlag.

Mills, D. and C. Harris (1995). Neurofuzzy modelling and control of a six degree of freedom auv. Technical report, Image Speech and Intelligent Systems research group.

Moody, J. (1991). The effective number of parameters: An analysis of generalization and regularization in nonlinear learning systems. In J. Moody, S. Hanson, and R. Lippmann (Eds.), *Advances in Neural Information Processing Systems 4*, pp. 847–854. Morgan Kaufmann.

Murata, N., S. Yoshizawa, and S. Amari (1991). A criterion for determining the number of parameters in an artificial neural network model. In T. Kohonen, K. Makisara, O. Simula, and J. Kangas (Eds.), *Artificial Neural Networks*, pp. 9–14. Amsterdam:North Holland.

Nerenberg, M. and C. Essex (1990). Correlation dimension and systematic geometric effects. *Phys. Rev. A* 42, 7065.

Ott, E. (1993). *Chaos in Dynamical Systems*. Cambridge: University Press. natural measure is discussed in §2.3.3 p. 51 ff.

Papoulis, A. (1991). *Probability, Random Variables, and Stochastic Processes* (3rd. ed.). McGraw-Hill.

Pearl, J. (1995). Bayesian networks. In M. Arbib (Ed.), *The Handbook of Brain Theory and Neural Networks*, pp. 149–153. The MIT Press.

Press, W., B. Flannery, A. Saul, and W. Vetterling (1993). *Numerical Recipes in C. The Art of Scientific Computing*. Cambridge University Press.

Price, C., D. Prichard, and E. Hugenson (1992). Do the sunspot numbers form a ‘chaotic’ set? *J. Geophys. Res.* 97.

Prichard, D. (1993). An investigation of the non-linear response of the magnetosphere. Master’s thesis, University of Alaska Fairbanks, Fairbanks, Alaska. 1993.

Primas, H. (1994). Endo- and exo-theories of matter. In H. Almanspacher and G. J. Dalenoort (Eds.), *Inside Versus Outside, Endo- and ExoConcepts of Observation and Knowledge in Physics, Philosophy and Cognitive Science*, pp. 163–193. Berlin: Springer.

Risken, H. (1996). *The Fokker-Planck Equation* (2nd. ed.), Volume 18 of *Springer Series in Synergetics*. Berlin: Springer Verlag.

Rössler, O. E. (1992). *Endophysik*. Berlin: Merve.

Ruelle, D. (1990). Deterministic chaos: the science and the fiction. *Proc. R. Soc. Lond. A* 427, 241.

Ruelle, D. and F. Takens (1971). On the nature of turbulence. *Comm. Math. Phys.* 20, 167.

Sano, M. and Y. Sawada (1985). Measurement of the Lyapunov spectrum from chaotic time series. *Phys. Rev. Lett.* 55, 1082.

Satsuma, J. and N. Yajima (1947). Initial value problems of one-dimensional self-modulation of nonlinear waves in dispersive media. *Prog. Theor. Phys., Suppl.* 55, 284–306.

Scheck, F. (1990). *Mechanics: From Newton's Laws to Deterministic Chaos*. Berlin: Springer Verlag.

Schilhabel, T. (1996). Chaotic dynamics of Ballistic missiles. Technical report, Image, Speech, and Intelligent Systems research group, ECS, University of Southampton.

Schilhabel, T. (1999). Linear dynamics in an endo-observer's frame of reference. Technical report, Image, Speech, and Intelligent Systems research group, ECS, University of Southampton.

Schilhabel, T. (2000). Pattern formation of a multicellular bacterium described by a schrödinger-like partial differential equation. In *XVII Sitges Conference Euroconference*, Sitges-Barcelona, Spain, pp. poster.

Schilhabel, T. and C. Harris (1998a). Autonomous decision making using nonlinear dynamics. In *FUSION'98*, Volume 2, Las Vegas, USA, pp. 920–924.

Schilhabel, T. and C. Harris (1998b). Channel coding in the hilbert space for neuron activity. In *XV Sitges Conference Euroconference*, Sitges-Barcelona, Spain, pp. poster.

Schilhabel, T. and C. Harris (1998c). A mathematical model for shared variables among different observers. In *FUSION'98*, Volume 2, Las Vegas, USA, pp. 897–907.

Schilhabel, T. and C. Harris (1998d). A probabilistic Hilbert space approach towards understanding nonlinear dynamical systems in an observer's endo-and exovariables. In *Proceedings of the 3rd International Conference on Artificial Life and Robotics AROB III'98*, Bepu, Oita, Japan.

Schilhabel, T. and Z. Wu (1997). Why the lorenz attractor is almost inaccessible with neuro-fuzzy systems. Personal communications.

Schlögel, F. (1989). *Probability and Heat: Fundamentals of Thermostatistics*. Braunschweig/Wiesbaden: Vieweg.

Schreiber, T. and H. Kantz (1998). Nonlinear projective filtering ii: Application to real time series. In *Proceedings of NOLTA 1998*, Lausanne. Presses Polytechniques et Universitaires Romandes.

Schuster, H. (1989). *Deterministic Chaos: An Introduction* (2nd. ed.). Weinheim: VCH Publishers.

Schwarz, U. (1994). *Zeitreihenanalyse astrophysikalischer Aktivitätsphänomene*. Ph.D. thesis, Universität Potsdam, Potsdam.

Shumway, R. (1988). *Applied Statistical Time Series Analysis*. Englewood Cliffs, New Jersey: Prentice Hall.

Sir Popper, K. (1972). *Objective Knowledge; An Evolutionary Approach*. Oxford University Press.

Sjöberg, J., A. Zhang, Q. and Benveniste, B. Deylon, H. Hjalmarsson, A. Juditsky, and L. Ljung (1995). Nonlinear black-box modelling in system identificatio: a unified overview. *Automatica* 31(12), 1691–1724.

Smith, L. (1988). Intrinsic limits on dimension calculations. *Phys. Lett. A* 133, 283.

Stark, J. (1999). Delay embeddings of forced systems: I deterministic forcing. *Nonlinear Sci.* 9, 255–332.

Stark, J., D. Broomhead, M. Davies, and J. Huke (1997). Takens embedding theorems for forced and stochastic systems. *Nonlinear Analysis* 30, 5303–5314.

Systems, J. W. (1985). 1984-85. Jane's Publishing Company Limited.

Takens, F. (1993). Detecting nonlinearities in stationary time series. *Int. J. Bifurcation* 3, 241–256.

Takens, F. (Warwick 1981). Detecting strange attractors in turbulence. In *Dynamical Systems and Turbulence*, Volume 898 of *Lect. Notes Math.*, pp. 366. Berlin: Springer–Verlag.

Theiler, J. (1986). Spurious dimensions from correlation algorithms applied to limited time series data. *Phys. Rev. A* 34, 2427.

Thodberg, H. (1996). A review of bayesian neural networks with an application to near infrared spectroscopy. *IEEE Trans. Neural Networks* 7(1), 56–72.

Thornton, S. and J. Marion (1995). *Classical Dynamics of Particles and Systems* (4th. ed.). Fort Worth, USA: Saunders College Publishing.

Tong, H. (1995). *Non-linear Time Series, A Dynamical System Approach* (3rd ed.), Volume 6 of *Oxford Statistical Science Series*. Oxford: Oxford Science Publications.

Tsay, R. (1986). Nonlinearity tests for time-series. *Biometrika* 73(2), 461–466.

Vapnik, V. (1999). An overview of statistical learning theory. *IEEE Transactions on Neural Networks* 10(5), 988–998.

Weigend, A. S. and N. A. Gershenfeld (Eds.) (1993). *Time series prediction: Forecasting the future and understanding the past*. Reading, MA: Addison Wesley.

Whitney, H. (1936). Differentiable manifolds. *Ann. Math.* 37, 645 – 680.

Wolf, A., J. Swift, H. Swinney, and J. Vastano (1985). Determining Lyapunov exponents from a time series. *Physica D* 16, 285.

Wolff, R. C. L. (1994). Independence in time series: another look at the BDS test. *Philos. Trans. Roy. Soc. A* 348(1688), 383–395.

Wu, Z. and C. Harris (1997). Neurofuzzy network structure for modelling and state estimation of unknown nonlinear systems. *International Journal of Systems Science* 28, 335–345.

Wu, Z. and T. Schilhabel (1997). Estimation of the lorenz attractor with neuro-fuzzy systems. Personal communications.

Zakharov, V. and A. Mikhailov (1978). *Soc. Phys.-JTEP* 47, 1017.